

263
CIVIL ENGINEERING STUDIES
D. 2 STRUCTURAL RESEARCH SERIES NO. 263



Metz Reference Room
Civil Engineering Department
B106 C. E. Building
University of Illinois
Urbana, Illinois 61801

DEFLECTIONS OF REINFORCED CONCRETE FLOOR SLABS

By

M. D. VANDERBILT

M. A. SOZEN

C. P. SIESS

A Report to

THE REINFORCED CONCRETE RESEARCH COUNCIL
OFFICE OF THE CHIEF OF ENGINEERS, U. S. ARMY

GENERAL SERVICES ADMINISTRATION

PUBLIC BUILDINGS SERVICE

HEADQUARTERS, U. S. AIR FORCE
DIRECTORATE OF CIVIL ENGINEERING

and

U. S. NAVY, ENGINEERING DIVISION
BUREAU OF YARDS AND DOCKS

UNIVERSITY OF ILLINOIS
URBANA, ILLINOIS
APRIL 1963

DEFLECTIONS OF
REINFORCED CONCRETE FLOOR SLABS

by

M. D. Vanderbilt
M. A. Sozen
C. P. Siess

A Report on a Research Project
Conducted by the

CIVIL ENGINEERING DEPARTMENT
UNIVERSITY OF ILLINOIS

in cooperation with the

REINFORCED CONCRETE RESEARCH COUNCIL

OFFICE OF THE CHIEF OF ENGINEERS, U. S. ARMY

GENERAL SERVICES ADMINISTRATION, PUBLIC BUILDINGS SERVICE

HEADQUARTERS, U. S. AIR FORCE

and

U. S. NAVY, ENGINEERING DIVISION, BUREAU OF YARDS AND DOCKS
NBy 37633

UNIVERSITY OF ILLINOIS

URBANA, ILLINOIS

April 1963

TABLE OF CONTENTS

	Page
List of Tables	v
List of Figures.	vi
1. INTRODUCTION	1
1.1 Object and Scope of Investigation	1
1.2 Object and Scope of Report	4
1.3 Acknowledgments.	6
1.4 Notation	7
2. CURRENT BUILDING CODE PROVISIONS ON DEFLECTIONS	10
2.1 Introductory Remarks	10
2.2 Current Building Code Specifications Governing Deflections	10
2.3 Comparison of Thickness Requirements	19
2.4 Philosophy Underlying Code Provisions on Deflections . . .	20
3. THEORETICAL AND APPROXIMATE ANALYSES FOR DEFLECTIONS	23
3.1 Theoretical Methods of Analysis for Deflections.	23
3.2 Factors Affecting Deflections of Elastic Structures. . . .	29
3.3 Approximate Methods of Analyses for Deflections.	37
4. FRAME ANALYSIS	39
4.1 Introductory Remarks	39
4.2 Approximate Solution for the Mid-Panel Deflection of a Clamped Plate on Rigid Supports.	41
4.3 Effects of Stiffness Parameters and Aspect Ratio on Frame Loading	43
4.4 Details of Frame Analysis.	47
4.5 Application of the Frame Analysis to Elastic Structures. .	56
5. DEFLECTIONS OF REINFORCED CONCRETE STRUCTURES	60
5.1 Introductory Remarks	60
5.2 Description of University of Illinois Test Structures. . .	61
5.3 Comparisons of Computed with Measured Deflections.	66
5.4 Time-Dependent Deflections	79
5.5 Further Applications of Frame Analysis	86
6. DESIGN CONSIDERATIONS	90
6.1 Introductory Remarks	90
6.2 Nonsymmetrical Layouts	91

TABLE OF CONTENTS (continued)

	Page
7. SUMMARY AND CONCLUSIONS	93
7.1 Summary.	93
7.2 Conclusions.	95
BIBLIOGRAPHY.	97
TABLES	101
FIGURES	124
APPENDIX A. EXTRACT FROM FRENCH BUILDING CODE ON DEFLECTIONS . . .	257
A.1 Introductory Remarks	257
A.2 Extract on Deflections	257
APPENDIX B. DESCRIPTION OF COMPUTER PROGRAM.	263
B.1 Introductory Remarks	263
B.2 Input Data	264
B.3 Finite Difference Operator	264
B.4 Flow Diagrams.	266
B.5 Output Data and Estimation of Running Time	269
B.6 Validity of Program.	269
B.7 Availability	270
APPENDIX C. ILLUSTRATIVE EXAMPLE	277
C.1 Introductory Remarks	277
C.2 Selection of Frames.	277
C.3 Computations of Stiffness and Carry-Over Factors	278
C.4 Determination of Loading	281
C.5 Computations of Moments, Slopes, and Deflections for Uncracked Sections	281
C.6 Computations of Slopes and Deflections Based on Fully Cracked Sections	284

LIST OF TABLES

<u>Number</u>		<u>Page</u>
1	Building Code Limitations on $\frac{\text{Thickness}}{\text{Span}}$ Ratios.	101
2	Building Code Minimum Thickness Limitations.	102
3	Comparison of Thicknesses Required for U. of I. Test Slabs by Various Building Codes	103
4	Deflections of Uniformly Loaded Rectangular Plates on Nondeflecting Supports	104
5	Deflections of Plates Continuous over Flexible Beams	107
6	Deflections of a Nine-Panel Slab	109
7	Deflection Coefficients for Interior Panels, $I_S = I_L$	110
8	Bending Moments in Long Direction at Various Points in Interior Panels, $I_S = I_L$	111
9	Bending Moments in Short Direction at Various Points in Interior Panels, $I_S = I_L$	112
10	Deflection Coefficients for Interior Panels, $I_S = (S/L)I_L$	113
11	Bending Moments in Long Direction at Various Points in Interior Panels, $I_S = (S/L)I_L$	114
12	Bending Moments in Short Direction at Various Points in Interior Panels, $I_S = (S/L)I_L$	115
13	Deflection Coefficients for Interior Panels, $I_S = (S/L)^2 I_L$	116
14	Bending Moments in Long Direction at Various Points in Interior Panels, $I_S = (S/L)^2 I_L$	117
15	Bending Moments in Short Direction at Various Points in Interior Panels, $I_S = (S/L)^2 I_L$	118
16	Deflection Coefficients for Nine-Panel Slabs, All Panels Loaded.	119
17	Deflection Coefficients for Nine-Panel Slabs, Corner and Interior Panels Loaded.	122
18	Deflections and End Moments for a Symmetrically-Loaded Prismatic Beam	123

LIST OF FIGURES

Figure No.		Page
3.1	Variation of Mid-Panel Deflection with H_L , $S/L = 1.0$.	124
3.2	Variation of Mid-Beam Deflection with H_L , $S/L = 1.0$.	125
3.3	Variation of Mid-Panel Deflection with H_L , $S/L = 0.8$, $I_S = (S/L)I_L$	126
3.4	Variation of Mid-Panel Deflection with H_L , $S/L = 0.6$, $I_S = (S/L)I_L$	127
3.5	Variation of Mid-Panel Deflection with H_L , $S/L = 0.4$, $I_S = (S/L)I_L$	128
3.6	Direction and Designation of Bending Moments in a Typical Interior Panel	129
3.7	Variation of Deflection with c/L Ratio, $S/L = 1.0$. .	130
3.8	Variation of Deflection with c/L Ratio, $S/L = 0.8$, $I_S = (S/L)I_L$	131
3.9	Variation of Deflection with c/L Ratio, $S/L = 0.6$, $I_S = (S/L)I_L$	132
3.10	Variation of Deflection with c/L Ratio, $S/L = 0.4$, $I_S = (S/L)I_L$	133
3.11	Variation of Mid-Panel Deflection with Aspect Ratio, $I_S = (S/L)I_L$	134
4.1	Deflected Shape of a Portion of a Continuous Structure	135
4.2	Typical Layout of a Nine-Panel Floor Slab.	136
4.3	Rotation of Beam Under Applied Unit Twisting Moment. .	137
4.4	Constant for Torsional Rotation of a Rectangular Cross Section	138
4.5	Comparisons of Theoretical and Frame Analyses Solutions, $J = 0.25$, $K = 10$, All Panels Loaded	139
4.6	Comparisons of Theoretical and Frame Analyses Solutions, $J = 0.25$, $K = 30$, All Panels Loaded	140
4.7	Comparisons of Theoretical and Frame Analyses Solutions, $J = 0.25$, $K = 90$, All Panels Loaded	141

LIST OF FIGURES (continued)

Figure No.		Page
4.8	Comparisons of Theoretical and Frame Analyses Solutions, $J = 1.0$, $K = 10$, All Panels Loaded	142
4.9	Comparisons of Theoretical and Frame Analyses Solutions, $J = 1.0$, $K = 30$, All Panels Loaded	143
4.10	Comparisons of Theoretical and Frame Analyses Solutions, $J = 1.0$, $K = 90$, All Panels Loaded	144
4.11	Comparisons of Theoretical and Frame Analyses Solutions, $J = 2.5$, $K = 10$, All Panels Loaded	145
4.12	Comparisons of Theoretical and Frame Analyses Solutions, $J = 2.5$, $K = 30$, All Panels Loaded	146
4.13	Comparisons of Theoretical and Frame Analyses Solutions, $J = 2.5$, $K = 90$, All Panels Loaded	147
4.14	Comparisons of Theoretical and Frame Analyses Solutions, $H = J = 0.25$, Corner and Interior Panels Loaded	148
4.15	Comparisons of Theoretical and Frame Analyses Solutions, $H = J = 2.5$, Corner and Interior Panels Loaded	149
5.1	View of Flat Slab (F2)	150
5.2	View of Two-Way Slab with Deep Beams (T1)	151
5.3	View of Flat Slab (F4)	152
5.4	Layout of Flat Plate Test Structure (F1)	153
5.5	Bottom Steel in the Flat Plate Test Structure (F1) . .	154
5.6	Top Steel in the Flat Plate Test Structure (F1) . . .	155
5.7	Arrangement of Reinforcement in Beams in the Flat Plate Test Structure (F1)	156
5.8	Arrangement of Column Reinforcement in Flat Plate Test Structure (F1)	157
5.9	Layout of Flat Slab Test Structures (F2, F3)	158

LIST OF FIGURES (continued)

Figure No.		Page
5.10	Bottom Steel in the Flat Slab Test Structure Reinforced with 1/8-in. Square Bars (F2)	159
5.11	Top Steel in the Flat Slab Test Structure Reinforced with 1/8-in. Square Bars (F2)	160
5.12	Arrangement of Reinforcement in Beams in the Flat Slab Test Structures (F2, F3).	161
5.13	Arrangement of Column Reinforcement in Flat Slab Test Structures (F2, F3)	162
5.14	Comparison of Cross-Sectional Areas of Slab Positive Reinforcement Provided in Test Structures No. 2 and No. 5	163
5.15	Comparison of Cross-Sectional Areas of Slab Negative Reinforcement Provided in Test Structures No. 2 and No. 5	164
5.16	Layout of Two-Way Slab Test Structures (T1, T2)	165
5.17	Arrangement of Bottom Reinforcement in Typical Two-Way Slab (T1)	166
5.18	Arrangement of Top Reinforcement in Typical Two-Way Slab (T1)	167
5.19	Arrangement of Reinforcement in Beams in Typical Two-Way Slab Test Structure (T1)	168
5.20	Arrangement of Bottom Reinforcement in Two-Way Slab with Shallow Beams	169
5.21	Arrangement of Top Reinforcement in Two-Way Slab with Shallow Beams (T2).	170
5.22	Arrangement of Reinforcement in Beams of Two-Way Slab with Shallow Beams (T2)	171
5.23	Arrangement of Column Reinforcement in Two-Way Slabs (T1, T2)	172
5.24	Arrangement of Bottom Reinforcement in the Flat Slab (F5).	173
5.25	Arrangement of Top Reinforcement in the Flat Slab (F5).	174

LIST OF FIGURES (continued)

Figure No.		Page
5.26	Arrangement of Beam Reinforcement Flat Slab Test Structure (F5)	175
5.27	Arrangement of Column Reinforcement in the Flat Slab (F5)	176
5.28	Location and Designation of Deflection Dial Gages for all Test Structures	177
5.29	Deflections and Deflection Coefficients for the Flat Plate (F1) Based on Uncracked Sections	178
5.30	Deflections and Deflection Coefficients for the Flat Plate (F1) Based on Fully Cracked Sections	179
5.31	Deflections and Deflection Coefficients for the Flat Slab (F2) Based on Uncracked Sections	180
5.32	Deflections and Deflection Coefficients for the Flat Slab (F2) Based on Fully Cracked Sections	181
5.33	Deflections and Deflection Coefficients for the Flat Slab (F3) Based on Fully Cracked Sections	182
5.34	Deflections and Deflection Coefficients for the Flat Slab (F5) Based on Fully Cracked Sections	183
5.35	Deflections and Deflection Coefficients for the Two-Way Slab with Deep Beams (T1) Based on Uncracked Sections	184
5.36	Deflections and Deflection Coefficients for the Two-Way Slab with Deep Beams (T1) Based on Fully Cracked Sections	185
5.37	Deflections and Deflection Coefficients for the Two-Way Slab with Shallow Beams (T2) Based on Uncracked Sections	186
5.38	Deflections and Deflection Coefficients for the Two-Way Slab with Shallow Beams (T2) Based on Fully Cracked Sections	187
5.39	Load-Deflection Curve, Flat Plate (F1), Point A_0 . . .	188
5.40	Load-Deflection Curves, Flat Plate (F1), Points A_1 and A_2	189

LIST OF FIGURES (continued)

Figure No.		Page
5.41	Load-Deflection Curve, Flat Plate (F1), Point B_0 . . .	190
5.42	Load-Deflection Curve, Flat Plate (F1), Point B_1 . . .	191
5.43	Load-Deflection Curves, Flat Plate (F1), Points B_2 and D_1	192
5.44	Load-Deflection Curves, Flat Plate (F1), Points C_3 and G_4	193
5.45	Load-Deflection Curve, Flat Plate (F1), Point E_0 . . .	194
5.46	Load-Deflection Curve, Flat Plate (F1), Point E_2 . . .	195
5.47	Load-Deflection Curve, Flat Plate (F1), Point F_0 . . .	196
5.48	Load-Deflection Curve, Flat Plate (F1), Point F_1 . . .	197
5.49	Load-Deflection Curve, Flat Plate (F1), Point F_2 . . .	198
5.50	Load-Deflection Curves, Flat Plate (F1), Points F_3 and H_4	199
5.51	Load-Deflection Curve, Flat Plate (F1), Point G_0 . . .	200
5.52	Load-Deflection Curve, Flat Plate (F1), Point J_0 . . .	201
5.53	Load-Deflection Curve, Flat Plate (F1), Point J_1 . . .	202
5.54	Load-Deflection Curve, Flat Slab (F2), Point A_0 . . .	203
5.55	Load-Deflection Curves, Flat Slab (F2), Points A_1 and A_2	204
5.56	Load-Deflection Curve, Flat Slab (F2), Point B_0 . . .	205
5.57	Load-Deflection Curve, Flat Slab (F2), Point B_1 . . .	206
5.58	Load-Deflection Curves, Flat Slab (F2), Points B_2 and D_1	207
5.59	Load-Deflection Curve, Flat Slab (F2), Point C_0 . . .	208
5.60	Load-Deflection Curves, Flat Slab (F2), Points C_2 and G_1	209
5.61	Load-Deflection Curve, Flat Slab (F2), Point D_2 . . .	210

LIST OF FIGURES (continued)

Figure No.		Page
5.62	Load-Deflection Curve, Flat Slab (F2), Point E_0 . . .	211
5.63	Load-Deflection Curves, Flat Slab (F2), Points E_1 and H_2	212
5.64	Load-Deflection Curve, Flat Slab (F2), Point F_0 . . .	213
5.65	Load-Deflection Curve, Flat Slab (F2), Point J_0 . . .	214
5.66	Load-Deflection Curve, Flat Slab (F2), Point J_2 . . .	215
5.67	Load-Deflection Curves, Flat Slab (F2), Points J_3 and J_4	216
5.68	Load-Deflection Curve, Flat Slab (F3), Point A_0 . . .	217
5.69	Load-Deflection Curves, Flat Slab (F3), Points A_1 and A_2	218
5.70	Load-Deflection Curves, Flat Slab (F3), Points B_1 and C_1	219
5.71	Load-Deflection Curve, Flat Slab (F3), Point C_0 . . .	220
5.72	Load-Deflection Curve, Flat Slab (F3), Point D_0 . . .	221
5.73	Load-Deflection Curve, Flat Slab (F3), Point E_0 . . .	222
5.74	Load-Deflection Curves, Flat Slab (F3), Points E_2 , F_1 and H_2	223
5.75	Load-Deflection Curves, Flat Slab (F3), Points F_0 and H_0	224
5.76	Load-Deflection Curves, Flat Slab (F3), Points F_2 and J_1	225
5.77	Load-Deflection Curve, Flat Slab (F3), Point J_0 . . .	226
5.78	Load-Deflection Curve, Flat Slab (F4), Point A_0 . . .	227
5.79	Load-Deflection Curve, Flat Slab (F4), Point B_1 . . .	228
5.80	Load-Deflection Curve, Flat Slab (F4), Point D_0 . . .	229
5.81	Load-Deflection Curve, Flat Slab (F4), Point H_0 . . .	230

LIST OF FIGURES (continued)

Figure No.		Page
5.82	Load-Deflection Curve, Flat Slab (F5), Point A_0 . . .	231
5.83	Load-Deflection Curve, Flat Slab (F5), Point A_1 . . .	232
5.84	Load-Deflection Curve, Flat Slab (F5), Point B_1 . . .	233
5.85	Load-Deflection Curve, Flat Slab (F5), Point D_0 . . .	234
5.86	Load-Deflection Curve, Flat Slab (F5), Point G_0 . . .	235
5.87	Load-Deflection Curve, Two-Way Slab (T1), Point A_0 . .	236
5.88	Load-Deflection Curve, Two-Way Slab (T1), Point A_1 . .	237
5.89	Load-Deflection Curve, Two-Way Slab (T1), Point B_0 . .	238
5.90	Load-Deflection Curve, Two-Way Slab (T1), Point B_1 . .	239
5.91	Load-Deflection Curves, Two-Way Slab (T1), Points B_2 and D_1	240
5.92	Load-Deflection Curve, Two-Way Slab (T1), Point E_0 . .	241
5.93	Load-Deflection Curves, Two-Way Slab (T1), Points E_1 and E_2	242
5.94	Load-Deflection Curve, Two-Way Slab (T2), Point A_0 . .	243
5.95	Load-Deflection Curve, Two-Way Slab (T2), Point A_1 . .	244
5.96	Load-Deflection Curve, Two-Way Slab (T2), Point B_0 . .	245
5.97	Load-Deflection Curve, Two-Way Slab (T2), Point B_1 . .	246
5.98	Load-Deflection Curves, Two-Way Slab (T2), Points B_2 and D_1	247
5.99	Load-Deflection Curve, Two-Way Slab (T2), Point E_0 . .	248
5.100	Load-Deflection Curves, Two-Way Slab (T2), Points E_1 and E_2	249
5.101	Method of Construction of Parabolic Transition Curve	250
5.102	Strain Distribution in a Reinforced Concrete Beam . .	251
5.103	Shrinkage Curvature in Reinforced Concrete Beams . . .	252

LIST OF FIGURES (continued)

Figure No.		Page
5.104	Load-Deflection Curves for PCA Test Slab	253
5.105	Typical Interior Panel, Structure C	254
5.106	Deflection-Time Curves, Interior Panel, Structure C. .	255
6.1	Schematic Layout of a Typical Nonsymmetrical Structure	256
B.1	Finite Difference Operator Pattern and Addresses . . .	271
B.2	General Flow Diagram	272
B.3	Detailed Flow Diagram	273
B.4	Layout of One-Quarter of Interior Plate	275
B.5	Check on Validity of Computer Program, $S/L = 0.8$, $c/L = 0$	276
C.1	Ersatz Frames for Two-Way Slab with Shallow Beams (T2)	287

1. INTRODUCTION

1.1 Object and Scope of Investigation

This report is one of a continuing series of reports written as part of the investigation of multiple-panel reinforced concrete floor slabs which is currently being conducted at the University of Illinois. The floor slab investigation has as its over-all objective the development of a unified design procedure for floor slabs.

A floor slab consists essentially of a continuous plate supported on columns. If supporting beams are placed so that they span between columns the beams act to stiffen the structure and to enhance the load-carrying capability of the structure. Structures without beams, excepting spandrel beams, are termed either flat slabs or flat plates depending upon whether the tops of the supporting columns are flared to form column capitals. The slabs with supporting beams are termed two-way slabs.

The current design specifications for slabs contained in the ACI Building Code (1)* treat the two types of construction in entirely different approaches. An extensive discussion of the design of flat slabs and plates is given while the design of two-way slabs is treated briefly in a separate chapter.

The total moment capacities provided by the two methods of design are quite different. For example, for a square interior panel of a flat slab the total moment provided is

$$M_o = 0.09WLF \left[1 - \frac{2c}{3L} \right]^2 \quad (1.1)$$

where W = the total load on the panel,

* Numbers in parentheses refer to entries in the bibliography.

L = the span,

c = the effective support size, and

F = $1.15 - c/L$, but not less than one.

For a square interior panel of a two-way slab the total moment provided is $0.15WL$ which is 120 percent of the static moment of $0.125WL$. For a ratio of c/L of zero the two-way slab would provide 145 percent of the moment provided by the flat slab. Conversely, the flat slab would provide 83 percent of the static moment and 69 percent of the moment for the two-way slab. For ratios of c/L of 0.15 and larger the flat slab is required to carry only 72 percent of the static moment. The fact that the two methods lead to such differences in required moment capacity, and hence amounts of reinforcing steel, results in the anomalous situation that the inherently stronger two-way system is economically justifiable only for light design loads for which thickness limitations govern the design of flat slabs.

The reasons for the differences between the two types of design procedures stem from the ways in which they were developed. Flat slabs literally were invented and were constructed for years before any analysis was developed. When Nichols (2) in 1914 first gave the expression defining the static moment in an interior panel as

$$M_o = 0.125WL \left[1 - \frac{2c}{3L} \right]^2 \quad (1.2)$$

many practicing engineers refused to believe it since it placed a lower bound on the total moment in a panel that was higher than the total capacity current practice then provided.

During the early days of flat slab construction it was common practice for the owner of a new building to specify that acceptance would be made only upon the successful completion of a load test. These tests usually

included the loading of only a few panels and hence the unloaded panels immediately adjacent to the loaded panels were able to assist in carrying the load. Since building codes can do little more than reflect current practice, whenever the current practice appears to give reasonable results, the regulations adopted by the ACI and other codes provided for only a portion of the static moment as is shown by Eq. 1.1.

Analyses of load tests made by Westergaard and Slater in 1921 (3) are often cited to prove the correctness of Eq. 1.1. However, these analyses did not properly take into account the influence of the tensile forces in the concrete and the aid of the unloaded panels adjacent to the loaded panels. Hence the high factors of safety shown by these studies were incorrect.

The design procedures for two-way slabs were developed on the bases of solutions for moments in plates on nondeflecting supports. Effects of pattern loadings were considered and the final procedures thus developed required more than adequate moment-carrying capacity. Chronologically, method 2 was the first method developed. This method was developed based on studies made by Westergaard (4). Method 1 was developed by Di Stasio and Van Buren for inclusion in the New York City Building Code (5) and was later incorporated into the ACI and other codes. A third procedure, similar in form to the German code, is included in the 1963 ACI code (6). This method is in most cases the most conservative method of the three (7).

In view of the inequities of the disparate design provisions for two-way and flat slabs, an investigation of floor slabs was initiated at the University of Illinois in 1956. This investigation has included both theoretical and experimental studies. The theoretical studies have included considerations of the effects of openings in slabs and the effects of varying column stiffnesses on moments and deflections of slabs (8,9). The experimental

phase has included the testing of five nine-panel reinforced concrete floor slabs. Previous reports have given details of the construction and testing of these slabs and the results of analyses for moments (10,11,12,13,14,15). Effects of beam and column stiffnesses on moments and the correlation between computed and measured moments have been studied (16).

1.2. Object and Scope of Report

The adequate design of a structure requires that at least two different types of criteria be satisfied: those of safety and serviceability. The criterion of safety is satisfied if the structure provides adequate strength. The serviceability criteria are less easily defined. Such diverse factors as color, finish, ability to resist spalling and dusting, etc., may be considered to serve as indices of serviceability. Perhaps the most commonly cited criterion is that of deflections.

Excessive deflections of a floor slab may render a structure unusable both from an esthetical and a functional point of view. Deflections of a floor may in themselves cause worry to the occupants of a building since to the layman noticeable deflection often signifies incipient collapse. However, the major effect of large deflections is usually to cause damage to construction carried by the floor. Such damage is shown by cracking of brittle partitions, jamming and mis-alinement of doors in partitions and the like. Current trends towards the use of lightweight-aggregate concretes and higher allowable steel stresses will increase the possibility of large deflections.

The problem of deflections has long been recognized by the engineering profession. Building codes attempt to provide adequate stiffness by specifying minimum allowable thicknesses and/or thickness-to-span ratios. Design engineers commonly provide for a certain amount of camber. The

inadequacy of these provisions is shown by the number of cases of structures which become unserviceable because of deflections. Since such cases often are matters of litigation they are seldom publicized. No simple method of analyses for deflections of continuous structures has previously been developed.

The effect of deflections on strength is also a matter of interest. The yield-line method for assessing the strength of slabs is an upper-bound method but it normally underestimates the strength by 10 to 30 percent. In exceptional cases, where a slab is surrounded by essentially rigid beams, the load-carrying capacity of a panel may be several times that predicted by the yield-line procedure (17). It has been postulated (11) that the large deflections accompanying the formation of yield lines in a slab serve to increase the lever arms of the positive reinforcement thereby increasing the capacity. It is possible that a method of determining the effect of deflections on strength may be developed after a method of computing the deflections at and beyond yield has been developed.

This report describes the results of a study of deflections of reinforced concrete floor slabs. The study is concerned with the problem of deflections as a serviceability criterion and does not include a discussion of the effects of deflections on strength. The current building code provisions on deflections contained in the codes of a number of countries are discussed in Chapter 2. The theoretical methods of determining deflections of plates and the factors affecting the deflections of plates in continuous structures are described in Chapter 3. The development of an approximate method of analyses for deflections through the use of a frame analysis is given in Chapter 4. The agreement between computed and measured deflections for several reinforced concrete structures is shown in Chapter 5. Additional

design considerations are contained in Chapter 6 and Chapter 7 is a summary of the report.

1.3 Acknowledgments

This report was prepared as part of an investigation conducted in the Structural Research Laboratory of the Civil Engineering Department at the University of Illinois in cooperation with the following organizations:

Reinforced Concrete Research Council
Directorate of Civil Engineering, Headquarters, U. S. Air Force
General Services Administration, Public Buildings Service
Office of the Chief of Engineers, U. S. Army
Bureau of Yards and Docks, Engineering Division, U. S. Navy

The program of investigation has been guided by an advisory committee on which the following persons have served:

Douglas McHenry, Chairman of the Advisory Committee, Portland Cement Association
L. H. Corning, Past Chairman, Portland Cement Association
G. B. Begg, Jr., Public Buildings Service, General Services Administration
W. J. Bobisch, BuDocks, Department of the Navy
Frank Brown, Wire Reinforcement Institute, Inc.
J. Di Stasio, Sr., Consulting Engineer, Di Stasio and Van Buren (Deceased)
A. S. Neiman, Headquarters, U. S. Air Force
N. M. Newmark, University of Illinois
D. H. Pletta, Virginia Polytechnic Institute
J. R. Powers, Headquarters, U. S. Air Force
Paul Rogers, Consulting Engineer, Paul Rogers and Associates
E. J. Ruble, Association of American Railroads
W. E. Schaem, Office of the Chief of Engineers, U. S. Army
M. P. Van Buren, Consulting Engineer, Di Stasio and Van Buren
C. A. Willson, American Iron and Steel Institute

The project has been under the over-all direction of Dr. C. P. Siess, Professor of Civil Engineering, and the immediate supervision of Dr. M. A. Sozen, Associate Professor of Civil Engineering.

Invaluable assistance in programming for electronic computers has been furnished by Dr. J. W. Melin, Assistant Professor of Civil Engineering.

This report was prepared as a Ph. D. thesis under the direction of Professor M. A. Sozen.

1.4 Notation

The symbols used throughout the text are defined below and where first introduced in the text. Symbols that are used only once in the text are not repeated below.

A_s = cross-sectional area of tensile reinforcement

A'_s = cross-sectional area of compressive reinforcement

a, b = spans of a rectangular plate, also spans in the x and y directions, respectively; also portions of the span of a symmetrically-loaded beam as defined in Table 18

b = width of a beam

C = a measure of the torsional rigidity of a beam

c = a dimension defining the effective support size

d = effective depth of a reinforced concrete section or depth from compression face to centroid of tensile reinforcement

d_1 = larger dimension of a rectangular cross section for use in Eq. 4.5

$D = \frac{Et^3}{12(1-\nu^2)}$ = unit plate flexural rigidity

ϵ = strain

E = modulus of elasticity

E_s, E_c = modulus of elasticity of steel and concrete, respectively

f'_c = compressive strength of concrete

f_r = modulus of rupture of concrete

f_s = steel stress

f_y = yield stress of steel

G = modulus of elasticity in shear

$H_L = \frac{(EI)_L}{DS}$ = ratio of flexural rigidity of beam in long direction to plate flexural rigidity in short direction

$$H_S = \frac{(EI)_S}{DL} = \text{ratio of flexural rigidity of beam in short direction to plate flexural rigidity in long direction}$$

$$I_L, I_S = \text{moments of inertia of beams spanning in long and short directions, respectively}$$

$$j = \text{ratio of distance between compressive and tensile forces acting on a reinforced concrete beam cross section to the effective depth } d.$$

$$J = \frac{GC}{DL} = \text{ratio of torsional rigidity of a beam to the flexural rigidity of a plate}$$

$$k = \text{ratio of depth from compression face to neutral surface of a reinforced concrete section to the effective depth}$$

$$K = \frac{\sum 4(EI)_{col}/L_{col}}{D} = \text{ratio of total stiffness of a column to the unit plate flexural rigidity}$$

$$L = \text{the longer span of a rectangular plate}$$

$$M_O = \text{the static moment in a panel of a slab}$$

$$m, n = \text{positive integers}$$

$$m = \text{a factor defined by Eq. 5.8}$$

$$m_c = \text{the bending moment acting on a column as used in Eq. 4.3}$$

$$N = \text{number of simultaneous equations in a matrix}$$

$$p = A_s/bd = \text{ratio of cross-sectional area of tensile reinforcement to the product } bd$$

$$p' = A'_s/bd = \text{ratio of cross-sectional area of compressive reinforcement to the product } bd$$

$$q = \text{intensity of uniformly distributed load}$$

$$R = S/L = \text{ratio of short to long spans or aspect ratio}$$

$$S = \text{the shorter span of a rectangular plate}$$

$$t = \text{thickness of a plate}$$

$$t_1 = \text{the smaller dimension of a rectangular section for use in Eq. 4.5}$$

$$u = \text{Poisson's ratio, which is taken as zero in this report}$$

w = deflection, also weight of concrete

W = the total load on a panel

α = an angle defining the load to be applied to the ersatz frame

β = a factor used in finding C

Δ = deflection

$\lambda_L = \frac{(EI)_L}{DL} =$ ratio of flexural rigidity of beam in long direction to plate flexural rigidity in long direction

$\lambda_S = \frac{(EI)_S}{DS} =$ ratio of beam flexural rigidity in short direction to plate flexural rigidity in short direction

θ = slope

θ_t = the average rotation of a beam caused by a unit twisting moment as given by Eq. 4.4

θ_f = the rotation of a column caused by the unit twisting moment applied to the beam framing into the column

ϕ = curvature

Φ = unit rotation caused by unit twisting moment applied to a beam

2. CURRENT BUILDING CODE PROVISIONS ON DEFLECTIONS

2.1 Introductory Remarks

The deflection of a flexural member is a function of the support conditions, applied loading and span, and the flexural rigidity of the member. The majority of the building codes do not concern themselves with computations of deflections but rather with attempting to provide minimum values of flexural rigidity. These limitations upon the rigidity are usually presented in the form of minimum ratios of thickness and/or minimum ratios of thickness to span. The thickness and thickness-to-span limitations imposed by the codes available for study are listed in Tables 1 and 2. Of the building codes which are currently available for study, only those of the Netherlands, Sweden, France, USSR, and the United States contain any provisions pertaining to deflections other than the minimum thickness and thickness-to-span limitations listed in Tables 1 and 2.

A more detailed discussion of the provisions concerning deflections that are included in certain codes is given in Section 2.2. A comparison of the thicknesses required by the various codes for the University of Illinois test structures is given in Section 2.3. A discussion of the philosophy underlying the majority of the code provisions on deflections is contained in Section 2.4.

2.2 Current Building Code Specifications Governing Deflections

The majority of the codes attempt to insure adequate rigidity by specifying a minimum ratio of either thickness to span or effective depth to span. The span in most cases is defined as either the distance from center-to-center of supports or this distance plus the effective depth at mid-span. Certain codes also give limiting absolute values of thickness. The tacit

assumption appears to be made in all codes that all panels in a floor slab are rectangular in shape and are supported rigidly at least at the corners.

A complete code specification pertaining to deflections should consider both short-time and long-time deflections. However, among the codes studied only the Swedish, French and the USSR codes considered long-time deflections explicitly. While no longer a serviceability criterion, a method is given by the USSR code to calculate deflections at the formation of yield lines. The provisions concerning deflections given by certain codes are given below.

(A) Netherlands Code (18)

The building code of the Netherlands attempts to limit deflections by specifying a minimum allowable depth. The formula given by the code is a function of steel strain, which in turn is a function of the load and the shape of the panel, live load to dead load ratio, and span.

The Netherlands code presents a formula which gives the minimum depth as

$$d \geq 67 \frac{f_s}{E_s} \left[\frac{LL}{DL + LL} \right] L_{\min}$$

where

d = depth from extreme compressive fiber to center of tensile reinforcement

LL = live load

DL = dead load

f_s = design steel stress

E_s = modulus of elasticity of steel

L_{\min} = shorter span

The additional stipulations are made that when the slab is continuous over one edge, then L_{\min} shall be taken as 0.85 times the span perpendicular to this edge. If the slab is continuous over two opposite edges, L_{\min} is to be taken as 0.7 times the span perpendicular to these edges. The minimum $LL/(DL + LL)$ ratio to be used is 0.5.

This formula is based on a maximum allowable deflection to short span ratio of 1/250 for total load or 1/500 for live load, whichever governs.

The formula was developed on the basis of the assumption that the concrete in the tensile zone of the short span of a panel will be cracked at service load levels and that therefore the steel stress governs the design. The discussion of this formula (18) states that the formula gives results which agree fairly well with results of tests of simply supported slabs, but that for other cases rather large deviations may be expected.

(B) Swedish Code (18,19)

The Swedish code specifies that proper consideration should be given to the influence of cracking in the tension zone. The thickness of plates supported on four sides and carrying walls,* and which may be harmed by deformations, should be at least

$$t_{\min} = \sqrt{\frac{7m_{\text{pos}}}{f_r}}$$

where m_{pos} = largest positive design moment, and

f_r = modulus of rupture of concrete (given by Table 9.311 of the Swedish State Concrete Regulations).

The commentary on this provision (19) which accompanies the code states that this formula was developed so as to prevent, as nearly as possible, the development of cracks in the positive moment regions. The intended result was that the uncracked stiffness would be preserved, thereby limiting

* Presumably "clamped down by walls at the periphery."

deflections. Based on the assumption of uncracked sections, the code further specifies that deflections may be calculated using the theory of elasticity with an apparent modulus of elasticity for the concrete. A numerical value of the apparent modulus is given for each of several grades of concrete. The code further specifies that for short-time loadings, calculations involving vibrations, etc., a modulus of elasticity up to three times that given in the code may be used. The commentary states that roughly the same value of t_{min} would be obtained if the code specified a maximum deflection to short span ratio of 1/1000.

A number of the variables which affect deflections are considered, at least implicitly, by this code. Type of loading, aspect ratio and span length affect the value of positive moment chosen for use in the formula for the minimum thickness. The effects of different material properties are considered in the value of the modulus of rupture used in the formula and in the value of the modulus of elasticity for concrete used in elastic calculations of deflections. However, the inadequacy of these specifications is pointed out in the commentary.

(C) The USSR Code (20)

The USSR code presents a number of empirical formulas for the determination of deflections and moments at first cracking, and deflections when sufficient yield lines have formed to produce a collapse mechanism. These formulas appear to be based in part on tests performed by W. I. Murashev and discussed briefly in a text by Sachnovski (21). However, the stipulated methods do not appear to be realistic, especially those pertaining to deflections at yield.

The USSR code states that attention shall be paid to the beginning of cracking, the width of cracks, and to the magnitude of deflections.

Approximate methods for the determination of crack widths and deflections are given. The specifications governing deflections are as follows:

(1) Two-way slabs

(a) Short-time deflections may be determined using tabulated values for elastic plates that were developed by Galerkin.

(b) In cracked slabs it is recommended that the deflection be determined approximately by linear interpolation between the deflection Δ_r , corresponding to the formation of the first cracks, and the deflection Δ_y , which immediately precedes collapse, by using the formula

$$\Delta = \Delta_r + (\Delta_y - \Delta_r) \left[\frac{P - P_r}{P_y - P_r} \right]$$

where

$$P_r < P < P_y$$

P = load

P_r = load at formation of first crack

P_y = failure load

Δ_r is determined as for an isotropic elastic slab with consideration given to creep where necessary. Time dependent effects are considered by multiplying the elastic deflection by two.

(c) When the ratio of reinforcement is 0.5 percent or less, the cracking moment may be determined from the equation

$$M_r = \frac{t^2(f_t)}{3.5}$$

where M_r = largest positive bending moment in the panel under consideration,

t = thickness, and

f_t = tensile strength of concrete.

(d) For two-way slabs Δ_y is determined based on a consideration of the pattern of yield lines that would exist at the formation of a failure mechanism for the given panel. At the formation of the mechanism corresponding to the lowest failure load the panel is assumed to be divided into rigid segments connected by bands of yielded material. The minimum failure angle between adjacent rigid segments is taken as $w'\phi$ where w' is the width of the yield band and $\phi = \frac{\epsilon_s}{d - kd}$ is the curvature of the slab when the steel yields. For rectangular panels w' may be assumed as $0.4S$ where S = the shorter side of the panel. The value of the width w' was determined from tests.

(2) Flat Slabs

(a) Uncracked deflection

$$\Delta = 0.018 \frac{P(L_x^4 + L_y^4)}{Eh^3} \text{ but } < \frac{L}{1000}$$

(b) Cracking moment

$$M_r = \frac{f_t t^2}{5}$$

(c) Load at cracking

$$P_r = \frac{10 M_r}{(L - 2c)^2}$$

(d) Δ_y for a square panel with square column capitals is given by the equation

$$\Delta_y = 0.1 L_1 f_s \frac{(0.5L - c)}{E_s (d - kd)}$$

where

L_1 = clear span between capitals

L = span center-to-center of columns

f_s = design steel stress

E_s = modulus of elasticity of steel

kd = depth from compression face to neutral surface.

For other than square panels it is necessary to consider the pattern of yield lines corresponding to the minimum yield load. The maximum absolute deflection of a flat slab, assuming no cracking, is limited to $1/1000$ of the span center-to-center of columns.

The mid-panel deflection at the yield load level was computed for the interior panels of the two two-way U. of I. test structures using the procedure outlined in (1d) above. The comparison between measured deflections at yield with the predicted deflections shows that the procedure specified for the computation of Δ_y greatly overestimates the correct value.

<u>Type of two-way structure</u>	<u>Measured mid-panel deflection less average beam deflection</u>	<u>Predicted Δ_y using (1d)</u>
Shallow beams	$0.24'' - 0.15'' = 0.09''$	0.57''
Deep beams	$0.30'' - 0.08'' = 0.22''$	0.50''

(d) French Code (22)

The French code prescribes only that deflections shall be small enough so that no structural damage shall occur and that in no case shall a thickness be used that is less than 5.0 cm. for on-site construction or 3.75 cm. for slabs prefabricated in shops. However, the commentary accompanying the code contains a discussion of some of the factors affecting deflections and suggests methods for computing deflections. The rules and commentary thereon are contained in Appendix A.

The relationships presented in the commentary for use in computing absolute values of deflections are basically conventional methods. For instance, the relationship given for the computation of Δ_1 (Eq. A.3) is nearly that which would be obtained for a uniformly loaded, simply supported beam assuming a fully-cracked section and using a modular ratio (ratio of elastic moduli) of 15. The term θ appearing in Eqs. A.3 and A.4 is evidently introduced

to account for the increased deflection that may be expected to occur for the shallower section which would result from the use of a high percentage of reinforcement.

(E) United States Code

A number of building codes are currently in force in various parts of the United States. The one perhaps most commonly recognized has been developed by the American Concrete Institute (1). The ACI code (318-56) gives provisions concerning minimum thickness and thickness-to-span limitations for both two-way and flat slabs. These provisions are included in Tables 1 and 2. In addition, minimum thickness formulae are given for flat slabs which are functions of span, load and concrete strength. These formulae were developed using the conventional straight-line formula to insure that the maximum flexural concrete stress in a flat slab would be less than the allowable stress. Hence, while these formulae affect stiffness, they were not developed to govern stiffness.

For two-way construction the minimum thickness is to be taken as four inches or the perimeter divided by 180, whichever is the larger. For a square panel the second requirement would reduce to

$$\frac{t}{L} \geq \frac{1}{45} \quad (2.1)$$

which is in the range of values included in Table 1. For an aspect ratio of 0.5, the second requirement would reduce to

$$\frac{t}{L_{\min}} \geq \frac{1}{30} \quad (2.2)$$

where the notation is that of Table 1. This ratio is more conservative than any of those included in Table 1 requiring, for example, twice the thickness for this case that would be required by the German, Austrian and Greek codes.

The definition of the minimum allowable thickness as a function of the perimeter was first suggested by Di Stasio and Van Buren (5). In the form first developed the minimum thickness was given by the relationship

$$t_{\text{minimum}} = \frac{A+B - 0.1N}{72} \left[\sqrt[3]{\frac{2000}{f'_c}} \right] \quad (2.3)$$

where A and B = span lengths,

N = sum of edges A and B which are continuous with adjacent panels, and

f'_c = 28 day concrete strength.

The development of the formula was based on limiting the deflection of a panel to a definite ratio of the span "consistent with all conditions of rectangularity and continuity." For simply supported, one-way construction a minimum thickness-to-span ratio of $1/24$ was commonly accepted at the time of the development of Eq. 2.3. For a square, simply supported panel the equivalent uniform load ratio was taken as $2/3$.^{*} In order to have a deflection equal to that of a one-way slab of the same span, the required thickness would be $1/36$ th of the span.

The authors further stated that, for equal deflections, a continuous, uniformly loaded beam with a mid-span moment of $qL^2/12$ ^{**} would require a

* This was based on the maximum moment in a square simply supported plate being $qL^2/24$ which is $2/3$ of $qL^2/16$ where $qL^2/16$ is the mid-panel moment in each direction based on a crossing-beam analogy. The average moment across a diagonal of a square simply supported plate is $qL^2/24$ while the mid-panel moment is about $qL^2/27$. Considering the purposes intended, the use of $qL^2/24$ in the derivation of Eq. 2.3 was adequate though not precise.

** This is the moment that would occur at the center of a loaded span of a prismatic beam if the beam were divided into an infinite number of similar spans with every other span uniformly loaded and the remaining spans unloaded.

thickness equal to 85% of the thickness required for a similarly loaded simple span, and that for two-way slabs this could be reduced to 80%. The cube root factor was added to provide for cases where concrete was used having a 28 day strength other than the 2000 psi commonly in use at the time Eq. 2.3 was developed.

The reduction factor of 0.85 given above may be readily derived using conventional methods of analysis of reinforced concrete sections and the t/L ratio of $1/24$ for one-way construction.

If f'_c is taken as 3000 in Eq. 2.3 and if all four edges of a rectangular panel are assumed continuous then Eq. 2.3 reduces to

$$t_{\min} = \frac{\text{perimeter}}{183} \quad (2.4)$$

which is closely the form now included in the ACI code (318-56).

The only other provisions given in the ACI code concerning deflections are criteria to be used in judging the results of load tests. All of these criteria are of the form $D = \text{maximum allowable deflection} = L^2/\eta t$ where L is the longer span, t the thickness, and η a constant specified by the code.

2.3 Comparison of Thickness Requirements

It is of interest to compare the thicknesses that would have been required by the various codes for the construction of the prototype flat slabs and two-way slabs of the University of Illinois test series. These thicknesses are listed in Table 3 as well as an indication of whether the minimum thickness or minimum thickness-to-span ratio was the controlling criterion. It is seen that the thickness required ranges from 3.2 to 8.0 in. with the majority of values in the range of 6 to 8 in. The thicknesses

(in inches) that would have been required on the basis of the Netherlands and Swedish formulae are as follows:

<u>Code</u>	<u>Flat Slabs (Nos. 2 and 5)</u>	<u>Two-way (No. 3)</u>	<u>(No. 4)</u>
Swedish	10.1	10.5	9.3
Netherlands	6.25	4.6	4.6
As Designed	7	6	6

The values shown for the Swedish code were computed based on the moduli of rupture used in the analyses of the test structures.

2.4 Philosophy Underlying Code Provisions on Deflections

The absolute value of the deflection of a point on a panel in a continuous structure is a function of the size and shape of the panel, the type and extent of the loading, the torsional and flexural stiffnesses of the beams (if any) supporting the panel, the flexural stiffnesses of the supporting columns, and the properties of the materials used in construction. In addition, the deflections of a reinforced concrete structure are influenced by the amount, type and arrangement of the compressive and tensile reinforcement, cracking of the concrete, the non-linearity of the stress-strain curve for concrete, and time-dependent deformations of the concrete.

The serviceability of a structure is affected by both absolute and relative deflections. If the absolute deflection of a point in a structure is too great it may render the structure unusable from either an esthetical or functional point of view. The relative deflection between points on a structure affects the serviceability not so much of the structure itself, but of adjuncts to the structure such as partitions, surface toppings, curtain walls, and the like.

The basic approach that most building codes incorporate in attempting to limit deflections is that of limiting relative deflections by specifying

some minimum allowable ratio of thickness to span. This type of specification considers only the size of the panel in question. Some codes attempt to introduce the effects of rectangularity by specifying that a given depth to span ratio is applicable only within a certain range of aspect ratios. The U.S. code is unique in specifying a minimum thickness for two-way construction which varies continuously with varying aspect ratios. Again, however, this specification considers only size and shape and is unaffected by boundary conditions, except that it presumably includes the assumption that all four edges are continuous.

Some codes do attempt to consider the effects of continuity. The Yugoslavian code specifies a minimum depth to span ratio with the span being taken as the span between lines of inflection. This provision is affected by boundary rotations, but does not include the effects of boundary deflections. Hence it may be expected to affect the relative deflection more than the absolute deflection. The minimum depth formulae given by the codes of Sweden and the Netherlands are functions of the bending moments in a panel. If the bending moments were functions of all the factors mentioned above as affecting deflections then these formulae could be expected to give good results. This is not the case, however, as the Swedish code states that moments are found by combining the moments for various cases of individual plates, all of which are cases of plates on nondeflecting supports, and the Netherlands formula was developed based on studies of simply supported reinforced concrete plates.

A limitation upon the allowable value of the absolute deflection could be specified by a code as a maximum deflection-to-span ratio. The commentary accompanying the French code suggests that the maximum deflection should be $1/500$ th of the clear span or even less for large spans. The minimum

depth formulae of the Swedish and Netherlands codes were developed with the intention of providing a maximum deflection of $1/1000$ th of the short span in the case of the Swedish code and either $1/250$ th or $1/500$ th of the short span in the case of the Netherlands code.

The maximum allowable absolute or relative deflection is a function of the use for which the structure is intended. Hence, the decision as to the allowable deflection should be made by the designing engineer. It is advisable, however, that guide lines be established by the codes.

3. THEORETICAL AND APPROXIMATE ANALYSES FOR DEFLECTIONS

3.1 Theoretical Methods of Analysis for Deflections

The problem of finding solutions giving the deflections and bending moments of elastic plates is one that has attracted the interest of investigators for the last century and a half. The differential equation governing the deflection of medium-thick elastic plates was first suggested by Lagrange in 1811, although a satisfactory derivation was not found until 1829 when it was developed by Poisson. This equation may be stated as follows:

$$\frac{\partial^4 w}{\partial x^4} + 2 \frac{\partial^4 w}{\partial x^2 \partial y^2} + \frac{\partial^4 w}{\partial y^4} = \frac{q}{D} \quad (3.1)$$

where w = deflection
 q = load
 $D = Et^3/12(1-u^2)$ = unit plate rigidity
 t = plate thickness
 u = Poisson's ratio, and
 E = the modulus of elasticity.

The derivation of this equation from conditions of equilibrium and compatibility may be found in Reference 23.

The solution to Eq. 3.1 is affected by the shape of the plate, type and extent of the loading on the plate, and the boundary conditions of deflections, rotations, moments and shears. Exact solutions have been found for various combinations of loadings and boundary conditions by a number of investigators. For purposes of discussion the theoretical methods of finding solutions to plate problems are grouped under the following headings:

(a) Closed form,

- (b) Infinite series,
- (c) Energy methods,
- (d) Finite differences, and
- (e) Moment distribution.

Brief discussions of these methods are given below.

(a) Closed Form Solution

A closed form solution is one which defines the deflected shape of a plate by means of a single equation containing a finite number of terms. The accuracy of the solution does not depend upon the number of terms of an infinite series which must be evaluated and in this respect a closed-form solution is an "exact" solution. Solutions of this form have been found for only a few isolated cases. For example Timoshenko (23) gives closed-form solutions for uniformly loaded circular plates on nondeflecting supports.

(b) Series Solutions

Many of the earlier solutions to Eq. 3.1 for the case of rectangular plates on nondeflecting supports were in the form of double Fourier series. An example of a series of this type is given by the expression

$$w = \frac{qC_1}{D} \sum_{m=1,2..}^{\infty} \sum_{n=1,2..}^{\infty} A_{mn} \sin \frac{m\pi x}{a} \sin \frac{n\pi y}{b} \quad (3.2)$$

where a and b are the spans in the two orthogonal directions,

x and y are distances measured along the a and b spans,

C_1 is a constant which is a function of the spans,

m and n are positive integers, and

A_{mn} is a function of the load distribution, spans, and boundary conditions.

The first known solution to Eq. 3.1, which was developed by Navier in 1820 for

the case of a simply supported plate, utilized an infinite series similar to Eq. 3.2.

A second type of series solution, which is applicable to the case of a rectangular panel having two opposite edges simply supported and the other two edges supported in any manner, was developed by M. Levy in 1899. Levy suggested taking the solution to Eq. 3.1 in the form of a series

$$w = \sum_{m=1,2,\dots}^{\infty} Y_m \sin \frac{m\pi x}{a} \quad (3.3)$$

where Y_m is a function of y only,
 a is the span between simply supported edges, and
 m is a positive integer.

The expressions defining the deflected surface of the plate which result from the use of Eq. 3.3 contain a number of hyperbolic terms which are functions of m and y only. Each term is modified by a constant which is a function of m , the boundary conditions, and the type and extent of the loading.

The Levy method has recently been extended by S. J. Fuchs (24) to include the case of plates supported on all edges by beams having any values of torsional and flexural rigidity.

A series solution for the deflected shape of a plate is exact to the extent that the deflection or moment at any point on a plate may be determined to any desired number of significant figures by evaluating additional terms of the infinite series. Usually it is necessary to evaluate only the first few terms of the series to obtain sufficient accuracy.

(c) Energy Methods

A second procedure incorporating an infinite series has been developed on the concept that when a loaded plate is in a state of equilibrium

with the applied loads the total energy of the system is at a minimum. In applying the method the deflected shape of a plate is assumed to be defined by a function or functions which must satisfy only the geometrical boundary conditions. The deflected shape may be assumed to be defined by a series in the form

$$w = a_1 f_1(x,y) + a_2 f_2(x,y) + \dots a_n f_n(x,y) \quad (3.4)$$

where $a_1 \dots a_n$ are arbitrary constants, and $f_1(x,y) \dots f_n(x,y)$ are functions of x and y which satisfy the geometrical boundary conditions.

The total energy I of the system is the strain energy V of the plate and the change in potential energy U of the loads caused by the deflections. Setting the partial derivative of I with respect to successive values of $a_1 \dots a_n$ equal to zero leads to a series of equations from which the values of the constants $a_1 \dots a_n$ may be evaluated. Ordinarily only the first few terms of the series represented by Eq. 3.4 need be evaluated to have sufficient accuracy.

A second type of function which may be assumed as representing the deflected surface of the plate is the S-function (25). This function has the form

$$S_m(\xi) = \frac{4m+1}{2m!} \frac{d^{2m-2}}{d\xi^{2m-2}} \left[\xi^{2m} (1-\xi)^{2m} \right] \quad (3.5)$$

where $\xi = \frac{x}{a}$, a dimensionless parameter,
 $m =$ any positive integer, and
 $a =$ the span in the x direction.

S-functions were used by Sutherland, et al, (26) in an investigation of uniformly loaded plates supported on flexible beams. The beams were assumed

to have no width and the plates were assumed to undergo no edge rotation. The final deflection function derived by Sutherland was given as

$$\frac{w}{qa^4D} = \sum_m \sum_n \alpha_{mn} S_m(\xi) S_n(\eta) + \sum_m \beta_m S_m(\xi) + \sum_n \gamma_n S_n(\eta) \quad (3.6)$$

where α_{mn} , β_m , and γ_n were coefficients found in the same manner as the coefficients $a_1 \dots a_n$ in Eq. 3.4,

$\eta = \frac{y}{b}$, a dimensionless parameter,

n = any positive integer, and

b = the span in the y direction.

The second and third terms in Eq. 3.6 represent the supporting beams in the x and y directions, respectively.

Deflection coefficients obtained by various investigators are given in Tables 4 and 5 for a number of cases of uniformly loaded rectangular plates. Included are cases of plates on nondeflecting supports and plates supported at all four edges by flexible beams. Deflections are given as coefficients of $(q/D) (\text{span})^4$ where q is the unit intensity of the uniformly distributed load and D is the unit plate rigidity. The span to be considered is the shorter span S for plates on nondeflecting supports and the longer span L for plates on flexible supports. The coefficients are presented in this form because as the aspect ratio S/L approaches zero the deflection coefficient for a plate on nondeflecting supports approaches that of a beam having similar end conditions and spanning in the short direction, while the deflection coefficient of a plate on flexible supports approaches that of a beam spanning in the long direction.

(d) Finite Difference Method

The method of determining deflections by means of using the method of finite differences is based on satisfying the conditions of equilibrium and

continuity only at discrete points on the plate considered. The procedure followed in applying the method consists of generating N simultaneous equations by applying the appropriate finite difference pattern or operator to N node or pivotal points on the plate. The N unknowns are the deflections at the N points. The necessity of using a high-speed electronic digital computer for the solving of the large number of simultaneous equations, which must be generated for solution of all but simple problems, is the major limitation on the method. The finite difference method may be used in the solution of problems which cannot be solved by other methods.

Finite difference operators may be derived directly from the governing differential equation (Eq. 3.1) or from a physical analog of the plate or structure under consideration. The use of the analog allows a consideration of the effects of beam and column stiffnesses to be made. The accuracy of the method may be improved by reducing the grid spacing between node points.

(e) Moment-Distribution Methods

In addition to the methods discussed above two procedures have been developed which utilize a form of moment distribution for plates analogous to the Cross moment-distribution process for the analysis of frames.

In a method developed by Ang (27) the stiffness and carry-over factors for unit deflections and rotations for a number of points along each edge of each panel of the structure under consideration are determined using finite difference solutions. In addition, fixed-end moments and reactions for nondeflecting supports are determined. The procedure of unlocking a joint at a node point, balancing the moments, performing carry-overs and relocking the joint that is used with this method is similar to that used with frames except that the carry-overs are made only to adjacent node points. The procedure

requires the use of a high-speed electronic computer. Deflections for a nine-panel structure found using this method are given in Table 6.

A similar procedure developed by Ewell, et al, (28) consists of dividing each panel into a gridwork of intersecting beams having flexural and torsional stiffness. After distribution factors have been determined, each joint in turn is displaced, the resulting fixed-end moments determined, and moments distributed as above.

3.2 Factors Affecting Deflections of Elastic Structures

The factors affecting the deflection of a point on a panel in a continuous structure are the sizes and stiffnesses of the supporting beams and columns, the size and shape of the panel, and the type and extent of the applied loading. The effects of these factors are discussed in detail below.

(a) Beam Flexural Rigidity

In discussing the effects of beam flexibility on deflections of symmetrical rectangular panels it is more convenient to deal with dimensionless ratios of beam-to-plate rigidity than with absolute values of beam rigidity. These ratios may be expressed as

$$H_L = \frac{(EI)_L}{DS} \quad \text{and} \quad H_S = \frac{(EI)_S}{DL} \quad (3.7)$$

or as

$$\lambda_L = \frac{(EI)_L}{DL} \quad \text{and} \quad \lambda_S = \frac{(EI)_S}{DS} \quad (3.8)$$

where L = span in longer direction,

S = span in shorter direction, and

I_L, I_S = moments of inertia of beams in long and short directions, respectively.

The product EI is termed the flexural rigidity of the beam.

The use of either the H or the λ definition is valid. The ratio λ relates the rigidity of the beam to the plate rigidity in the same direction. Hence the use of one particular value of λ_L in the analyses of a number of plates having different aspect (S/L) ratios would mean that the beams in the long direction for each case would have the same absolute value of $(EI)_L$. The term H relates the beam rigidity to the total plate rigidity in the span perpendicular to the beam considered. This in effect relates the beam to the portion of the plate acting as a beam in the same direction. The ratio H is used throughout the remainder of this report.

As may be expected, the effect of increasing H is to decrease deflection. This is shown graphically in Figs. 3.1 through 3.5 which are plots of mid-panel or mid-beam deflection^{*} versus H_L for various aspect ratios and column sizes. The term c/L appearing in these figures is defined in 3.2b below. The type of plate considered in Figs. 3.1 through 3.5, and in the following discussion on the effects of column size, is one which is part of an infinite array of identical plates, all uniformly loaded and supported on flexible beams. The relationship between H_L and H_S is defined as $H_S = R^2 H_L$ where R is the aspect ratio S/L . This corresponds to a ratio of I_S/I_L equal to R .

For each of the curves shown there is a large decrease in deflection as H_L increases from zero to one and a lesser decrease with further increase in H_L . For example, the mid-panel deflection of a square plate is less than half as great for $H = 1.0$ as it is for $H = 0$, but the deflection for $H = 4.0$ is still about three-fourths as large as for $H = 1.0$.

A comparison of Figs. 3.1 and 3.2 shows that the mid-panel deflection for a square plate on flexible supports is about equal to the mid-beam

* The term "mid-beam deflection" will be used throughout the report to denote the deflection at the middle of a center line connecting two columns.

deflection plus a constant amount. This constant amount is nearly the deflection of a square clamped plate on nondeflecting supports. For other than square panels the mid-panel deflection is given closely by the sum of (a) the deflection at the center of a long beam and (b) the mid-panel deflection of a rigidly supported plate having the same shape and carrying the same loading as the panel under consideration. In short, if the longer edges of a rectangular plate are deflected by some amount the center of the plate tends to deflect by the same amount.

(b) Column Size

Relatively little study has been made in the past concerning the effects of finite column size (or size of support area) on deflections and moments. In order to study these effects the method of finite differences was used to find solutions for several cases of typical interior plates supported on flexible beams and nondeflecting columns. The beams were assumed to have no width and the neutral axes of the beams were assumed to coincide with the neutral surface of the plate. This latter assumption was necessary in order to preclude T-beam action.

The columns were taken as square for all aspect ratios. The relationship between the size of the column and the plate was defined by the ratio of width of column to long span or the ratio c/L . In addition to deflections, bending moments were obtained at each of the node points in the two orthogonal directions defined by the two spans. Mid-panel and mid-beam deflections and bending moments for selected points are given for a number of cases in Tables 7 through 15. The layout of a typical interior panel and the locations of the points for which moments are given are shown in Fig. 3.6. A description of the computer program is given in Appendix B.

The curves depicted in Figs. 3.1 through 3.5 show that the effect of increasing column size is, as would be expected, to decrease deflection. Figures 3.7 through 3.10 are plots of mid-panel and mid-beam deflections versus the ratio c/L for the different values of H and R considered. These curves show that the reduction in deflection was nearly a linear function of the increase in column size or the ratio c/L . The decrease in deflection accompanying increased column size is of course the result of the decreased spans of the supporting beams and the reduction of the total load to be carried by the plate. Figure 3.11 is a plot of mid-panel deflections versus the aspect ratio.

If it is desired to use the tabulated deflection coefficients to determine the deflection coefficient for an interior plate supported on other than square columns it is suggested that the actual columns be replaced by square columns having the same area in cross section. Entering the appropriate table with the ratio of c/L for the equivalent columns and interpolating linearly between the tabulated deflection coefficients will give a value sufficiently accurate for use.

(d) Column Stiffness

The only available extensive investigation of the effects of column stiffness on deflections and moments in continuous structures was performed by Simmonds (9) using the method of finite differences. This investigation was limited to analyses of a number of "mathematical models" of symmetrical elastic structures. The model structure considered contained nine square panels arranged three-by-three. The panels were supported on beams having both flexural and torsional rigidity and on inextensible columns having flexural stiffness. The beams were assumed to have no width and the ratio c/L was zero. A square grid having a spacing of $h = L/8$ was used.

The column stiffness was related to the unit plate rigidity by the dimensionless parameter

$$K = \frac{\sum 4(EI)_{col}/L_{col}}{D} \quad (3.9)$$

where $\sum 4(EI)_{col}/L_{col}$ was the total flexural stiffness of the column. The beam torsional rigidity was related to the plate rigidity by the dimensionless parameter

$$J = \frac{GC}{DL} \quad (3.10)$$

where G = shear modulus of elasticity = $E/2(1+\mu)$,

C = a measure of the torsional rigidity of the beam cross section, and

L = span of square panel.

The ratio of beam to plate flexural rigidities was defined by $H = EI/DL$.

Due to the limitations imposed by the capacity of the computer used it was necessary to define the values of H , J , and K for the exterior beams and columns as constant functions of the corresponding values for the interior members. H and J for the edge beams were taken as five-eighths of the value of H and J for the interior beams. K for the corner columns was taken as twenty percent of K for the interior column. For an edge column K for bending about an axis perpendicular to the discontinuous edge was seventy percent of K for the interior column and K for bending about an axis parallel to the edge was thirty percent that of K for the interior column. These proportions were similar to those for the two-way slab test structures tested during other phases of the floor-slab investigation. In further discussion the values of H , J , and K referred to are those for the interior columns and beams.

Solutions were determined for the case of a uniform load on all nine panels for values of H and J of 0.25, 1.0, and 2.5 and for values of K of

0, 10, 30, 90, and ∞ . Tabulated values of deflections for seven points on the structures are given in Table 16. Solutions were also obtained for a limited range of parameters for a pattern loading with the interior and the corner panels loaded. Deflections for this case are given in Table 17. Points No. 1, 3 and 6 in Tables 16 and 17 represent the centers of the interior, edge and corner panels, respectively. The remaining points are located on the beams midway between columns. The maximum deflections in the edge and corner panels were only a few percent greater than the mid-panel deflections given and occurred close to the mid-panel points.

The effects of column stiffness and beam torsional stiffness were most pronounced on the corner panel deflections. An increase in the column stiffness or beam torsional stiffness reduced the deflections in a corner panel and increased the deflections in the interior panel, but by a smaller amount. The limiting case would occur for $J = K = \infty$. For this case the action of each panel would be identical.

For values of K other than zero, the mid-panel and mid-beam deflections for the interior panel, for all panels loaded, are given approximately by the coefficients tabulated in Table 10. For example, for $H = 0.25$ the deflection coefficient for the center of the interior panel (Δ_1) ranged from 0.00385 for $J = 0.25$ and $K = 10$ to 0.00463 for $J = 2.5$ and $K = \infty$. The mid-panel coefficient for a typical square interior panel for $H = 0.25$ is 0.00415.

(e) Partial Loadings

The arrangement of the loading on a structure has a large effect on the ways in which the structural elements participate in carrying the load. Consider the nine-panel structures discussed in Section 3(d) above. Loading all nine panels caused relatively little rotation of the interior beams and

hence the torsional resistance to rotation of the interior beams and the flexural stiffnesses of the interior columns had little effect on deflections. However, for the checkerboard loading* a much larger rotation of the interior beams and columns occurred, thus increasing the torsional moments in the interior beams and the bending moments in the interior columns.

The changes in rotation of the beams and columns occurring for CB loading had the effect of increasing the deflections of the loaded panels. The magnitude of this increase was a function of the resistance to rotation afforded by the beams and columns. However, the increase in deflections of the loaded panels was in large part offset by the reduction in deflections of the beams adjacent to unloaded panels. With only the interior and corner panels loaded, the interior beams were required to carry only about half as much load as when all panels were loaded. The reduced beam deflections in turn reduced the deflections of the loaded panels thus effectively canceling the increase in deflections due to beam and column rotations.

The deflections at the center of the loaded interior panel (Δ_1 in Table 17) did not vary by more than 14 percent from the deflections for all panels loaded. For $K = 0$ the value of Δ_1 for CB loading was 5 percent greater for flexible beams ($H = J = 0.25$) and 14 percent greater for stiff beams ($H = J = 2.5$), but for $K = \infty$ the deflection at this point was 12 percent less for flexible beams and 4 percent less for stiff beams compared to all panels loaded. The deflections at the center of the loaded corner panel (Δ_6) were slightly less in all cases for CB loading than for all panels loaded. For flexible beams the difference was about 5 percent and for stiff beams it was about 2 percent.

* To be referred to as a "CB loading."

Pattern loadings have a greater effect on moments than on deflections. For a corner panel the mid-panel deflection was less for the CB loading than for all panels loaded but the corresponding moments were a small amount greater. For the interior panel the CB loading caused a mid-panel moment which was as much as 50 percent greater than the moment for all panels loaded. The 50 percent increase was for $K = 0$ and $H = J = 0.25$. For $H = J = 2.5$ and $K = \infty$ the increase was 5 percent although for this case the deflection for CB loading was 4 percent less than for all panels loaded.

Two different types of patterns of partial loadings may be considered in analyses for maximum moments and deflections. For structures containing stiff beams, various forms of checkerboard loadings may be expected to cause maximum deflections and moments, although as shown above this may not always be true for deflections. For structures containing no beams or beams of low stiffness various arrangements of strip loadings cause maximum moments and may cause maximum deflections.

For a continuous array of square plates for which $H = 0$ and $c/L = 0.2$ the deflection at the center of a loaded panel is $0.00289 qL^4/D$ for all panels loaded. With every other row of panels loaded the deflection coefficient at the center of a loaded panel is 0.00292 which represents an increase of one percent. The deflection on a line mid-way between column centers is $0.00173 qL^4/D$ for all panels loaded. For the strip loading this deflection is reduced by one-half for the point between a loaded and an unloaded strip, while for the point between loaded panels it is increased by six percent to $0.00184 qL^4/D$. While the strip loading causes a negligible increase in deflections it has a much larger effect on moments. The mid-panel moment for all panels loaded is $0.0224 qL^2$ while for strip loading the mid-panel moment

in a direction perpendicular to the centerline of a loaded strip is $0.0278 qL^2$ which is an increase of 24 percent.

Deflection coefficients are given in Table 6 for a nine-panel structure arranged three-by-three for which $H = 0$, $c/L = 0.1$ and $K = \infty$. The mid-panel deflection for the corner panel was about two percent greater for the edge row of panels loaded than for all panels loaded. Loading a center row of panels caused a deflection at the center of the interior panel which was about four percent larger than for all panels loaded.

3.3 Approximate Methods of Analyses for Deflections

The complexity of the theoretical methods of analyses of plates has led various investigators to attempt to formulate simple methods of analyses. The basic assumption upon which the majority of these methods have been based is that the action of a plate may be taken as similar to that of a gridwork of intersecting or crossing beams, hence the term "crossing-beam analogy."

One of the first appearances of the crossing-beam analogy was in an early text (1904) on reinforced concrete design by Marsh (29). Marsh suggested replacing a uniformly loaded plate by a grid of uniformly loaded beams. From the condition that the deflections of the long and short beams must be equal at mid-panel, the load distribution factor defining the proportion of the uniformly distributed load q to be carried in the short direction was found to be

$$r_s = \frac{L^4}{S^4 + L^4} \quad (3.11)$$

where L was the longer and S the shorter span of the plate considered. The remaining load of $(1 - r_s) q$ was then assigned to the beams spanning in the longer direction.

Since the crossing-beam analogy neglected the presence of twisting moments in the plate the use of Eq. 3.11 was a gross over-simplification and led to large errors. The early investigators were primarily interested in moments rather than deflections. However, it is of interest to note that the use of Eq. 3.11 for uniformly loaded rectangular plates, rigidly clamped on all edges, gives values of deflections which are close to those found by "exact" theory.

Recognizing that the use of Eq. 3.11 neglected the effect of twisting moments Marcus (30) developed a procedure incorporating a modified crossing-beam approach. The relationships developed for moments and deflections contained a modifying factor which was a function of the number of clamped edges and the aspect ratio. As the procedure was only applicable to cases of plates supported on nondeflecting supports, for which theoretical solutions were already available, it was of little value.

The deflection at the center of a uniformly-loaded typical interior plate for which $H = c/L = 0$ may be estimated by taking a beam of unit width having a span equal in length to the diagonal dimension of the plate (31). The beam is assumed to have fixed ends and a loading equal to that on the plate.

Since the presence of flexible beams and columns in a structure has a large effect on deflections and the distribution of moments a reasonable method of analysis for moments or deflections cannot be developed on the bases of solutions for plates on rigid supports. An approximate method of analysis for deflections in continuous structures which does take into account the flexibilities of the supporting beams and columns is presented in the next chapter.

4. FRAME ANALYSIS

4.1 Introductory Remarks

This chapter describes the development of a two-dimensional analysis for deflections of floor slabs. The two-dimensional analysis is based on three-dimensional analyses of structures having uniformly loaded rectangular panels supported at all corners. Although the basic development of the method refers to a linearly elastic structure, the effects of cracking, yielding, and time-dependent deformations may be taken into account. These factors are considered in Chapter 5.

The terms "structure," "slab" and "floor slab" are used interchangeably. All terms refer to a three-dimensional structure containing beams, plates, and columns. Each floor of the structure is assumed to be at a single level. The columns are assumed to be inextensible but to have a finite flexural stiffness. Hence, the term "deflection" refers to the movement of a portion of the structure parallel to the axis of the columns. Unless noted otherwise, the datum plane for deflections is the unloaded position of the structure.

The frame analysis method is based upon a concept of the way in which a multiple-panel continuous slab deflects. Figure 4.1 represents a portion of such a structure showing the deformed shape that the structure would assume under uniform load. Consideration of the bending moments in a given span of the slab leads to the conclusion that there are lines of contraflexure in the slab analogous to the points of contraflexure in a continuous beam. The lines of contraflexure deviate slightly from a straight line, the deviation depending on the size and stiffness of the beams and columns.

However, plate solutions for interior panels indicate that lines of contraflexure in a given span are located approximately two-tenths of the span considered from each of the supporting beams. Thus, for the panel shown in Fig. 4.1, the lines of contraflexure in the spans S and L may be considered with little error to be located as shown by the broken lines.

For the purpose of making a frame analysis, the real structure is assumed to be replaced by a "physical analog" consisting of beam and plate elements, these elements being delimited by the lines of contraflexure. Thus, in Fig. 4.1 the two beam elements in the long direction are shown shaded. Only one-half of the beam elements in the short direction are shown. The plate element is the portion of the panel bordered by the four beam elements.

The division of the structure into elements allows the deflection at the center of a panel to be computed as the sum of the deflections of the constituent elements. A beam element tends to form an anticlastic or saddle-shaped surface when deformed. Hence, the deflection at the center of the beam on a line between column centers is less than the deflection at the free edge of the beam at the same distance from column centers. The total deflection at the center of the symmetrical panel would then be the sum of (a) the deflection at the center of the beam in respect to its supporting columns (Δ_a in Fig. 4.1), (b) the deflection at the edge of the beam in respect to its center (Δ_b), and (c) the additional deflection of the plate element (Δ_c).

The frame analysis described in the following sections leads directly only to the deflections at the centers of the beam elements (Δ_a in Fig. 4.1). A second procedure is described by which the additional deflections (Δ_b and Δ_c) may be found.

The computations involved in making a frame analysis for deflections may be divided into four phases as follows:

1. A portion of the three-dimensional structure is selected for use in a two-dimensional analysis. In further discussion this portion is termed the "ersatz frame."
2. The stiffness parameters to be used in the analysis, which are functions of the flexural and torsional rigidities of the constituent parts of the ersatz frame, are computed.
3. The loading to be applied to the ersatz frame is determined.
4. An analysis of the frame for moments, slopes, and deflections is made using conventional methods.

The procedure outlined above gives the elastic deflections of points on the ersatz frame. The deflection at the center of a panel with respect to its supporting beams is given by a second procedure which is referred to as the S-method. This method is described in Section 4.2. The method of determining the load to be applied to the ersatz frame is discussed in 4.3 and the details of the frame analysis are described in 4.4. The application of the method to elastic structures is considered in 4.5. Discussion of time-dependent strains, cracking of the concrete and yielding of the reinforcement is deferred to Chapter 5.

4.2 Approximate Solution for the Mid-Panel Deflection of a Clamped Plate on Rigid Supports

The frame analysis method for deflections gives directly only the deflections at the centers of the spans between the columns. To determine the deflection at the center of a given panel with respect to its supporting beams it is necessary to add to the deflections of the supporting beams an additional quantity. For a typical interior panel this additional quantity is approximately the deflection that would be obtained for a plate with all four edges clamped and having the same size and loading as the panel of the floor slab

under consideration. For other than an interior panel this additional quantity is about what would be obtained for a clamped plate subjected to some edge rotation.

In view of this, it is necessary to have at hand some approximate procedure with which to compute the deflections of clamped plates which will allow edge rotations to be taken into account. Such a procedure is outlined below and is termed the S-method.

Consider a fixed-ended beam carrying a uniformly distributed load. The beam mid-span deflection may be readily determined using conventional methods considering the entire beam. The mid-span deflection may also be determined by assuming that the beam acts as a "structure" consisting of two cantilever beams, each extending from its fixed support to a point of contraflexure, and a simply supported beam spanning between points of contraflexure. Each beam would have acting on it the uniformly distributed load and in addition each cantilever would have acting at its free end the reaction from the simply supported span. The deflection at the center of the "structure" may then be obtained by summing the deflections of the constituent parts. Since it is necessary to know the locations of the points of contraflexure the S-method affords no savings of labor in beam analysis. However, the same approach may be applied to the analysis of a clamped plate and the resulting method will permit the approximate analysis of clamped plates subjected to some edge rotation.

The method as applied to a clamped plate differs from the method as applied to a fixed beam in that the points of contraflexure in the fixed beam becomes lines of contraflexure in the clamped plate and the simply supported span in the beam becomes a simply supported plate within the clamped plate. For a square clamped plate the distance from the center of an edge to a line

of contraflexure for moments in a given span is slightly greater than twenty percent of the span. For other than square clamped plates a study of the moments obtained for typical interior panels, as discussed in Chapter 3 and Appendix B, show that this is still nearly the case.

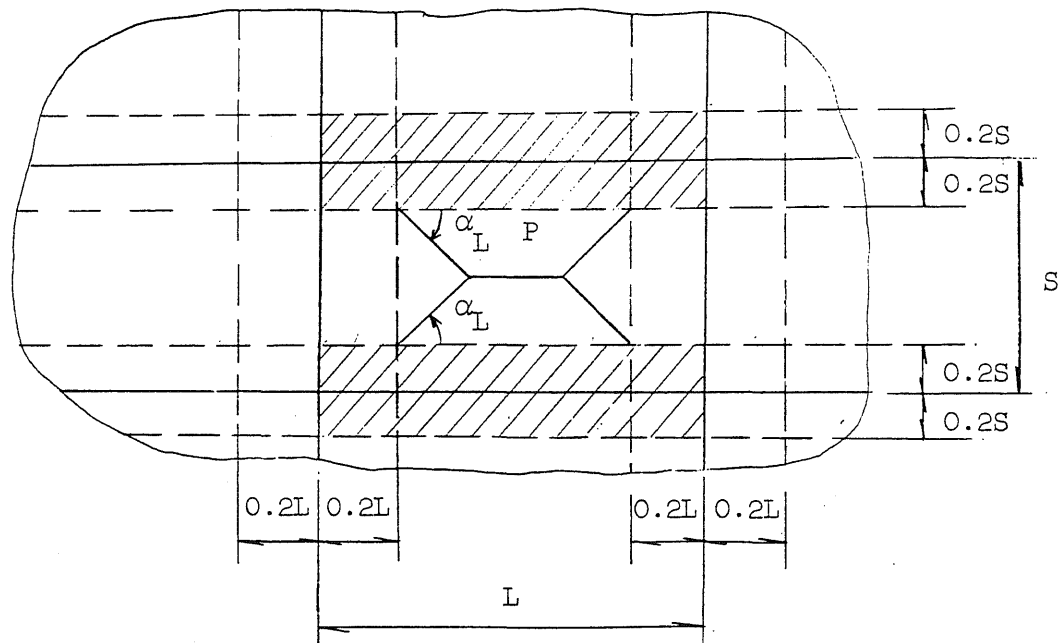
The deflection at the center of the square clamped plate may be determined by computing the deflection of a cantilever "stub" beam extending from the center of an edge and having a length equal to one-fifth the span, and adding to this deflection that of a simply supported square plate having a span equal to three-fifths that of the clamped plate. The deflection of the cantilever "stub" beam is computed assuming it to have a unit width and a loading consisting of a uniform loading over its length and a concentrated load at its free end. The area assumed to contribute to the concentrated load has unit width and extends from the end of the "stub" to the center of the plate.

The deflection at the center of a square, uniformly loaded, clamped plate on rigid supports is $0.001265 \, qL^4/D$. The deflection computed using the S-method is $0.00153 \, qL^4/D$ which is 21 percent greater than the correct value. This error is on the conservative side and is largest for a square panel. As the aspect ratio decreases from one to zero, the deflection coefficient approaches that of a fixed beam. The effect of a known edge rotation of the plate may be taken into account by assuming that the rotation is applied to the supported end of the cantilever "stub" and then proceeding through the S-method for clamped plates as described above.

4.3. Effects of Stiffness Parameters and Aspect Ratio on Frame Loading

As pointed out in previous discussion, the deflection at the center of an interior panel supported on flexible beams may be determined approximately

by adding to the beam mid-span deflection that quantity given by the S-method. The difficulty in determining, by an approximate method, the mid-panel deflection of a plate supported on flexible beams lies in computing the beam mid-span deflection. The beam mid-span deflection may be computed in the following manner. Consider an infinite array of uniformly loaded, similar panels, supported on flexible beams. A portion of this array would appear as shown in Sketch A.



SKETCH A

The lines of contraflexure are assumed to be located as shown by the broken lines in Sketch A. The deflections of the beams spanning in the long direction have a greater effect on the mid-panel deflection than do the deflections of the short beams. Hence in making a frame analysis, the ersatz frame to be considered for a structure having finite dimensions, or the ersatz beam to be considered when dealing with an infinite array of panels would

consist of that portion of the slab containing the beam (if any) in the long direction and lying between lines of contraflexure. Thus for panel P in Sketch A the two areas shown hatched would constitute the ersatz beams.

The load assigned to each of these ersatz beams includes the load within the confines of the hatched area plus a portion of the load on the segment of the panel lying between ersatz beams. This segment of the panel represents the simply supported plate discussed in the description of the S-method. The additional load carried by the ersatz beam may be considered as the reaction of this simply supported plate.

The additional portion of the load to be taken as acting on the ersatz beam is most conveniently defined by the angle α_L where α_L is the angle between the edge of the ersatz beam spanning in the long direction and the border of the area considered as contributing load to the ersatz beam. The angle α_L is shown in Sketch A.

The altitude of the trapezoid or triangle defined by the angle α_L may be less than or equal to, but not more than one-half the distance between edges of opposite ersatz beams.

The factors affecting α_L for a symmetrical interior panel are the aspect ratio, R, of the plate and the ratio of beam to slab rigidities, H. The path by which the load on a plate is transferred to the beams and then to the columns is affected by both H and R. The stiffer the beam supporting a panel the greater is the tendency for the load to travel to the beam and then to the column.

For the practical range of values of H_L and R considered in computing the deflections and moments summarized in Tables 7 - 15, the following expression defines a satisfactory relationship between α_L and the parameters H_L and R.

$$\alpha_L = 45^\circ \left[1 - (1 - R) \frac{(4 - H_L)}{2(1 + H_L)} \right] \quad (4.1)$$

which is valid for $0.5 \leq R \leq 1.0$ and $\frac{1}{H_L} > 0$.

Thus, for a square panel this expression would require that α_L be 45° for all values of H . The values required to fit the data in Table 10 for a square panel range from 41° for $H = 0$ to 47° for $H = 4$. As the deflection is not very sensitive to errors in α , this expression is satisfactory. For R less than one-half the panel may be considered to be acting as a beam in the long direction.

Similarly, the loading to be taken as acting on a beam spanning in the short direction is defined by an angle α_S such that

$$\alpha_S = 90^\circ - \alpha_L \quad (4.2)$$

The expression for α_L given above is strictly applicable only for the relationship between H_L and H_S considered in obtaining Table 10. However, for nonsquare panels the deflection of a beam spanning in the long direction is primarily a function of the rigidity in the long direction and is affected little by the rigidity of the beams in the short direction. This is shown by the similarity of the coefficients given in Tables 7, 10, and 13. Hence, the expressions given above in Eqs. 4.1 and 4.2 may be considered as applicable to most practical cases of nonsquare interior panels, provided that the parallel beams in the long direction have the same flexural rigidity.

For square panels or nearly square panels having beams of unequal rigidities in the different spans the mid-panel deflection may be found approximately by assuming that the α_L function as given in Eq. 4.1 may be used for each span. The average of the ersatz beam deflections thus obtained would be taken as the quantity to use in conjunction with the S-method. However, the beam deflections obtained may be expected to be in error.

The expression for α_L given above was developed upon considerations of the behavior of interior panels. For a real structure containing edge and corner panels the load distribution in a row of panels adjacent to a discontinuous edge would be somewhat different than for an interior row of panels. This difference could be accounted for by reducing the distance between the discontinuous edge and the line of contraflexure or by changing the α_L function. Either the α_L function or the distance between discontinuous edge and line of contraflexure, or both would then have to be functions of the aspect ratio, the stiffness of the beams perpendicular to and parallel with the discontinuous edge, the stiffnesses of the interior and edge columns, and the torsional stiffnesses of the edge beams. The complexity of the function or functions necessary to describe the effects of these variables would preclude their use. Hence in all further discussion the assumption is made that the ersatz frame may be cut from the edge and corner panels just as for the interior panels. It will be shown in Section 4.5 that this assumption leads to some error but that the results obtained compare well with "exact" results.

4.4 Details of Frame Analysis

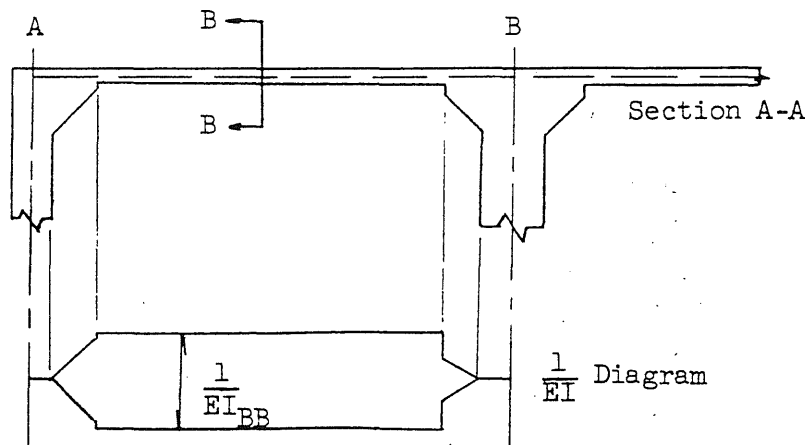
The four basic steps in the method for the frame analysis of a structure for deflections consist of (a) selecting a portion of the structure to act as the ersatz frame, (b) selecting the load to act on this frame, (c) determining the stiffness and carry-over factors for the frame, and (d) performing an analysis for moments, slopes and deflections using conventional means. The details of the method may best be explained by means of an example. Consider the layout of a floor slab as shown in Fig. 4.2. This layout is representative of the structures tested at the University of Illinois during other phases of the floor slab investigation.

The first step in the frame analysis for deflections is to cut an ersatz frame out of the three-dimensional structure. For the structure shown in Fig. 4.2 there are two types of ersatz frames, an interior frame and an edge frame. The portions of the structure to be used in these frames are shown shaded in Fig. 4.2.

The second step is the determination of the loading. Assuming the beams in perpendicular directions to have similar rigidities, the load to be applied to each of the ersatz frames would comprise the load included between the edges of the ersatz frame and the additional load defined by an α_L angle of 45° . The contributing areas defined by $\alpha_L = 45^\circ$ are shown bordered by dotted lines and the edges of the ersatz frames in Fig. 4.2.

The third step is the determination of the stiffness and carry-over factors of the frame for use in the Cross moment-distribution method. These may be computed considering the uncracked sections of the ersatz frame.

Assume that section A-A in Fig. 4.2 has the following cross section.



SKETCH B

An assumption commonly made in structural analysis is that a frame having finite dimensions may be reduced to a "line" structure for purposes of analysis. The "line" representation of Section A-A is shown by broken lines in Sketch B. The horizontal portions of the "line" structure in Sketch B are located at mid-depth of the panel thickness in the case of a flat plate or flat slab. If beams are present the "line" portions are taken as coinciding with the neutral axes of the T-beam portions of the ersatz frame. Studies have shown that the computed stiffnesses of the columns are relatively unaffected by small changes in the location of the horizontal "line" portions.

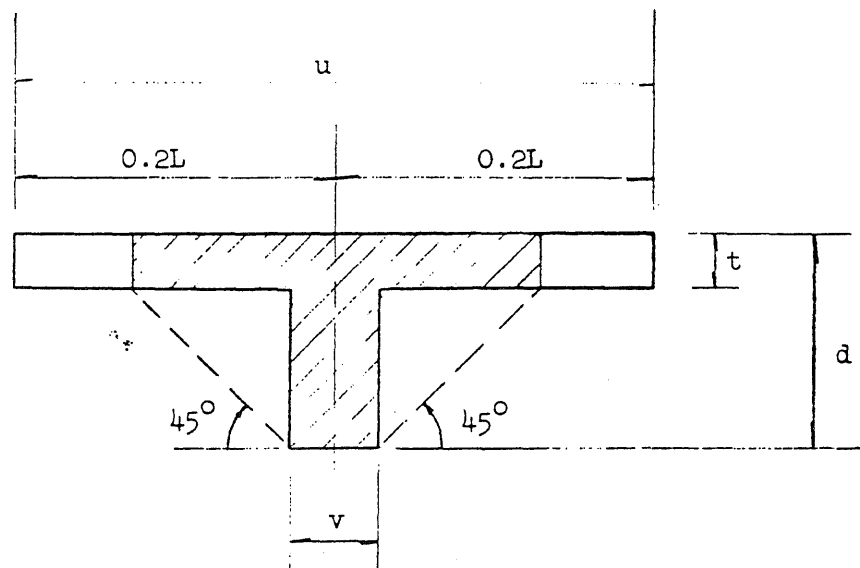
In determining the stiffness parameters for the ersatz frame it is necessary to consider two types of members. The first of these is a flexural element such as the beam spanning between the columns in Sketch B. The second type is a combined torsional-flexural member made up of a column and the beams framing into it from a direction perpendicular to the longitudinal axis of the ersatz frame. The stiffnesses for these two types of members may be determined as follows:

(a) Flexural Members

The stiffnesses and carry-over factors for the beam portions of the ersatz frame may be determined using conventional methods such as the column analogy. In using the column analogy method it is necessary to construct a $1/EI$ diagram for the member under consideration. The $1/EI$ diagram for the beam AB shown in Sketch B has been drawn directly beneath the beam. In preparing this diagram it was assumed that the portion of the structure between the face of the column and the column center line could be treated as rigid. Hence the $1/EI$ diagram for this portion of the diagram is a line. It is sufficiently accurate to assume a linear variation in the $1/EI$ diagram between

the face of a column and the edge of a column capital. The uncracked moment of inertia of a section is computed about its own centroid.

If, for the Section A-A shown in Sketch B, a cross section through the center of the ersatz beam were rectangular in form then the value of H would evidently be zero and the question of T-beam action could be neglected. However, if the ersatz beam included both slab and beam it would be necessary to consider the question of T-beam action in order both to compute the value of H and to compute the composite value of the moment of inertia for the ersatz beam. Assume that the Section B-B in Sketch B has the cross section shown in Sketch C.



SKETCH C

The amount of slab that acts with the beam to form a T-beam is difficult to assess. A greater amount of the slab may be expected to participate in T-beam action in the positive moment region of the slab than in the negative moment region, and the amount of slab participation varies with the amount of cracking that takes place. A number of studies have been made in attempts to determine how much T-beam action occurs and most building codes contain provisions for defining the amount of slab to be assumed as acting

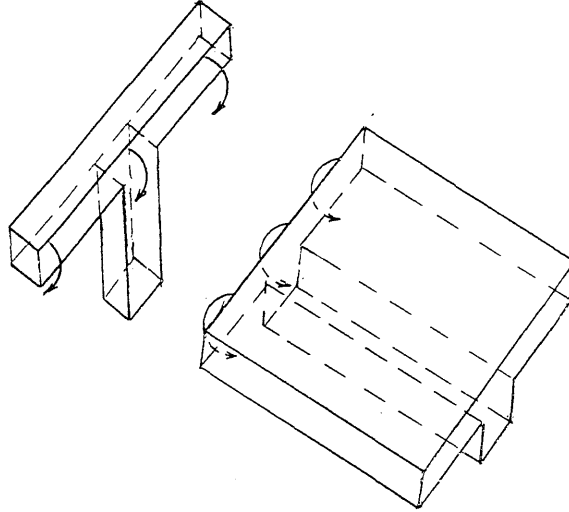
as the flanges of a T-beam (32,33). However, the problem is still undefined and it appears satisfactory to assume an amount of slab to be acting with the beam as would be defined by a line drawn from the bottom of the beam to the bottom of the slab and at the angle of 45° with the vertical face of the beam web. Following this suggestion the T-beam for the section shown in Sketch C is as shown by the hatched area. The value of H would then be computed as the ratio of the moment of inertia of the T-beam to the sum of the moments of inertia of the portions of the adjacent panels lying between the edges of the T-beam and the centers of the panels. The composite value of the moment of inertia of the ersatz beam would be the sum of the value for the T-beam and the values of the portions of the slab lying between the edges of the T-beam and the edges of the ersatz frame, the value for each section being computed about its own centroid.

For the case of a concrete slab supported on steel beams the rigidity of the steel beam alone would be used in analysis if there were little or no provision for transfer of shear between the lower surface of the slab and the upper flanges of the steel beam. If shear connectors were adequate a portion of the slab as defined above could be considered as acting with the steel beam. In either case the tributary area for purposes of determining the load to be carried by the beam would be as previously defined.

(b) Flexural-Torsional Members

At the junction of the ersatz beam in an ersatz frame with an end column there is a transfer of bending moment from ersatz beam to column. Some of this moment is transferred directly from ersatz beam to column and some is transferred from ersatz beam to the spandrel beam lying perpendicular to the longitudinal axis of the ersatz beam and thence is carried to the column by twisting moments in the edge beam. This action is shown in the "exploded" view

of a beam-column connection (Sketch D). At an interior column the difference in end moments between the adjacent ersatz beams is transferred to the column in a similar fashion.



SKETCH D

The action of the edge beam in assisting in the transfer of bending moment between column and ersatz beam has the effect of "softening" the beam-column connection. Hence it is necessary to compute the stiffness of the combined column-edge beam combination. This combined stiffness is a function of the flexural stiffness of the column and the torsional stiffnesses of the beams framing into either side of the column.

The combined stiffness of the beam-column combination may be found assuming the beam and the column to act essentially as two springs in series. The combined stiffness may be defined by the expression

$$K_{bc} = \frac{m_c}{\theta_t + \theta_f} \quad (4.3)$$

where K_{bc} is the stiffness of the beam-column combination, m_c is the moment acting on the column, θ_f is the rotation at the near end of the column caused

by m_c , and θ_t is the average rotation of the beam with respect to the column. The term θ_f may be found by conventional methods assuming the far ends of the column to be fixed. Expression 4.1 and the following procedure for determining θ_t were developed by Corley (34).

In developing a method for computing θ_t it is necessary to make certain simplifying assumptions. It is assumed that a unit twisting moment is applied along the length of the beams framing into the column under consideration. This unit twisting moment causes a unit rotation to occur at each point of the beam as shown in Fig. 4.3. The angle θ_t , as defined by Corley, was one-half the area under the unit rotation diagram between the edge of the column and the center of a beam framing into the column. Since in the procedure for frame analysis for deflections the ersatz frame is taken as including only one-fifth the width of the panel lying on either side of the center line of the frame, rather than one-half of each panel as in Corley's procedure, only the portion of the unit rotation diagram lying between the edges of the ersatz frame is considered in computing θ_t . Hence for a value of $\Phi_{\max} = \frac{(1 - c/L)}{2GC}$ the value of θ_t would be

$$\theta_t = \frac{L[0.64 - 2.0(c/L) + (c/L)^2]}{16GC} \quad (4.4)$$

In expression 4.3 the term G represents the modulus of elasticity in shear. The modulus of elasticity in shear is related to the modulus of elasticity E by the expression $G = E/2(1+u)$ where u is Poisson's ratio. It is sufficiently accurate to neglect u and to take G as $E/2$ in Eq. 4.4.

The term C in expression 4.3 is a measure of the torsional rigidity of the cross section of the beam. For a rectangular section Timoshenko (35) has developed the following expression for C :

$$C = \beta d_1 t_1^3 \quad (4.5)$$

where d_1 is the larger and t_1 the smaller dimension of the cross section and β is a factor which is a function of the ratio of t_1 to d_1 . For very small ratios of t_1/d_1 (0.1 or less) β is $1/3$. For the range of t_1/d_1 ratios commonly used for reinforced concrete beams β may be taken as $1/3(1 - 0.630t_1/d_1)$. The value of β as a function of the t_1/d_1 ratio is shown graphically in Fig. 4.4.

The value of C for a T-beam is given by Nylander (36) as

$$C_T = C_R + (t^3)(0.33u - 0.17v - 0.21t) \quad (4.6)$$

where C_T is the torsional constant for the T-beam, C_R is the torsional constant for the rectangular beam, and the other terms are the dimensions as shown in Sketch C.

Rather than use expression 4.6 in determining the total value of C for a T-beam it is sufficiently accurate to sum the values of C computed for each of the rectangular elements forming the T-beam. These elements are the stem, having a depth equal to the total depth of the T-beam, and the flange or flanges. Hence the final value of C for the T-beam would be

$$C = \sum \beta d_1 t_1^3 \quad (4.7)$$

If the values of θ_t computed for each of the beams framing into a column are different than the average of the two values may be used in expression 4.3.

If no edge or interior beams are present in the slab then a strip of slab equal in width to the width of the column may be considered as acting as beams for the purpose of computing θ_t .

After the stiffnesses have been found, bending moments, slopes, and deflections may be computed by conventional means. The rotation of a column may be computed by dividing the column moment by the column stiffness.

Assuming the slope caused by the column rotation remains constant from the

center of the column to its faces or the junctures of the column capital (if any) with the slab, it may be seen that the column rotation has the effect of imparting an end deflection and rotation to either beam element framing into the column. The effects of these initial displacements on the beam mid-span deflection may be found using ordinary procedures.

The additional deflection of the beam caused by the loads on the beam may be found assuming the beam to act as a prismatic member with a span equal to the clear distance between column faces or, if column capitals are present, to the distance between the points at which the capitals intersect the lower surface of the slab. The load on a beam includes a uniformly distributed load and a load having a trapezoidal or triangular distribution. Formulae for deflections for this latter type of loading are given in Table 18. The formulae given in Table 18 are for a beam having a load placed symmetrically about the mid-point of the span. For a beam having a loading that is not quite symmetrical about mid-span the formulae may be used by substituting into the formulae the smaller of the values of aL computed for the beam under consideration.

Once the beam mid-span deflections have been determined the frame analysis is completed. The mid-panel deflections may next be obtained using the S-method. Consider the nine-panel structure shown in Fig. 4.2. For the symmetrical structure shown there are only seven points for which deflections need be determined.

Assume that deflections in the form of coefficients of qL^4/D have been obtained for points 2, 4, 5, and 7 using the frame analysis, and that slopes in the form of coefficients of qL^3/D have been obtained at the points A, C, E and G. In the discussion of the S-method it was shown that the deflection coefficient obtained by application of the method was $0.00153 qL^4/D$ for a square clamped plate. Hence, if there were no rotation

of the beams in the structure shown in Fig. 4.2 then the deflection at point No. 1 would be $\Delta_2 + 0.00153qL^4/D$. The actual rotation of the beams is difficult to determine. However, if it is assumed that the beam containing point No. 2 undergoes a constant rotation θ_C throughout its length (about its longitudinal axis) then the effect of beam rotation may be taken into account in an approximate manner. The rotation of the beam would have the effect of rotating the "stub" cantilever beam discussed in Section 4.2. Thus the deflection at point No. 1 would be

$$\Delta_1 = \Delta_2 + (0.00153 \frac{qL^4}{D}) - 0.2(\theta_C)(L) \quad (4.8)$$

where $0.2L$ is the length of the "stub" beam.

In like manner the deflection of point No. 3 may be obtained as

$$\Delta_3 = \Delta_5 + (0.00153 \frac{qL^4}{D}) - 0.2L \frac{(\theta_C + \theta_G)}{2} \quad (4.9)$$

For this point only the deflection of the interior ersatz frame is considered in obtaining the center of panel deflection. For the corner panel the mid-panel deflection is

$$\Delta_6 = (0.00153 \frac{qL^4}{D}) + 0.5 \left\{ \left[\Delta_5 + 0.2L \left(\frac{\theta_C + \theta_G}{2} \right) \right] + \left[\Delta_7 + 0.2L \left(\frac{\theta_A + \theta_E}{2} \right) \right] \right\} \quad (4.10)$$

Since for the corner panel both the edge and the interior beams have a large effect on the mid-panel deflection their average contribution is used.

4.5 Application of the Frame Analysis to Elastic Structures

The procedure described in the previous sections was used to analyze a number of the elastic structures considered by Simmonds (9). These were idealized structures containing line beams and line columns as discussed in

Chapter 3. The beams had finite torsional and flexural stiffnesses and the column stiffnesses ranged from zero to infinity. The layout of these structures was as shown in Fig. 4.2. Both uniform and checkerboard loadings were considered.

(a) Uniform Loading

Results of analyses of uniformly loaded structures are given in Figs. 4.5 through 4.13 for the complete range of beam torsional and flexural stiffnesses considered by Simmonds and for a wide range of column stiffnesses. The cases of zero column stiffness and rigid columns are the only cases not shown. The results are given in the form of ratios of the deflection at given points to the maximum deflection measured in the structure. The deflections obtained by Simmonds are referred to as the theoretical deflections. The point considered at which the maximum deflection occurred was point No. 6 in all cases and the deflection at this point was always greatest for a value of $H = EI/DL = 0.25$. In each of the figures the results obtained by Simmonds are shown by solid lines and the results obtained using the frame analysis are shown by broken lines.

In general the agreement between the deflections found by the theoretical and frame analysis methods is good. In most cases the deflections based on the frame analysis tend to underestimate the correct deflections by a small amount. Many of the curves based on the frame analysis fall beneath the "exact" curves by a nearly constant value. This difference represents a small percentage error at lower values of H but for higher values of H the percentage error is large. However, for the higher values of H the beam deflections contribute a relatively small proportion of the mid-panel deflections and errors in beam deflections are relatively insignificant.

While the cases of infinitely stiff columns and columns offering zero stiffness are not practical, the frame analysis was applied to several examples of these cases. The results obtained for the value of zero column stiffness were considerably in error. For this extreme case the frame analysis is not applicable. For the case of rigid columns the analysis is made by taking θ_f in Eq. 4.3 as zero. Results obtained from the analyses of a number of structures having rigid columns showed good agreement between correct deflections and those given by the frame analysis. Hence it may be concluded that the frame analysis method can be used in the analysis of structures for deflections for any value of column stiffness other than zero. Note that good results were obtained for a value of $K = 10$ as shown in Figs. 4.5, 4.8, and 4.11. For a value of interior column stiffness ratio of $K = 10$ the corner column had a value of $K = 2$ and the edge column had a value of $K = 3$ in the direction perpendicular to the edge beam. Even for these low values of K the frame analysis method gives acceptable agreement.

(b) Checkerboard Loading

Results of analyses of structures having only the interior panel and the corner panels loaded are given in Figs. 4.14 and 4.15 for the two combinations of H and J considered by Simmonds. For the case of $H = J = 2.5$ the deflections obtained using the frame analysis method compare favorably with those obtained using the method of finite differences. The greatest percentage difference occurs at the center of an unloaded edge panel but here the absolute deflection is small.

For $H = J = 0.25$ there is a large difference in the results given by the two methods for some points on the structure. The largest percentage difference occurs at the center of an unloaded edge panel but for this case also the absolute value of this deflection is small.

A comparison of the effects of the uniform and checkerboard loadings shows that the deflections at the center of the interior and corner panels is about the same for each type of loading. The maximum difference between the two loading cases is only 14 percent. In view of this the large differences between the frame analysis and theoretical deflections for some points that were obtained for the structure with flexible beams are not serious.

5. DEFLECTIONS OF REINFORCED CONCRETE STRUCTURES

5.1 Introductory Remarks

This chapter contains a discussion of the results obtained from the application of the frame analysis method to compute deflections for eight reinforced concrete test structures. Comparisons of predicted and measured deflections are given and several factors affecting deflections of reinforced concrete structures are discussed. The majority of the structures considered were the test structures constructed at the University of Illinois. A description of the floor slabs that have been tested to date at the University of Illinois is given in Section 5.2.

The development of the frame analysis for deflections referred to ideal structures that were linearly elastic. The application of this method to actual reinforced concrete structures is confronted with problems at two different levels: problems related to inelasticity of reinforced concrete and problems related to quality control. In a practical case, the major problem is the determination of the permanent and transient loads. However, this can be ignored in calculating deflections of test structures for which the loads are known with reasonable certainty.

Problems related to inelasticity of reinforced concrete involve cracking and yielding in addition to the inherent inelasticity and time-dependence of the stress-strain relationship for plain concrete.

The use of poor materials and construction practices may have significant effects on the deflections of reinforced concrete structures. Deflections of reinforced concrete structures have been observed to be influenced by over-finishing, which brings excess fines to the upper surface of the concrete,

thereby weakening it, finishing that is not true to grade, which is usually evidenced by low finishing at mid-panel and high finishing around the columns, misplacement or omission of tensile reinforcement, addition of water to the concrete to aid in its placement, and overloading of uncured concrete with construction materials. In the test structures described in Section 5.2 these problems were eliminated. However, even with careful control of both the quality of the construction materials and construction practices non-uniformity is unavoidable.

Comparisons of computed and measured deflections for the University of Illinois test slabs are given in Section 5.3. Included in this section is a discussion of the effects of cracking and yielding on deflections and of the modulus of deformation of the concrete. The influence on deflections of time-dependent behavior of concrete is discussed in Section 5.4. Comparisons between predicted and measured deflections for structures other than the University of Illinois test slabs are given in Section 5.5. While the quality of the workmanship attending the erection of a structure may have a large effect on its behavior, the control of the workmanship is a construction problem, not one of design. Hence it is not considered further here other than to point out the necessity for careful control and the desirability of having the designing engineer or his representative specify and observe the construction practices used in executing the design.

5.2 Description of University of Illinois Test Structures

The experimental phase of the floor slab investigation has included the construction, testing, and analyses of seven small-scale test structures. Brief descriptions are given below of (a) the layout and reinforcement of the test structures, (b) the physical properties of the concrete and reinforcing steel used in their construction, and (c) their instrumentation and the

testing programs to which they were subjected. More extensive descriptions are given in References 10 through 15.

(a) Layout and Reinforcement of University of Illinois Test Slabs

The prototype structure for each of the test slabs contained nine square panels arranged three-by-three with a center-to-center of column spacing of 20 feet. The first five test structures were quarter-scale models of the prototypes and the sixth and seventh test slabs were one-sixteenth scale models. The type and designation of these slabs is given below in chronological order of testing.

<u>Structure No.</u>	<u>Type of Structure</u>	<u>Designation</u>	<u>Scale</u>
1	Flat Plate	F1	1/4
2	Flat Slab	F2	1/4
3	Two-Way Slab with Deep Beams	T1	1/4
4	Two-Way Slab with Shallow Beams	T2	1/4
5	Flat Slab Reinforced with Welded-Wire Fabric	F3	1/4
6	Flat Slab	F4	1/16
7	Flat Slab	F5	1/16

All of the test structures except Nos. 4 and 7 were designed according to the regulations set forth in the ACI Building Code (318-56). Test structure No. 4 was designed to carry the full static moment and to have a strength and behavior intermediate between those of the flat slab (F2) and the typical two-way slab (T1). Test structure No. 7 had the same geometry as structures 2, 5 and 6 but was reinforced to carry the full static moment and had the reinforcement distributed following the suggestions given by Hatcher (13). Figures

5.1, 5.2, and 5.3 are photographs of structures No. 2, 3, and 7, respectively, showing the loading and testing equipment in place.

Each of the prototype floor slabs was considered as being representative of an intermediate story in a building and hence had columns extending above and below the floor level. Each of the test slabs had columns extending only below the level of the floor. The columns of each of the test structures were supported on steel balls. The length of an interior column, measured from center of floor to center of ball, was taken so that the flexural stiffness of an interior column in the model was equal to that of the corresponding column extending above and below the floor in the prototype. The far ends of the column in the prototype were assumed to be fixed and computations for stiffnesses were based on the moments of inertia of the uncracked sections.

The panels of slabs 1, 2, 3 and 4 were reinforced with 1/8-in. square plain bars. A cover of 3/16 in. was provided for the top steel and for the bottom steel running in a north-south direction. The east-west bottom steel had a cover of 5/16 in. Welded-wire fabric was used in slab No. 5 and 20 gauge (0.035 in. diameter) wire was used in slabs 6 and 7. The layout of the five quarter-scale slabs and the amounts and arrangements of the reinforcement used in structures 1 to 4 are shown in Figs. 5.4 to 5.23. The amount and arrangement of the reinforcement used in slab No. 7 is shown in Figs. 5.24 through 5.27. In making an analysis for deflections of a reinforced concrete structure, the amount and placement of the tensile reinforcement is of interest only in computing the moments of inertia of the fully-cracked sections. A comparison of the amounts of tensile reinforcement provided at the various design sections in slabs Nos. 2 and 5 is given in Figs. 5.14 and 5.15.

The design loads for the prototype structures were as follows:

<u>Structure No.</u>	<u>Dead Load, psf</u>	<u>Live Load, psf</u>	<u>Total Load, psf</u>
1	85	70	155
2, 5, 6, 7	85	200	285
3, 4	75	70	145

The total dead load on the quarter-scale test structures, including 22 psf contributed by the weight of the loading equipment, was 44 psf for slabs 1, 2 and 5 and 41 psf for slabs 3 and 4. For slabs 6 and 7 the dead load, including 16 psf for the loading equipment, was 21 psf.

(b) Physical Properties of Materials

The physical properties of the concrete and reinforcement used in the seven test structures are given below. The concrete properties are those at the beginning and end of testing. The modulus of deformation of the concrete, E_c , is the average initial tangent modulus measured in tests of 2 by 4 and 4 by 8-in. cylinders. The yield points for the high-strength steel used in slab No. 5 varied with the size of the wires used. The range of these yield points is given below. The moduli of rupture of the concrete are given in Section 5.3.

Slab No.	f_y , ksi	<u>Beginning of Testing</u>			<u>End of Testing</u>		
		f'_c , psi	E_c , ksi	Age, days	f'_c , psi	E_c , ksi	Age, days
1	36.7	2510	2400	76	2680	2800	140
2	42.0	2760	3100	78	2320	3100	168
3	42.0	3020	3000	76	2510	3000	185
4	47.6	3660	3300	50	4020	3300	92
5	61-76*	3800	3700	55	3820	3700	100
6	46.0	--	--	--	3700	3700	156
7	47.8	3140	3100	40	3140	3100	40

* Based on an offset strain of 0.002.

(c) Instrumentation and Testing Program

Each of the test structures was constructed in place in its testing frame. Each column of a test structure was supported on a steel ball. These balls were in turn supported on tripod reaction dynamometers for the quarter-scale models or on a reaction frame for the one-sixteenth scale models. Extreme care was taken in the construction of the test slabs to insure close dimensional control.

Loading was applied equally to sixteen points on each panel by means of a load distribution system. These points were symmetrically spaced about the center of each panel. Elastic studies have shown that the moments and deflections obtained for this type of loading are nearly equal to those obtained for a uniform loading covering the entire panel.

The loading system for the quarter-scale models was placed entirely above the upper surface of the slab. The equipment for one panel consisted of 16 eight-in. square steel plates resting on rubber pads. These plates were connected by four small H frames and one large H frame. Load was applied to the center of the larger H frame by a hydraulic jack which reacted against a frame extending above the slab. Applied load was measured by means of two dynamometers, one placed directly below the jack and the second being formed by the larger H frame. Pressure was supplied to the jacks by means of a pump and a system of hoses and valves. Load could be applied to all panels or to any desired pattern of panels.

The loading system for each of the one-sixteenth scale slabs was placed beneath the slab. Load was applied to each of the 16 two-in. square plates on a panel by means of a rod which passed through the slab. A small hydraulic jack, a load dynamometer and a system of bars to distribute load from the jack to the 16 rods completed the load system for a panel.

Deflections were measured at the center of each panel and at each mid-beam point for a total of 33 points on each structure. The designation of these points is given in Fig. 5.28. For the quarter-scale slabs the deflections were measured by means of dials permanently mounted beneath the slabs. Deflections were read for slab No. 6 using a movable bridge on which were mounted seven deflection dials. For slab No. 7 deflections were read using 49 dials fixed in position above the slab. For slabs 6 and 7 the shortening of each column was recorded as well as the deflections at the 33 points described above. The deflection dials used read directly to 0.001 in. with the fourth decimal place being estimated.

Each of the quarter-scale slabs was also instrumented for the reading and recording of strains at selected points on the concrete and on the tensile reinforcement.

The testing program for the quarter-scale slabs consisted of subjecting each structure to a series of loadings of different patterns and at different load levels. The sequence of load tests for a given structure consisted of a test in which all panels were loaded in successive steps to a desired level of load and then a series of tests in which one or more panels were loaded in like manner to the same load level. At the completion of a sequence of tests a second similar series was conducted but at a higher load level. Deflections and strains were recorded after the application of each load increment of each test. As many as 44 load tests were performed on some of the test structures. A total of three load tests were performed on slab No. 6 and slab No. 7 was loaded to failure in one continuous test.

5.3 Comparisons of Computed with Measured Deflections

This section contains a discussion of (a) the deflection coefficients for the test structures that were computed on the bases of both uncracked and

fully-cracked sections, (b) the cumulative load-deflection curves for various points on the test structures, (c) the transition curve between uncracked and fully-cracked deflections, and (d) a discussion of the modulus of deformation for concrete.

(a) Computed Deflection Coefficients

Deflection coefficients are given in Figs. 5.29 through 5.38 for the seven test structures. Figures 5.29, 5.31, 5.35 and 5.37 give coefficients which were determined using the frame analysis assuming all sections to be uncracked. The remaining figures give deflection coefficients that were computed assuming all sections to be fully cracked. The coefficients for uncracked sections given in Fig. 5.31 for the slab (F2) are also applicable to the other flat slabs (F3, F4, and F5) since the geometrical relationships for the uncracked flat slabs were all the same.

Although the frame analysis method is an approximate procedure the deflection coefficients are given to five significant places after the decimal point in each of Figs. 5.29 - 5.38 in order to show the effects of beam torsional rigidity on deflections. In Fig. 5.31 the deflection coefficient for point A_2 on the flat slab is shown to be slightly greater than that for point C_2 . The torsional rigidity of a deep beam in the flat slab was about one and one-half times that of a shallow beam. For the flat plate the torsional rigidities of the deep and shallow beams (considering T-beam action) were about the same and were taken as equal in computing the deflection coefficients.

In addition to deflection coefficients, deflections for a load of 100 psf are given in each figure. In computing these deflections Poisson's ratio was taken as zero and the initial tangent modulus of elasticity of the concrete at the beginning of testing was used.

The deflection coefficients given for the fully-cracked sections were computed using the coefficients for uncracked sections. For a point at the center of a beam the coefficient for fully-cracked sections was obtained by multiplying the coefficient for uncracked sections by the ratio of the moment of inertia for the uncracked section to that of the cracked section. The moment of inertia for the cracked section was taken as the average of the sum of (a) the moment of inertia for the positive mid-beam section, and (b) the average of the two negative end-of-beam sections. The mid-panel deflections were computed using the same procedure as for the uncracked structure except that the term $0.00153 qL^4/D$, which results from the use of the S-method for a square panel (see Section 4.2), was multiplied by the ratio of the average of the negative and positive moments of inertia for the panel to the uncracked moment of inertia. The rotation for each column was determined by multiplying the rotation computed assuming the column to be uncracked by the ratio of uncracked to cracked moments of inertia. The alternative to using the procedure outlined above for predicting deflections for cracked sections would be to perform a second frame analysis using the moments of inertia for cracked sections. Note that all of the deflection coefficients given for fully cracked sections are given in terms of qL^4/D where D is for the uncracked section. The moments of inertia for the cracked sections were computed using conventional straight-line methods.

Deflections in inches for a load of 100 psf for the fully-cracked structures are given for slabs Nos. 1, 2, 3, 4, 5 and 7 in Figs. 5.30, 5.32 - 5.34, 5.36 and 5.38. The deflection coefficients given in Fig. 5.33 for slab No. 5 (F3) for the mid-beam points were taken as being the same as those computed for slab No. 2 (F2) since the percentages of reinforcement provided in these two structures were nearly the same. The coefficients for fully-cracked sections given in Fig. 5.32 are also applicable to slab No. 6 (F4)

since this structure contained the same percentages of slab reinforcement as did F2. Test structure No. 7 (F5) contained greater percentages of reinforcement than any of the other flat slabs and hence had a somewhat greater rigidity when fully cracked than did the other flat slabs. The deflection coefficients for this slab assuming fully cracked sections are given in Fig. 5.34.

An Illustrative Example, containing a step-by-step description of the computation of the deflection coefficients for the two-way slab with shallow beams (T2), is given in Appendix C.

(b) Cumulative Load-Deflection Curves

Cumulative load-deflection curves for the seven test structures are given in Figs. 5.39 - 5.100. The figure numbers for the load-deflection curves for each test structure are as follows:

<u>Structure Number</u>	<u>Figure Numbers</u>
1 (F1)	5.39 - 5.53
2 (F2)	5.54 - 5.67
5 (F3)	5.68 - 5.77
6 (F4)	5.78 - 5.81
7 (F5)	5.82 - 5.86
3 (T1)	5.87 - 5.93
4 (T2)	5.94 - 5.100

The load-deflection curves for structures 1 through 5 include the effects of the dead load of the slab and loading system. For slabs 6 and 7 deflections are given for applied load only as those for dead load were very small. The deflections given for slabs 6 and 7 are four times those actually measured. This is done in order to allow direct comparisons to be made among the curves for the flat slabs. The effects of column shortening were included in constructing the curves for slab No. 6. However, these effects were very small.

The cumulative load-deflection curve for a particular point on a given structure was prepared using the data recorded during a number of different load tests. The tests considered were those in which all panels were loaded to the same level of applied load. Where space permits the load-deflection curves for the separate tests in which all panels were loaded are shown by broken curves. The difference in deflection shown between the end of one broken curve and the beginning of the next broken curve for a given point represents the increase in residual deflection accrued at that point during the intervening tests.

The curves given for test structure No. 6 (F4) were obtained from the data recorded in the third of the three load tests performed on this structure. In the second test a maximum applied load of 220 psf was reached which probably caused some cracking although none could be detected by visual inspection. At this point one of the loading wires extending through the slab failed and it was necessary to discontinue testing. Since the residual deflections accrued in the second test were not included in constructing Figs. 5.78 - 5.81 the initial portion of these curves are rebound or reloading curves.

The single panel and pattern loadings that were applied to the structures caused maximum moments at various sections and hence caused additional cracking and loss of stiffness beyond that which occurred during the tests with all panels loaded. This loss in stiffness caused by the partial loadings is shown by the decrease in slopes of the broken curves for successively higher loading tests. It may be expected that similar structures loaded continuously in one test from no applied load to failure would exhibit somewhat smaller deflections for loads intermediate between the cracking load and the failure load than were measured for the quarter-scale test slabs.

Two straight lines, one marked "uncracked" and the other marked "cracked," are plotted on each of the cumulative load-deflection curves. These lines represent the computed deflections based on uncracked and fully-cracked sections, respectively.

The load-deflection curves for the flat plate (F1) all terminate at a load of 306 psf although the maximum load carried by this structure was 360 psf. The deflections given for the load of 306 psf were the last deflections measured before the slab failed. Failure was characterized by the punching through of column No. 7. A broken line is used on each of the curves for the flat plate to connect the deflection measured at 306 psf with that measured after failure.

The load-deflection curves for slab No. 5 (F3) all terminate at a load of 587 psf. The interior tripod reaction dynamometers buckled at a load somewhat higher than this and it was necessary to replace them by steel blocks in order to continue loading the structure to failure.

In general, the agreement between the initial portion of each of the measured load-deflection curves and the straight line computed on the basis of uncracked sections is good. The poorest agreement is for the deep edge beams in the flat plate and flat slabs and for the beams in the two-way slab with deep beams (T1). However, the magnitude of the deflections of the deep beams was small. Hence the large percentage errors between computed and measured deflections for these sections is relatively insignificant in so far as both beam and mid-panel deflections are concerned.

(c) Transition Curve Between Cracking and Yielding

Consider a typical load-deflection curve for a point on a continuous slab. After an initial straight-line portion the slope of the curve begins to decrease steadily with increase in load. This reduction in slope is caused by

the losses in stiffness accompanying cracking of the concrete and the reduction of the "modulus of deformation" which also occurs concomitantly with increased loading. The shape of the curved portion of the load-deflection cannot be defined with exactitude.

The effect of cracking of the concrete is more noticeable in an isolated beam than in a continuous structure. Cracks occurring in an isolated beam tend to form completely across the width of the beam. Hence there is a large decrease in stiffness and an accompanying large increase in curvature at each crack. A load-deflection curve constructed for such a beam would show a sudden decrease in slope at the point of first cracking.

The effect of first cracking in a slab is to cause some slight redistribution in moments and a negligible decrease in stiffness. Consequently it is difficult to detect any change in shape of the load-deflection curve for a slab corresponding to the point of first cracking. In most of the test structures first cracking could be determined only by a decrease in slope of load-steel strain curves with first visual observation of cracks being made at much higher loads.

Since the point at which the load-deflection curve for a slab begins to exhibit noticeable deviation from a straight line is difficult to determine, the following approximate method for defining this point is suggested.

In using the frame analysis it is necessary to determine the end-moments for each of the "ersatz beams" included in the "ersatz frame." Having the end-moments, the mid-beam moments may be determined using the formulae given in Table 18. By setting the mid-beam moment equal to the cracking moment the load corresponding to cracking at mid-beam may be computed. The cracking moment at mid-beam may be determined from the relationship

$$M_{cr} = f_r Z \quad (5.1)$$

where f_r = the modulus of rupture of the concrete, and

Z = the section modulus of the ersatz beam.

The cracking loads computed for the test structures are indicated on each of the cumulative load-deflection curves. The cracking load given for a point at the center of an interior panel was taken as equal to the cracking load computed for one of the four adjacent mid-beam points. This is in keeping with the concept that when the boundaries of a plate are deflected the center of the plate tends to deflect by the same amount. Hence when cracking begins to affect the slope of the load-deflection curve for a mid-beam point it may be expected that the slope of the mid-panel curves for adjacent panels will also be affected.

For an edge panel the cracking load at mid-panel was taken as equal to that of one of the ersatz beams perpendicular to the discontinuous edge. For a corner panel the average of the cracking loads for an edge and interior beam were used. The deflection corresponding to the cracking load is referred to as the cracking deflection in subsequent discussion.

In computing the cracking moments the moduli of rupture of the concrete that were used were those assumed in the analyses of the test structure for moments. Tests by Mila (37) have shown that the effective modulus of rupture of concrete in a structure is less than that for plain specimens cast from the same batches of concrete. This reduction is caused by stresses arising from the resistance to shrinkage of the concrete furnished by the presence of the reinforcing steel.

The moduli of rupture used in analyzing the quarter-scale test structures for moments and the average moduli in psi measured for unreinforced beams that were cast at the same times as the test structures are listed below.

Slab No.	<u>Beginning of Testing</u>		<u>End of Testing</u>		f_r , effective
	f'_c	f_r , plain	f'_c	f_r , plain	
1	2510	700	2680	620	310
2	2760	600	2320	---	360
3	3020	590	2510	---	350, beams 400, slab
4	3660	---	4020	940	500, beams 550, slab
5	3800	750	3820	800	600

Two different values for the effective modulus of rupture were used for the two-way slabs since the beams in these structures contained higher percentages of reinforcement than the slabs, thereby causing a greater reduction in the effective modulus.

The point at which the cumulative load-deflection curve crosses the line marked "cracked" on the curves occurs in the vicinity of the yield load. The yield load is defined as the load level at which sufficient yield lines form in the structure to allow unrestrained deflection to take place.

When a structure fails by general yielding of the reinforcement one of two patterns of yield lines may form. If the supporting beams are sufficiently strong each panel may fail separately. If no beams are present or if the supporting beams have relatively low strength then the pattern of yield lines will extend through the beams and the structure as a whole will participate in the failure. The computed and measured yield loads in psf for the test structures were as shown on the following page.

The yield loads indicated on the cumulative load-deflection curves for the flat plate and the flat slabs are those computed for the structural failure mechanism in which a positive yield line extended through each edge panel and into the corner panels. For each of these structures the capacity

<u>Slab No.</u>	<u>Computed Yield Load and Pattern</u>	<u>Measured Yield Load</u>
1(F1)	270 Interior panel only* 320 Edge and corner panels	360
2(F2)	460 Interior panel only* 565 Edge and corner panels	550
3(T1)	395 Interior panel 435 Edge panel 440 Corner panel 530 End row of panels 610 Interior row of panels	537
4(T2)	390 End row of panels 405 Interior row of panels	466
5(F3)	1010 Edge and corner panels	952
6(F4)	650 Edge and corner panels	620
7(F5)	800 Edge and corner panels	710

* Computed assuming the interior panel to be one of an infinite array
- of similar panels.

of the interior panel was less than that of the structure as a whole. However, since each structure could continue to carry additional load after the interior panel yielded, the structural capacity is indicated on the curves. For the two-way slabs the yield load indicated on a curve for a particular point is the one corresponding to the failure mechanism which would include the point. The deflection corresponding to the yield load is referred to as the yield deflection below.

The portion of a load-deflection curve lying between cracking and yield deflections is termed the transition curve. The measured transition curve appears to be approximately parabolic in shape. A graphical method of predicting the shape of the transition curve, assuming it to be a parabola, is given in Fig. 5.101. The shape of the predicted transition curves are indicated by a number of small circles in each of Figs. 5.39, 5.42, 5.45, 5.48, 5.54, 5.56, 5.68, 5.87, 5.94, 5.95, 5.96 and 5.99.

For design purposes it is suggested that the deflections computed on the basis of uncracked sections be used if the design load is not more than twice the cracking load for the point under consideration. Where the design load is greater than twice the cracking load a linear transition curve between the yield deflection and a point corresponding to twice the cracking load appears to give reasonably close comparisons between measured and computed deflections. This curve is shown by a broken line in several load-deflection curves.

Considering the number of variables that affect deflections of reinforced concrete structures the agreement between the measured and predicted transition curves cannot be expected to be more than approximately close. For most of the figures in which a comparison is given the agreement is reasonable. The poorest agreement occurs for slab No. 2 (F2). The edge and corner columns of this structure were lightly reinforced. Hence the columns allowed a large amount of rotation to take place thus increasing the slab deflections. It was necessary to provide external reinforcing on these columns in order to load the structure to its yield load capacity. More column reinforcement was provided in slabs No. 5, 6, and 7 and better agreement is shown for these slabs.

(d) Modulus of Elasticity of Concrete

The use of the term "modulus of elasticity" is not strictly applicable in discussing the properties of concrete. By definition a modulus of elasticity is the constant of proportionality between stress and strain. For some materials, such as steel, the modulus is well defined in the early stages of stressing and may be assumed to be constant. Concrete, however, exhibits a nonlinear stress-strain relationship from first loading to failure. This is shown by the multiplicity of definitions of the so-called "modulus of

elasticity" for concrete, which include tangent and secant definitions at arbitrarily chosen stresses. The modulus of elasticity might better be termed the "modulus of deformation."

The modulus of deformation obtained for a particular test cylinder is affected by the duration of the test. If the specimen is tested to failure in a very short time a substantially higher modulus is obtained than if the specimen is tested at the standard rate (38). Also if the duration of the test is very long an appreciably lower modulus is obtained. In addition to speed of testing the type of aggregate and mix proportions have large effects on the modulus obtained (39). For instance, lightweight concrete may develop strengths comparable to those of normal-weight concretes but usually exhibit considerably lower moduli of deformation. It is apparent that the modulus of deformation is an index value which may be assumed to represent the behavior of the concrete in a structure in an approximate manner.

Various expressions have been assumed to define the modulus of elasticity for concrete. The simplest is the secant definition

$$E_c = 1000 f'_c \quad (5.2)$$

where E_c = modulus of elasticity in psi, and

f'_c = concrete compressive strength in psi determined from a test of a 6-in. by 12-in. cylinder. This equation was first included in the 1928 edition of the ACI Building Code (40) and continued in use through the 1956 edition (1). Since this expression tends to overestimate the modulus for high concrete strengths various investigators have proposed formulae that give better fits to experimental data. Among these are the formula proposed by Jensen (41)

$$E_c = \frac{30,000,000}{5 + \frac{10,000}{f'_c}} \quad (5.3)$$

and Lyse (42)

$$E_c = 1,800,000 + 460 f'_c \quad (5.4)$$

for normal-weight concretes. In an effort to present one formula applicable to all weights of concrete Pauw (43) suggested the formula

$$E_c = 33w^{1.5} \sqrt{f'_c} \quad (5.5)$$

where w is the weight of the concrete in pounds per cubic foot.

The value of the modulus reported in Section 5.2(b) for a given test structure is an average value which was determined from tests of a number of cylinders cast at the same time as the test slab. The initial portion of the stress-strain curve drawn for each cylinder was nearly linear and the modulus reported is the average slope of these initial portions - hence the designation "initial tangent modulus." Although the mixing and casting of the concrete for each test structure was carefully controlled and the testing of the cylinders was performed in a standard manner there was still an appreciable amount of scatter in the values of the moduli determined for a particular slab. A comparison of the moduli computed using Eqs. 5.2 - 5.5 is given below in the form of ratios of computed values to the initial values at the beginning of testing. Equation 5.3 was modified by replacing the factor 5 by a 6.

<u>Slab No.</u>	<u>1000f'_c</u>	<u>Jensen</u>	<u>Lyse</u>	<u>Pauw</u>
1	1.05	1.26	1.23	1.26
2	0.89	1.01	0.98	1.15
3	1.01	1.07	1.06	1.10
4	1.11	1.04	1.05	1.11
5	1.03	0.94	0.96	1.01
6	1.00	0.93	0.95	0.99
7	1.01	1.05	1.04	1.09

For the small aggregate mixes used in the test structures the relationship $E_c = 1000 f'_c$ gives the best fit with measured data.

For normal-weight concretes the modified form of Eq. 5.3 is adequate in the absence of measured data. For lightweight concretes the data reported by various investigators shows considerable scatter and it is recommended that a design value of E_c for a concrete of this type should be determined by tests for specific cases.

5.4 Time-Dependent Deflections

The deflection of a point on a reinforced concrete structure is the sum of the instantaneous deflection that occurs upon the first application of load and the time-dependent deflection resulting from the effects of creep and shrinkage. The deflection caused by shrinkage is assumed to be independent of the loading while creep deflection is largely a function of the amount and history of the loading. Knowledge on creep and shrinkage deformations of concrete under actual working conditions is limited. However, the determination of the portion of the total load that may be considered as permanent is perhaps the most critical unknown factor in computing long-time deflections. So far in this study, only instantaneous deflections have been considered. However, in design it is the total deflection that is of interest and the larger portion of the total deflection may result from the time-dependent effects.

The time-dependence of deformations of reinforced concrete construction has been the subject of numerous investigations. Several controlled studies have been made of isolated structural elements, such as flexural and axially loaded members, and procedures have been developed that allow the prediction of the long-time deformations of such elements to be made with some

accuracy. However, time-dependent deflections of floor slabs have received little organized attention. Three cases of long-time tests of continuous structures have been reported. These are described briefly below although neither of the first two structures is representative of current design practice.

In 1917 a single panel of the Schwinn Building was loaded to twice the design load and this load was maintained for over one year (44). The Schwinn Building was a multistory flat slab structure three bays wide by several bays long. The reinforcement in each panel was placed in four layers, two top and two bottom, with one of each of the top and bottom layers oriented parallel to the column centerlines and the remaining layers at 45 degree angles to the column centerlines. Each layer was continuous over the width of the panel. The loaded panel was an edge panel located in an intermediate story. The test panel measured 27 by 25 feet and was ten in. thick. The mid-panel deflection at first loading was about $4 \frac{3}{4}$ in. This deflection increased to about $8 \frac{1}{4}$ in. after 379 days, an increase of about 175 percent.

In 1919 a single story two-way test structure was constructed by the U.S. Bureau of Standards at Waynesville, Ohio (45). This structure contained 18 panels arranged three by six, and was constructed of reinforced concrete with hollow tile fillers. A number of load tests were performed with some of the loads remaining in place for several weeks. The deflections showed some tendency to increase with time. When the loads were removed most of the deflection was recovered.

In 1959 a flat plate test structure was constructed and tested in Melbourne, Australia (46). This structure contained nine panels arranged three-by-three. Each panel was 9 by 12 ft. by $3 \frac{1}{2}$ in. thick. In addition there was a 6-ft. cantilever extension at both of the narrower ends of the

structure so that the over-all dimensions of the slab were 28 ft. 5 1/2 in. by 48 ft. However, 48 days after the formwork had been removed an 18-in. wide strip of the cantilever was cut off at both ends of the slab. The slab was supported on slender steel columns and contained no spandrel beams. The slab was constructed under field conditions and no special care was taken to insure proper compaction of the concrete. Hence the completed slab contained considerable voids.* A lightweight-aggregate concrete was used which weighed 114 pcf. The average 28-day compressive strength was 2500 psf and the 28-day modulus of rupture of plain specimens was about 290 psi. The sonic modulus of elasticity of the concrete showed considerable variation. An average value was about 1,500,000 psi.

Deflections were measured at numerous points using an engineers level. Deflections were recorded at the time the formwork was removed, which was ten days after casting, and at various times during the following 200 days. During this time only the 31 psf dead load was acting. Difficulties were encountered in measuring deflections since some columns rose and others settled. At the time the formwork was removed the deflection at the center of the interior panel, corrected for apparent column settlement, was about 0.05 in. This deflection increased to about 0.44 in. at an age of 50 days and continued increasing more slowly to a total of about 0.59 in. at 200 days.

The deflection of the interior panel was computed using a coefficient obtained by interpolating between values given in Table 10. For $S/L = 0.75$, $c/L = 0.06$, and $H = 0$ the coefficient was found to be $0.0032 qL^4/D$. For a

* It is stated in Reference 46 that "After the formwork was stripped a visual assessment was made of the quality of the concrete in each bay, judging by the compactness of the surface. Although one bay was estimated to be defective through incomplete compaction over 50 percent of its area, the average for the whole slab was 15 percent."

modulus of 1,500,000 psi the deflection was computed as 0.06 in. based on uncracked sections. There was a considerable increase with time in the amount of cracking that was visible on both the top and bottom surfaces of the slab. This cracking was attributed to shrinkage, thermal stresses, and stresses caused by differential settlements. For a slab as lightly reinforced as this one was, the moment of inertia for cracked sections is about one-fifth to one-fourth as large as the moment of inertia for uncracked sections. Assuming the slab to be fully cracked and taking the long-time deflection as twice that of the initial deflection computed on the basis of cracked sections gives a computed long-time deflection of 0.5 in. This compares favorably with the observed deflection of 0.59 in. Note that the structure was subjected to carrying its own weight while the concrete was still uncured. It is probable that if the formwork had been allowed to remain in place for an additional two or three weeks that the total deflections would have been less.

Since there is a paucity of data concerning time-dependent behavior of continuous structures it is necessary to consider the behavior of isolated flexural members in order to arrive at an intelligible method of predicting long-time deflections of slabs. Accordingly, a discussion anent the effects of (a) creep and (b) shrinkage on deformations of beams is given below and (c) an analytical interpretation of the time-dependent behavior of beams is extended to slabs.

(a) Effects of Creep on Beam Deflection

The effect of creep on beam deflections is influenced by the amount of cracking that has taken place and whether compressive reinforcement is present. Consider first the case of a fully-cracked section and assume that no compressive reinforcement is present. For this case the instantaneous curvature corresponding to the linear distribution of strains shown in

Fig. 5.102(a) is

$$\phi_i = \frac{\epsilon_i}{kd} \quad (5.6)$$

Assuming that the steel strain computed on the basis of a fully cracked section does not change then the relationship between instantaneous curvature and curvature after creep is

$$\frac{\phi_c}{\phi_i} = \frac{k\epsilon_c}{\epsilon_i} \quad (5.7)$$

where ϵ_i = initial strain at first loading,

ϵ_c = increase in strain due to creep,

ϕ_i = instantaneous curvature,

ϕ_c = increase in curvature due to creep, and

kd = depth from compression face to neutral surface.

This is an over-simplified explanation of the effects of creep since in a real beam the steel stress will increase somewhat with time, thus affecting the distribution of concrete stress, but it does suffice to show that the increase in deflection due to creep is not as great as the increase in strains. Based on test data it has been determined (47) that the ratio ϵ_c/ϵ_i in Eq. 5.7 may be replaced by a factor m such that

$$m = 3 - \frac{p'}{p} \quad (5.8a)$$

for rectangular section or T-beam sections with $kd \leq \frac{2t}{3}$, and for T-beam sections with $kd \geq \frac{2t}{3}$

$$m = 3(2 - \frac{p'}{p}) \quad (5.8b)$$

where p and p' = ratios of cross-sectional areas of compressive and tensile steel, respectively, to bd ,

b = width of rectangular beam or width of compressive portion of T-beam,

d = effective depth of beam, and

t = thickness of flange of T-beam.

The factor m in Eq. 5.8 is a function of the concrete properties and variation in concrete stress.

As shown by the presence of the factor p' in Eq. 5.8 the use of compressive reinforcement tends to decrease the deflections due to creep. As the concrete in the compressive region of a beam creeps the compressive steel, becoming effectively more rigid, is forced to carry more of the compressive force which in turn acts to decrease the load causing the concrete to creep.

Consider next the case of an uncracked section. The strain distributions across the cross section before and after creep for this case would be about as shown in Fig. 5.102(b). Almost no data have been collected for this case and consequently no simple relationship between initial and creep curvature, such as Eq. 5.8, can be developed. However, qualitatively, at least, it can be concluded that creep will cause relatively more increase in the deflections of an uncracked beam than of a fully cracked beam. As for the cracked member, the presence of compressive reinforcement would tend to reduce the creep deflections.

(b) Effect of Shrinkage on Beam Deflections

There are two cases for which shrinkage strains alone will cause little or no deflection. If a plain concrete beam is unrestrained then shrinkage will cause some axial shortening. If a rectangular reinforced concrete beam contains equal amounts of top and bottom reinforcement placed symmetrically about mid-depth of the beam then shrinkage would not cause any deflection although it might cause cracking.

For rectangular beams containing unequal amounts of tensile and compressive reinforcement, with the compression steel placed above the upper

kern limit and the tensile steel placed below the lower kern limit of the concrete, it may be shown (47) that the curvature caused by shrinkage is

$$\varphi_{sh} = \frac{K_1 \epsilon_{sh} (p-p')}{d} \quad (5.9)$$

where K_1 = a constant which is a function of the dimensions of the cross section and the long-time modular ratio, and

ϵ_{sh} = the free shrinkage strain.

Based on available data (47) the following simplified relationship has been developed.

$$\varphi_{sh} = \frac{0.035(p-p')}{d} \quad (5.10)$$

Given the curvatures due to shrinkage strains the shrinkage deflection may be computed. For example, consider the simply-supported beam of Fig. 5.103(a). Assuming a uniform shrinkage curvature the mid-span deflection is readily determined to be

$$\Delta = \frac{\varphi_{sh} L^2}{8} \quad (5.11)$$

where L is the span. However, for the fixed-ended beam of Fig. 5.103(b) the boundary conditions impose the requirement that the area of the negative curvature diagram equal that of the positive curvature diagram and hence there may be little or no shrinkage deflection. The shrinkage would have an indirect effect on deflections in this case in that the cracking resulting from shrinkage would cause a loss of stiffness.

(c) Long-Time Deflections of Slabs

The current state of knowledge concerning the effects of time-dependent behavior of concrete allows the long-time deflections of statically determinate beams to be predicted with reasonable accuracy if the load is

known. However, for continuous slabs, although time-dependent behavior may be expected to cause the same qualitative effects, sufficient data are not available to allow an intelligible analysis to be made for long-time deflections. Until such data become available it is suggested that the long-time increase in deflection be taken as the instantaneous deflection times a multiplier of three, if the instantaneous deflection was calculated on the basis of uncracked sections, or one, if based on fully cracked sections. The instantaneous deflection to be used is that corresponding to the dead load plus the portion of the live load considered as being permanent.

5.5 Further Applications of Frame Analysis

A three-quarter scale model of the prototype flat plate structure was constructed and tested at the Portland Cement Association Structural Laboratory in Skokie, Illinois. The percentages and distribution of the reinforcement in this structure were identical to those of the quarter-scale test structure (F1) and the deflection coefficients of Fig. 5.29 and 5.30 are applicable to this structure. The major difference between the two test structures, other than scale, was that the PCA slab contained normal deformed reinforcing bars and large-aggregate concrete, while the quarter-scale slab contained plain bars and small-aggregate concrete.

The PCA test structure failed at almost the same load and in the same manner as the quarter-scale slab. Figure 5.104 shows load-deflection curves for six mid-panel points on the PCA slab. The curves are for the applied load and do not include the 73 psf dead load. On each curve the slope predicted on the basis of uncracked sections is given. Note that the computed slopes and the initial portions of each of the curves coincide. The load-deflection curves for the quarter-scale flat plate in most cases show no noticeable deviation from the straight line representing the uncracked slope

until loads of about 80 to 100 psf were reached. The curves for the PCA slab show the same behavior. Hence it may be expected that the curves corresponding to the 73 psf dead load would be straight lines falling on the computed slopes. If the slope of one of the curves in Fig. 5.104 is projected backwards to the zero load-zero deflection origin then the slope for the fully cracked sections may be plotted from this origin. These slopes are not shown due to lack of space. However, as for the quarter-scale slab, the deflections at working load computed on the basis of fully cracked sections are about three times the measured deflections while the measured deflections are only a small amount greater than those computed for uncracked sections.

The load-deflection data also showed that, allowing for differences in scale and moduli of deformation for concrete, the deflections for corresponding points on the two test slabs were nearly identical in the earlier stages of loading. For higher loads the PCA structure exhibited somewhat less deflection than the quarter-scale structure. This is the behavior that would be predicted by the frame analysis since the yield point of the reinforcement of the PCA slab was 44.5 ksi, which was 25 percent greater than that of the quarter-scale slab.

One additional structure has been studied. This was a three-story flat slab structure designed to serve as a library addition. Each floor contained thirty square panels arranged five by six. In further discussion this structure is referred to as structure C. The dimensions of a typical interior panel are shown in Fig. 5.105. The structure was designed to carry a dead load of 88 psf and a live load of 90 psf. Steel was provided in excess of the amounts required by the ACI Code (318-56). The discontinuous sides of the edge and corner panels were supported on walls.

The second and third floors of structure C began to show large deflections shortly after construction was completed. Hence the owners recorded

the deflections at each of the mid-panel and mid-beam points on these floors for a period of five years beginning shortly after construction. A composite deflection-time diagram for a mid-panel point is shown in Fig. 5.106. This curve was constructed from the deflections measured for a number of panels as all of the panels, including edge and corner panels, showed nearly the same behavior. The deflection data were obtained with the aid of an engineers level and were subject to some error.

The deflections for this structure were predicted using the tabulated coefficients of Table 10. Since the column capitals were round a ratio of c/L of 0.17 was used in determining the deflection coefficients. The deflection coefficients are

$$\begin{array}{ll} \text{mid-panel} & \frac{0.0033qL^4}{D} \\ \text{mid-beam} & \frac{0.0021qL^4}{D} \end{array}$$

The computed short-time deflections for the total design load of 178 psf are

<u>Point</u>	<u>Uncracked</u>	<u>Cracked</u>
mid-panel	0.25 in.	0.73 in.
mid-beam	0.16 in.	0.47 in.

A modulus of deformation of 3,000 ksi was used for the concrete.

The average of the mid-panel deflections measured at a time shortly after the completion of construction was about three-fourths in. and the average mid-beam deflection was about one-half in. After five years these deflections had increased to about 2.5 and 1.5 in., respectively. There was no evidence of foundation or first floor settlement. The owner estimated that only about 25 psf live load had been acting continuously during this period. Since the deflections were measured in respect to the columns about

one-fourth in. of the deflection was attributed to high finishing around the columns and low finishing at mid-panel.

This structure exhibited an unacceptable amount of deflection and ultimately required extensive filling with lightweight aggregate concrete to achieve level floor surfaces. Investigation into the causes of the extraordinarily large deflections revealed a number of contributing factors. The aggregate used caused abnormally high shrinkage resulting in extensive cracking. Coring and x-ray examination showed that a large number of the reinforcing bars in the negative moment areas around the columns had been placed below the specified elevation. Also the structure had been erected during a wet season and the third floor was rained on during casting. The shoring was removed after about 20 days and the still uncured floor was then loaded. These factors all serve to show that the best design is worthless unless the construction is carefully controlled.

6. DESIGN CONSIDERATIONS

6.1 Introductory Remarks

The purpose of making a frame analysis is to determine whether or not a proposed design will prove unserviceable because of excessive deflections. If the computed deflections are felt to be objectionable then the design may either be revised or a certain amount of camber may be provided. The camber may be introduced into the structure by constructing the mid-panel and mid-beam points of the formwork above grade by amounts equal to the long-time deflections calculated for the permanent load.

Certain types of construction are particularly susceptible to developing unacceptable deflections. Flat slab and flat plate structures, being the most flexible form of structure, are those that most often show excessive deflections. A flat plate floor erected by the "lift-slab" technique is normally supported by steel columns affording very small support areas and restraint. Hence this type of structure is probably most prone to developing objectionable deflections. Some lift-slab structures are designed with cantilever portions of the slab extending beyond the edge columns. These cantilever portions act to decrease the deflections of the edge and corner panels.

In previous chapters the frame analysis has been shown to give good results in the prediction of deflections of nine-panel test structures. In the following section the application of the frame analysis to multiple-panel floor slabs with nonsymmetrical layouts is discussed. The discussion is based on the assumption that analysis will be performed on structures with all panels uniformly loaded.

6.2 Nonsymmetrical Layouts

Consider the schematic layout of a typical multiple-panel structure shown in Fig. 6.1. In order to determine the mid-panel deflection of panel A it is necessary to analyze three and perhaps four frames. If these frames were taken as extending the full width of the structure a prohibitive amount of labor would be required in their analyses. Since it may be expected that a column more than two panels from a discontinuous edge will undergo little rotation about an axis parallel to that edge, it may be assumed that each of the frames is fixed at the third column from the edge. Based on this assumption the frames to be used in computing the deflections of panel A are those shown either as shaded or as bordered by broken lines in Fig. 6.1.

If the two east-west oriented frames, numbered 1 and 2 in Fig. 6.1, are similar then only one of these frames need be analyzed. The effect of the rotation of frame number 1 about its longitudinal axis on the deflections of panels A and C is found by analyzing frames 3 and 4. The final mid-panel deflection of panel A is the sum of the average of the mid-span deflections of the longer supporting beams, the effect of the edge rotation, and the factor determined using the S-method.

The mid-panel deflection of panel B may be found using the frame analysis. However, if the supporting beams in the long direction are similar then the deflection may be predicted reasonably well using the tabulated deflection coefficients of Tables 7, 10 and 13. That this is true even for the interior panel of the test structures described in Chapter 5 is shown by the following comparison of computed with tabulated coefficients. All coefficients are of qL^4/D . For panels located more than two panels from a discontinuous edge tabulated coefficients may be used.

Slab No.	Computed Coefficients		Coefficients from Table 10	
	Mid-panel	Mid-beam	Mid-panel	Mid-Beam
1 (F1)	0.00424	0.00289	0.00441	0.00304 ($H=0, \frac{c}{L} = 0.1$)
2 (F2)	0.00287	0.00162	0.00289	0.00173 ($H=0, \frac{c}{L} = 0.2$)
3 (T1)	0.00194	0.00048	0.00161	0.00035 ($H=3.6, \frac{c}{L} = 0.1$)
4 (T2)	0.00273	0.00132	0.00258	0.00130 ($H=0.6, \frac{c}{L} = 0.1$)

Note that the coefficients given for slab No. 2 (F2) are for a c/L ratio of 0.2. This ratio corresponds to the size of the column capital at the line of intersection of the capital with the bottom of the drop panel. The curvature occurring within the limits of the column capital would contribute to the deflections but this contribution would be offset to some extent by the stiffening effect of the drop panel. Finite difference solutions for a square panel containing a drop panel showed the presence of the drop decreased the mid-beam and mid-panel deflections by less than one percent compared with the same panel without drops. The case considered was one for which $H = 0$ and $c/L = 0.2$. The thickness through the drop was taken as twice that of the remaining panel. The width of the drop from an edge to the adjacent column face was taken as one-twentieth of the span.

7. SUMMARY AND CONCLUSIONS

7.1 Summary

An adequate design of a structure must provide for both safety and serviceability. Safety is assured if the requisite strength is provided. The purpose of this study was to develop a means of determining whether a design which provided adequate strength would also meet the serviceability criterion of deflections. To this end the current building code provisions concerning deflections were examined. The discussion of these codes included in Chapter 2 points out that all of the codes attempt to control deflections by insuring adequate rigidity through specifying minimum thicknesses or minimum thickness-to-span ratios.

The classical theoretical methods of finding solutions for deflections of plates are discussed in Chapter 3. Here it is shown that the deflections of a panel in an ideally elastic structure are influenced by the size and shape of the panel, the size and flexural stiffness of the supporting columns, the flexural and torsional rigidity of the supporting beams, and the type and extent of the loading. Solutions for interior plates supported on rigid columns of finite cross-sectional area are given for the first time.

Based on the concept of the way in which a continuous structure deforms, an approximate method of analysis for deflections is developed in Chapter 4. This method is applicable to continuous uniformly loaded structures containing rectangular panels supported at their corners. Solutions for interior plates on flexible supports showed that the lines of inflection for bending moments in the directions of the long and short spans were located about one-fifth the span considered from the supporting beams. The approximate method consists of finding the mid-beam deflections by selecting portions of

the three-dimensional structures for analyses as two-dimensional frames. Each of the frames is taken as including a row of columns and beams and extending from a discontinuous edge of the structure to an interior point which may be assumed to undergo no rotation. The width of the frame is taken as including one-fifth the width of each panel lying on either side of the column center-line. The loading to be applied to the frame includes that on the frame plus additional portions of the total load on each of the contiguous panels. These additional portions are defined as functions of the ratios of sides and beam-to-slab rigidities. Once the mid-beam deflections have been determined the mid-panel deflections are found using the mid-beam deflections plus a second procedure.

The frame analysis was used to compute the deflections of 33 cases of mathematical models of nine-panel elastic structures for which the column and beam stiffnesses were known. The deflections of these structures for a uniform loading had previously been determined using finite differences. The results of the analyses showed good agreement between computed and finite difference solutions for the 27 cases for which all panels were loaded. For the six cases for which only the interior and corner panels were loaded the solutions found using the two procedures gave poorer agreement. However, for these cases the theoretical deflections were in most cases less for the partial loadings than for all panels loaded.

In addition to the factors affecting deflections of ideally elastic structures, the deflections of reinforced concrete structures are further influenced by cracking of the concrete, yielding of the reinforcement, the nonlinearity of the stress-strain curve for concrete, and the time-dependent behavior of concrete. Applications of the approximate procedure to the analyses of real reinforced concrete structures are discussed in Chapter 5.

The results obtained show good agreement in most cases between predicted deflections and the deflections measured while the structure was nearly uncracked. The poorest agreement between measured and predicted deflections was for the deep beams in the flat plate and flat slab test structures and for the beams of the two-way slab with deep beams. A method of predicting the shape of the load-deflection curve between cracking and yielding is given. Additional design considerations and discussions of the analyses of non-symmetrical layouts are given in Chapter 6.

7.2 Conclusions

The current building code provisions on deflections consider, in an implicit manner, only a few of the many factors affecting deflections. Hence the thickness and thickness-to-span limitations prescribed by the codes cannot be expected to prevent excessive deflections in all cases.

The frame analysis method does take into account all of the factors affecting deflections of both ideally elastic and reinforced concrete structures. In using the frame analysis to compute the deflections of a structure the loading case to be considered is that of all panels uniformly loaded. The data available indicate that while pattern loadings cause maximum moments at various points they seldom cause maximum deflections, and when they do cause maximum deflections these are usually not appreciably larger than the deflections for all panels loaded. Hence the major effect of pattern loadings appears to be that of causing additional cracking which in turn may help to increase deflections.

The efficacy of the frame analysis method was shown by the results of analyses of both ideally elastic and reinforced concrete structures. The structures considered all contained nine square panels arranged three-by-three.

Additional tests of structures containing more panels with other arrangements of panel layouts are required to prove that the method may be extended to these cases. However, for structures with nonsymmetrical regular layouts the frame analyses may be expected to give acceptable results.

The major unknown in predicting the total deflections of a reinforced concrete slab, other than the amount of the live load to assume as acting permanently, is how much increase in deflection will be caused by time-dependent effects. This is one area in which much additional research effort is still required. Additional information is also needed concerning how much relative deflection can be tolerated by different types of construction supported on slabs.

The frame analysis procedure developed in this report makes available a method of predicting deflections of multiple-panel reinforced concrete floor slabs. The application of the procedure does not require an excessive amount of office time and computations need only be made to within slide rule accuracy.

BIBLIOGRAPHY

1. American Concrete Institute, Building Code Requirements for Reinforced Concrete, (ACI 318-56).
2. Nichols, J. R., "Statistical Limitations Upon the Steel Requirement in Reinforced Concrete Flat Slab Floors," ASCE Transactions, Vol. 77, 1914, pp. 1670-1681.
3. Westergaard, H. M., and W. A. Slater, "Moments and Stresses in Slabs," ACI Proceedings, Vol. 17, 1921, pp. 415-538.
4. Westergaard, H. M., "Formulas for the Design of Rectangular Floor Slabs and their Supporting Girders," ACI Proceedings, Vol. 22, 1926, pp. 26-46.
5. Di Stasio, J., and M. P. Van Buren, "Slabs Supported on Four Sides," ACI Proceedings, Vol. 32, 1936, pp. 350-364.
6. "Proposed Revision of Building Code Requirements for Reinforced Concrete (ACI 318-56)," ACI Proceedings, Vol. 59, 1962, pp. 145-276.
7. Casillas, J., and C. P. Siess, "Comparative Studies of Design Procedures for Two-Way Reinforced Concrete Slabs," Structural Research Series No. 215, Department of Civil Engineering, University of Illinois, June 1961.
8. Fluhr, W. E., A. Ang, and C. P. Siess, "Theoretical Analysis of the Effects of Openings on the Bending Moments in Square Plates with Fixed Edges," Structural Research Series No. 203, Department of Civil Engineering, University of Illinois, July 1960.
9. Simmonds, S. H., and C. P. Siess, "Effects of Column Stiffness on the Moments in Two-Way Floor Slabs," Structural Research Series No. 253, Department of Civil Engineering, University of Illinois, July 1962.
10. Mayes, G. T., M. A. Sozen, and C. P. Siess, "Tests on a Quarter-Scale Model of a Multiple-Panel Reinforced Concrete Flat Plate Floor," Structural Research Series No. 181, Department of Civil Engineering, University of Illinois, September 1959.
11. Hatcher, D. S., M. A. Sozen, and C. P. Siess, "An Experimental Study of a Reinforced Concrete Flat Slab Floor," Structural Research Series No. 200, Department of Civil Engineering, University of Illinois, June 1960.
12. Gamble, W. L., M. A. Sozen, and C. P. Siess, "An Experimental Study of a Two-Way Floor Slab," Structural Research Series No. 211, Department of Civil Engineering, University of Illinois, June 1961.
13. Hatcher, D. S., M. A. Sozen, and C. P. Siess, "A Study of Tests on a Flat Plate and a Flat Slab," Structural Research Series No. 217, Department of Civil Engineering, University of Illinois, July 1961.

14. Vanderbilt, M. D., M. A. Sozen, and C. P. Siess, "An Experimental Study of a Reinforced Concrete Two-Way Floor Slab with Flexible Beams," Structural Research Series No. 228, Department of Civil Engineering, University of Illinois, November 1961.
15. Jirsa, J. O., M. A. Sozen, and C. P. Siess, "An Experimental Study of a Flat Slab Floor Reinforced with Welded Wire Fabric," Structural Research Series No. 249, Department of Civil Engineering, University of Illinois, June 1962.
16. Gamble, W. L., M. A. Sozen, and C. P. Siess, "Measured and Theoretical Bending Moments in Reinforced Concrete Floor Slabs," Structural Research Series No. 246, Department of Civil Engineering, University of Illinois, June 1962.
17. Wood, R. H., "Plastic and Elastic Design of Slabs and Plates," Thames and Hudson, London, 1961.
18. Report of Committee No. 10, Slabs, Bulletin D'Information No. 29, Comité Européen du Béton, 8 Avenue de L'Arsenal, Luxembourg, November 1960.
19. "Specifications for Design Methods, Comments, and Numerical Examples Relating to Regulations for Design of Massive Concrete Slabs," Swedish State Concrete Committee, 1957.
20. "Instruction for the Design of Statically Indeterminant Reinforced Concrete Structures with Consideration of Stress Redistribution," Academy of Building and Architecture USSR, Institute of Scientific Research on Plain and Reinforced Concrete (NIIZhB), Moscow, 1960. [English translation available as Foreign Literature Study No. 330, Library, Portland Cement Association]
21. Sachnowski, K. W., "Stahlbetonkonstruktionen," Veb Verlag Technik, Berlin, 1956.
22. "Regles Pour Le Calcul et L'Execution des Constructions en Beton Arme," Regles BA 1960, La Documentation Technique du Batiment et des Travaux Publics, Paris, December 1960.
23. Timoshenko, S. P., and S. Woinowsky-Krieger, "Theory of Plates and Shells," Second Edition, McGraw-Hill Book Co., New York, 1959.
24. Fuchs, S. J., "Plates with Boundary Conditions of Elastic Support," ASCE Transactions, Vol. 119, 1954, p. 935.
25. Duncan, W. J., "Normalized Orthogonal Deflexion Functions for Beams," Aero. Res. Council, R. and M. 2281, 1951, p. 23.
26. Sutherland, J. G., L. E. Goodman, and N. M. Newmark, "Analysis of Plates Continuous over Flexible Beams," Structural Research Series No. 42, Department of Civil Engineering, University of Illinois, January 1953.

27. Ang, A., "The Development of a Distribution Procedure for the Analysis of Continuous Rectangular Plates," Structural Research Series No. 176, Department of Civil Engineering, University of Illinois, May 1959.
28. Ewell, W. W., Okubo, and J. I. Abrams, "Deflections in Gridworks and Slabs," ASCE Transactions, Vol. 117, 1952, pp. 869-912.
29. Marsh, C. F., "Reinforced Concrete," D. Van Nostrand Co., New York, 1904, p. 283.
30. Marcus, H., "Die Theorie elasticsher Gewebe und ihre Anwendung auf die Berechnung biegsamer Platten," Julius Springer, Berlin, 1932.
31. Modern Developments in Reinforced Concrete No. 22, Portland Cement Association, Chicago.
32. "Study Regarding the Design of T-Sections (T-Beams) with Consideration of Present Codes," Comité Européen du Béton, Bulletin D'Information No. 8, Committee No. 9, T-Beams, November 1958.
33. Brendel, G., "Study Regarding the Design of T-Beams with Consideration of Present Codes," Dresden, 1958.
34. Corley, W. G., M. A. Sozen, and C. P. Siess, "The Equivalent Frame Analysis for Reinforced Concrete Slabs," Structural Research Series No. 218, Department of Civil Engineering, University of Illinois, June 1961.
35. Timoshenko, S. P., and J. N. Goodier, "Theory of Elasticity," Second Edition, McGraw-Hill Book Company, New York, 1951, p. 277.
36. Nylander, H., "Torsion and Torsional Restraint of Concrete Structures," (in Swedish), Statens Kommitté för Byggnadsforskning, No. 3, Meddelanden, Stockholm, 1945.
37. Mila, F. J., "Relationship Between Reinforcement Strain and Bending Moment in Reinforced Concrete," a report of the research project "Investigation of Multiple-Panel Reinforced Concrete Floor Slabs," Department of Civil Engineering, University of Illinois, July 1960.
38. McHenry, D., and J. J. Shideler, "Review of Data on Effect of Speed in Mechanical Testing of Concrete," Bulletin D9, Development Department, Portland Cement Association.
39. Hansen, T. C., "Creep and Stress Relaxation of Concrete," Proceedings No. 31, Swedish Cement and Concrete Research Institute at the Royal Institute of Technology, Stockholm, 1960.
40. "Tentative Building Regulations for Reinforced Concrete," ACI Proceedings, Vol. 24, 1928, pp. 791-833. (Adopted after ammendments as ACI E-14-28T)
41. Jensen, V. P., "Ultimate Strength of Reinforced Concrete Beams as Related to the Plasticity Ratio of Concrete," Engineering Experiment Station Bulletin No. 345, University of Illinois, 1943.

42. Sutherland, H., and R. C. Reese, "Reinforced Concrete Design" (with chapters by Inge Lyse), John Wiley, New York, 1943, p. 36.
43. Pauw, A., "Static Modulus of Elasticity of Concrete as Affected by Density," ACI Proceedings, Vol. 57, 1960, pp. 679-688.
44. Lord, A. R., "Extensometer Measurements in a Reinforced Concrete Building Over a Period of One Year," ACI Proceedings, Vol. 13, 1917, pp. 45-60.
45. Slater, W. A., A. Hagener, and G. P. Anthes, "Test of a Hollow Tile and Concrete Floor Slab Reinforced in Two Directions," Technologic Papers of the Bureau of Standards, Vol. 16, 1923, pp. 727-796.
46. Experimental Lightweight Flat Plate Structure, Part III, Long-Term Deformations, Commonwealth Scientific and Industrial Research Organisation, Constructional Review, Vol. 34, April 1961.
47. Corley, W. G., and M. A. Sozen, unpublished report, Department of Civil Engineering, University of Illinois.

TABLE 1

BUILDING CODE LIMITATIONS ON $\frac{\text{THICKNESS}}{\text{SPAN}}$ RATIOS

	Slabs Supported in One Direction		Slabs Supported in Two Directions	
Country	Simply Supported	Fixed	Simply Supported	Fixed
Austria	$\frac{d}{L} \geq \frac{1}{35}$	$\frac{d}{L_o} \geq \frac{1}{35}$ or $\frac{d}{L} \geq \frac{4}{5} \frac{1}{35}$	$\frac{d}{L_{min}} \geq \frac{1}{50}$	$\frac{d}{L_{min}} \geq \frac{1}{60}$
Germany	"	"	"	"
Greece	[May be decreased to $\frac{d}{L} \geq \frac{1}{40}$ if		[Valid only if $\frac{L_{max}}{L_{min}} \leq \frac{3}{2}$, Otherwise	
Portugal	slab is seldom loaded]		use $\frac{1}{35}$]	
Turkey	"	"	"	"
Great Britain	$\frac{t}{L} \geq \frac{1}{30}$	$\frac{t}{L} \geq \frac{1}{35}$		
	[$\frac{t}{L} \geq \frac{1}{12}$ for cantilever slab]		$\frac{t}{L} \geq \frac{1}{35}$	$\frac{t}{L} \geq \frac{1}{40}$
Poland	$\frac{d}{L} \geq \frac{1}{35}$	$\frac{d}{L} \geq \frac{1}{40}$	$\frac{d}{L_{min}} \geq \frac{1}{35}$	$\frac{d}{L_{min}} \geq \frac{1}{50}$
			[For $\frac{L_{max}}{L_{min}} > 2$ use $\frac{1}{35}$]	
Yugoslavia	$\frac{d}{L_o} \geq \frac{1}{30}$		$\frac{d}{L_o} \geq \frac{1}{35}$	
U.S.A. (1956)			Two way: $t \geq \frac{\text{perimeter}}{180}$ Flat Slabs: $\frac{t}{L} \geq \frac{1}{40}$ if drop panels $\geq \frac{1}{3}L$; $\frac{t}{L} \geq \frac{1}{36}$ otherwise	
France	Minimum d/L ratio is a function of bending moment. See Appendix A.			

Notation: d = depth from compression face to center of tensile reinforcement
t = total thickness
L = span
L_o = span between lines of inflection
L_{min} = minimum span between opposite supports of slabs supported in two directions
L_{max} = maximum span between opposite supports of slabs supported in two directions

TABLE 2

BUILDING CODE MINIMUM THICKNESS LIMITATIONS

Two-way Slabs			Flat Slabs	Reference
Country	General	Roof		
Austria	7cm=2.76 in.	5cm=1.97 in.	15cm = 5.9 in.	DIN 1045 Art.22.2
Germany	"	"	"	
Greece	"	"	"	
Portugal	"	"	"	
Turkey	"	"	"	
France	5cm if cast in place, and nonmonolithic, $\frac{4}{3}$ if cast in place monolithically, $\frac{3}{4}$ above if prefabricated		Same as two-way	Regles B.A. 1960, Art. 4.36
Netherlands	8cm=3.15 in.	7cm	$\frac{1}{40}$ span if drops $\frac{1}{36}$ span, no drops	Gewapend Beton-voorschriften G.B.U. 1950 - Art. 24
Poland	none		15cm or $\frac{1}{32}$ span 12 or $\frac{1}{40}$ span if roof	Konstruckeje Zebsture PN - 56/B-03260 Art. 5.4.4
Sweden	d = 6cm = 2.36 in.		15cm or $\frac{1}{32}$ span	Statliga Betongbestimmelser 1957
Argentina			15cm	Codigo de la Edificacion Art. 8.7.1.5.
Spain			$\frac{1}{35}$ short span	Règlement du Ministère des Travaux Publics pour Le Béton Arme - Art. 46
U.S.A.	10.2cm=4 in. or $\frac{\text{Perimeter}}{180}$		$\frac{1}{40}$ span or 4 in. with drop panels $\frac{1}{36}$ span or 5 in. if no drops	ACI 318-56
Great Britain	Thickness governed by minimum thickness to span ratios only			Code of Practice No. 114 (1957) Art. 309.d

TABLE 3

COMPARISON OF THICKNESSES REQUIRED FOR U. OF I.
TEST SLABS BY VARIOUS BUILDING CODES

Country	Flat Slabs			Two-Way Slabs		
	Required Thickness	Criterion Which Controls		Required Thickness	Criterion Which Controls	
		Minimum t	Minimum t/L*		Minimum t	Minimum t/L*
Design	7"			6"		
U.S.	6"	(4")	+	5"	Perimeter 180	
Austria	5.9"	+	(5")	5"	(2.75")	+
Germany	5.9"	+		5"	(2.75")	+
Greece	5.9"	+		5"	(2.75")	+
Portugal	5.9"	+		5"	(2.75")	+
Turkey	5.9"	+		5"	(2.75")	+
France	8.5"	(1.6")	+	8.5"	(1.6")	+
Argentina	5.9"	+	NR**	--	NR**	
Poland	7.5"	(5.9")	+		NR	
Netherlands	6"	NR	+	3.2"	+	NR
Sweden	7.5"	(5.9")	+	3.4"		
Spain	6.9"	NR	+		NR	
Great Brit.	6"	NR	+	6"	NR	+
Yugoslavia	8"	NR	+	8"	NR	+

* Where a code specified a minimum effective d, a cover of 1" was assumed, i.e., $t = d + 1$ ". The span was taken as 240 inches in all cases.

** NR = no requirement.

+ Indicates controlling criterion.

Note: The minimum thickness formulae of the Swedish and Netherlands codes control the thicknesses for these cases. (See page 20.)

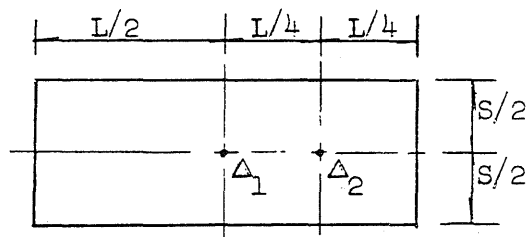
TABLE 4

DEFLECTIONS OF UNIFORMLY LOADED RECTANGULAR
PLATES ON NONDEFLECTING SUPPORTS

(Reference 23)

Case 1

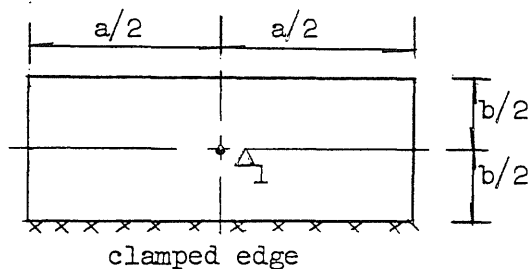
All Edges Simply Supported



L/S	S/L	$\Delta_1 D / qS^4$	$\Delta_2 D / qS^4$	L/S	S/L	$\Delta_1 D / qS^4$	$\Delta_2 D / qS^4$
1.0	1.0	0.00406	0.00293	1.8	0.56	0.00931	0.00666
1.1	0.91	0.00485	0.00350	1.9	0.53	0.00974	0.00696
1.2	0.83	0.00564	0.00407	2.0	0.50	0.01013	0.00724
1.3	0.77	0.00638	0.00460	3.0	0.33	0.01223	0.00872
1.4	0.71	0.00705	0.00508	4.0	0.25	0.01282	0.00914
1.5	0.67	0.00772	0.00553	5.0	0.20	0.01297	0.00924
1.6	0.62	0.00830	0.00594	∞	0	0.01302	0.01302
1.7	0.59	0.00883	0.00631				

Case 2

Three Edges Simply Supported, One Edge Clamped

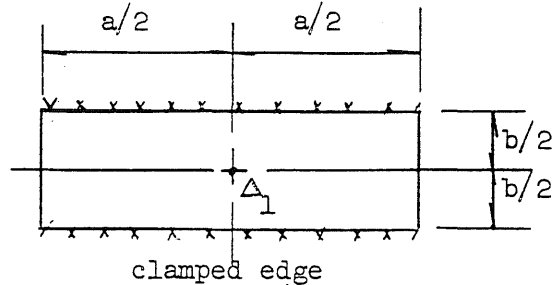


b/a	$\Delta_1 D / qb^4$	b/a	$\Delta_1 D / qa^4$
1.00	0.0028	1.1	0.0035
0.91	0.0032	1.2	0.0043
0.83	0.0035	1.3	0.0050
0.77	0.0038	1.4	0.0058
0.71	0.0040	1.5	0.0064
0.67	0.0042	2.0	0.0093
0.50	0.0049	∞	0.0130
0	0.0052		

TABLE 4 (Continued)

Case 3

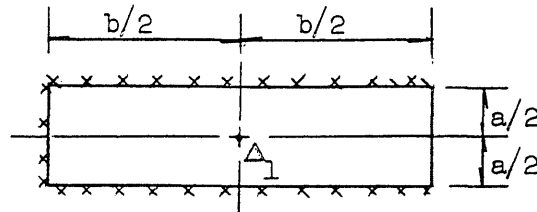
Two Opposite Edges Simply Supported, Two Edges Clamped



$b > a$			$b < a$		
b/a	$\Delta_1 D / qa^4$	b/a	$\Delta_1 D / qa^4$	a/b	$\Delta_1 D / qb^4$
1.0	0.00192	1.7	0.00668	1.0	0.00192
1.1	0.00251	1.8	0.00732	1.1	0.00209
1.2	0.00319	1.9	0.00790	1.2	0.00223
1.3	0.00388	2.0	0.00844	1.3	0.00234
1.4	0.00460	3.0	0.01168	1.4	0.00240
1.5	0.00531	∞	0.01302	1.5	0.00247
1.6	0.00603			2.0	0.00260
				∞	0.00260

Case 4

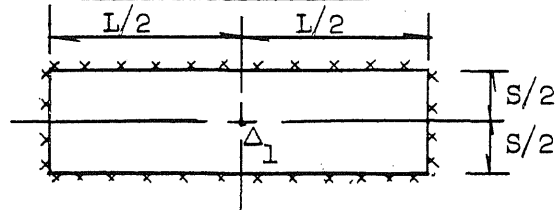
One Edge Simply Supported, Three Edges Clamped



$b/a = 2.0$	1.33	1.0	0.75	0.50
$\Delta_1 D / qb^4 = 0.000161$	0.000680	0.00157	0.00286	0.00449

Case 5

Four Edges Clamped

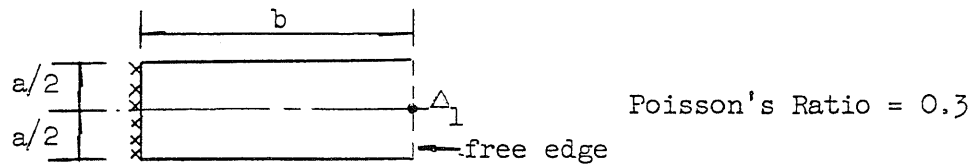


L/S	S/L	$\Delta_1 D / qS^4$	L/S	S/L	$\Delta_1 D / qS^4$
1.0	1.00	0.00126	1.6	0.62	0.00230
1.1	0.91	0.00150	1.7	0.59	0.00238
1.2	0.83	0.00172	1.8	0.56	0.00245
1.3	0.77	0.00191	1.9	0.53	0.00249
1.4	0.71	0.00207	2.0	0.50	0.00254
1.5	0.67	0.00220	∞	0	0.00260

TABLE 4 (Continued)

Case 6

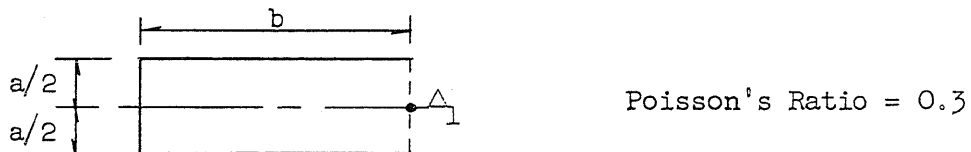
Two Edges Simply Supported, One Edge Clamped, One Edge Free



b/a	$\Delta_1 D / qb^4$	b/a	$\Delta_1 D / qa^4$
0	0.1250	3/2	0.0141
1/3	0.0940	2	0.0150
1/2	0.0582	3	0.0152
2/3	0.0335	∞	0.0152
1	0.0113		

Case 7

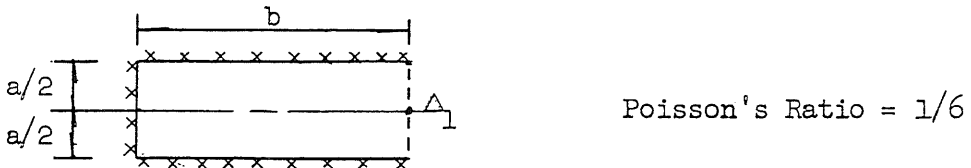
Three Edges Simply Supported, One Edge Free



b/a	$\Delta_1 D / qa^4$	b/a	$\Delta_1 D / qa^4$
0.50	0.00710	1.1	0.01341
0.67	0.00968	1.2	0.01384
0.72	0.01023	1.3	0.01417
0.79	0.01092	1.4	0.01442
0.83	0.01158	1.5	0.01462
0.91	0.01232	2.0	0.01507
1.00	0.01286	3.0	0.01520
		∞	0.01522

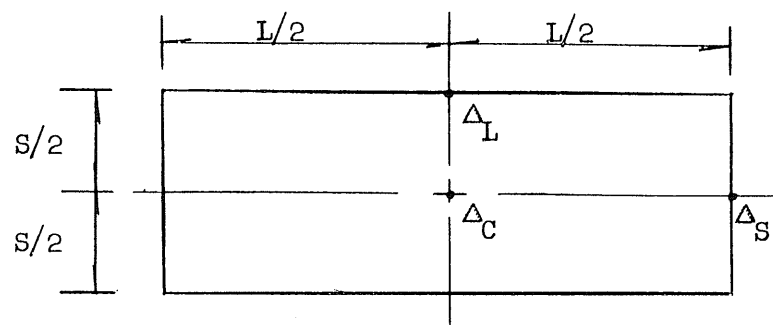
Case 8

Three Edges Clamped, One Edge Free



b/a	$\Delta_1 D / qa^4$	b/a	$\Delta_1 D / qa^4$
0.6	0.00271	1.0	0.00333
0.7	0.00292	1.25	0.00345
0.8	0.00308	1.5	0.00335
0.9	0.00323		

TABLE 5
DEFLECTIONS OF PLATES CONTINUOUS OVER FLEXIBLE BEAMS
(REFERENCE 26)



s/L	λ_L	λ_S	H_L	H_S	Δ_C^*	Δ_S^*	Δ_L^*	I_S/I_L
1.0	∞	∞	∞	∞	0.001265	0	0	-
	∞	5.0	∞	5.0	0.001435	0.0003324	0	0
	∞	2.0	∞	2.0	0.001622	0.0006977	0	0
	∞	1.0	∞	1.0	0.001829	0.001101	0	0
	∞	0.5	∞	0.5	0.002059	0.001549	0	0
	∞	0	∞	0	0.002604	0.002604	0	0
	5.0	5.0	5.0	5.0	0.001622	0.0003484	0.0003484	1.0
	5.0	2.0	5.0	2.0	0.001827	0.0007331	0.0003661	0.4
	5.0	1.0	5.0	1.0	0.002058	0.001160	0.0003860	0.2
	5.0	0.5	5.0	0.5	0.002315	0.001636	0.0004084	0.1
	5.0	0	5.0	0	0.002932	0.002772	0.0004639	0
	2.0	2.0	2.0	2.0	0.002058	0.0007726	0.0007726	1.0
	2.0	1.0	2.0	1.0	0.002315	0.001226	0.0008173	0.5
	2.0	0.5	2.0	0.5	0.002604	0.001736	0.0008681	0.25
	2.0	0	2.0	0	0.003311	0.002968	0.0009968	0
	1.0	1.0	1.0	1.0	0.002604	0.001302	0.001302	1.0

* Coefficients of qL^4/D

TABLE 5 (Continued)
DEFLECTIONS OF PLATES CONTINUOUS OVER FLEXIBLE BEAMS

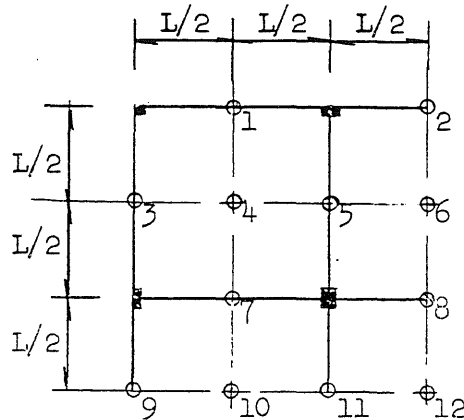
S/L	λ_L	λ_S	H_L	H_S	Δ_C^*	Δ_S^*	Δ_L^*	I_S/I_L
1.0	1.0	0.5	1.0	0.5	0.002933	0.001851	0.001389	0.5
	1.0	0	1.0	0	0.003754	0.003201	0.001616	0
	0.5	0.5	0.5	0.5	0.003312	0.001985	0.001985	1.0
	0.5	0	0.5	0	0.004284	0.003483	0.002346	0
	0	0	0	0	0.005800	0.004350	0.004350	-
0.8	∞	∞	∞	∞	0.0007463	0	0	-
	5.0	5.0	6.25	4.0	0.001017	0.0001506	0.0003179	0.8
	2.0	2.0	2.5	1.6	0.001345	0.0003425	0.0006962	0.8
	1.0	1.0	1.25	0.8	0.001750	0.0005926	0.001157	0.8
	0.5	0.5	0.625	0.4	0.002270	0.0009287	0.001739	0.8
	0.2	0.2	0.25	0.16	0.002973	0.001405	0.002508	0.8
	0	0	0	0	0.004052	0.002185	0.003654	-
	5.0	6.25	6.25	5.0	0.001008	0.0001236	0.0003165	1.0
	2.0	2.5	2.5	2.0	0.001324	0.0002894	0.0006902	1.0
	1.0	1.25	1.25	1.0	0.001717	0.0005169	0.001144	1.0
	0.89443	1.11803	1.11803	0.89443	0.001793	0.0005631	0.001230	1.0
	0.50	0.625	0.625	0.50	0.002226	0.0008402	0.001715	1.0
0.5	∞	∞	∞	∞	0.0001584	0	0	-
	5.0	5.0	10.0	2.5	0.0003756	0.0000243	0.0002309	0.5
	2.0	2.0	4.0	1.0	0.0006417	0.0000588	0.0005133	0.5
	1.0	1.0	2.0	0.5	0.0009766	0.0001085	0.0008681	0.5
	0.5	0.5	1.0	0.25	0.001413	0.0001828	0.001329	0.5
	0	0	0	0	0.002914	0.0005301	0.002900	-
	5.0	10.0	5.0	10.0	0.0003747	0.0000130	0.0002303	1.0
	2.0	4.0	4.0	2.0	0.0006385	0.0000339	0.0005108	1.0
	1.0	2.0	2.0	1.0	0.0009686	0.0000686	0.0008611	1.0
	0.70711	1.41421	1.41421	0.70711	0.001174	0.0000953	0.001079	1.0
	0.5	1.0	1.0	0.5	0.001397	0.0001292	0.001314	1.0

* Coefficients of qL^4/D

TABLE 6

DEFLECTIONS OF A NINE-PANEL SLAB

$H = J = 0, K = \infty, c/L = 0.1$ Poisson's Ratio = 0
(Reference 27)



1	2	3
4	5	6
7	8	9

Panel Designation

Point No.	Deflections for Panels 2, 5, 8, Loaded	Deflections for Panels 1, 4, 7, Loaded	Deflections for all Panels Loaded
1	-0.0001	0.0029	0.0028
2	0.0028	-0.0002	0.0024
3	0	0.0028	0.0028
4	-0.0001	0.0055	0.0054
5	0.0017	0.0018	0.0035
6	0.0049	0	0.0049
7	-0.0002	0.0037	0.0035
8	0.0035	-0.0002	0.0031
9	0	0.0024	0.0024
10	-0.0001	0.0050	0.0049
11	0.0016	0.0015	0.0031
12	0.0045	-0.0001	0.0043

Note: All deflections are given as coefficients of qL^4/D

TABLE 7
DEFLECTION COEFFICIENTS FOR INTERIOR PANELS

$$I_S = I_L$$

Location			Center of Panel			Center of Long Beam			Center of Short Beam		
c/L ratios =			0.0	0.1	0.2	0.0	0.1	0.2	0.0	0.1	0.2
S/L	H _L	H _S									
0.8	0.0	0.0	0.00420	0.00301	0.00189	0.00378	0.00262	0.00155	0.00230	0.00131	0.00057
	0.2	0.16	0.00316	0.00237	0.00159	0.00271	0.00192	0.00116	0.00149	0.00088	0.00040
	0.5	0.4	0.00246	0.00191	0.00136	0.00195	0.00138	0.00085	0.00099	0.00059	0.00028
	1.0	0.8	0.00191	0.00154	0.00117	0.00134	0.00095	0.00058	0.00063	0.00038	0.00018
	2.0	1.6	0.00147	0.00124	0.00100	0.00083	0.00058	0.00036	0.00036	0.00022	0.00011
	4.0	3.2	0.00116	0.00103	0.00089	0.00048	0.00033	0.00020	0.00019	0.00012	0.00006
0.6	0.0	0.0	0.00327	0.00234	0.00143	0.00321	0.00228	0.00137	0.00099	0.00040	0.00008
	0.2	0.12	0.00256	0.00189	0.00119	0.00246	0.00178	0.00108	0.00063	0.00027	0.00006
	0.5	0.3	0.00201	0.00150	0.00098	0.00187	0.00134	0.00082	0.00040	0.00017	0.00004
	1.0	0.6	0.00153	0.00116	0.00079	0.00135	0.00096	0.00059	0.00025	0.00011	0.00003
	2.0	1.2	0.00110	0.00085	0.00061	0.00087	0.00061	0.00037	0.00013	0.00006	0.00002
	4.0	2.4	0.00077	0.00063	0.00048	0.00051	0.00035	0.00022	0.00007	0.00003	0.00001
0.4	0.0	0.0	0.002843	0.002045	-	0.002841	0.002041	-	0.00031	0.00004	-
	0.2	0.08	0.00231	0.00166	-	0.00230	0.00165	-	0.00020	0.00003	-
	0.5	0.2	0.00183	0.00131	-	0.00181	0.00128	-	0.00012	0.00002	-
	1.0	0.4	0.00137	0.00098	-	0.00134	0.00094	-	0.00007	0.00001	-
	2.0	0.8	0.00093	0.00066	-	0.00088	0.00061	-	0.00004	0.000007	-
	4.0	1.6	0.00059	0.00042	-	0.00053	0.00036	-	0.00002	0.000004	-

Note: All deflections given as coefficients of $\frac{qL^4}{D}$

TABLE 8

BENDING MOMENTS IN LONG DIRECTION AT VARIOUS POINTS IN INTERIOR PANELS

$$I_S = I_L$$

Moment Coefficient			m_1/qL^2			$-m_2/qL^2$			m_3^*			$-m_4^*$		
c/L ratios =			0.0	0.1	0.2	0.0	0.1	0.2	0.0	0.1	0.2	0.0	0.1	0.2
S/L	H_L	H_S												
0.8	0.0	0.0	0.0346	0.0315	0.0259	0.0402	0.0351	0.0244	0.0496	0.0399	0.0357	0.2136	0.1243	0.0751
	0.2	0.16	0.0294	0.0264	0.0221	0.0398	0.0362	0.0277	0.0062	0.0055	0.0044	0.0171	0.0131	0.0087
	0.5	0.4	0.0247	0.0221	0.0188	0.0397	0.0369	0.0299	0.0118	0.0104	0.0083	0.0267	0.0220	0.0156
	1.0	0.8	0.0204	0.0183	0.0160	0.0394	0.0370	0.0313	0.0169	0.0146	0.0116	0.0340	0.0289	0.0211
	2.0	1.6	0.0165	0.0150	0.0135	0.0385	0.0367	0.0322	0.0214	0.0183	0.0145	0.0401	0.0344	0.0257
	4.0	3.2	0.0136	0.0126	0.0118	0.0374	0.0362	0.0327	0.0248	0.0209	0.0165	0.0455	0.0382	0.0289
0.6	0.0	0.0	0.0396	0.0353	0.0278	0.0512	0.0406	0.0198	0.0442	0.0396	0.0315	0.1677	0.1100	0.0700
	0.2	0.12	0.0331	0.0288	0.0228	0.0470	0.0380	0.0196	0.0043	0.0038	0.0031	0.0116	0.0093	0.0063
	0.5	0.3	0.0268	0.0229	0.0182	0.0429	0.0348	0.0191	0.0086	0.0075	0.0060	0.0193	0.0165	0.0117
	1.0	0.6	0.0206	0.0173	0.0140	0.0382	0.0313	0.0183	0.0126	0.0109	0.0086	0.0258	0.0225	0.0164
	2.0	1.2	0.0146	0.0122	0.0102	0.0329	0.0275	0.0175	0.0166	0.0141	0.0111	0.0318	0.0277	0.0206
	4.0	2.4	0.0098	0.0083	0.0073	0.0280	0.0244	0.0169	0.0197	0.0166	0.0130	0.0363	0.0313	0.0236
0.4	0.0	0.0	0.0416	0.0362	-	0.0630	0.0372	-	0.0421	0.0368	-	0.1269	0.0965	-
	0.2	0.08	0.0347	0.0297	-	0.0551	0.0316	-	0.0028	0.0024	-	0.0069	0.0058	-
	0.5	0.2	0.0278	0.0234	-	0.0470	0.0263	-	0.0056	0.0048	-	0.0123	0.0108	-
	1.0	0.4	0.0209	0.0173	-	0.0384	0.0212	-	0.0084	0.0071	-	0.0172	0.0151	-
	2.0	0.8	0.0140	0.0114	-	0.0291	0.0165	-	0.0112	0.0093	-	0.0219	0.0190	-
	4.0	1.6	0.0085	0.0069	-	0.0212	0.0129	-	0.0134	0.0111	-	0.0256	0.0219	-

* Coefficients of qL^3 except that for $H_L = H_S = 0.0$ the coefficient is of qL^2 .

TABLE 9
BENDING MOMENTS IN SHORT DIRECTION AT VARIOUS POINTS IN INTERIOR PANELS
 $I_S = I_L$

Moment Coefficient			m_5/qL^2			$-m_6/qL^2$			m_7^*			$-m_8^*$		
c/L ratios =			0.0	0.1	0.2	0.0	0.1	0.2	0.0	0.1	0.2	0.0	0.1	0.2
S/L	H_L	H_S												
0.8	0.0	0.0	0.0124	0.0116	0.0104	0.0130	0.0121	0.0103	0.0450	0.0376	0.0254	0.1946	0.0856	0.0380
	0.2	0.16	0.0126	0.0124	0.0118	0.0172	0.0175	0.0169	0.0053	0.0043	0.0029	0.0144	0.0087	0.0045
	0.5	0.4	0.0132	0.0134	0.0131	0.0221	0.0231	0.0229	0.0093	0.0074	0.0050	0.0209	0.0140	0.0080
	1.0	0.8	0.0141	0.0144	0.0143	0.0272	0.0283	0.0283	0.0123	0.0097	0.0066	0.0246	0.0176	0.0106
	2.0	1.6	0.0150	0.0154	0.0153	0.0322	0.0332	0.0330	0.0145	0.0114	0.0078	0.0268	0.0201	0.0127
	4.0	3.2	0.0159	0.0162	0.0160	0.0362	0.0369	0.0364	0.0157	0.0124	0.0087	0.0278	0.0216	0.0140
0.6	0.0	0.0	0.0034	0.0034	0.0033	0.0034	0.0034	0.0033	0.0337	0.0240	0.0100	0.1318	0.0397	0.0079
	0.2	0.12	0.0047	0.0052	0.0052	0.0070	0.0076	0.0078	0.0029	0.0020	0.0008	0.0078	0.0032	0.0009
	0.5	0.3	0.0062	0.0069	0.0070	0.0110	0.0119	0.0121	0.0049	0.0033	0.0014	0.0111	0.0054	0.0018
	1.0	0.6	0.0079	0.0086	0.0086	0.0152	0.0162	0.0163	0.0063	0.0042	0.0019	0.0127	0.0068	0.0026
	2.0	1.2	0.0097	0.0102	0.0101	0.0194	0.0202	0.0202	0.0070	0.0047	0.0023	0.0132	0.0078	0.0033
	4.0	2.4	0.0111	0.0115	0.0112	0.0229	0.0235	0.0232	0.0073	0.0050	0.0025	0.0137	0.0083	0.0038
0.4	0.0	0.0	0.0003	0.0004	-	0.0003	0.0004	-	0.0230	0.0083	-	0.0748	0.0037	-
	0.2	0.08	0.0013	0.0015	-	0.0023	0.0025	-	0.0013	0.0004	-	0.0032	0.0003	-
	0.5	0.2	0.0024	0.0026	-	0.0044	0.0046	-	0.0021	0.0007	-	0.0046	0.0007	-
	1.0	0.4	0.0034	0.0036	-	0.0066	0.0068	-	0.0025	0.0009	-	0.0051	0.0010	-
	2.0	0.8	0.0046	0.0047	-	0.0088	0.0089	-	0.0027	0.0010	-	0.0057	0.0014	-
	4.0	1.6	0.0055	0.0056	-	0.0105	0.0106	-	0.0028	0.0011	-	0.0059	0.0016	-

* Coefficients of qL^3 except that for $H_L = H_S = 0.0$ the coefficient is of qL^2 .

TABLE 10
DEFLECTION COEFFICIENTS FOR INTERIOR PANELS
 $I_S = (S/L) I_L$

Location			Center of Panel			Center of Long Beam			Center of Short Beam		
c/L ratios =			0.0	0.1	0.2	0.0	0.1	0.2	0.0	0.1	0.2
S/L	H _L	H _S									
1.0	0.0	0.0	0.00581 ⁺	0.00441	0.00289	0.00435 ⁺	0.00304	0.00173	Same as long beam		
	0.2	0.2	0.00438	0.00340	0.00240	0.00299	0.00207	0.00122			
	0.25	0.25	0.00415	0.00324	0.00233	0.00277	0.00192	0.00114			
	0.5	0.5	0.00331*	0.00271	0.00205	0.00198*	0.00141	0.00085			
	1.0	1.0	0.00260	0.00222	0.00179	0.00130	0.00092	0.00056			
	2.0	2.0	0.00206*	0.00184	0.00158	0.00077*	0.00054	0.00033			
	2.5	2.5	0.00196	0.00174	0.00153	0.00065	0.00045	0.00028			
	4.0	4.0	0.00174	0.00159	0.00144	0.00043	0.00030	0.00018			
	5.0	5.0	0.00162*	0.00154	0.00141	0.00035	0.00024	0.00015			
0.8	0.0	0.0	0.00405*	0.00301	0.00189	0.00365*	0.00262	0.00155	0.00218*	0.00131	0.00057
	0.2	0.128	0.00321	0.00240	0.00160	0.00274	0.00193	0.00116	0.00157	0.00093	0.00043
	0.5	0.32	0.00251	0.00193	0.00137	0.00198	0.00139	0.00085	0.00108	0.00065	0.00031
	1.0	0.64	0.00195	0.00156	0.00117	0.00136	0.00095	0.00059	0.00072	0.00043	0.00021
	2.0	1.28	0.00149	0.00125	0.00101	0.00084	0.00058	0.00036	0.00042	0.00026	0.00013
	4.0	2.56	0.00118	0.00104	0.00090	0.00048	0.00033	0.00020	0.00023	0.00014	0.00007
0.6	0.0	0.0	0.00327	0.00234	0.00143	0.00321	0.00228	0.00137	0.00099	0.00040	0.00008
	0.2	0.072	0.00260	0.00190	0.00119	0.00250	0.00178	0.00108	0.00070	0.00030	0.00007
	0.5	0.18	0.00204	0.00151	0.00098	0.00190	0.00135	0.00082	0.00049	0.00022	0.00006
	1.0	0.36	0.00156	0.00116	0.00079	0.00137	0.00096	0.00059	0.00032	0.00015	0.00004
	2.0	0.72	0.00111	0.00085	0.00061	0.00088	0.00061	0.00037	0.00019	0.00009	0.00003
	4.0	1.44	0.00078	0.00063	0.00049	0.00051	0.00035	0.00022	0.00010	0.00005	0.00002
0.4	0.0	0.0	0.002843	0.002045	-	0.002841	0.002041	-	0.00031	0.00004	-
	0.5	0.08	0.00185	0.00131	-	0.00182	0.00128	-	0.00016	0.00003	-
	1.0	0.16	0.00139	0.00098	-	0.00135	0.00094	-	0.00011	0.00002	-
	2.0	0.32	0.00094	0.00066	-	0.00089	0.00061	-	0.00006	0.000013	-
	4.0	0.64	0.00059	0.00042	-	0.00053	0.00036	-	0.00003	0.000009	-

Note: All deflections are given as coefficients of qL^4/D
⁺ Values reported by Timoshenko (Ref.23)
^{*} Values reported by Sutherland (Ref.26)

TABLE 11
BENDING MOMENTS IN LONG DIRECTION AT VARIOUS POINTS IN INTERIOR PANELS
 $I_S = (s/L) I_L$

Moment Coefficient			m_1/qL^2			$-m_2/qL^2$			m_3^*			$-m_4^*$		
c/L ratios =			0.0	0.1	0.2	0.0	0.1	0.2	0.0	0.1	0.2	0.0	0.1	0.2
S/L	H_L	H_S												
1.0	0.0	0.0	0.0278	0.0258	0.0224	0.0302	0.0277	0.0225	0.0577	0.0514	0.0407	0.2627	0.1394	0.0776
	0.2	0.2	0.0248	0.0233	0.0210	0.0336	0.0327	0.0296	0.0086	0.0075	0.0059	0.0233	0.0169	0.0109
	0.25	0.25	0.0243	0.0229	0.0207	0.0344	0.0337	0.0309	0.0101	0.0088	0.0070	0.0260	0.0194	0.0127
	0.5	0.5	0.0225 ⁺	0.0215	0.0199	0.0376 ⁺	0.0375	0.0354	0.0154 ⁺	0.0133	0.0105	0.0345 ⁺	0.0271	0.0187
	1.0	1.0	0.0208 ⁺	0.0202	0.0192	0.0417 ⁺	0.0416	0.0401	0.0208 ⁺	0.0179	0.0141	0.0417 ⁺	0.0341	0.0246
	2.0	2.0	0.0196	0.0192	0.0185	0.0450	0.0452	0.0439	0.0253	0.0215	0.0169	0.0468	0.0392	0.0292
	2.5	2.5	0.0193	0.0189	0.0184	0.0459	0.0461	0.0449	0.0265	0.0223	0.0176	0.0480	0.0405	0.0302
	4.0	4.0	0.0188	0.0185	0.0181	0.0475	0.0476	0.0465	0.0284	0.0238	0.0188	0.0504	0.0424	0.0320
	5.0	5.0	0.0185 ⁺	0.0184	0.0180	0.0486 ⁺	0.0481	0.0470	0.0290 ⁺	0.0244	0.0192	0.0510 ⁺	0.0430	0.0330
0.8	0.0	0.0	0.0345 ⁺	0.0315	0.0259	0.0395 ⁺	0.0351	0.0244	0.0492 ⁺	0.0399	0.0357	0.1243	0.0751	
	0.2	0.128	0.0291	0.0261	0.0219	0.0383	0.0347	0.0265	0.0063	0.0056	0.0045	0.0176	0.0131	0.0087
	0.5	0.32	0.0242	0.0217	0.0186	0.0375	0.0349	0.0284	0.0120	0.0104	0.0083	0.0275	0.0222	0.0156
	1.0	0.64	0.0199	0.0179	0.0158	0.0371	0.0351	0.0299	0.0170	0.0147	0.0116	0.0348	0.0291	0.0211
	2.0	1.28	0.0161	0.0147	0.0134	0.0366	0.0352	0.0312	0.0216	0.0184	0.0145	0.0408	0.0346	0.0258
	4.0	2.56	0.0133	0.0124	0.0117	0.0362	0.0352	0.0320	0.0249	0.0210	0.0166	0.0451	0.0384	0.0288
0.6	0.0	0.0	0.0396	0.0353	0.0278	0.0512	0.0406	0.0198	0.0442	0.0396	0.0315	0.1677	0.1100	0.0700
	0.2	0.072	0.0329	0.0287	0.0228	0.0448	0.0360	0.0187	0.0044	0.0039	0.0031	0.0121	0.0094	0.0063
	0.5	0.18	0.0264	0.0226	0.0182	0.0395	0.0321	0.0178	0.0086	0.0065	0.0059	0.0202	0.0166	0.0117
	1.0	0.36	0.0202	0.0171	0.0140	0.0347	0.0287	0.0171	0.0127	0.0109	0.0086	0.0268	0.0226	0.0164
	2.0	0.72	0.0142	0.0120	0.0101	0.0300	0.0256	0.0165	0.0167	0.0142	0.0111	0.0325	0.0278	0.0205
	4.0	1.44	0.0096	0.0082	0.0073	0.0261	0.0232	0.0162	0.0198	0.0166	0.0130	0.0370	0.0314	0.0235
0.4	0.0	0.0	0.0416	0.0362	-	0.0630	0.0372	-	0.0421	0.0368	-	0.1269	0.0965	-
	0.5	0.08	0.0278	0.0234	-	0.0436	0.0250	-	0.0056	0.0048	-	0.0128	0.0108	-
	1.0	0.16	0.0208	0.0173	-	0.0348	0.0199	-	0.0084	0.0071	-	0.0178	0.0151	-
	2.0	0.32	0.0139	0.0114	-	0.0262	0.0154	-	0.0112	0.0093	-	0.0225	0.0190	-
	4.0	0.64	0.0084	0.0069	-	0.0193	0.0122	-	0.0134	0.0111	-	0.0261	0.0219	-

* Coefficients of qL^3 except that for $H_L = H_S = 0.0$ the coefficient is of qL^2 .

+ Coefficients reported by Sutherland.

TABLE 12

BENDING MOMENTS IN SHORT DIRECTION AT VARIOUS POINTS IN INTERIOR PANELS

$$I_S = (s/L) I_L$$

Moment Coefficient			m_5/qL^2			$-m_6/qL^2$			m_7^*			$-m_8^*$		
c/L ratios =			0.0	0.1	0.2	0.0	0.1	0.2	0.0	0.1	0.2	0.0	0.1	0.2
s/L	H _L	H _S												
0.8	0.0	0.0	0.0122 ⁺	0.0116	0.0104	0.0126 ⁺	0.0121	0.0103	0.0446 ⁺	0.0376	0.0254	∞ ⁺	0.0856	0.0380
	0.2	0.128	0.0130	0.0128	0.0120	0.0176	0.0179	0.0171	0.0044	0.0036	0.0024	0.0124	0.0074	0.0038
	0.5	0.32	0.0138	0.0139	0.0133	0.0227	0.0236	0.0231	0.0081	0.0065	0.0044	0.0186	0.0125	0.0071
	1.0	0.64	0.0146	0.0149	0.0145	0.0278	0.0288	0.0285	0.0111	0.0088	0.0061	0.0226	0.0163	0.0098
	2.0	1.28	0.0155	0.0158	0.0154	0.0328	0.0336	0.0331	0.0135	0.0107	0.0075	0.0253	0.0192	0.0120
	4.0	2.56	0.0163	0.0164	0.0161	0.0365	0.0371	0.0365	0.0151	0.0120	0.0084	0.0269	0.0210	0.0136
0.6	0.0	0.0	0.0034	0.0034	0.0033	0.0034	0.0034	0.0033	0.0337	0.0240	0.0100	0.1318	0.0397	0.0079
	0.2	0.072	0.0049	0.0053	0.0053	0.0072	0.0078	0.0078	0.0019	0.0013	0.0006	0.0054	0.0020	0.0006
	0.5	0.18	0.0066	0.0071	0.0070	0.0113	0.0121	0.0122	0.0035	0.0024	0.0011	0.0084	0.0040	0.0013
	1.0	0.36	0.0082	0.0088	0.0087	0.0154	0.0163	0.0163	0.0049	0.0033	0.0016	0.0103	0.0055	0.0021
	2.0	0.72	0.0099	0.0104	0.0101	0.0197	0.0204	0.0202	0.0059	0.0041	0.0020	0.0114	0.0068	0.0029
	4.0	1.44	0.0113	0.0116	0.0112	0.0231	0.0236	0.0232	0.0066	0.0046	0.0024	0.0120	0.0076	0.0035
4.0	0.0	0.0	0.0003	0.0004	-	0.0003	0.0004	-	0.0230	0.0083	-	0.0748	0.0037	-
	0.5	0.08	0.0024	0.0026	-	0.0044	0.0046	-	0.0011	0.0004	-	0.0026	0.0004	-
	1.0	0.16	0.0035	0.0036	-	0.0066	0.0068	-	0.0015	0.0006	-	0.0033	0.0007	-
	2.0	0.32	0.0046	0.0047	-	0.0087	0.0089	-	0.0019	0.0008	-	0.0037	0.0011	-
	4.0	0.64	0.0055	0.0056	-	0.0105	0.0106	-	0.0021	0.0010	-	0.0038	0.0014	-

* Coefficients of qL^3 except that for $H_L = H_S = 0.0$ the coefficient is of qL^2 .

† Coefficients reported by Sutherland.

TABLE 13
DEFLECTION COEFFICIENTS FOR INTERIOR PANELS

$$I_S = (S/L)^2 I_L$$

Location			Center of Panel			Center of Long Beam			Center of Short Beam		
c/L ratios =			0.0	0.1	0.2	0.0	0.1	0.2	0.0	0.1	0.2
S/L	H _L	H _S									
0.8	0.0	0.0	0.00420	0.00301	0.00189	0.00378	0.00262	0.00155	0.00230	0.00131	0.00057
	0.2	0.1024	0.00325	0.00242	0.00161	0.00277	0.00194	0.00116	0.00164	0.00097	0.00047
	0.5	0.256	0.00255	0.00196	0.00138	0.00201	0.00140	0.00085	0.00117	0.00071	0.00034
	1.0	0.512	0.00199	0.00158	0.00118	0.00138	0.00096	0.00059	0.00080	0.00049	0.00024
	2.0	1.024	0.00152	0.00126	0.00102	0.00085	0.00059	0.00036	0.00049	0.00030	0.00016
	4.0	2.048	0.00119	0.00105	0.00090	0.00048	0.00033	0.00020	0.00028	0.00017	0.00009
0.6	0.0	0.0	0.00327	0.00234	0.00143	0.00321	0.00228	0.00137	0.00099	0.00040	0.00008
	0.2	0.0432	0.00263	0.00190	0.00119	0.00252	0.00179	0.00108	0.00074	0.00032	0.00008
	0.5	0.108	0.00208	0.00151	0.00098	0.00192	0.00135	0.00082	0.00056	0.00025	0.00007
	1.0	0.216	0.00158	0.00117	0.00079	0.00138	0.00096	0.00059	0.00040	0.00019	0.00005
	2.0	0.432	0.00113	0.00086	0.00061	0.00089	0.00061	0.00037	0.00026	0.00012	0.00004
	4.0	0.864	0.00079	0.00063	0.00048	0.00052	0.00035	0.00022	0.00015	0.00007	0.00002
0.4	0.0	0.0	0.002843	0.002045	-	0.002841	0.002041	-	0.00031	0.00004	-
	0.2	0.0128	0.00234	0.00166	-	0.00233	0.00165	-	0.00025	0.00003	-
	0.5	0.032	0.00186	0.00131	-	0.00183	0.00128	-	0.00019	0.00003	-
	1.0	0.064	0.00140	0.00098	-	0.00136	0.00094	-	0.00014	0.00003	-
	2.0	0.128	0.00094	0.00066	-	0.00089	0.00061	-	0.00010	0.00002	-
	4.0	0.256	0.00059	0.00042	-	0.00053	0.00036	-	0.00006	0.00002	-

TABLE 14
BENDING MOMENTS IN LONG DIRECTION AT VARIOUS POINTS IN INTERIOR PANELS

$$I_S = (s/L)^2 I_L$$

Moment Coefficients			m_1/qL^2			$-m_2/qL^2$			m_3^*			$-m_4^*$		
c/L ratios =			0.0	0.1	0.2	0.0	0.1	0.2	0.0	0.1	0.2	0.0	0.0	0.2
s/L	H_L	H_S												
0.8	0.0	0.0	0.0346	0.0315	0.0259	0.0402	0.0351	0.0244	0.0496	0.0399	0.0357	0.2136	0.1243	0.0751
	0.2	0.1024	0.0288	0.0259	0.0218	0.0370	0.0335	0.0255	0.0063	0.0056	0.0045	0.0180	0.0132	0.0087
	0.5	0.256	0.0238	0.0213	0.0184	0.0355	0.0330	0.0269	0.0120	0.0104	0.0083	0.0282	0.0223	0.0156
	1.0	0.512	0.0194	0.0176	0.0156	0.0348	0.0332	0.0285	0.0152	0.0147	0.0117	0.0356	0.0293	0.0211
	2.0	1.024	0.0156	0.0144	0.0132	0.0346	0.0336	0.0300	0.0218	0.0184	0.0145	0.0416	0.0348	0.0258
	4.0	2.048	0.0129	0.0122	0.0116	0.0347	0.0342	0.0313	0.0250	0.0210	0.0166	0.0456	0.0385	0.0290
0.6	0.0	0.0	0.0396	0.0353	0.0278	0.0512	0.0406	0.0198	0.0442	0.0396	0.0315	0.1677	0.1100	0.0700
	0.2	0.0432	0.0328	0.0286	0.0227	0.0433	0.0346	0.0179	0.0044	0.0039	0.0031	0.0124	0.0094	0.0063
	0.5	0.108	0.0261	0.0224	0.0181	0.0369	0.0299	0.0166	0.0086	0.0074	0.0059	0.0209	0.0167	0.0117
	1.0	0.216	0.0198	0.0168	0.0139	0.0314	0.0262	0.0157	0.0128	0.0110	0.0086	0.0277	0.0228	0.0164
	2.0	0.432	0.0138	0.0118	0.0101	0.0268	0.0233	0.0153	0.0168	0.0142	0.0111	0.0335	0.0279	0.0205
	4.0	0.864	0.0093	0.0080	0.0072	0.0237	0.0215	0.0153	0.0198	0.0166	0.0130	0.0376	0.0315	0.0235
0.4	0.0	0.0	0.0416	0.0362	-	0.0630	0.0372	-	0.0421	0.0368	-	0.1269	0.0965	-
	0.2	0.0128	0.0347	0.0297	-	0.0518	0.0302	-	0.0028	0.0024	-	0.0073	0.0058	-
	0.5	0.032	0.0277	0.0234	-	0.0416	0.0241	-	0.0056	0.0048	-	0.0132	0.0108	-
	1.0	0.064	0.0208	0.0173	-	0.0320	0.0187	-	0.0084	0.0071	-	0.0184	0.0151	-
	2.0	0.128	0.0139	0.0114	-	0.0232	0.0141	-	0.0112	0.0093	-	0.0231	0.0190	-
	4.0	0.256	0.0084	0.0068	-	0.0167	0.0110	-	0.0134	0.0111	-	0.0266	0.0219	-

* Coefficients of qL^3 except that for $H_L = H_S = 0.0$ the coefficient is of qL^2 .

TABLE 15
BENDING MOMENTS IN SHORT DIRECTION AT VARIOUS POINTS IN INTERIOR PANELS

$$I_S = (s/L)^2 I_L$$

Moment Coefficients			m_5/qL^2			$-m_6/qL^2$			m_7^*			$-m_8^*$		
c/L ratios =			0.0	0.1	0.2	0.0	0.1	0.2	0.0	0.1	0.2	0.0	0.1	0.2
S/L	H_L	H_S												
0.8	0.0	0.0	0.0124	0.0116	0.0104	0.0130	0.0121	0.0103	0.0450	0.0376	0.0254	0.1946	0.0856	0.0380
	0.2	0.1024	0.0134	0.0131	0.0122	0.0180	0.0182	0.0172	0.0036	0.0030	0.0020	0.0105	0.0063	0.0032
	0.5	0.256	0.0144	0.0143	0.0136	0.0233	0.0240	0.0233	0.0069	0.0056	0.0039	0.0163	0.0111	0.0062
	1.0	0.512	0.0153	0.0153	0.0147	0.0285	0.0293	0.0287	0.0099	0.0080	0.0055	0.0205	0.0149	0.0089
	2.0	1.024	0.0160	0.0161	0.0156	0.0334	0.0340	0.0333	0.0125	0.0100	0.0070	0.0237	0.0181	0.0114
	4.0	2.048	0.0166	0.0167	0.0162	0.0370	0.0374	0.0366	0.0144	0.0115	0.0081	0.0258	0.0203	0.0132
0.6	0.0	0.0	0.0034	0.0034	0.0033	0.0034	0.0034	0.0033	0.0337	0.0240	0.0100	0.1318	0.0397	0.0079
	0.2	0.0432	0.0051	0.0054	0.0053	0.0074	0.0079	0.0078	0.0012	0.0008	0.0004	0.0036	0.0014	0.0004
	0.5	0.108	0.0068	0.0073	0.0071	0.0115	0.0122	0.0122	0.0023	0.0017	0.0008	0.0060	0.0028	0.0009
	1.0	0.216	0.0086	0.0090	0.0087	0.0157	0.0165	0.0164	0.0035	0.0025	0.0012	0.0078	0.0043	0.0016
	2.0	0.432	0.0102	0.0106	0.0102	0.0199	0.0206	0.0203	0.0047	0.0034	0.0017	0.0093	0.0057	0.0024
	4.0	0.864	0.0115	0.0117	0.0113	0.0233	0.0237	0.0232	0.0057	0.0041	0.0021	0.0104	0.0069	0.0032
0.4	0.0	0.0	0.0003	0.0004	-	0.0003	0.0004	-	0.0230	0.0083	-	0.0748	0.0037	-
	0.2	0.0128	0.0013	0.0015	-	0.0023	0.0025	-	0.0002	0.0001	-	0.0007	0.0001	-
	0.5	0.032	0.0024	0.0026	-	0.0044	0.0046	-	0.0005	0.0002	-	0.0013	0.0002	-
	1.0	0.064	0.0035	0.0037	-	0.0066	0.0068	-	0.0008	0.0003	-	0.0018	0.0004	-
	2.0	0.128	0.0046	0.0047	-	0.0087	0.0089	-	0.0011	0.0005	-	0.0022	0.0007	-
	4.0	0.256	0.0055	0.0056	-	0.0105	0.0106	-	0.0014	0.0007	-	0.0027	0.0010	-

* Coefficients of qL^3 except that for $H_L = H_S = 0.0$ the coefficient is of qL^2 .

TABLE 16
(REFERENCE 9)

DEFLECTION COEFFICIENTS FOR NINE-PANEL SLABS, ALL PANELS LOADED.

H	J	K	Δ_1^*	Δ_2	Δ_3	Δ_4	Δ_5	Δ_6	Δ_7
0.25	0.25	0	0.001814	0.001865	0.006593	0.001204	0.006741	0.010760	0.005667
		10	0.003849	0.002885	0.005942	0.002137	0.004910	0.007661	0.003768
		30	0.004257	0.003047	0.005550	0.002237	0.004261	0.006671	0.003211
		90	0.004413	0.003094	0.005308	0.002258	0.003907	0.006149	0.002927
		∞	0.004492	0.003110	0.005144	0.002261	0.003680	0.005822	0.002754
	1.0	0	0.001837	0.001886	0.006540	0.001073	0.006677	0.010792	0.005596
		10	0.004003	0.002933	0.005902	0.002210	0.004824	0.007475	0.003832
		30	0.004417	0.003094	0.005442	0.002415	0.004096	0.006289	0.003261
		90	0.004553	0.003125	0.005128	0.002490	0.003672	0.005625	0.002956
		∞	0.004605	0.003123	0.004902	0.002526	0.003389	0.005192	0.002764
	2.5	0	0.001906	0.001896	0.006489	0.001007	0.006628	0.010823	0.005592
		10	0.004099	0.002960	0.005867	0.002255	0.004770	0.007388	0.003886
		30	0.004504	0.003115	0.005372	0.002526	0.004007	0.006094	0.003310
		90	0.004611	0.003132	0.005014	0.002636	0.003547	0.005348	0.002999
		∞	0.004631	0.003114	0.004745	0.002695	0.003229	0.004850	0.002802

* Coefficients of ql^4/D

TABLE 16 (Continued)
DEFLECTION COEFFICIENTS FOR NINE-PANEL SLABS, ALL PANELS LOADED.

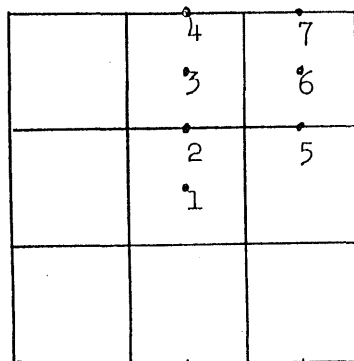
H	J	K	Δ_1^*	Δ_2	Δ_3	Δ_4	Δ_5	Δ_6	Δ_7
1.00	0.25	0	0.001030	0.000578	0.004122	0.000258	0.003627	0.006710	0.002828
		10	0.002170	0.001179	0.003873	0.000797	0.002754	0.005283	0.001986
		30	0.002582	0.001373	0.003633	0.000933	0.002281	0.004572	0.001595
		90	0.002770	0.001446	0.003428	0.000974	0.001955	0.004103	0.001347
		∞	0.002864	0.001471	0.003252	0.000984	0.001706	0.003755	0.001168
	1.00	0	0.001071	0.000592	0.004078	0.000232	0.003603	0.006703	0.002909
		10	0.002243	0.001196	0.003837	0.000829	0.002723	0.005144	0.002070
		30	0.002661	0.001391	0.003576	0.001006	0.002229	0.004330	0.001662
		60	0.002794	0.001445	0.003413	0.001057	0.001984	0.003941	0.001474
		90	0.002838	0.001460	0.003336	0.001072	0.001877	0.003774	0.001395
		120	0.002858	0.001466	0.003291	0.001080	0.001816	0.003681	0.001351
		∞	0.002911	0.001475	0.003119	0.001098	0.001599	0.003348	0.001197
	2.5	0	0.001102	0.000602	0.004034	0.000212	0.003577	0.006711	0.002973
		10	0.002298	0.001207	0.003800	0.000848	0.002697	0.005071	0.002131
		30	0.002714	0.001402	0.003527	0.001055	0.002194	0.004192	0.001710
		90	0.002877	0.001466	0.003264	0.001140	0.001827	0.003580	0.001432
		∞	0.002929	0.001472	0.003016	0.001177	0.001530	0.003102	0.001225
2.5	0.25	0	0.001019	0.000177	0.002926	0.000074	0.001920	0.004457	0.001335
		10	0.001518	0.000444	0.002825	0.000274	0.001577	0.003962	0.001095
		30	0.001825	0.000600	0.002713	0.000388	0.001305	0.003558	0.000880
		90	0.002013	0.000686	0.002580	0.000443	0.001064	0.003215	0.000704
		∞	0.002118	0.000720	0.002420	0.000462	0.000830	0.002892	0.000543

* Coefficients of qL^4/D

TABLE 16 (Continued)
DEFLECTION COEFFICIENTS FOR NINE-PANEL SLABS, ALL PANELS LOADED.

H	J	K	Δ_1^*	Δ_2	Δ_3	Δ_4	Δ_5	Δ_6	Δ_7
2.5	1.00	0	0.001046	0.000182	0.002861	0.000040	0.001914	0.004402	0.001483
		10	0.001560	0.000452	0.002780	0.000291	0.001563	0.003794	0.001162
		30	0.001870	0.000608	0.002664	0.000421	0.001285	0.003336	0.000932
		90	0.002053	0.000692	0.002516	0.000488	0.001034	0.002939	0.000740
		∞	0.002143	0.000721	0.002328	0.000514	0.000784	0.002556	0.000561
	2.5	0	0.001072	0.000191	0.002814	0.000036	0.001900	0.004346	0.001542
		10	0.001593	0.000459	0.002737	0.000301	0.001550	0.003698	0.001210
		30	0.001904	0.000614	0.002618	0.000444	0.001269	0.003204	0.000968
		90	0.002082	0.000696	0.002458	0.000520	0.001014	0.002772	0.000766
		∞	0.002156	0.000721	0.002247	0.000551	0.000752	0.002346	0.000576

* Coefficients of qL^4/D



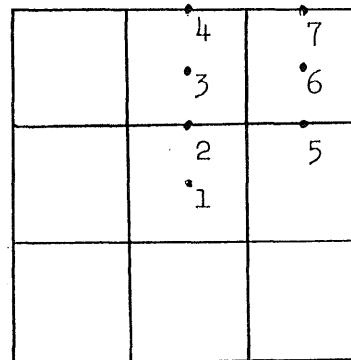
Point Designation

TABLE 17
(Reference 9)

DEFLECTION COEFFICIENTS FOR NINE-PANEL SLABS, CORNER AND INTERIOR PANELS LOADED.

H	J	K	Δ_1^*	Δ_2	Δ_3	Δ_4	Δ_5	Δ_6	Δ_7
0.25	0.25	0	0.001904	0.000367	0.000304	-0.003389	0.003944	0.010403	0.006860
		10	0.003495	0.001284	0.000588	-0.001127	0.002633	0.007135	0.004199
		30	0.003774	0.001426	0.000527	-0.000702	0.002237	0.006244	0.003498
		90	0.003877	0.001472	0.000466	-0.000532	0.002030	0.005801	0.003157
		∞	0.003927	0.001492	0.000418	-0.000441	0.001901	0.005532	0.002952
2.5	2.5	0	0.001218	-0.000097	-0.000003	-0.001164	0.001147	0.004309	0.001934
		10	0.001668	0.000144	0.000081	-0.000681	0.000870	0.003595	0.001457
		30	0.001909	0.000272	0.000111	-0.000372	0.000677	0.003088	0.001113
		90	0.002034	0.000337	0.000101	-0.000163	0.000521	0.002680	0.000835
		∞	0.002081	0.000358	0.000053	-0.000020	0.000378	0.002311	0.000586

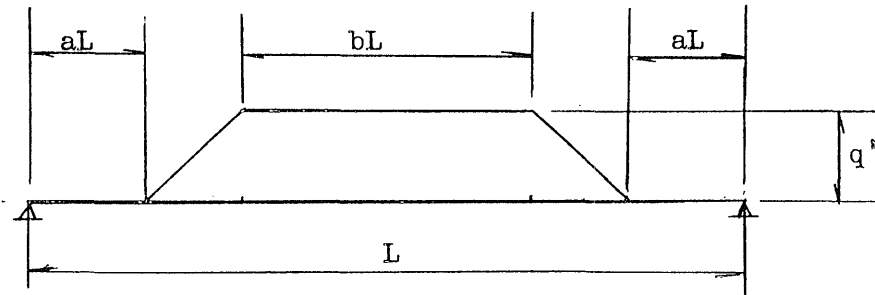
*Coefficients of qL^4/D



Point Designation

TABLE 18

DEFLECTIONS AND END MOMENTS FOR A SYMMETRICALLY-LOADED PRISMATIC BEAM

Center Deflection if Simply Supported

$$\Delta = \frac{q' L^4}{1920EI} [16a^4 + 8a^3(1-b) - 4a^2(9+2b-b^2) + 2a(-9+7b+3b^2-b^3) + 16(1+b) - 4b^2(1+b) + b^4]$$

Center Deflection if Both Ends Fixed

$$\Delta = \frac{q' L^4}{3840EI} [32a^4 - 8a^3(3+2b) + 4a^2(-3+b+2b^2) + 2a(-3+4b+b^2-2b^3) + 7(1+b) - 3b^2(1+b) + 2b^4]$$

Mid-Span Moment if Both Ends Simply Supported

$$M_o = \frac{q' L^2}{24} [-4a^2 - 2a + 2ab + 2b - b^2 + 2]$$

Fixed-End Moment if Both Ends Fixed

$$FEM = \frac{q' L^2}{96} [8a^3 - a^2(12+4b) + a(-6+4b+2b^2) + 5(1+b) - b^2(1+b)]$$

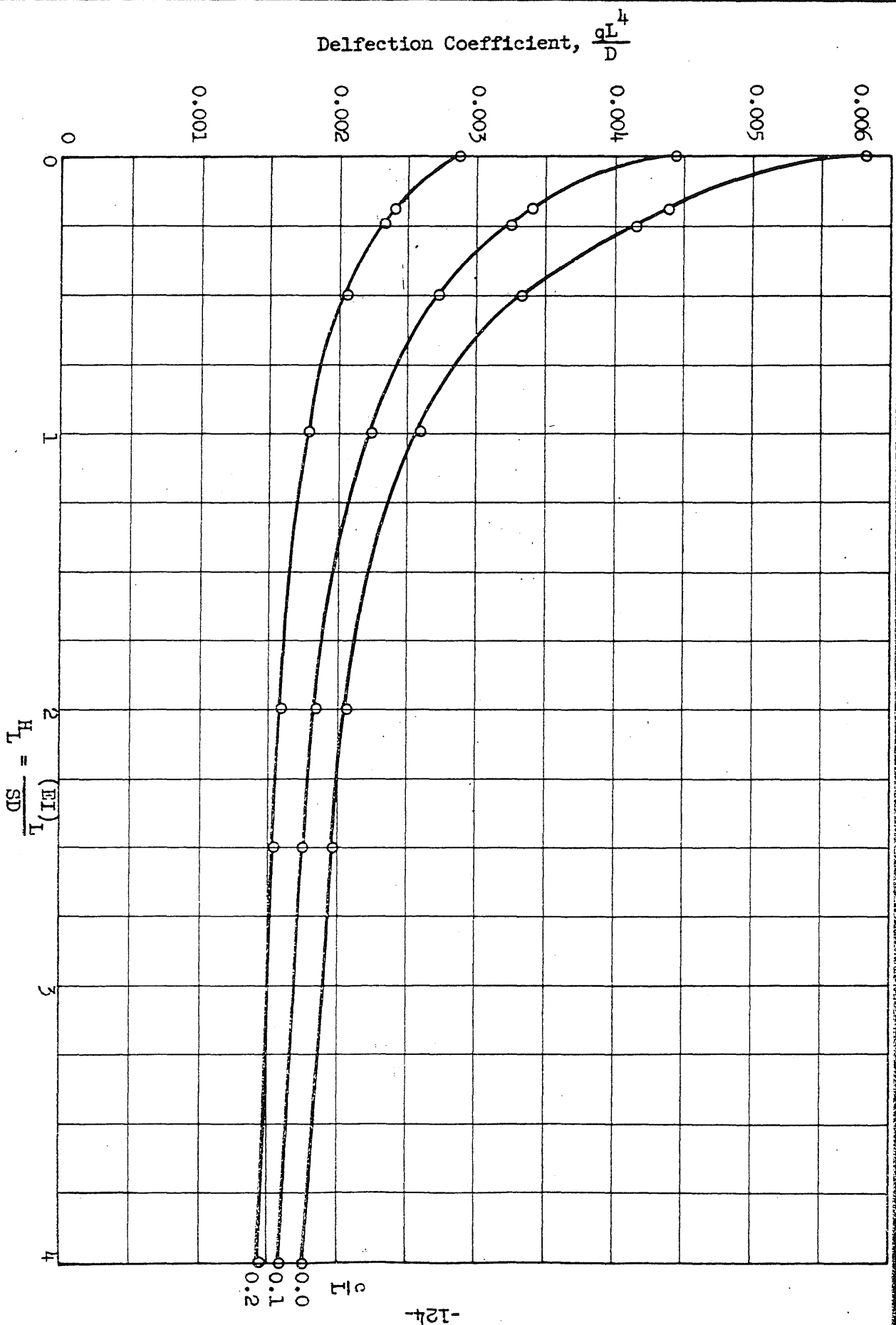


FIG. 3.1 VARIATION OF MID-PANEL DEFLECTION WITH H_L , $S/L = 1.0$

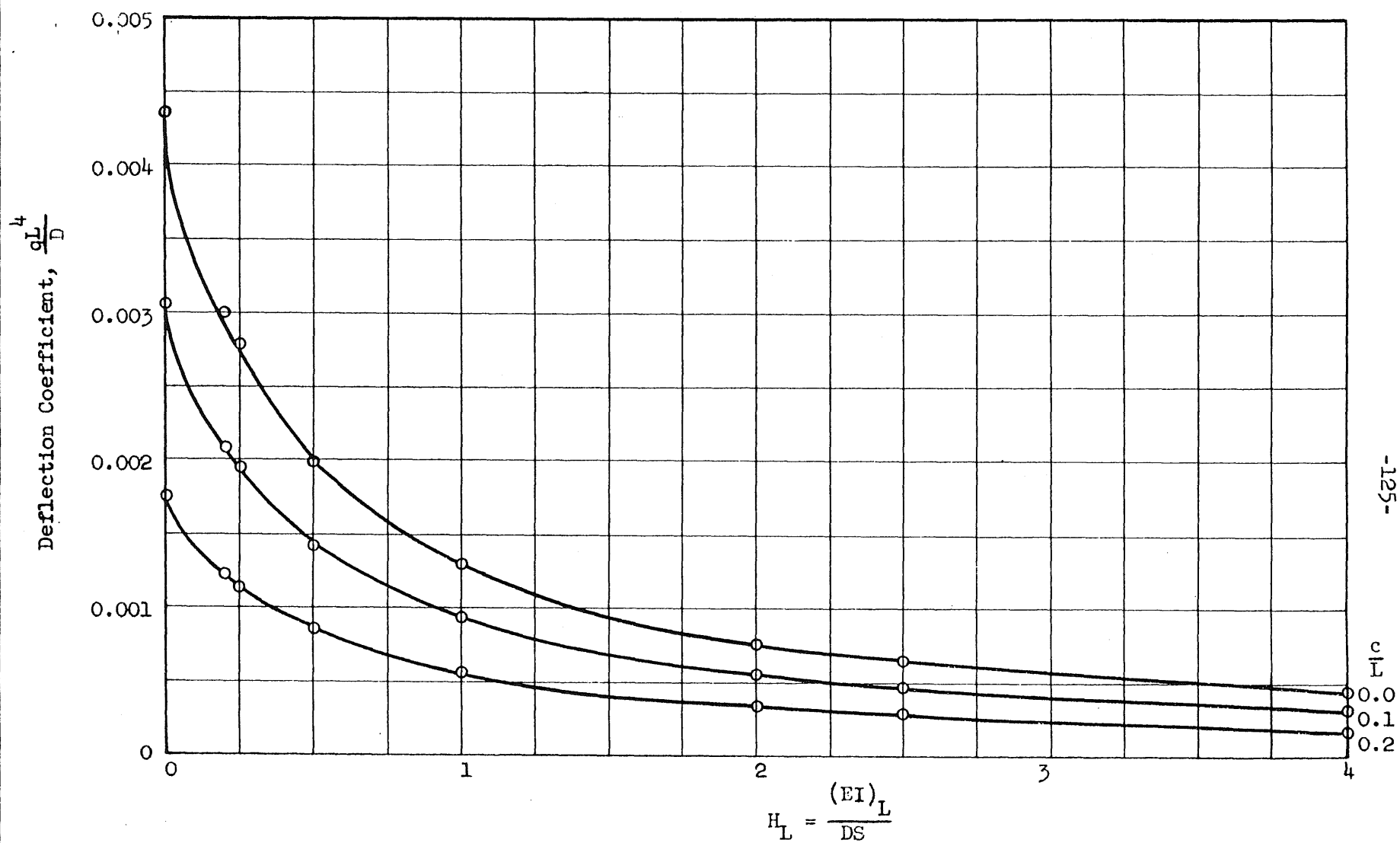


FIG. 3.2 VARIATION OF MID-BEAM DEFLECTION WITH H_L , $S/L = 1.0$

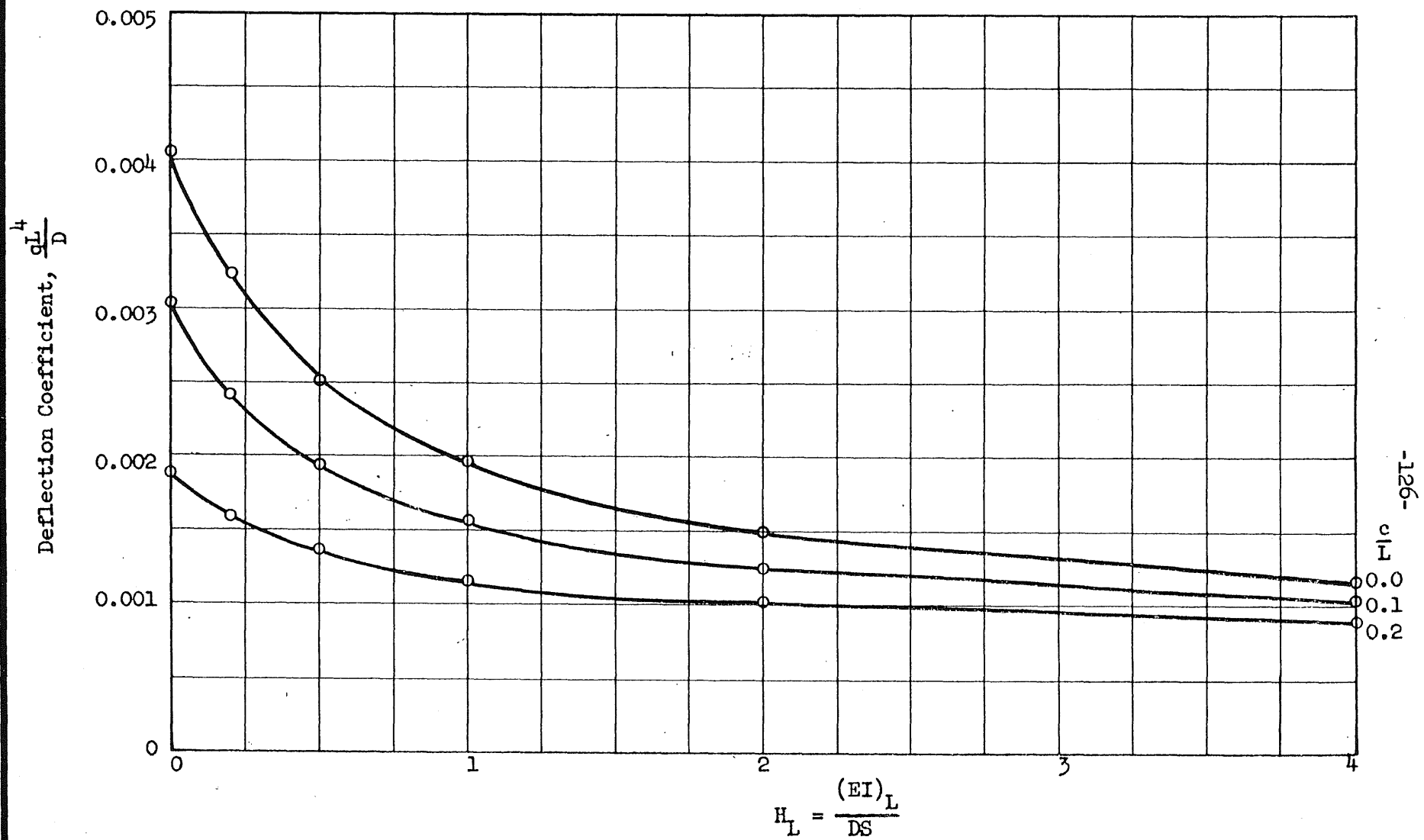


FIG. 3.3 VARIATION OF MID-PANEL DEFLECTION WITH H_L , $s/L = 0.8$, $I_S = (s/L) I_L$

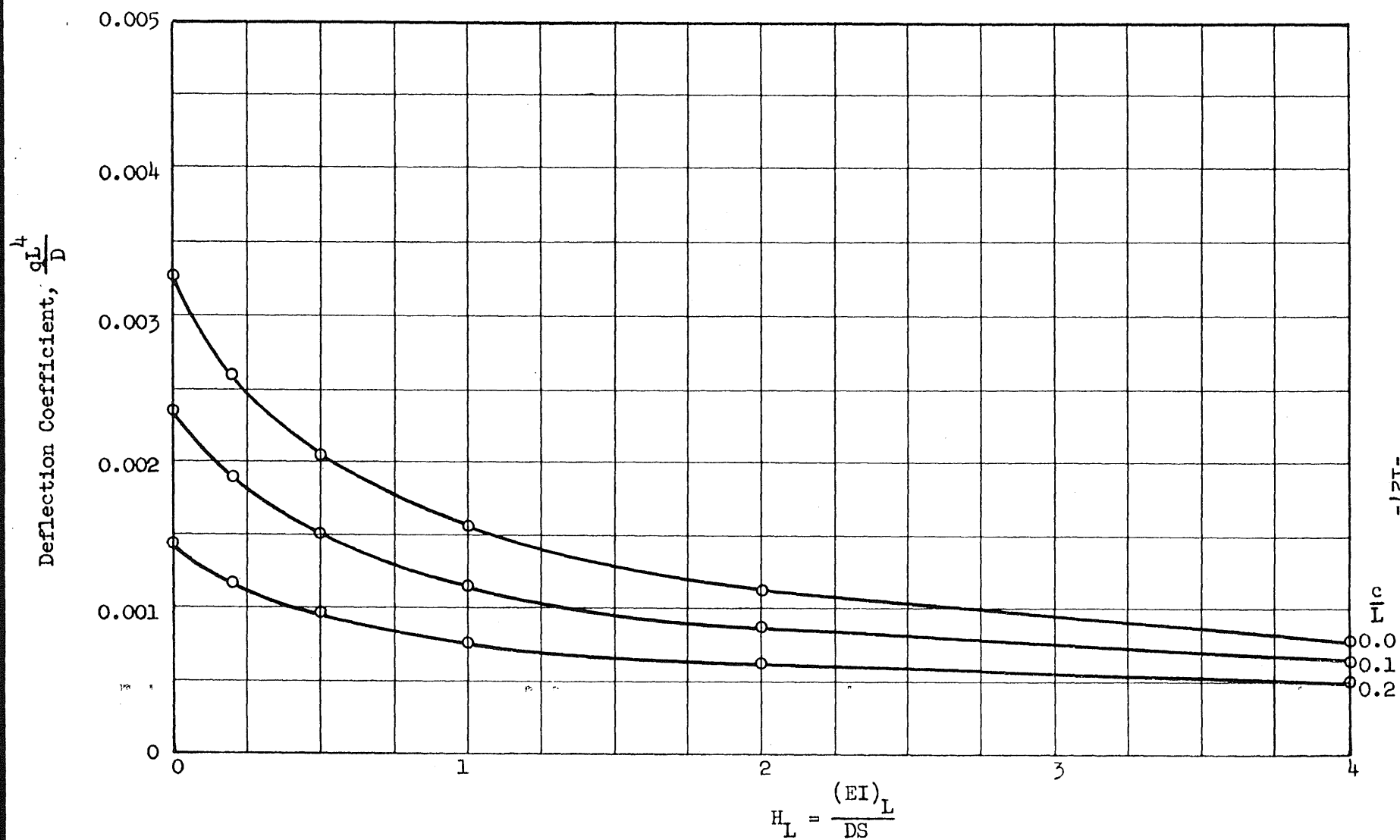


FIG. 3.4 VARIATION OF MID-PANEL DEFLECTION WITH H_L , $s/L = 0.6$, $I_S = (s/L) I_L$

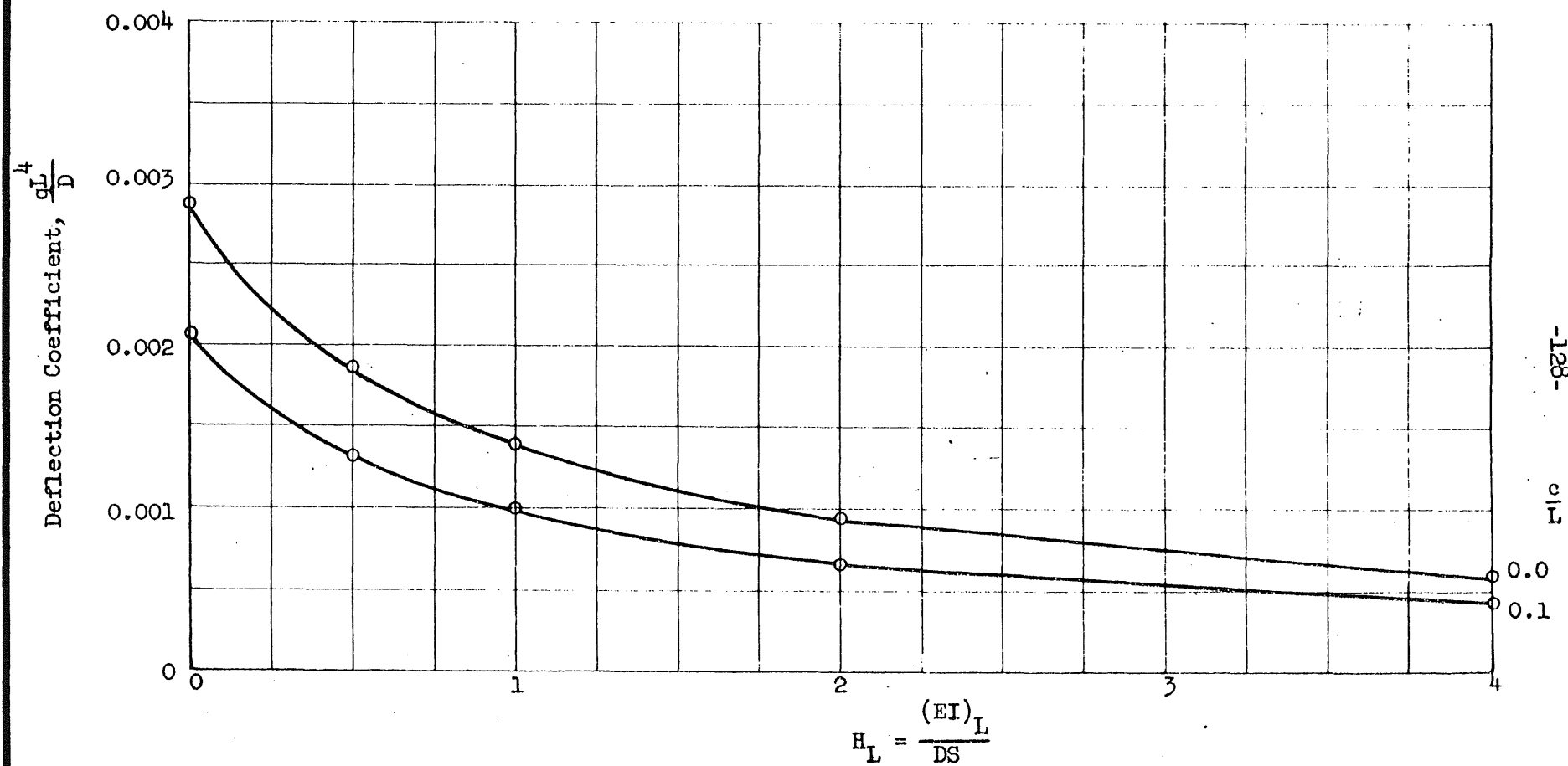


FIG. 3.5 VARIATION OF MID-PANEL DEFLECTION WITH H_L , $S/L = 0.4$, $I_S = (S/L) I_L$

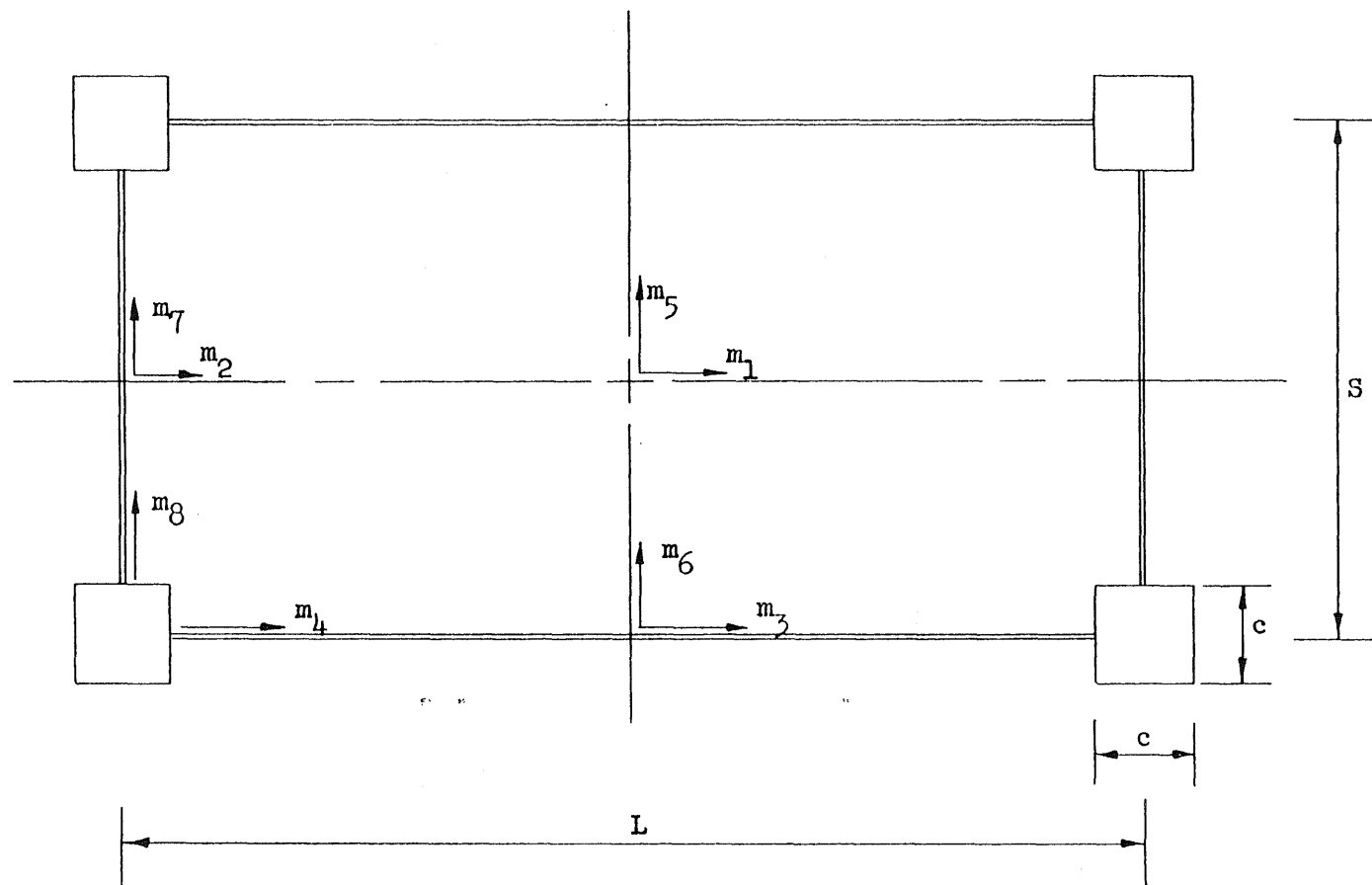


FIG. 3.6 · DIRECTION AND DESIGNATION OF BENDING MOMENTS IN A TYPICAL INTERIOR PANEL

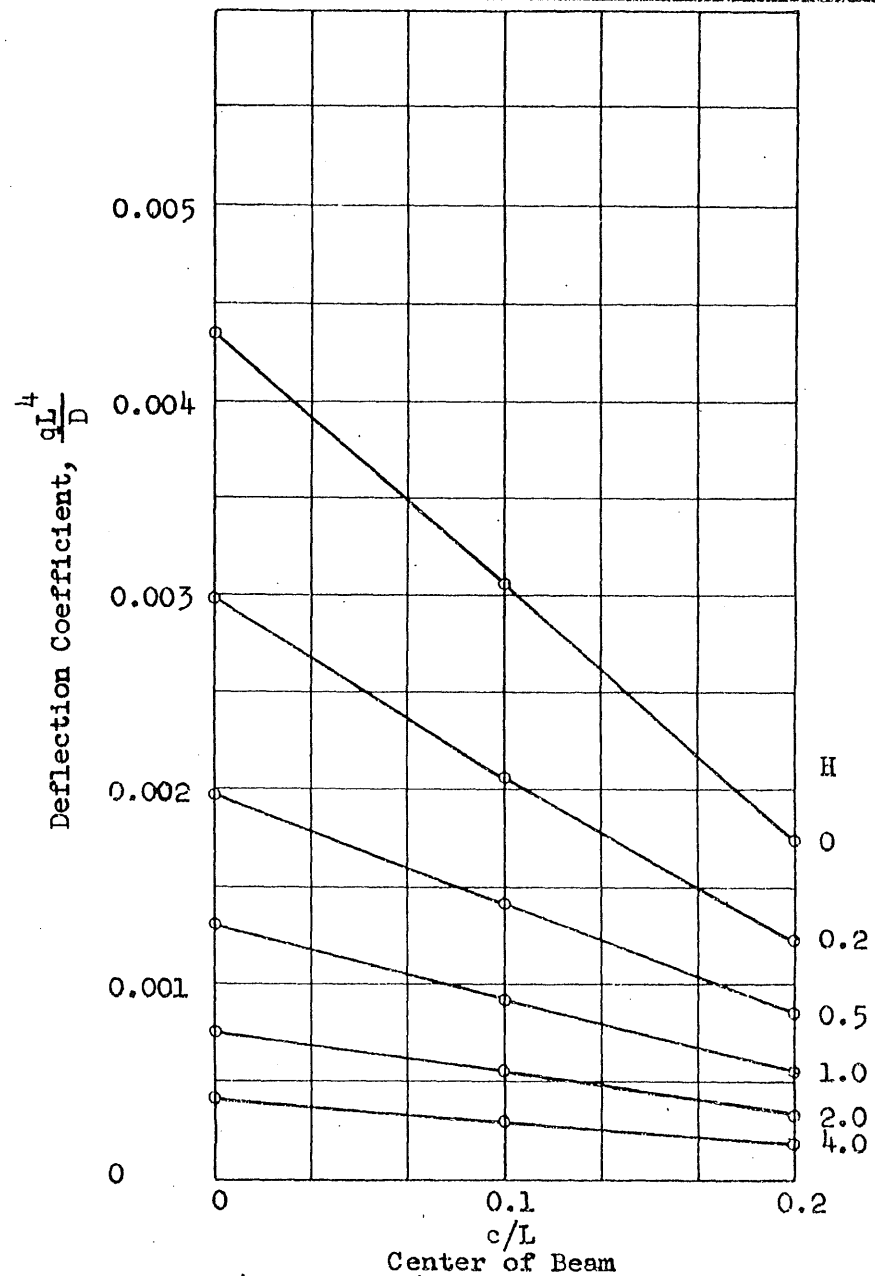
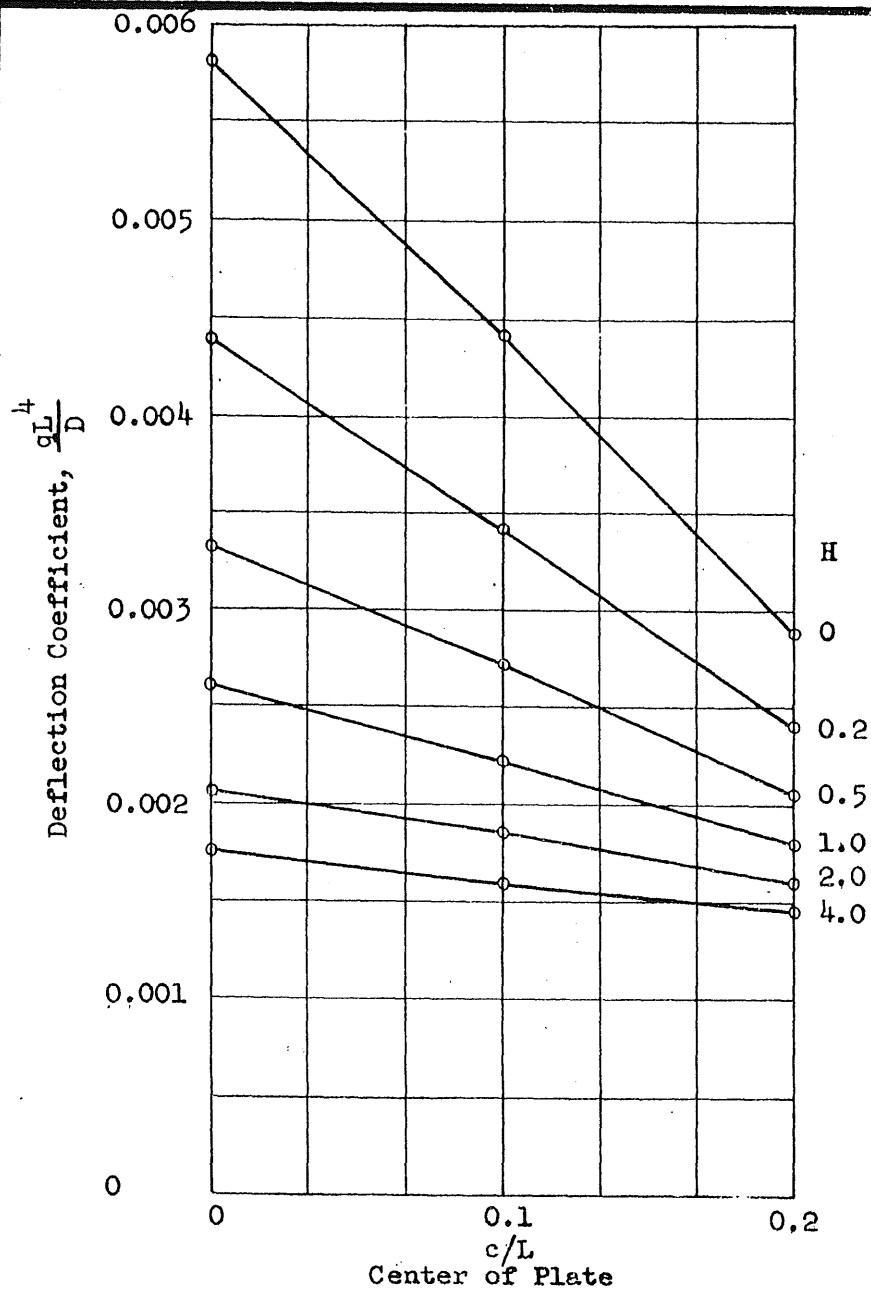


FIG. 3.7 VARIATION OF DEFLECTION WITH c/L RATIO, $S/L = 1.0$

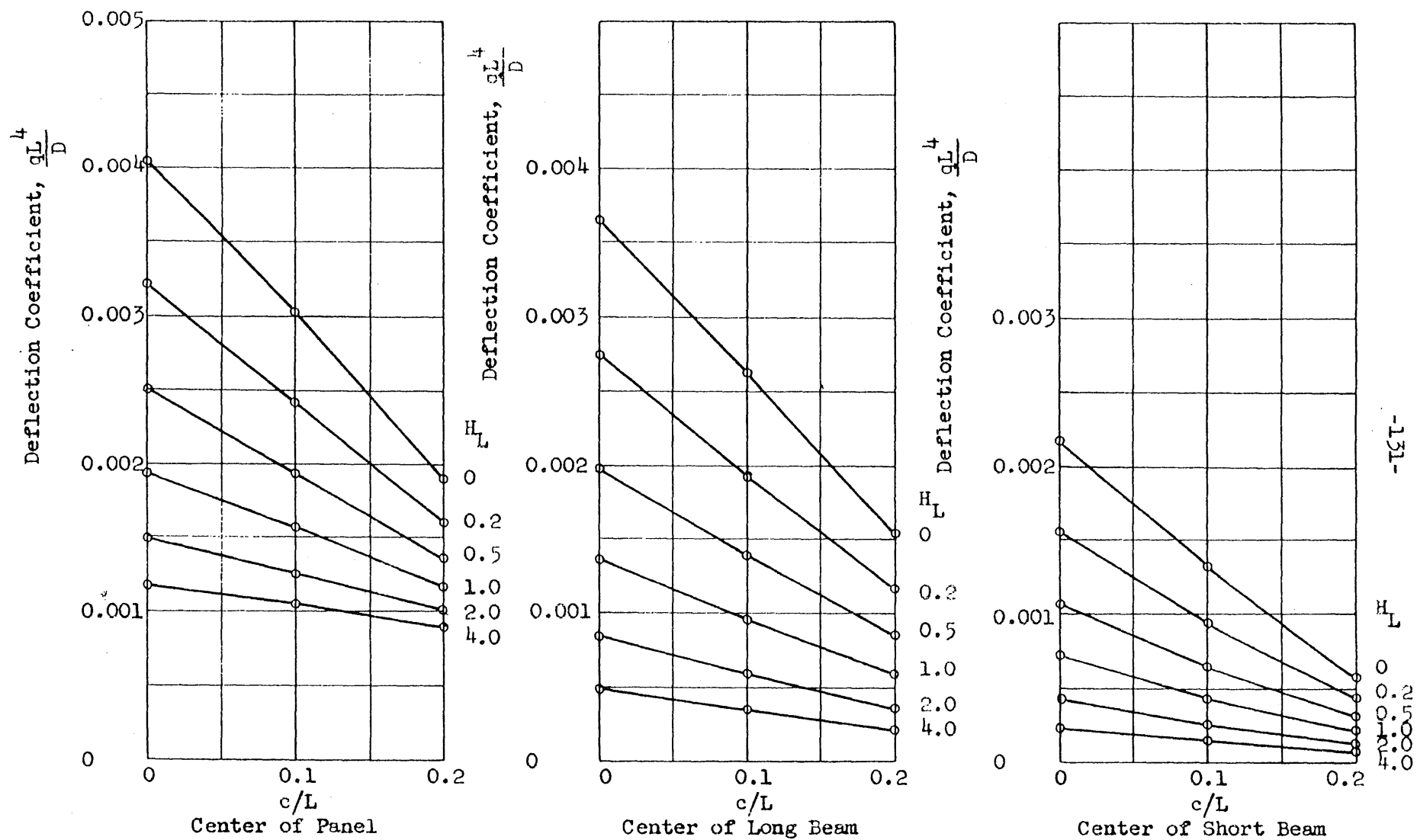


FIG. 3.8 VARIATION OF DEFLECTION WITH c/L RATIO, $S/L = 0.8$, $I_S = (S/L)I_L$

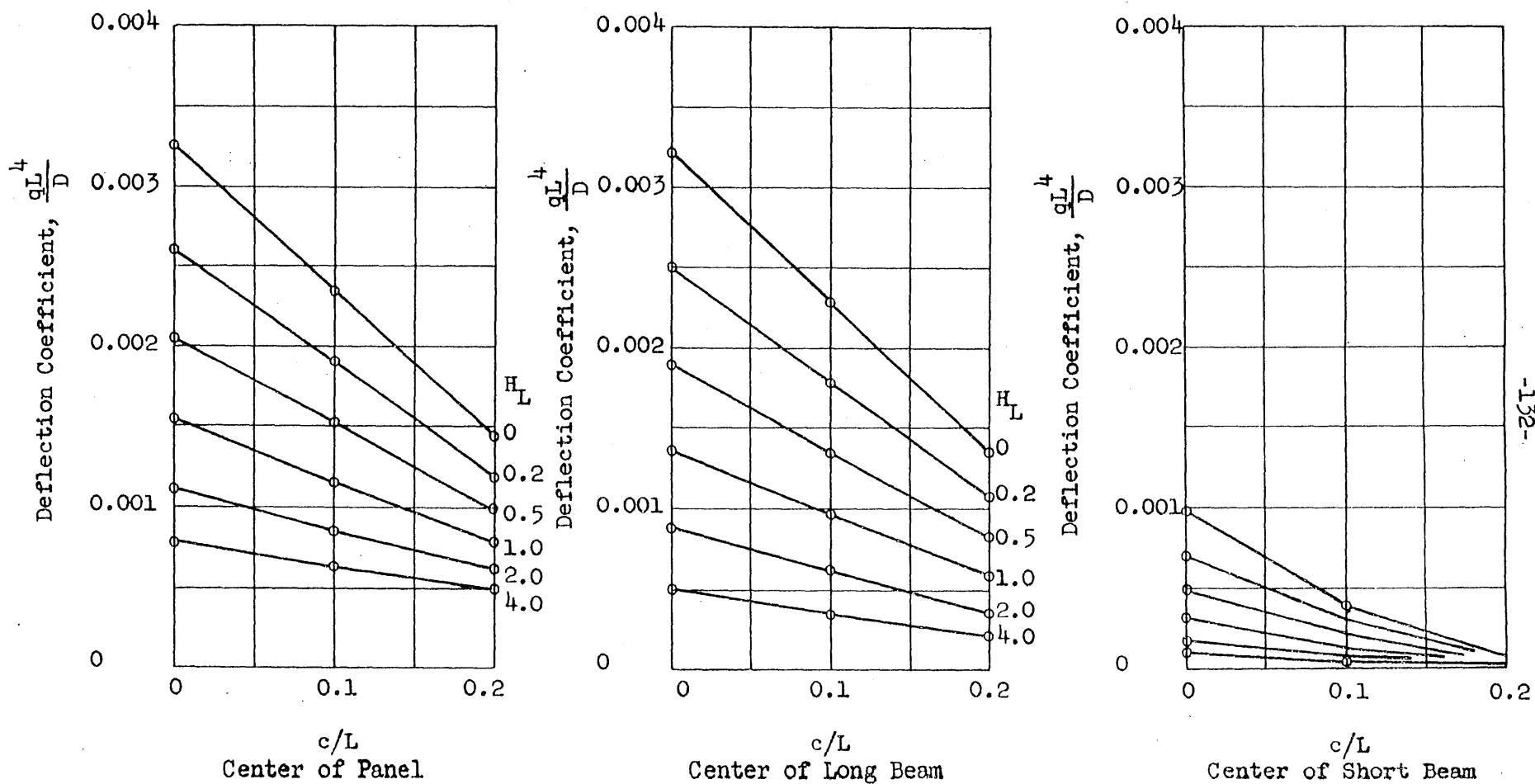
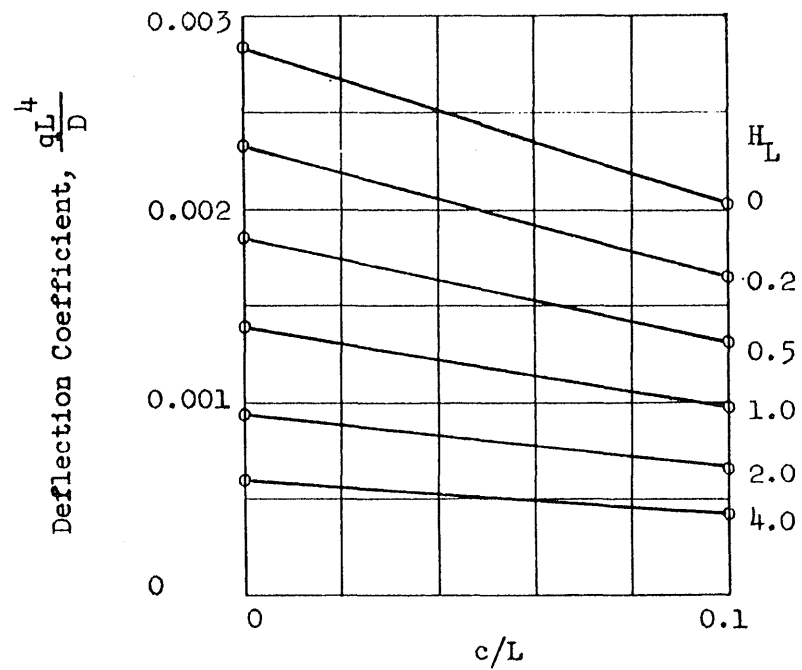
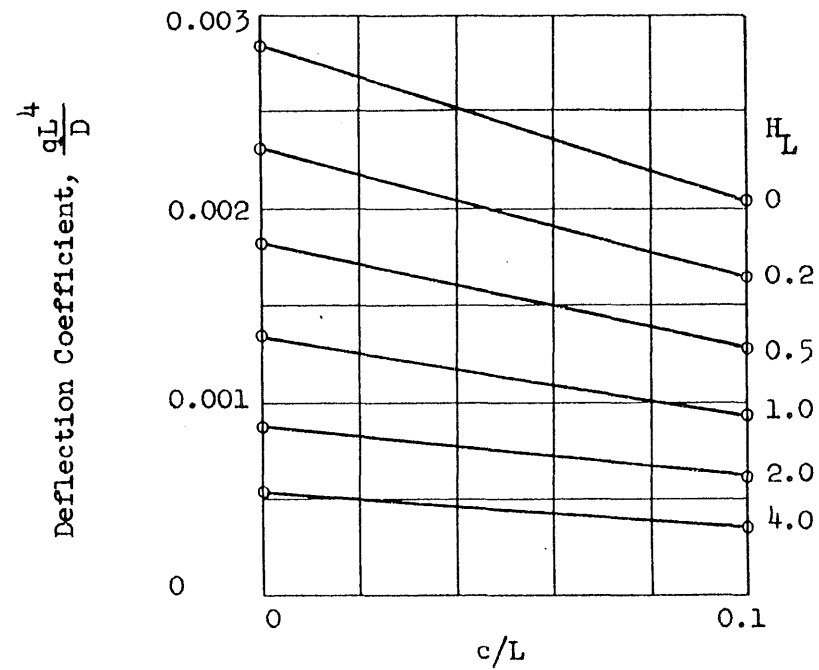


FIG. 3.9 VARIATION OF DEFLECTION WITH c/L RATIO, $S/L = 0.6$, $I_S = (S/L) I_L$

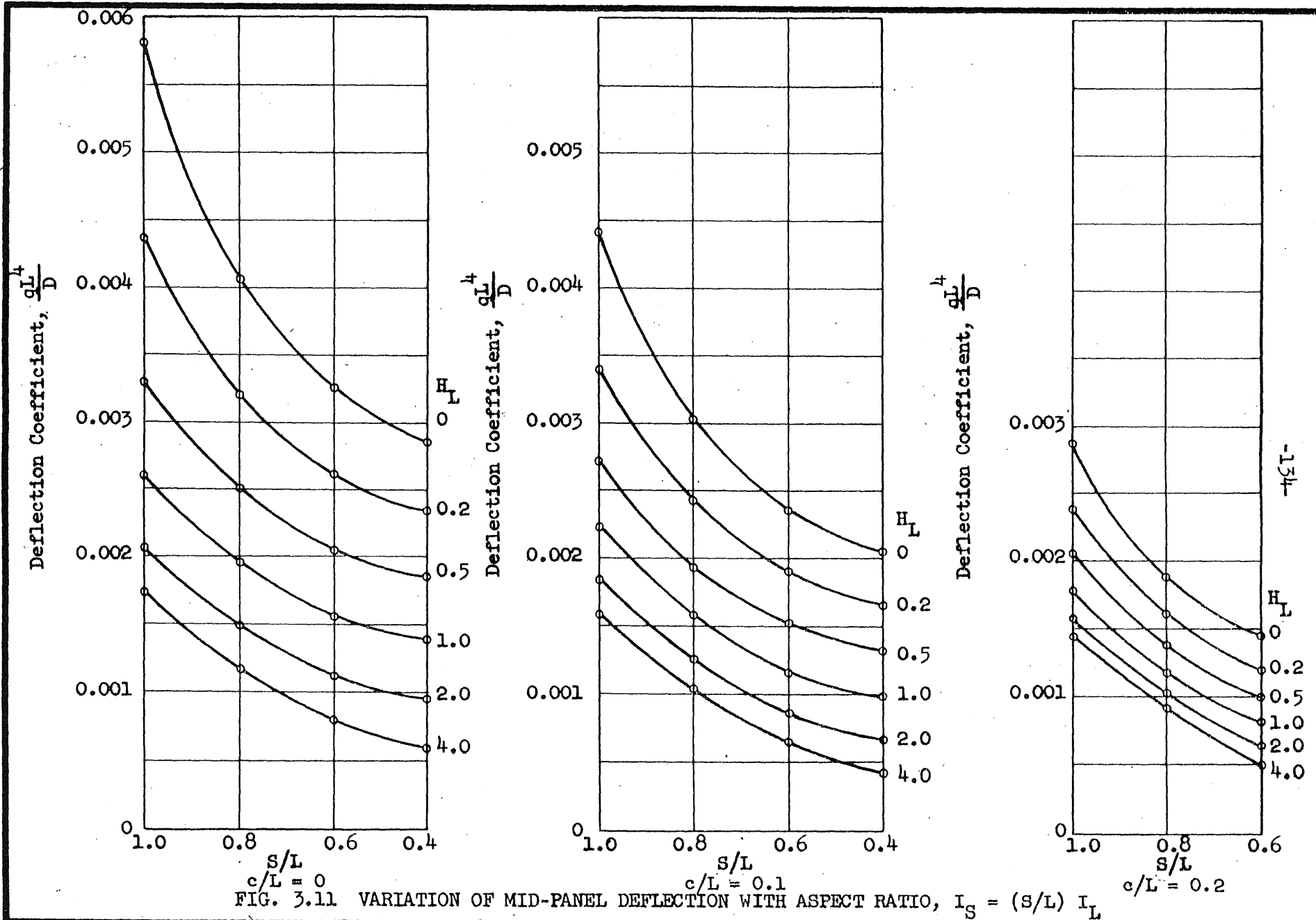


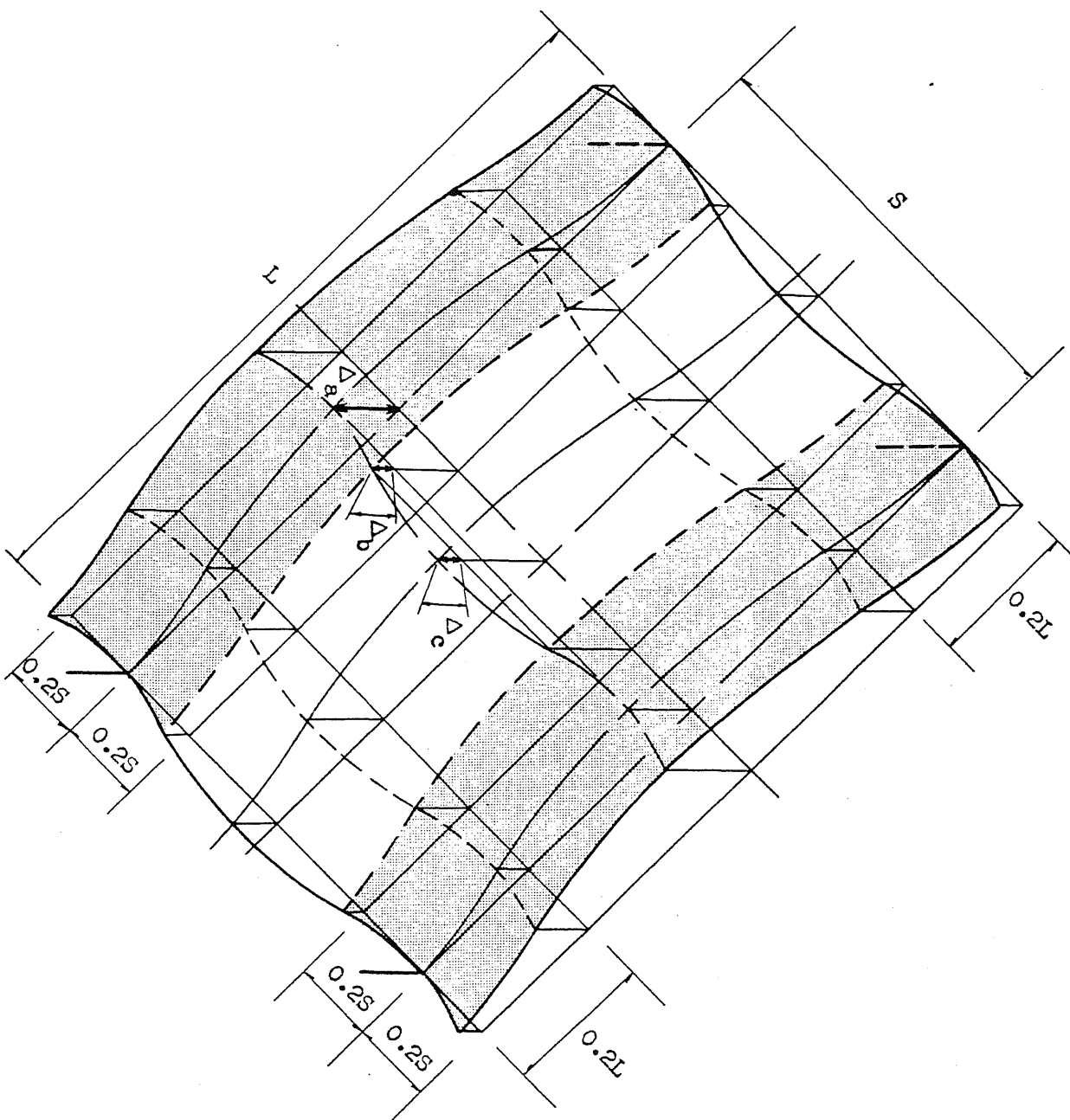
Center of Panel



Center of Long Beam

FIG. 3.10 VARIATION OF DEFLECTION WITH c/L RATIO, $S/L = 0.4$, $I_S = (S/L)I_L$





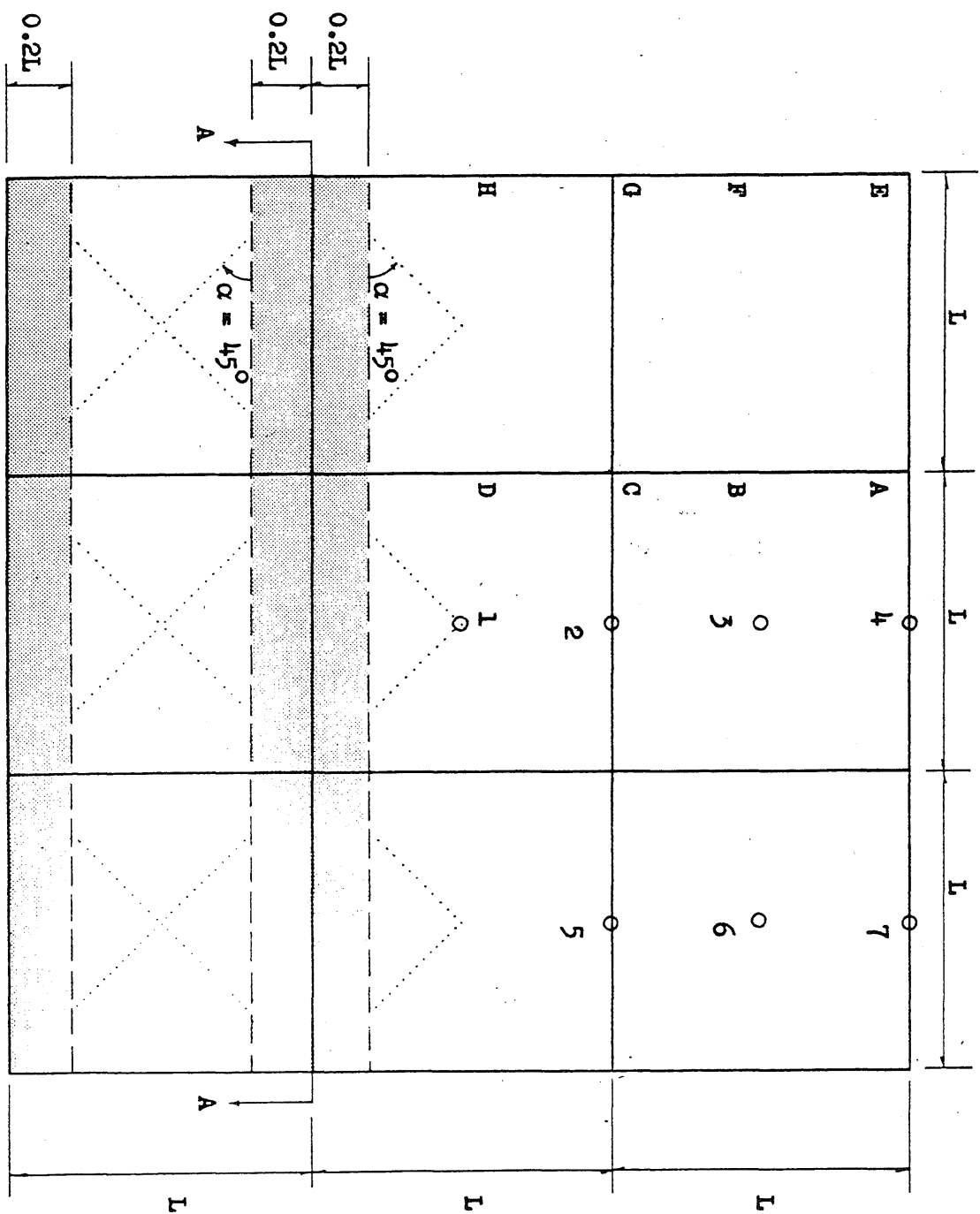
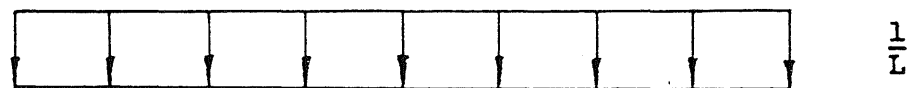
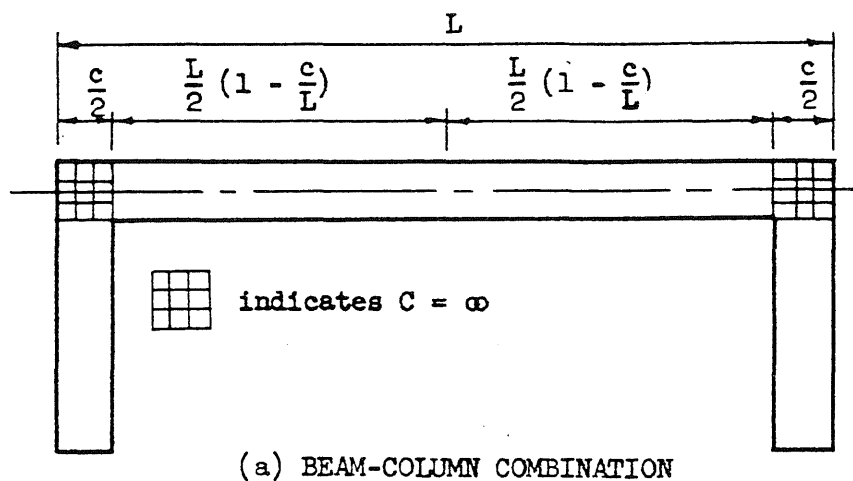
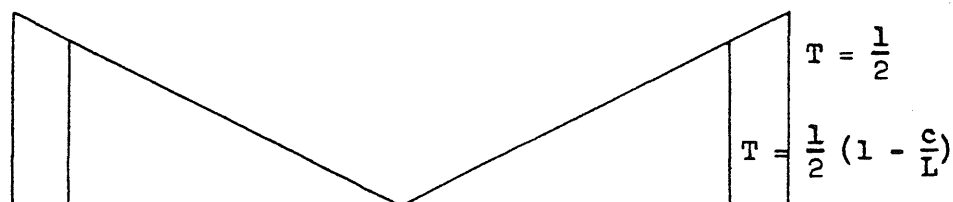


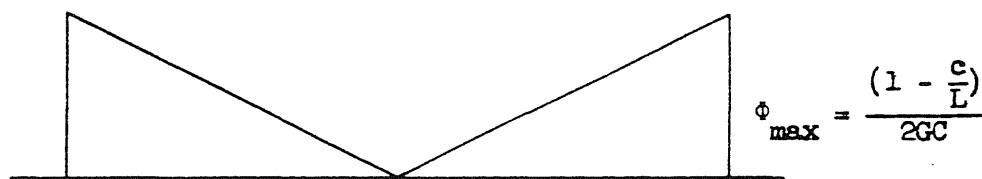
FIG. 4.2 TYPICAL LAYOUT OF A NINE-PANEL FLOOR SLAB



(b) TWISTING MOMENT APPLIED ALONG BEAM CENTERLINE

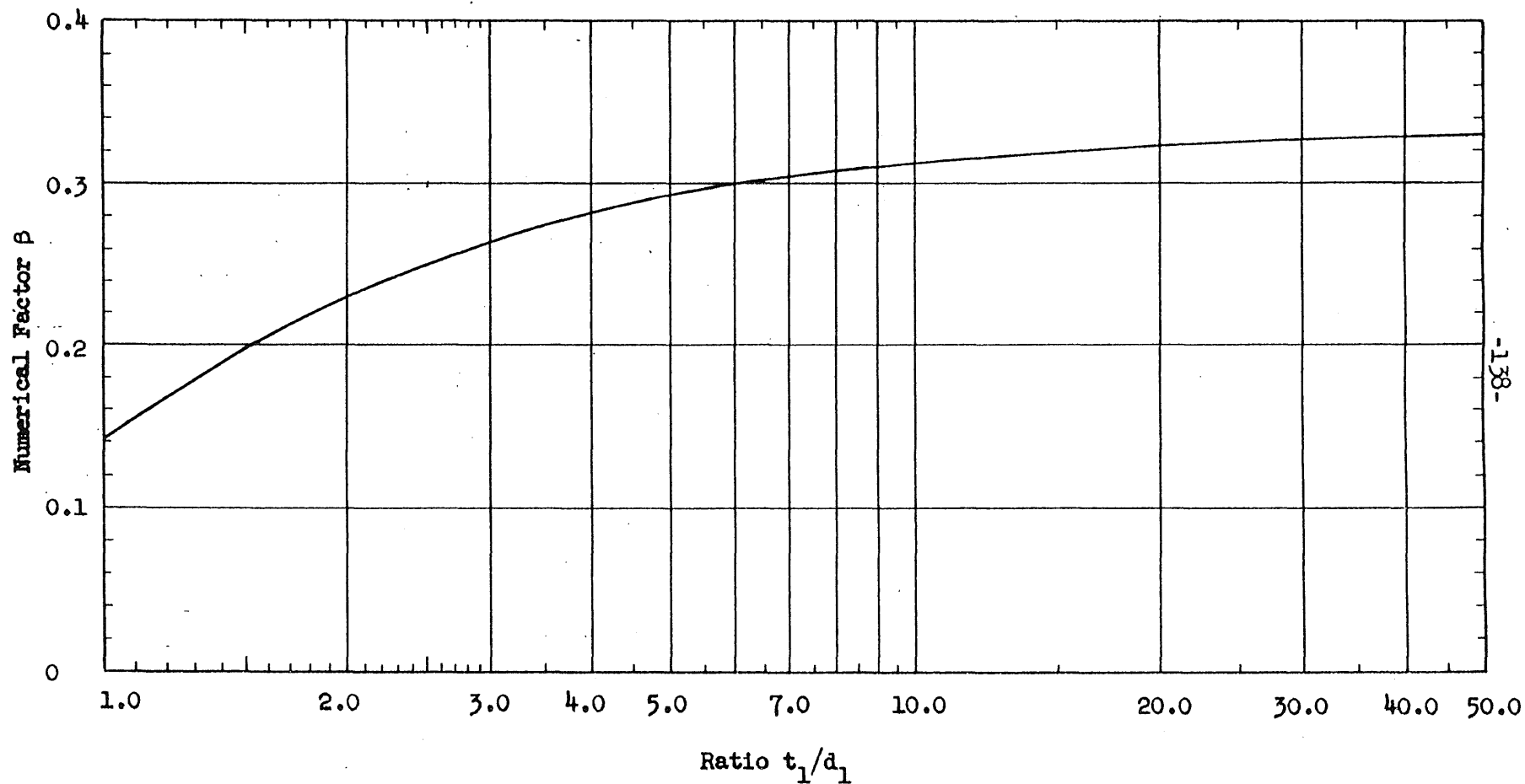


(c) TWISTING MOMENT DIAGRAM



(d) UNIT ROTATION DIAGRAM

FIG. 4.3 ROTATION OF BEAM UNDER APPLIED UNIT TWISTING MOMENT



-138-

FIG. 4.4 CONSTANT FOR TORSIONAL ROTATION OF A RECTANGULAR CROSS SECTION

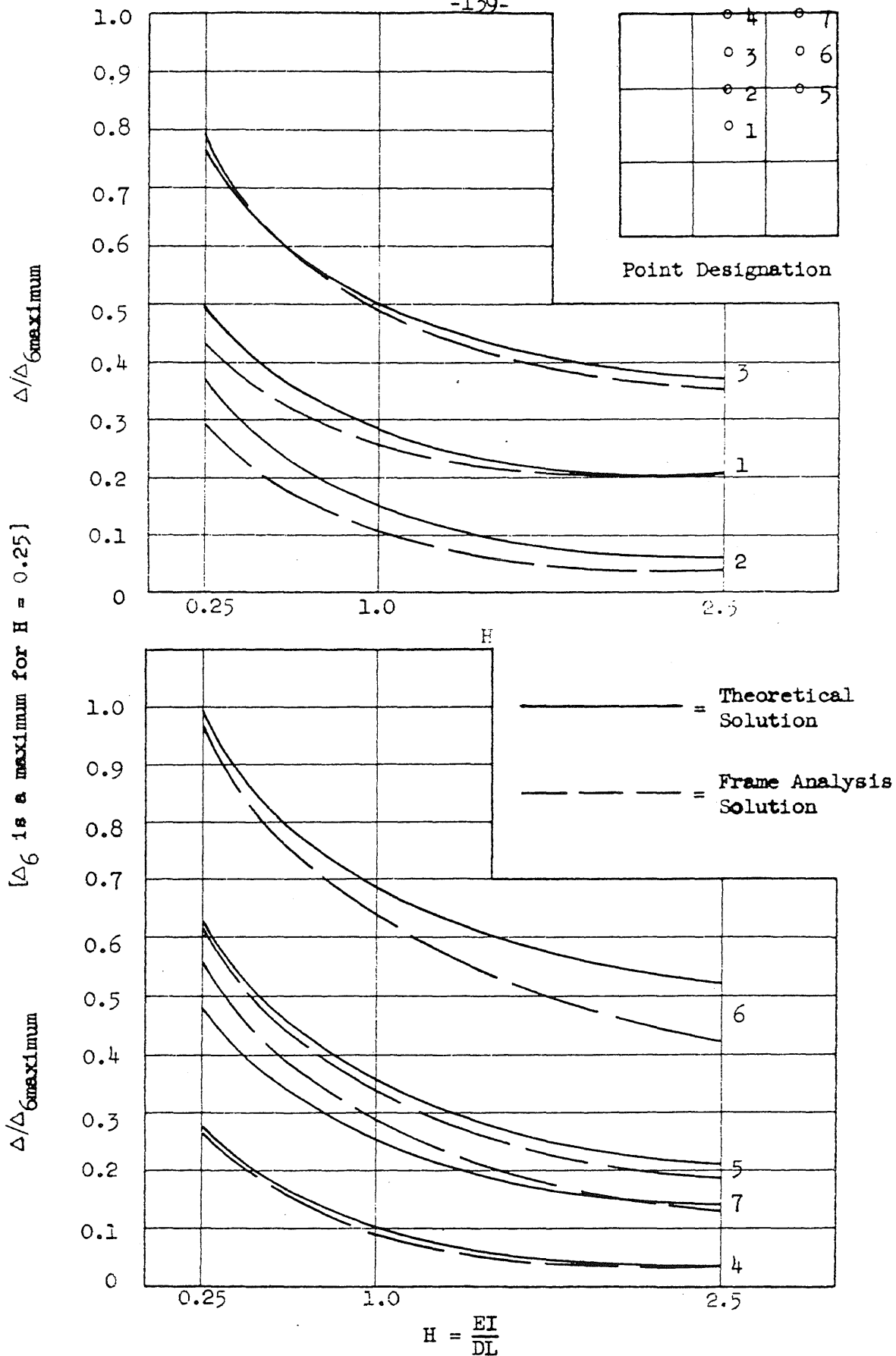


FIG. 4.5 COMPARISONS OF THEORETICAL AND FRAME ANALYSES SOLUTIONS, $J = 0.25$, $K = 10$, ALL PANELS LOADED

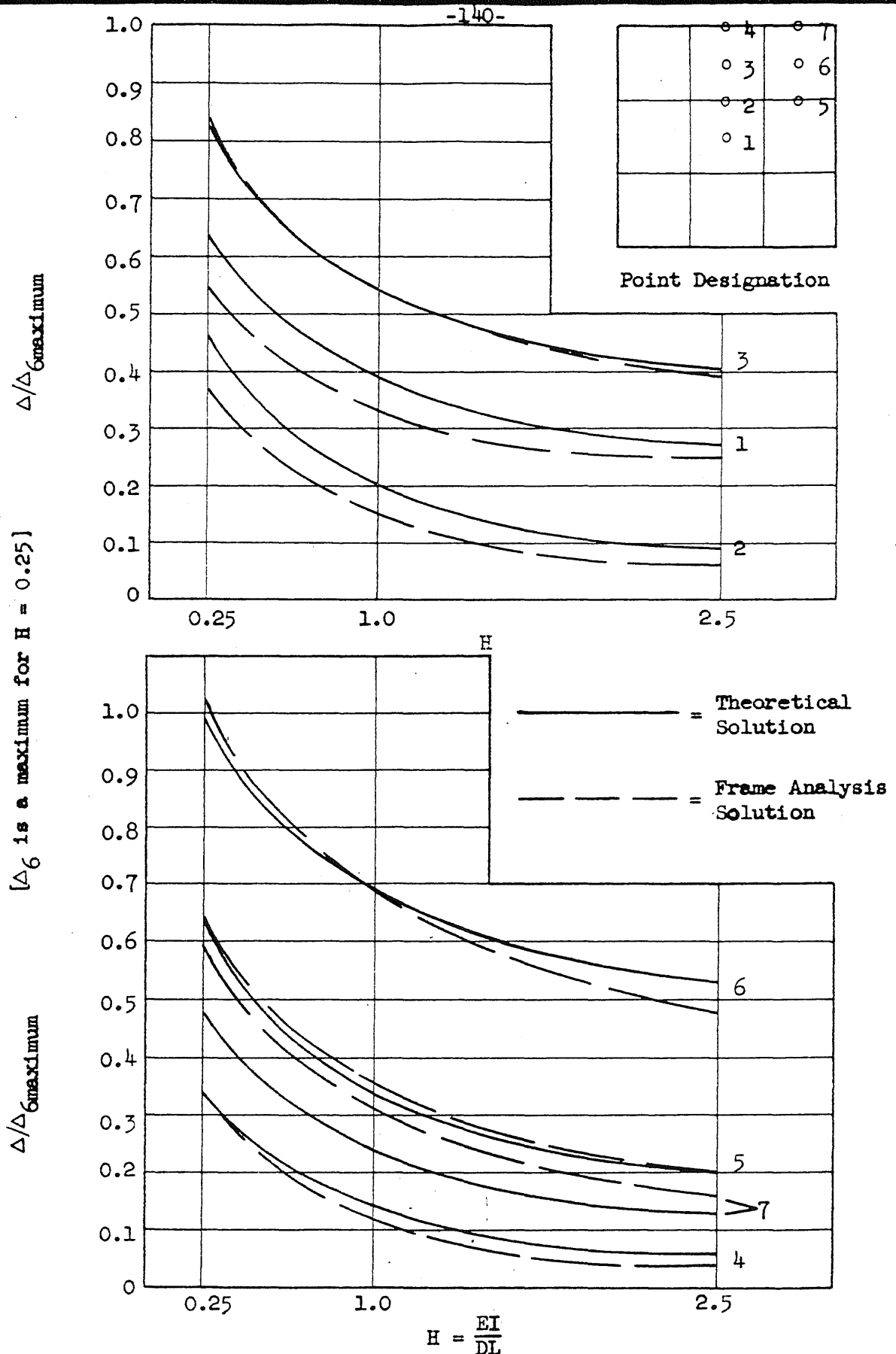


FIG. 4.6 COMPARISONS OF THEORETICAL AND FRAME ANALYSES SOLUTIONS, $J = 0.25$, $K = 30$, ALL PANELS LOADED

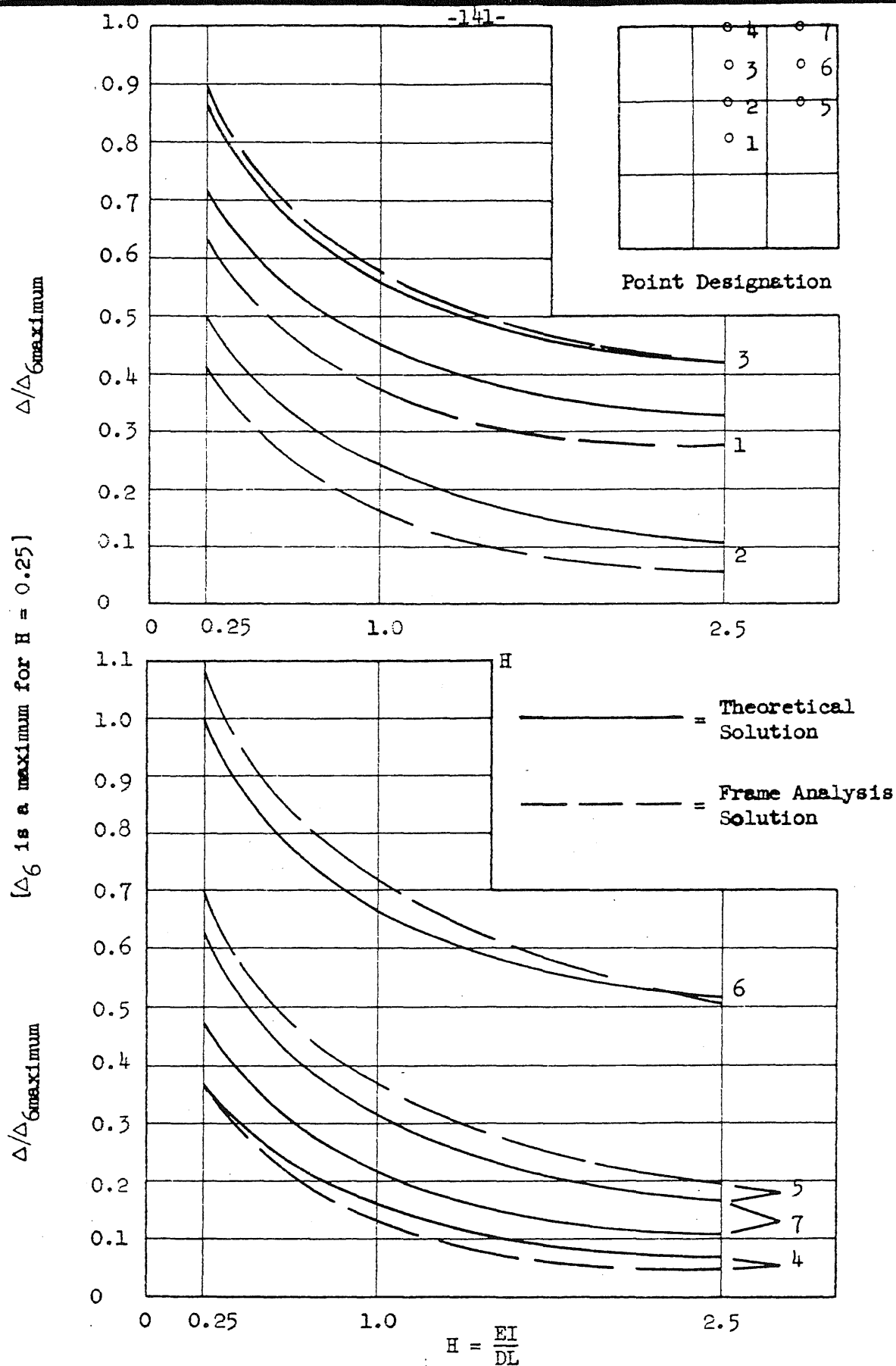


FIG. 4.7 COMPARISONS OF THEORETICAL AND FRAME ANALYSES SOLUTIONS, $J = 0.25$, $K = 90$, ALL PANELS LOADED.

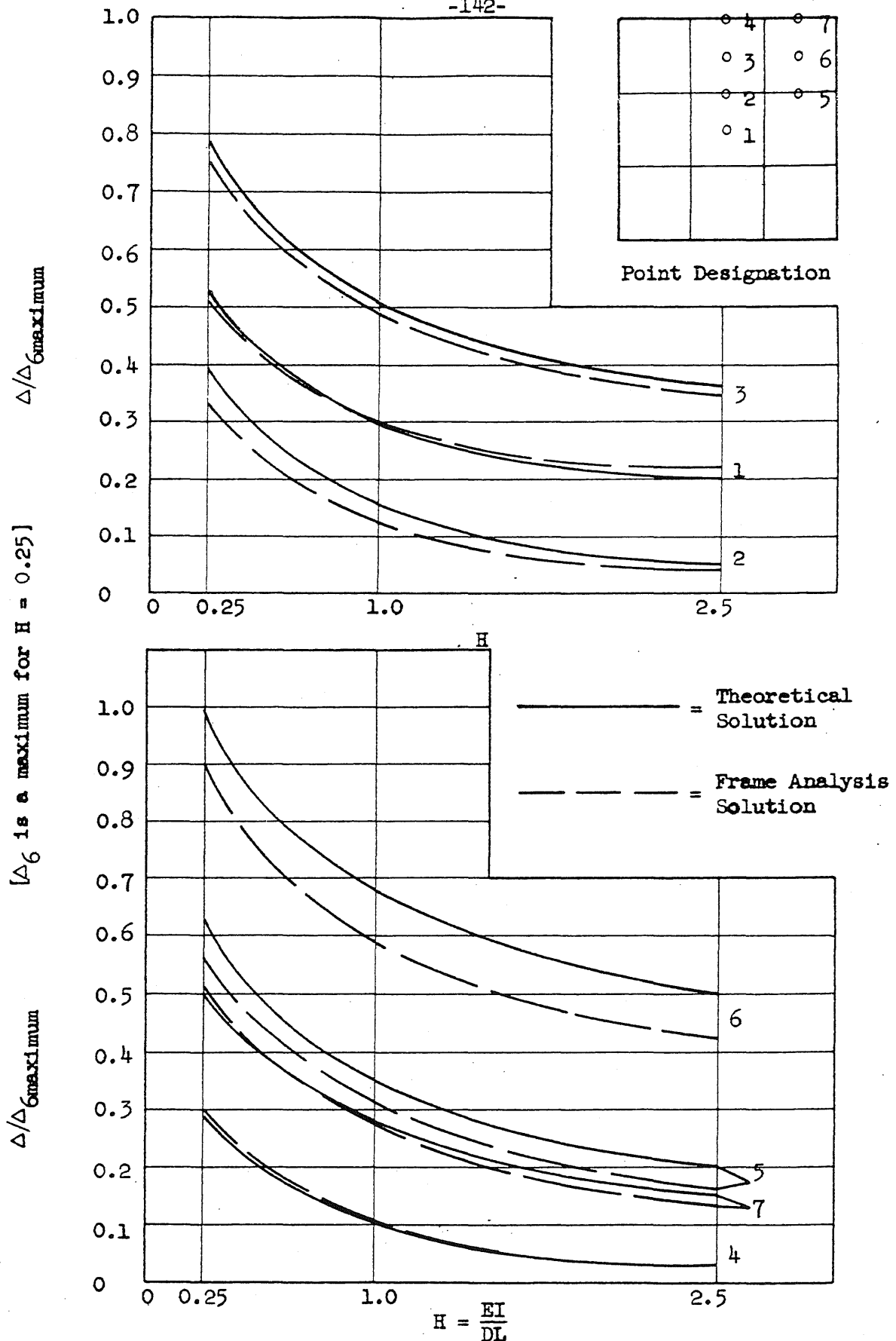


FIG. 4.8 COMPARISONS OF THEORETICAL AND FRAME ANALYSES SOLUTIONS, $J = 1.0$, $K = 10$, ALL PANELS LOADED

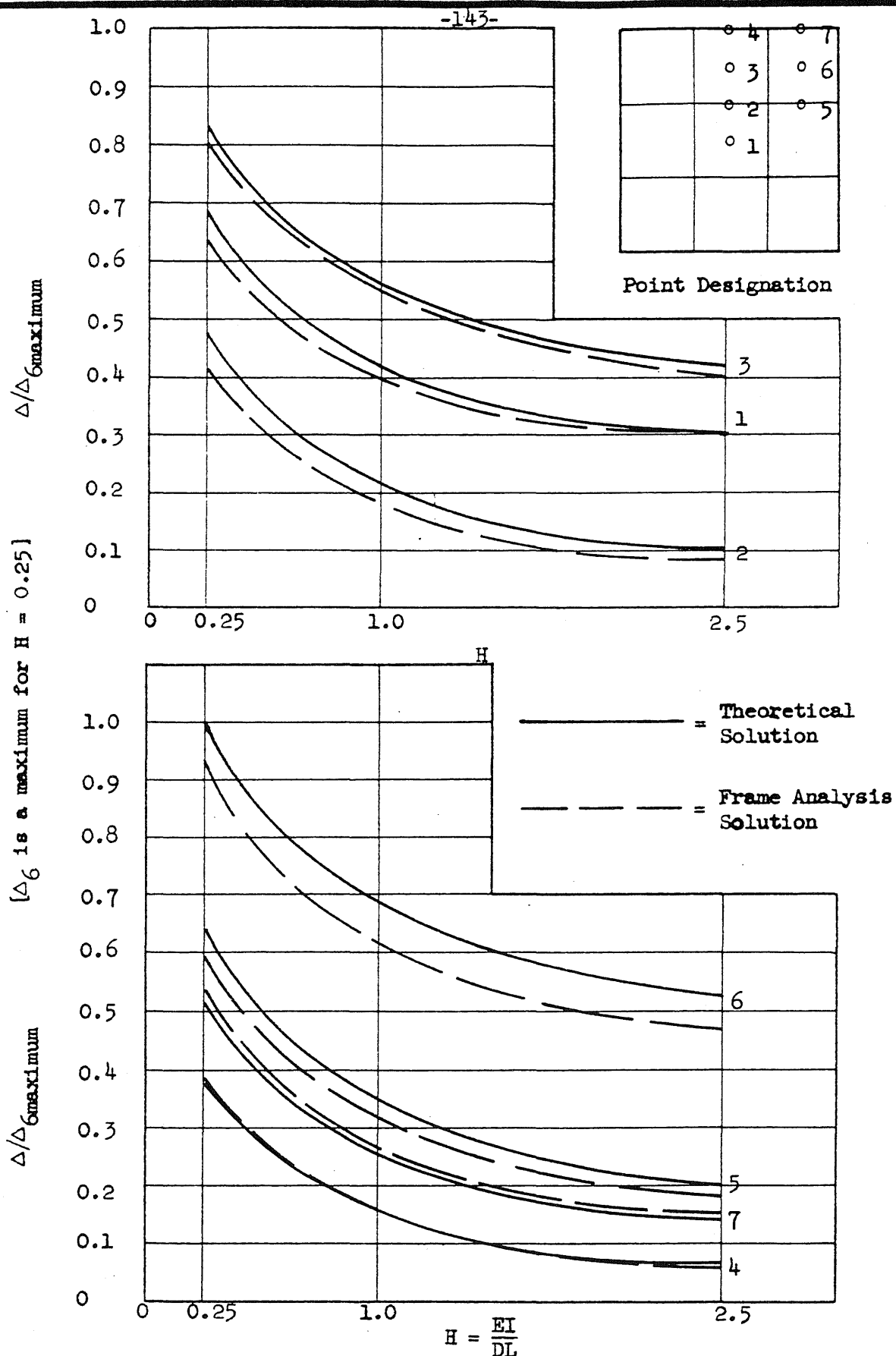


FIG. 4.9 COMPARISONS OF THEORETICAL AND FRAME ANALYSES SOLUTIONS, $J = 1.0$, $K = 30$, ALL PANELS LOADED

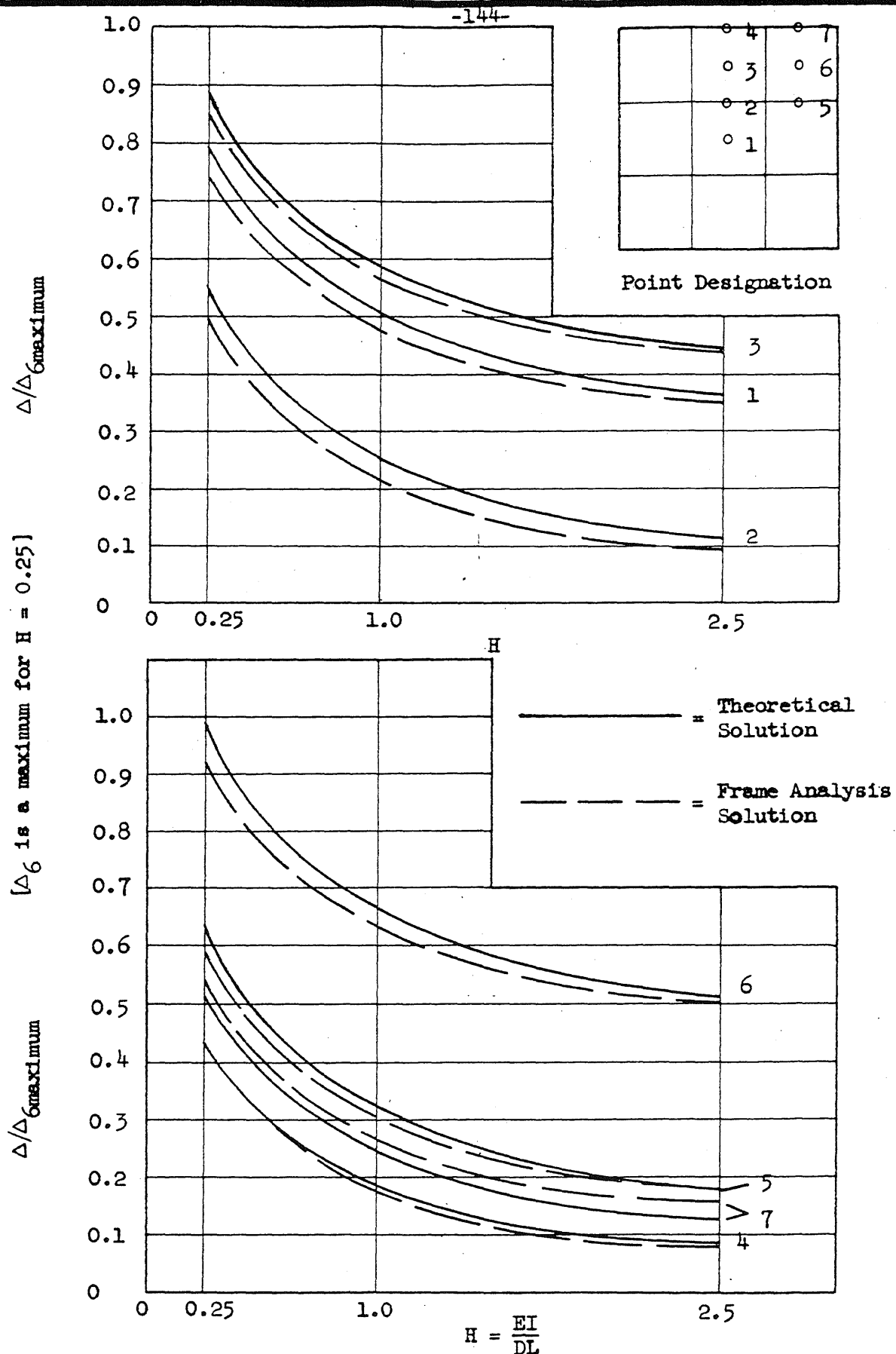


FIG. 4.10 COMPARISONS OF THEORETICAL AND FRAME ANALYSES SOLUTIONS, $J = 1.0$, $K = 90$, ALL PANELS LOADED

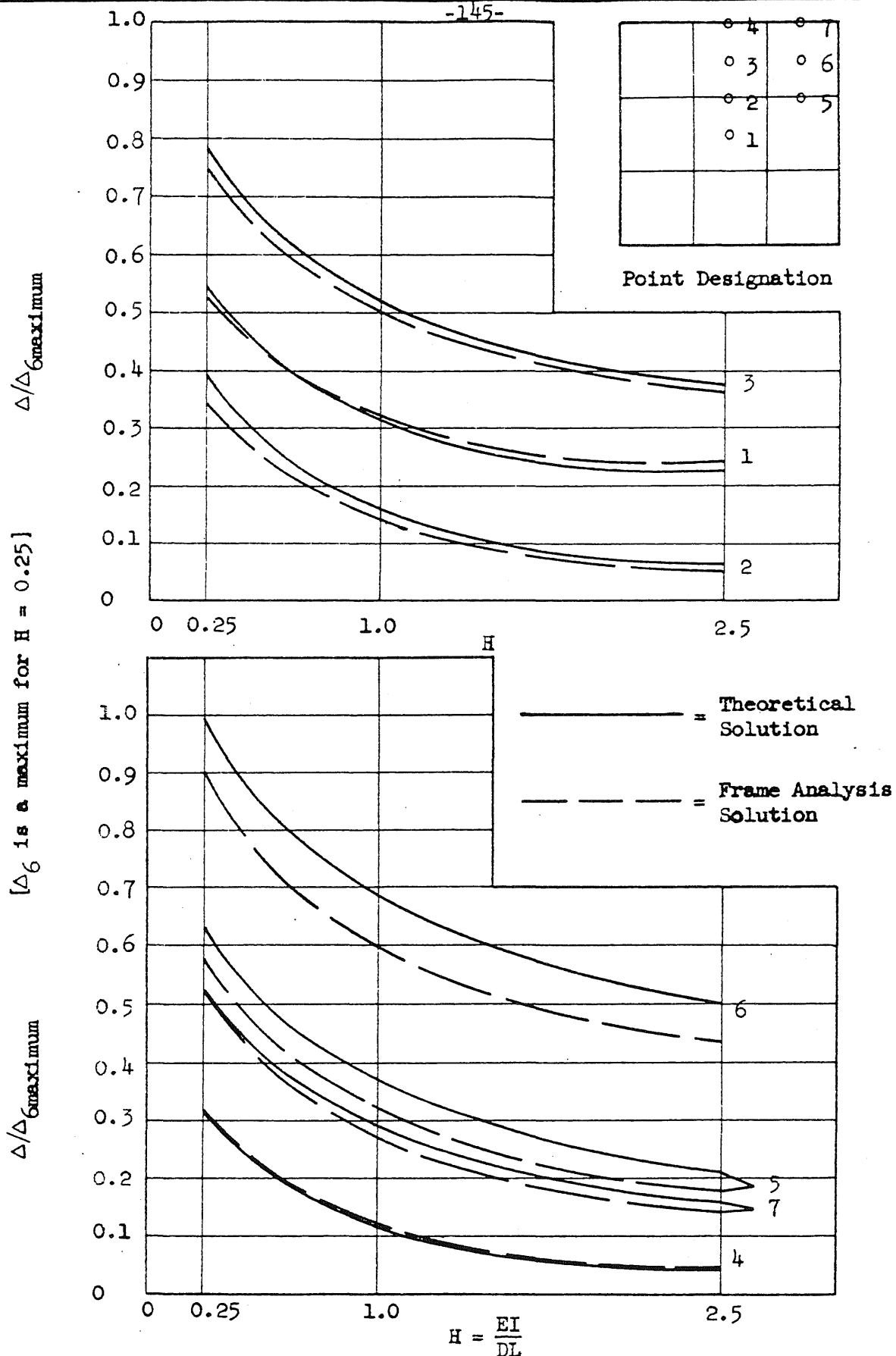


FIG. 4.11 COMPARISONS OF THEORETICAL AND FRAME ANALYSES SOLUTIONS, $J = 2.5$, $K = 10$, ALL PANELS LOADED

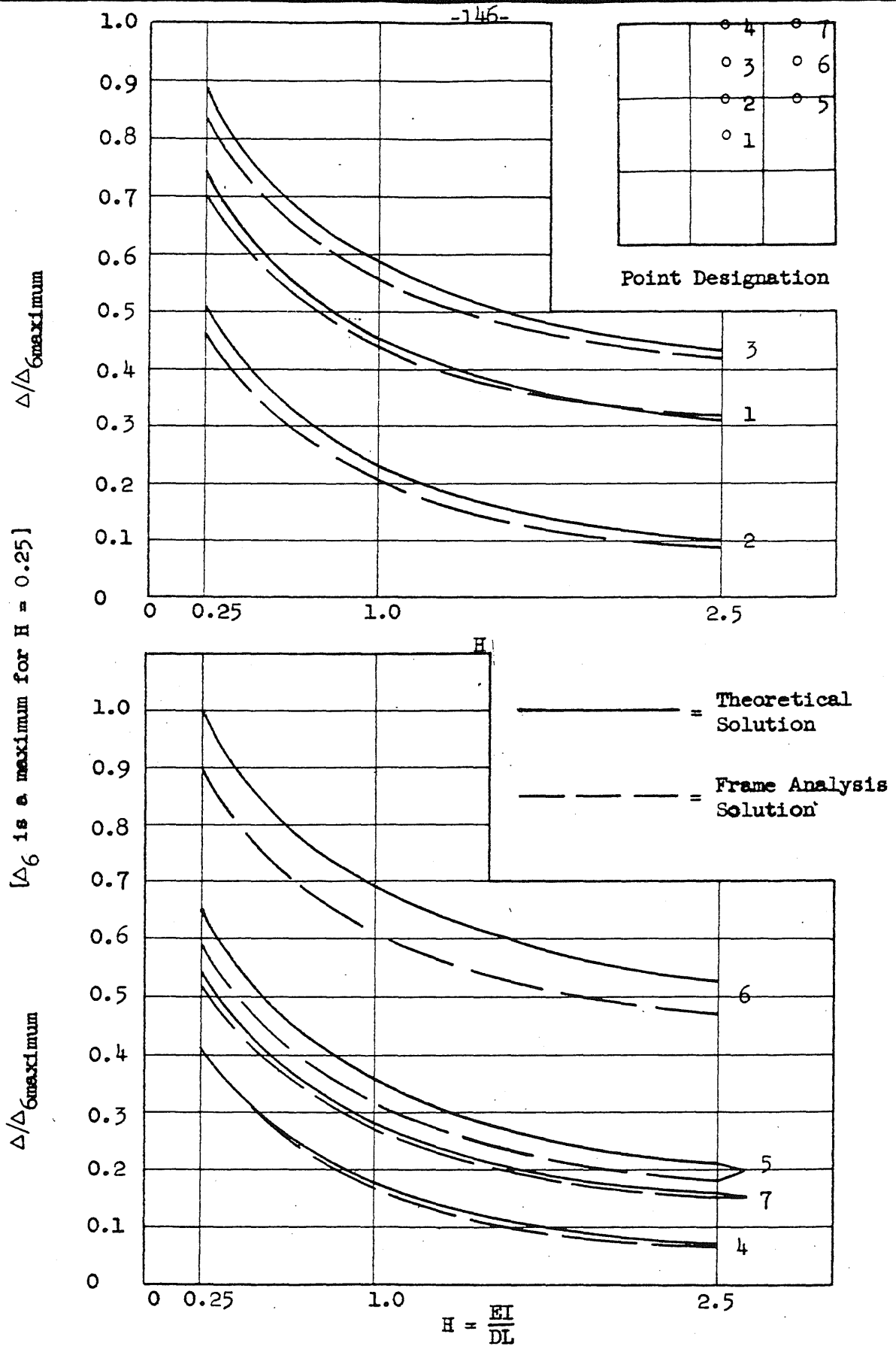


FIG. 4.12 COMPARISONS OF THEORETICAL AND FRAME ANALYSES SOLUTIONS, $J = 2.5$, $K = 30$, ALL PANELS LOADED

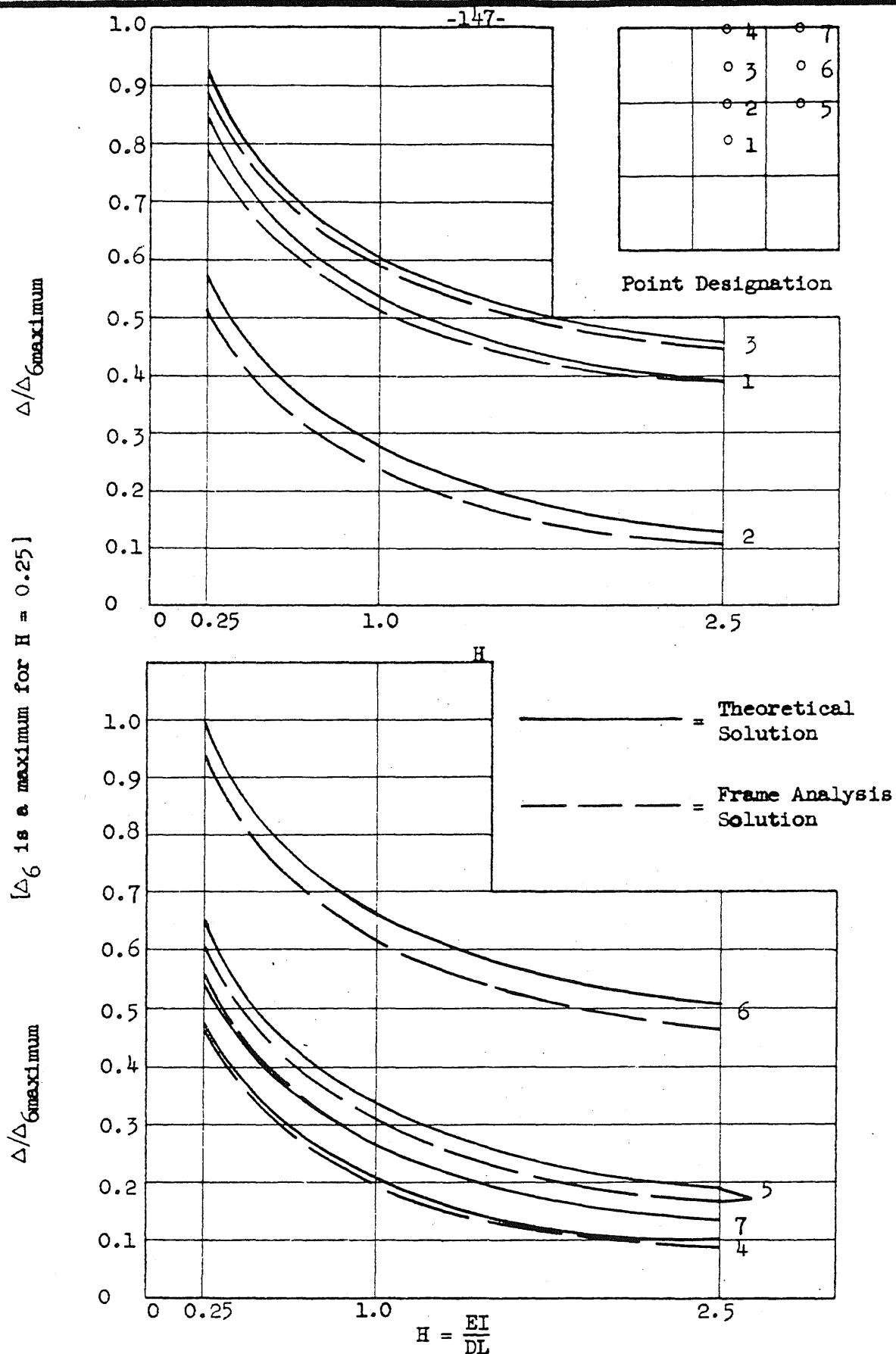


FIG. 4.13 COMPARISONS OF THEORETICAL AND FRAME ANALYSES SOLUTIONS, $J = 2.5$, $K = 90$, ALL PANELS LOADED

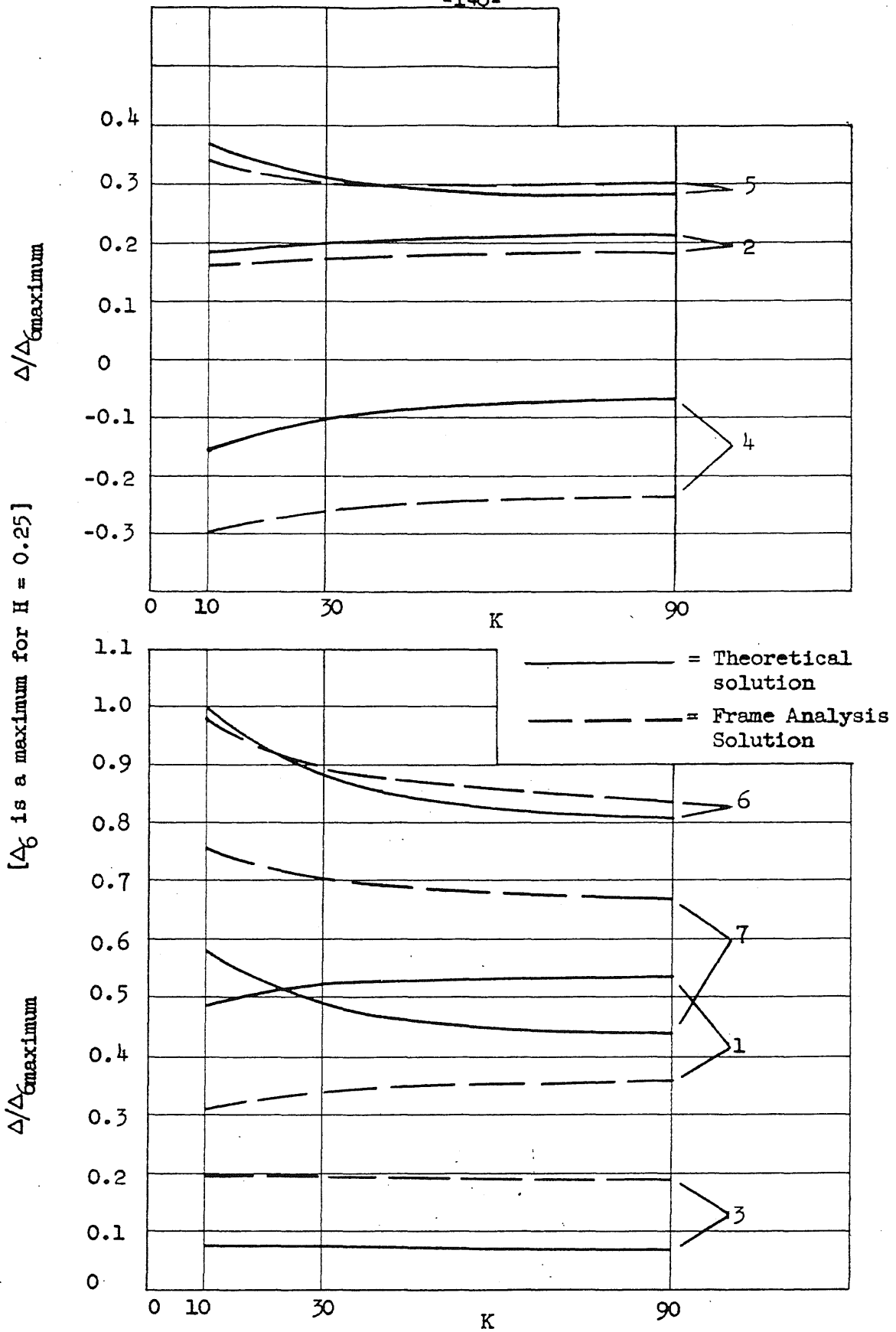


FIG. 4.14 COMPARISONS OF THEORETICAL AND FRAME ANALYSES SOLUTIONS, $H = J = 0.25$, CORNER AND INTERIOR PANELS LOADED

$\Delta/\Delta_{\text{maximum}}$

$[\Delta_6 \text{ is a maximum for } H = 0.25]$

$\Delta/\Delta_{\text{maximum}}$

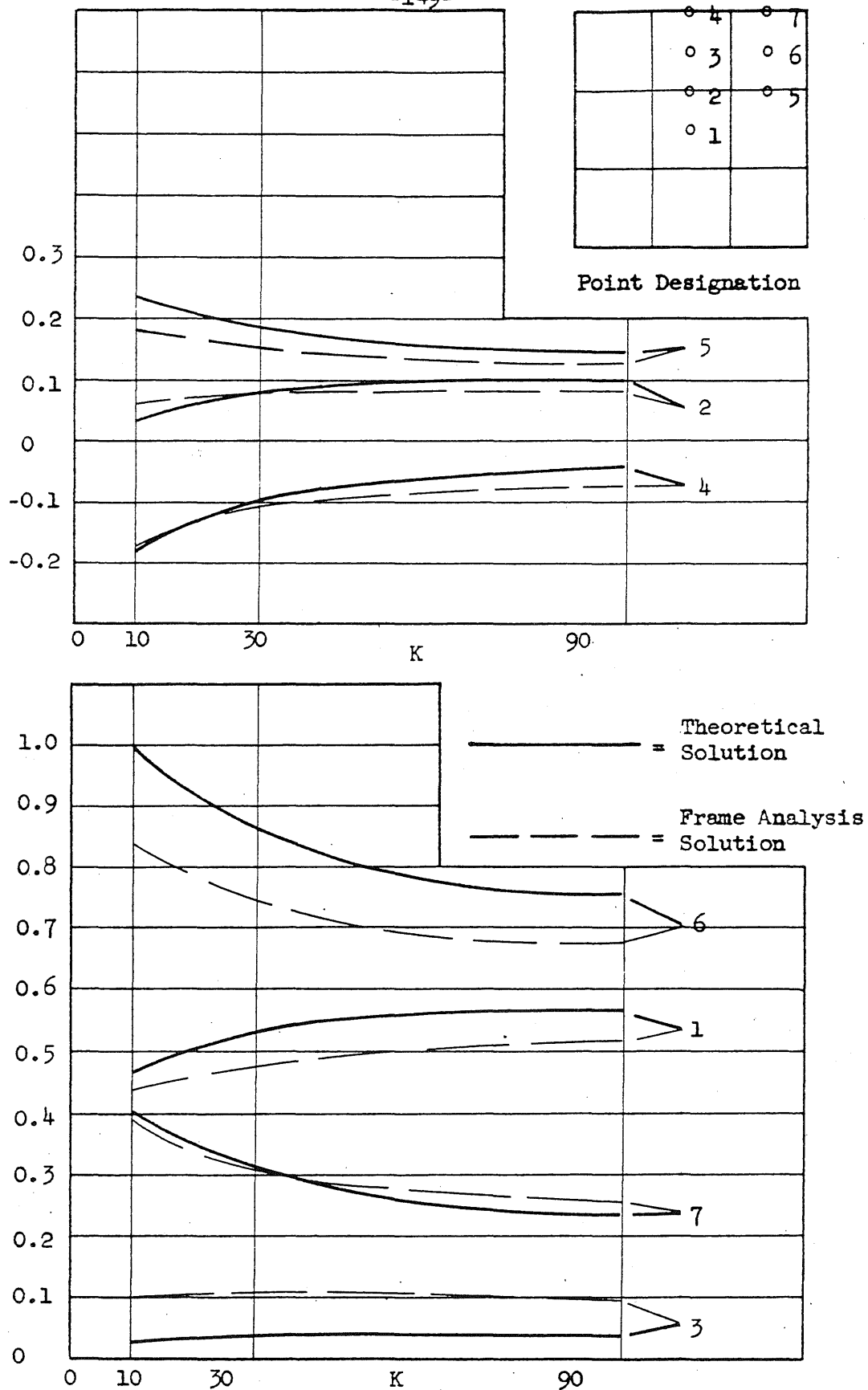


FIG. 4.15 COMPARISONS OF THEORETICAL AND FRAME ANALYSES SOLUTIONS, $H = J = 2.5$, CORNER AND INTERIOR PANELS LOADED

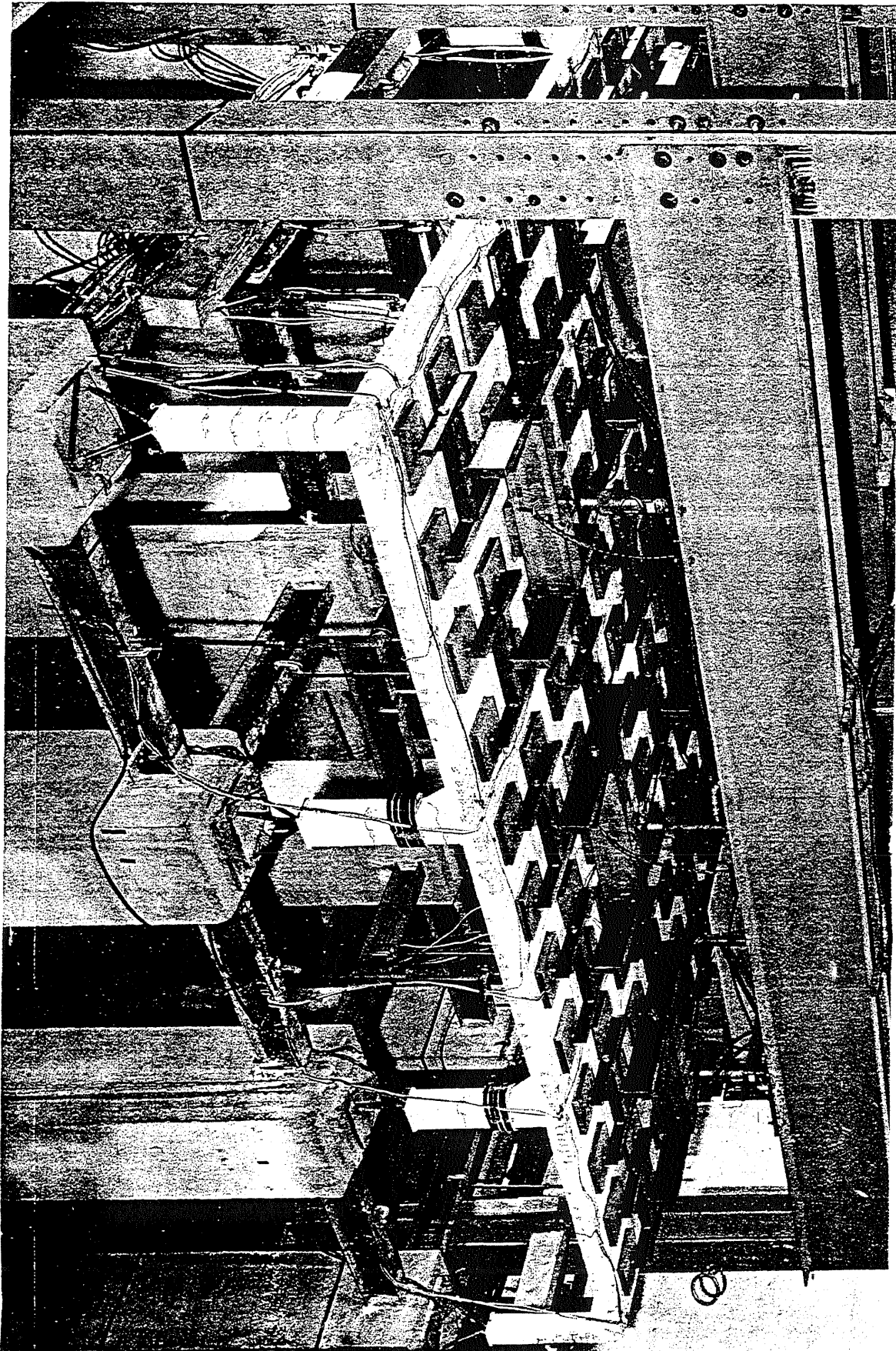


FIG. 5.1 VIEW OF FLAT SLAB (F2)

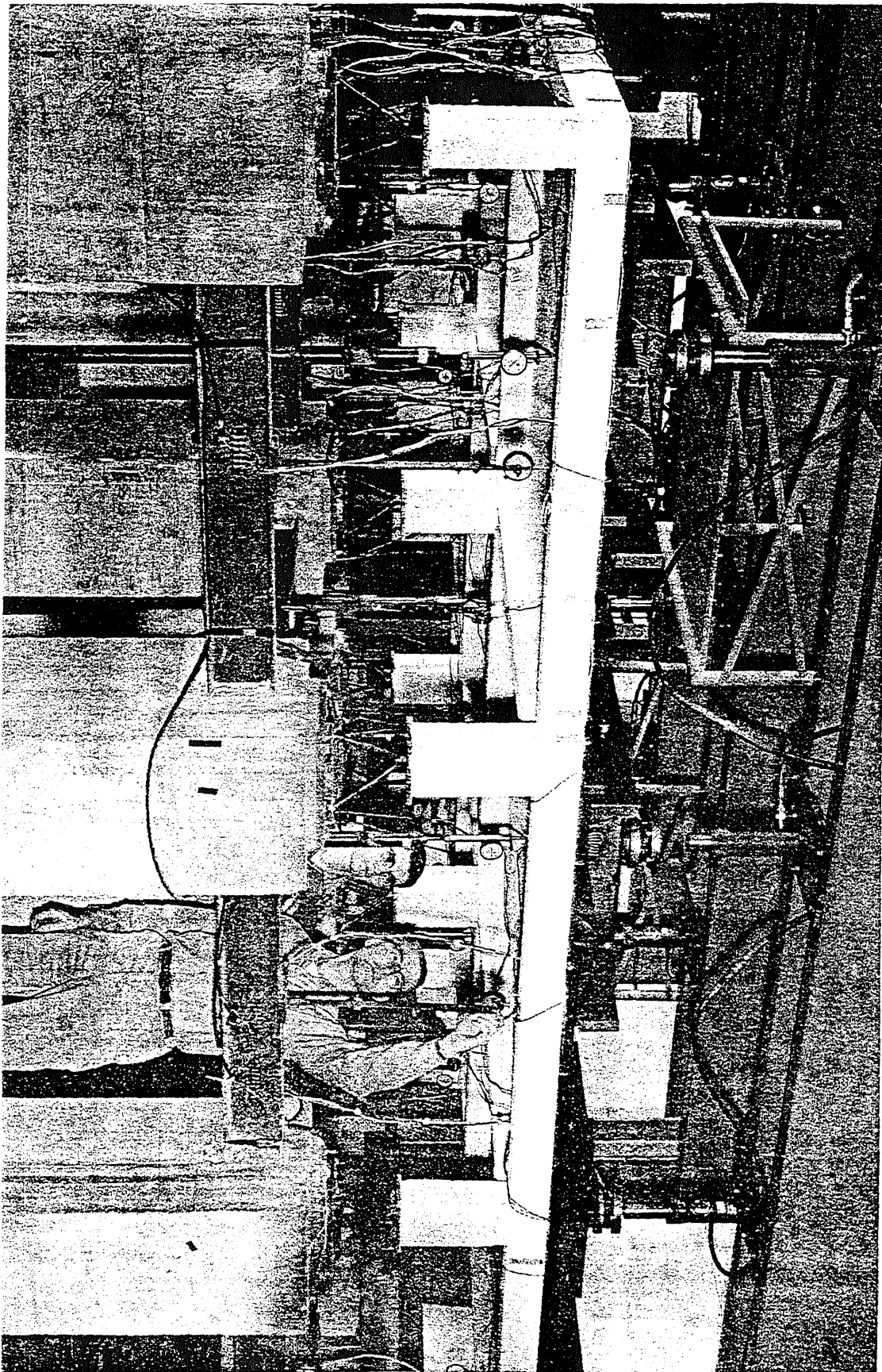


FIG. 5.2 VIEW OF TWO-WAY SLAB WITH DEEP BEAMS (T1)

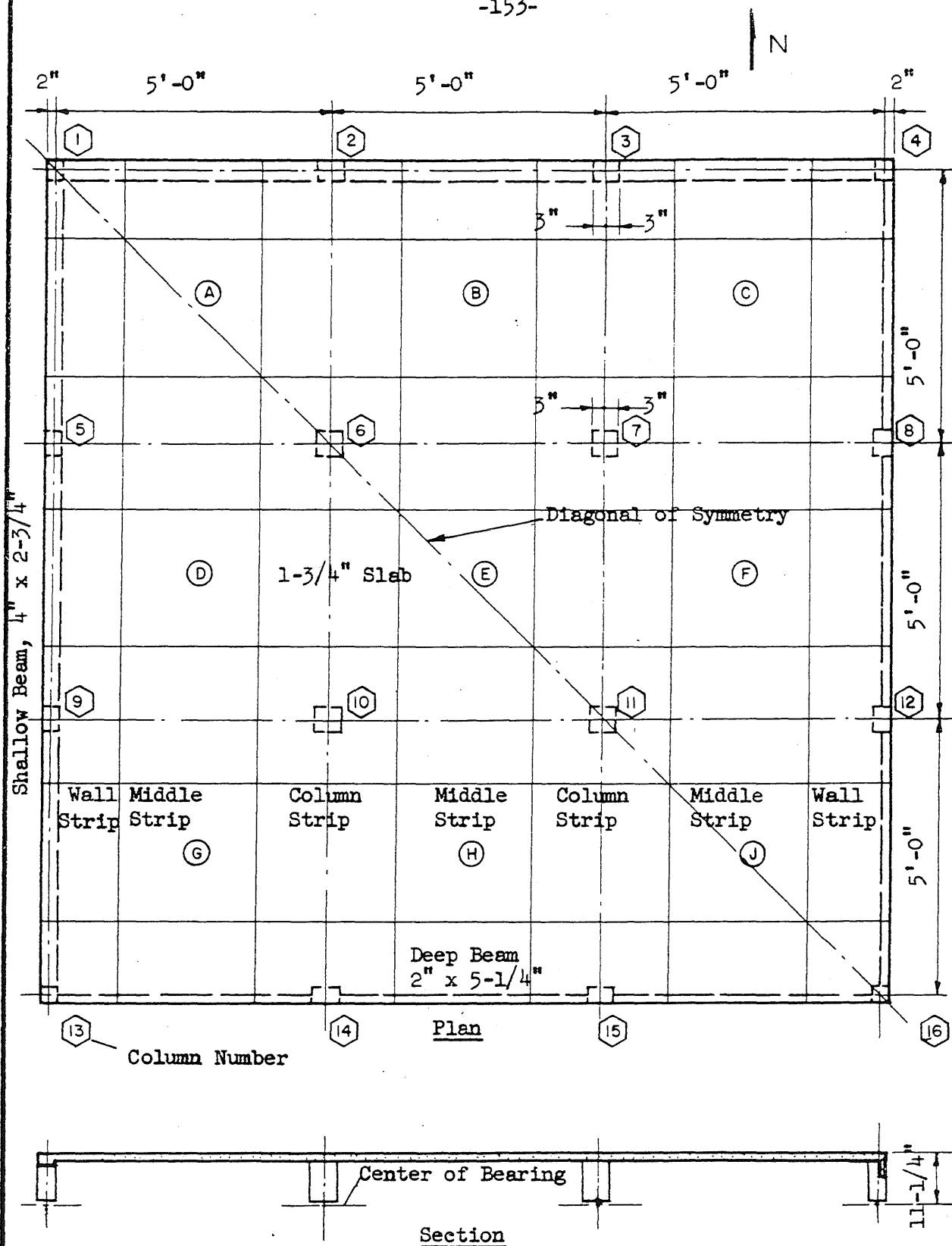


FIG. 5.4 LAYOUT OF FLAT PLATE TEST STRUCTURE (F1)

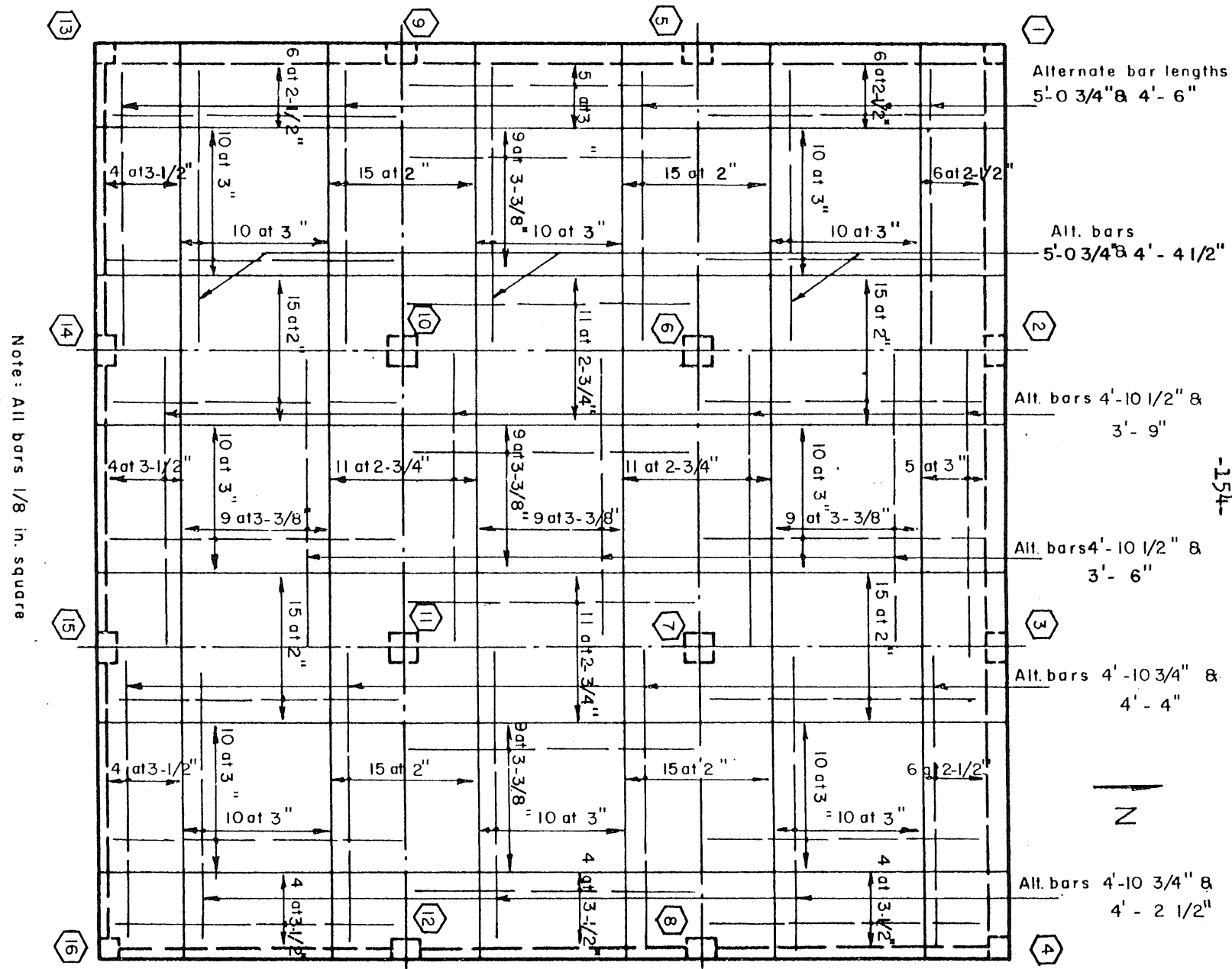
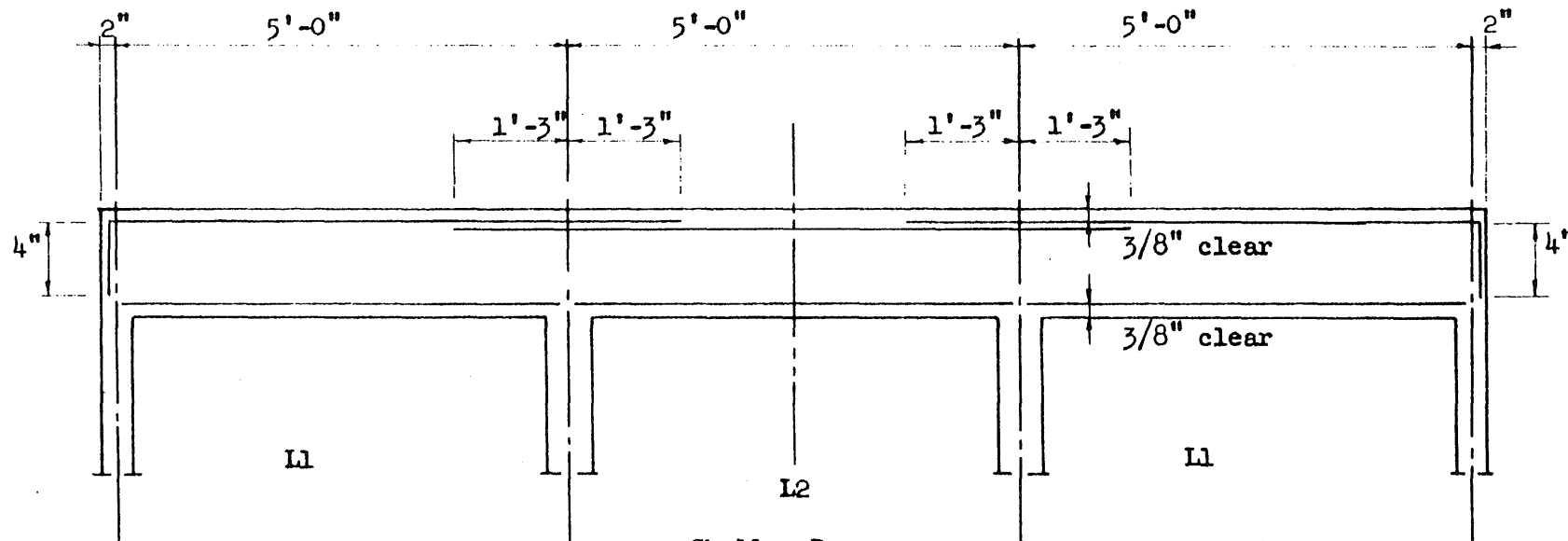


FIG. 5.5 BOTTOM STEEL IN THE FLAT PLATE TEST STRUCTURE (F1)





3-#2 x 6'-8" top
4-#2 x 5'-0" bottom

Shallow Beam
2-#2 x 7'-6" top
3-#2 x 4'-11" bottom

3-#2 x 6'-8" top
4-#2 x 5'-0" bottom

Deep Beam

2-#2 x 6'-8" top
4-#2 x 5'-0" bottom

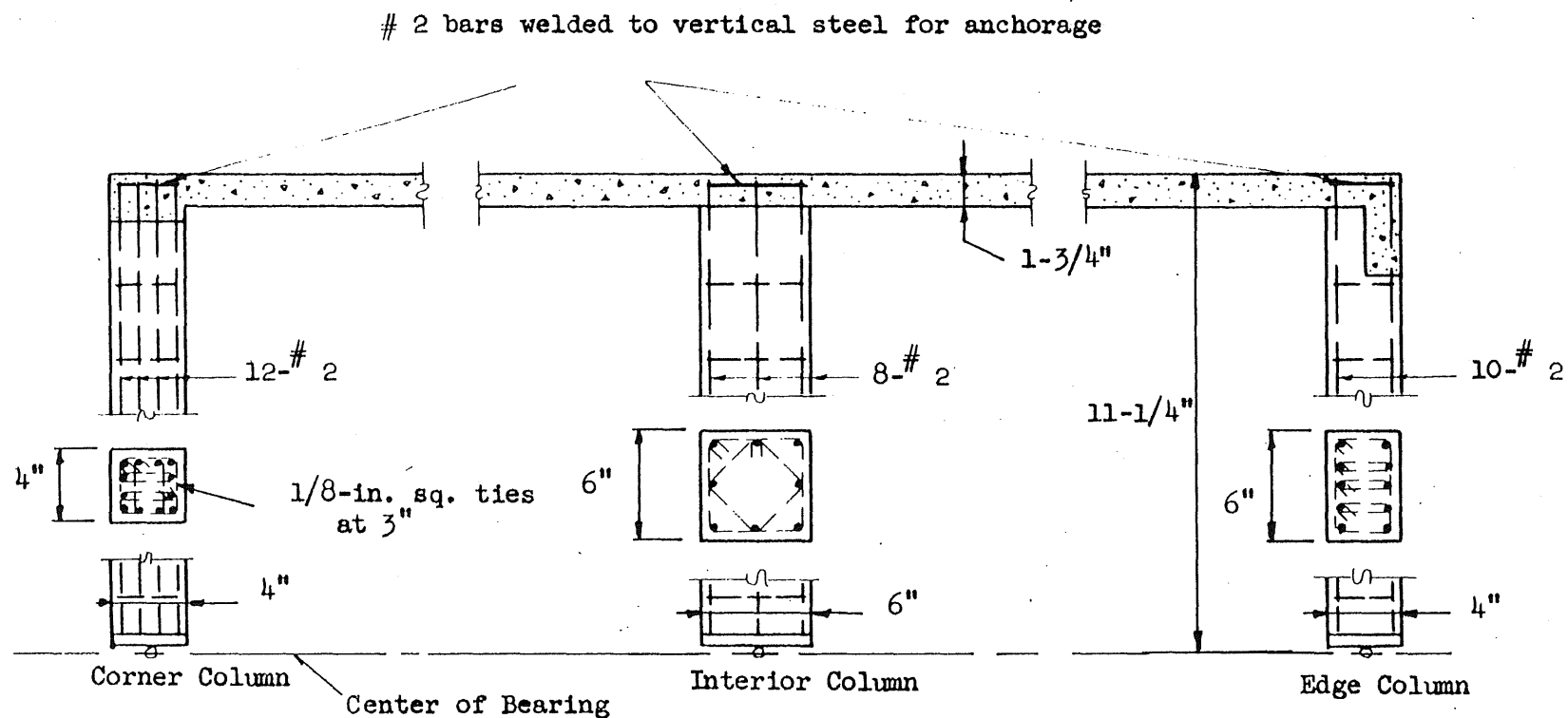
1-#2 x 7'-6" top
2-#2 x 4'-11" bottom

2-#2 x 6'-8" top
2-#2 x 5'-0" bottom

Stirrups

	Beam	No. Stirrups	Size	Spacing Each End from Face of Support
Shallow	L1	25	1/8-in. sq.	12 at 2-1/4"
	L2	25	1/8-in. sq.	12 at 2-1/4"
Deep	L1	12	1/8-in. sq.	5 at 4-3/4"
	L2	12	1/8-in. sq.	5 at 4-3/4"

FIG. 5.7 ARRANGEMENT OF REINFORCEMENT IN BEAMS IN THE FLAT PLATE TEST STRUCTURE (F1)



Note: Cover of 3/8 in. provided for vertical steel

FIG. 5.8 ARRANGEMENT OF COLUMN REINFORCEMENT IN FLAT PLATE TEST STRUCTURE (F1)

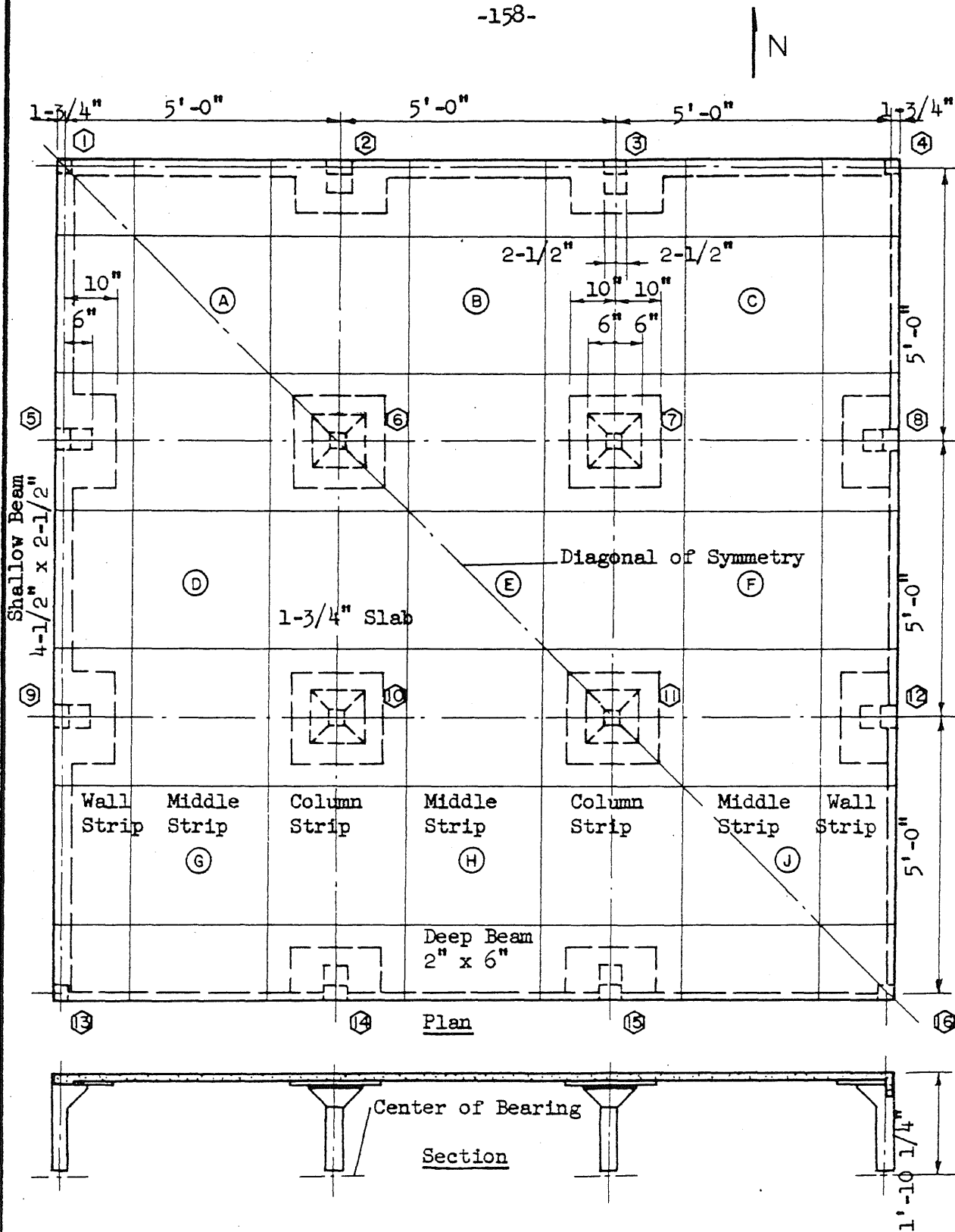


FIG. 5.9 LAYOUT OF FLAT SLAB TEST STRUCTURES (F2, F3)

Note: All bars 1/8-in. square in cross-section.



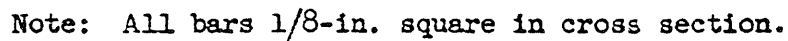
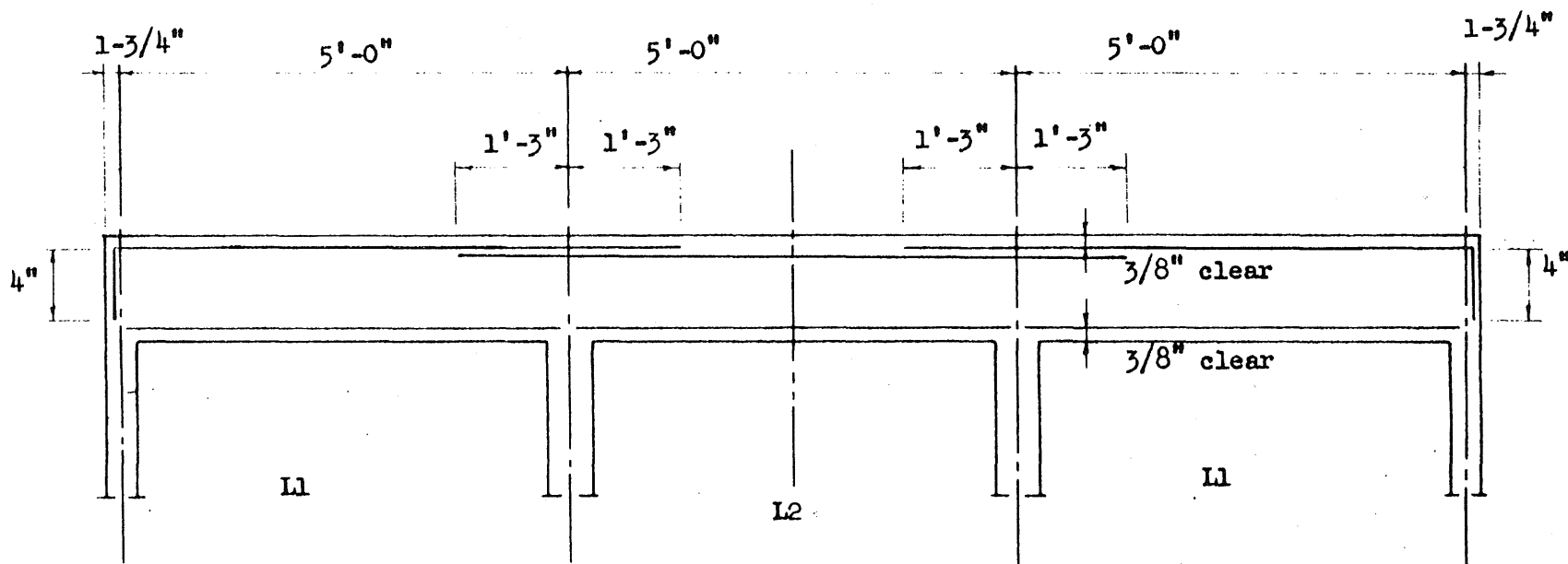


FIG. 5.11 TOP STEEL IN THE FLAT SLAB TEST STRUCTURE REINFORCED WITH 1/8-IN. SQUARE BARS (F2)



-161-

Shallow Beam

5-#2 x 6'-7 1/2" top
5-#2 x 5'-0 1/4" bottom

2-#2 x 7'-6" top
4-#2 x 4'-11 1/2" bottom

5-#2 x 6'-7 1/2" top
5-#2 x 5'-0 1/4" bottom

Deep Beam

3-#2 x 6'-7 1/2" top
3-#2 x 5'-0 1/4" bottom

1-#2 x 7'-6" top
3-#2 x 4'-11 1/2" bottom

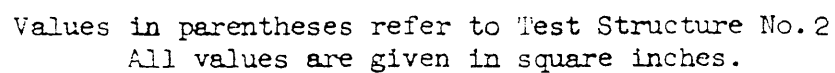
3-#2 x 6'-7 1/2" top
3-#2 x 5'-0 1/4" bottom

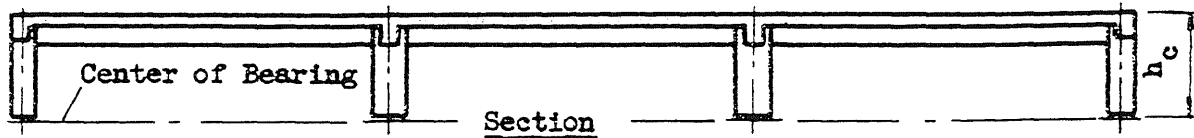
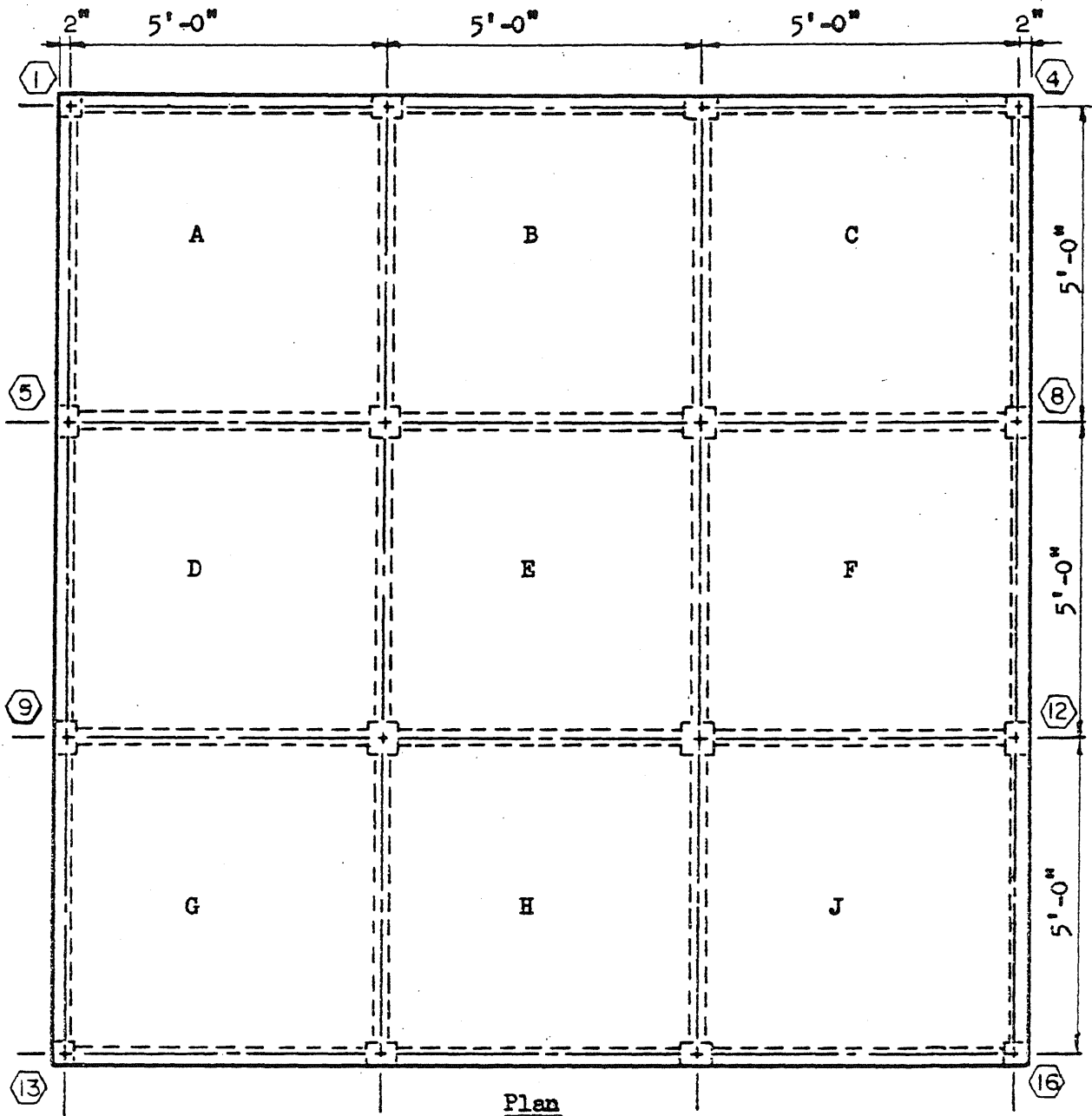
Stirrups

	Beam	No. Stirrups	Size	Spacing Each End from Face of Support
Shallow	L1	28	#10 wire	10 at 1", 1 at 2", 3 at 4-3/4"
	L2	28	#10 wire	10 at 1", 1 at 2", 3 at 4-3/4"
Deep	L1	18	#10 wire	8 at 2-5/8", 1 at 4-1/2"
	L2	18	#10 wire	8 at 2-5/8", 1 at 4-1/2"

Note: No. 2 plain round bars used in Test Structure No. 2 and No. 2 deformed bars in Test Structure No. 5

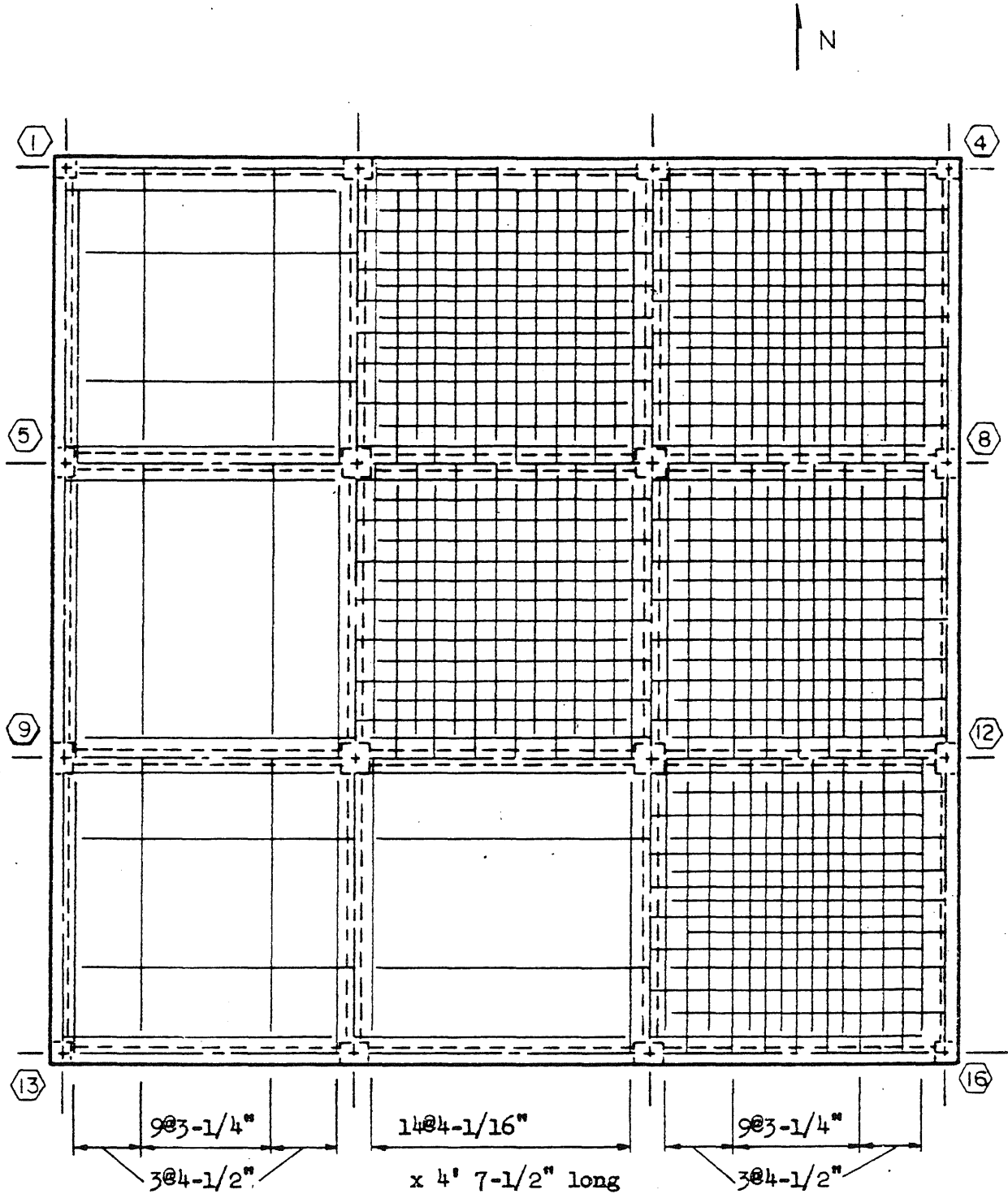
FIG. 5.12 ARRANGEMENT OF REINFORCEMENT IN BEAMS IN THE FLAT SLAB TEST STRUCTURES (F2, F3)





Note: Dimension $h = 16\text{-}5/8"$ in Typical Two-Way Slab (T1) and
 $h_c = 13\text{-}7/8"$ in Two-Way Slab with Shallow Beams (T2)

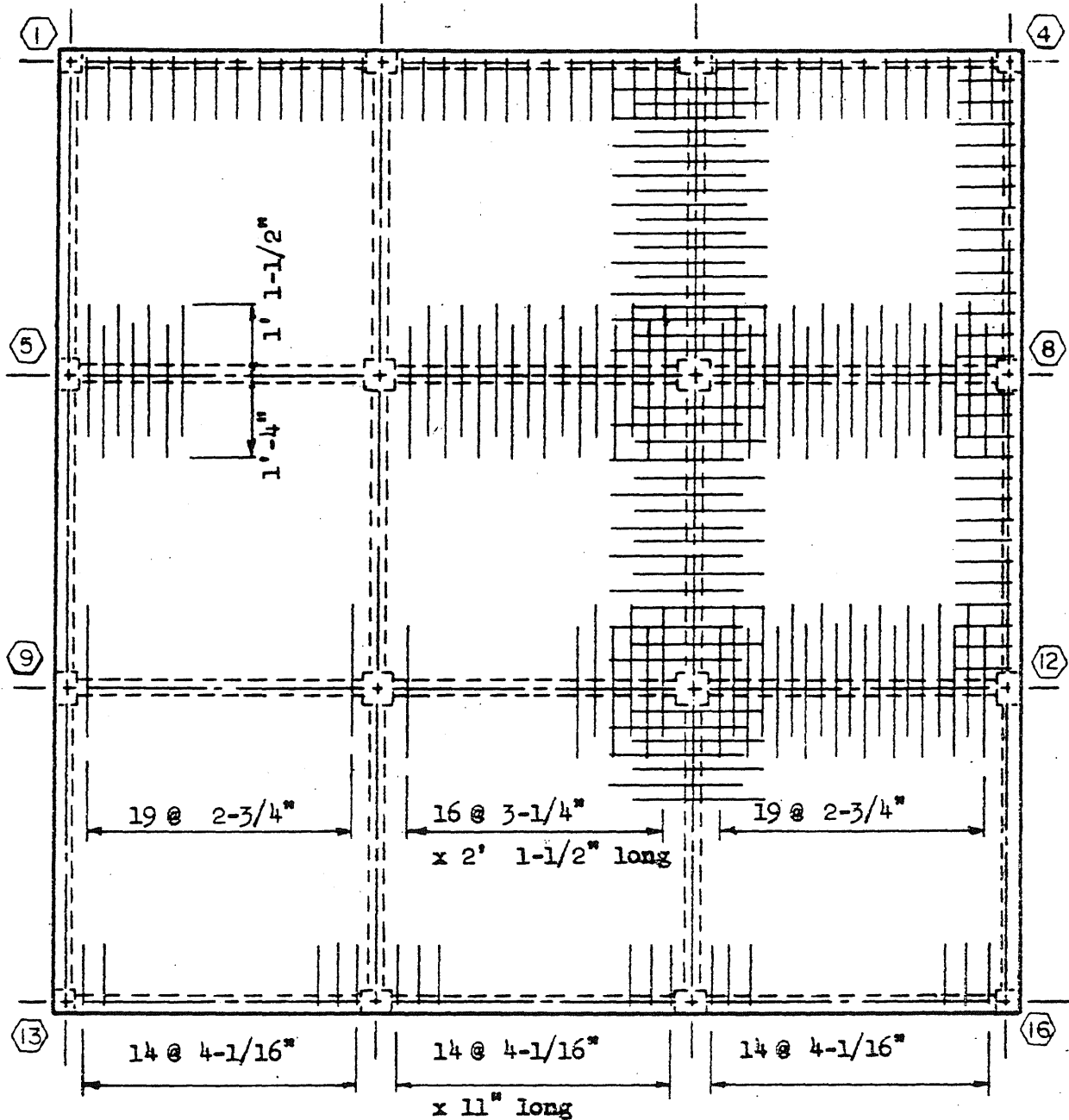
FIG. 5.16 LAYOUT OF TWO-WAY SLAB TEST STRUCTURES (T1 , T2)



Note: All bars are 1/8-in. square in cross section

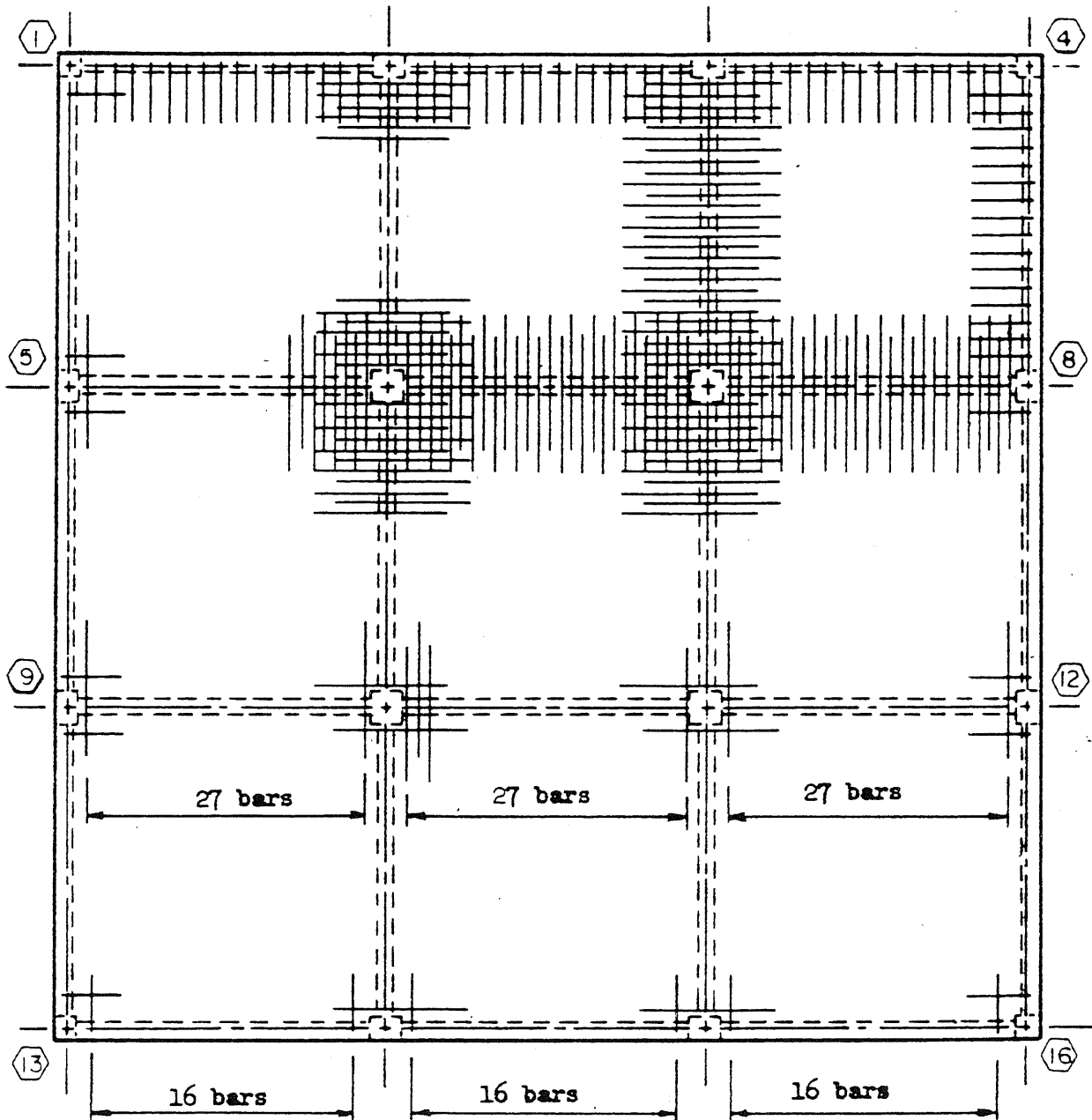
FIG. 5.17 ARRANGEMENT OF BOTTOM REINFORCEMENT IN TYPICAL TWO-WAY SLAB (T1)

N



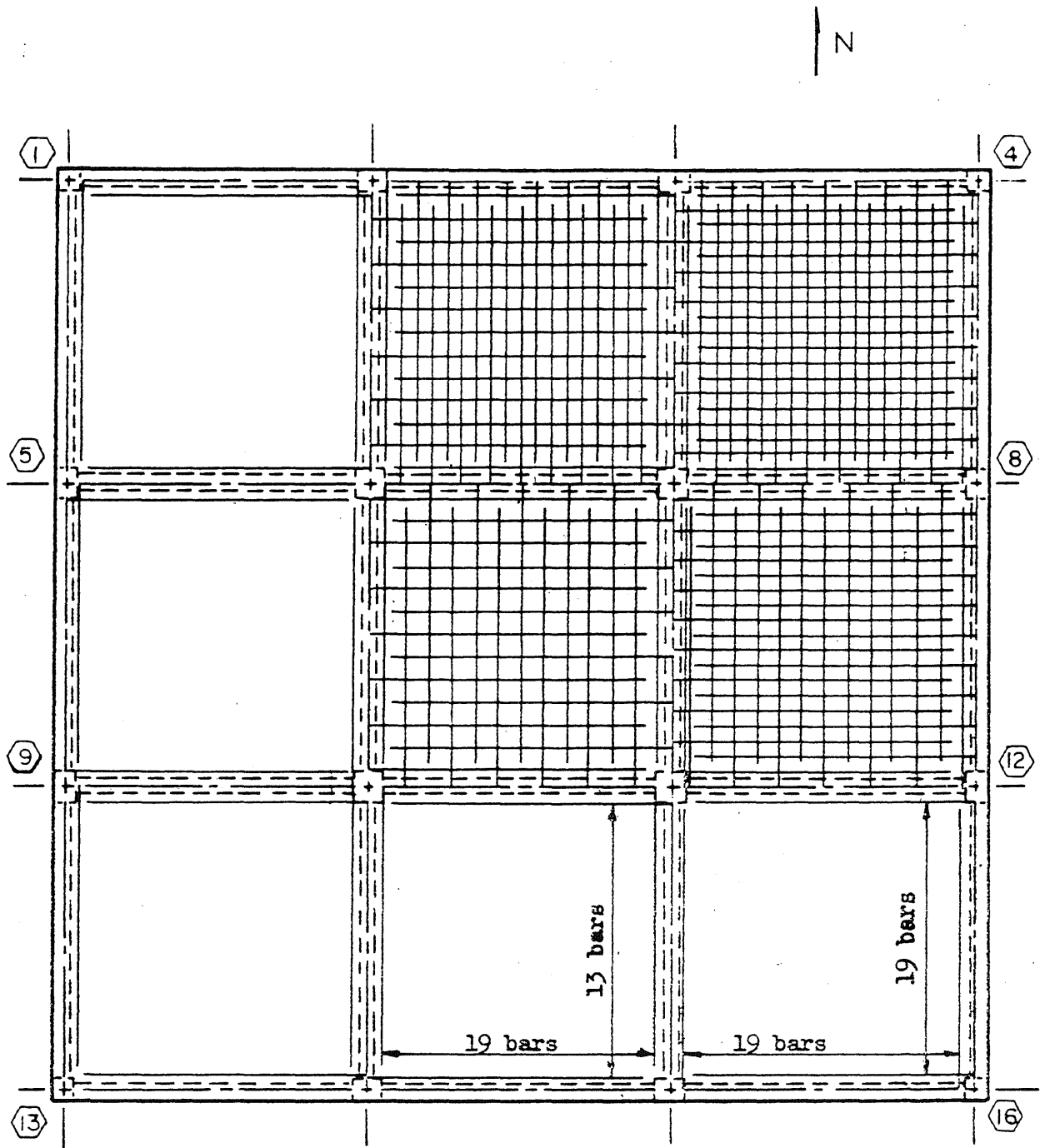
Note: All bars are 1/8-in. square in cross section

FIG. 5.18 ARRANGEMENT OF TOP REINFORCEMENT IN TYPICAL TWO-WAY SLAB (T1)



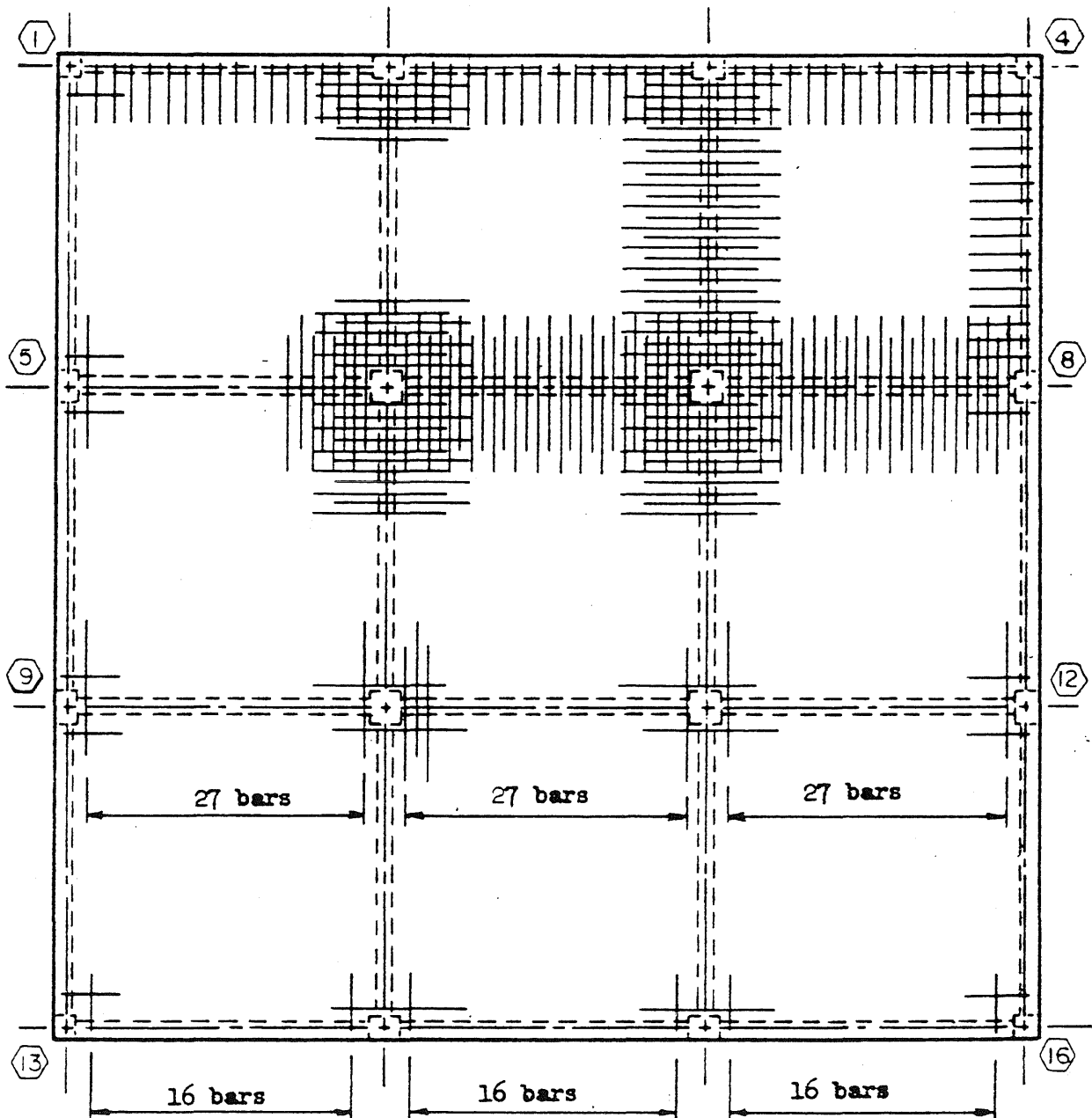
Note: All bars are 1/8-in. square in cross section and are spaced uniformly.

FIG. 5.21 ARRANGEMENT OF TOP REINFORCEMENT IN TWO-WAY SLAB WITH SHALLOW BEAMS (T2)



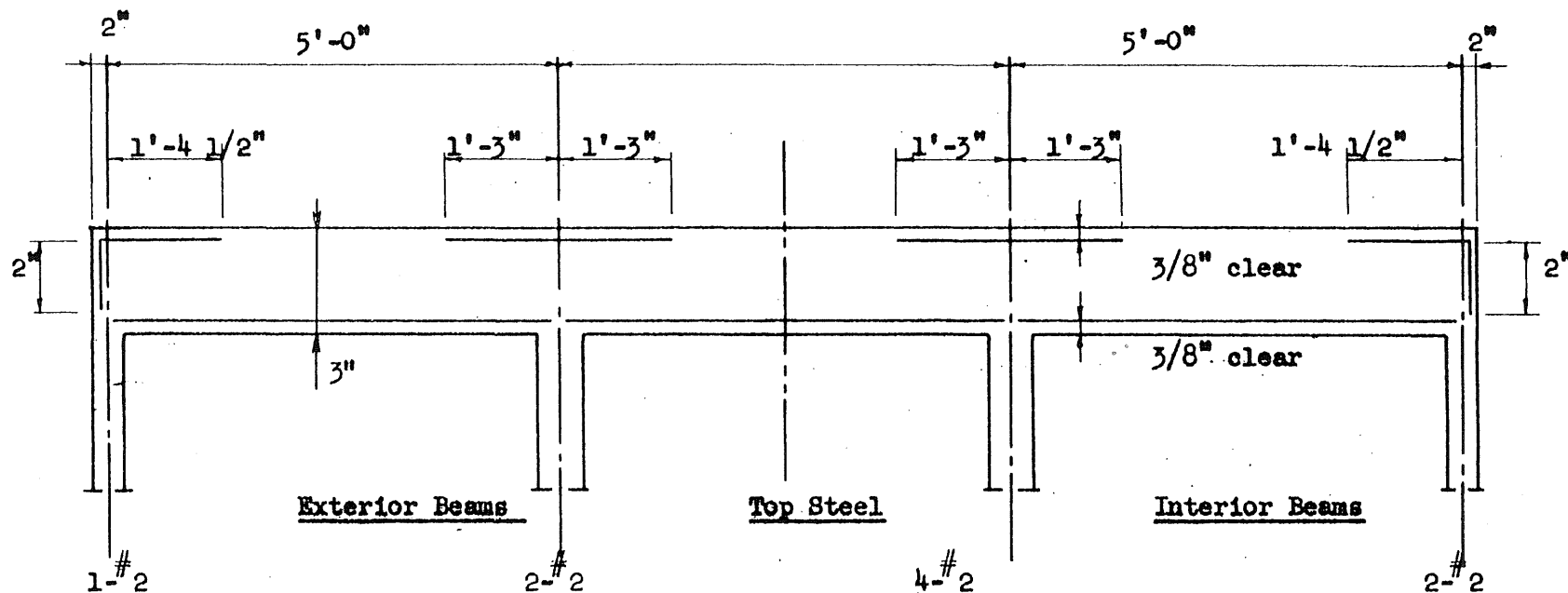
Note: All bars are 1/8-in. square in cross section and are spaced uniformly.

FIG. 5.20 ARRANGEMENT OF BOTTOM REINFORCEMENT IN TWO-WAY SLAB WITH SHALLOW BEAMS



Note: All bars are 1/8-in. square in cross section and are spaced uniformly.

FIG. 5.21 ARRANGEMENT OF TOP REINFORCEMENT IN TWO-WAY SLAB WITH SHALLOW BEAMS (T2)



1-#2 and 2-1/8-in. sq.
x 4' - 7"

1-#2
x 4' - 6"

Bottom Steel
2-#2
x 4' - 6"

3-#2
x 4' - 7"

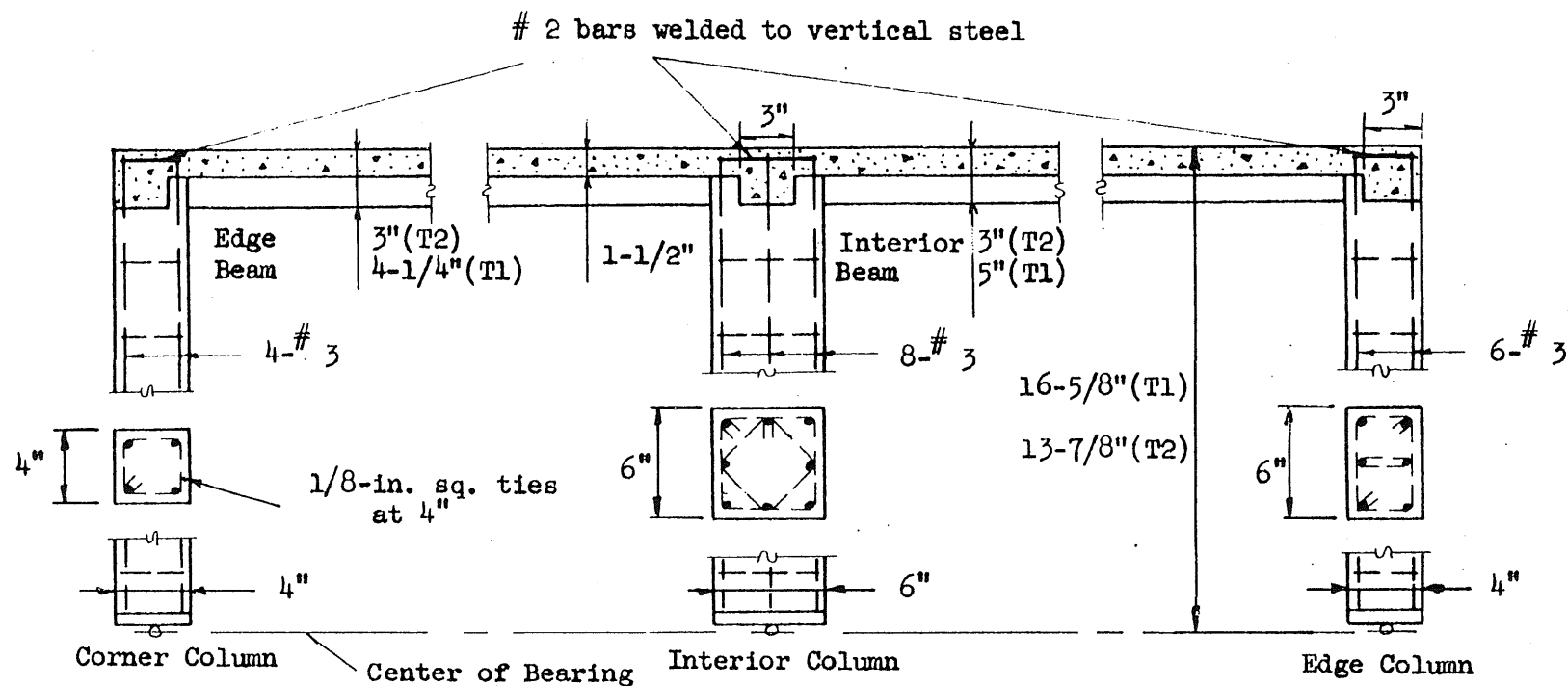
Stirrups

6 at 1" and 6 at 1-1/2" each end

6 at 1" and 10 at 1-1/2" each end

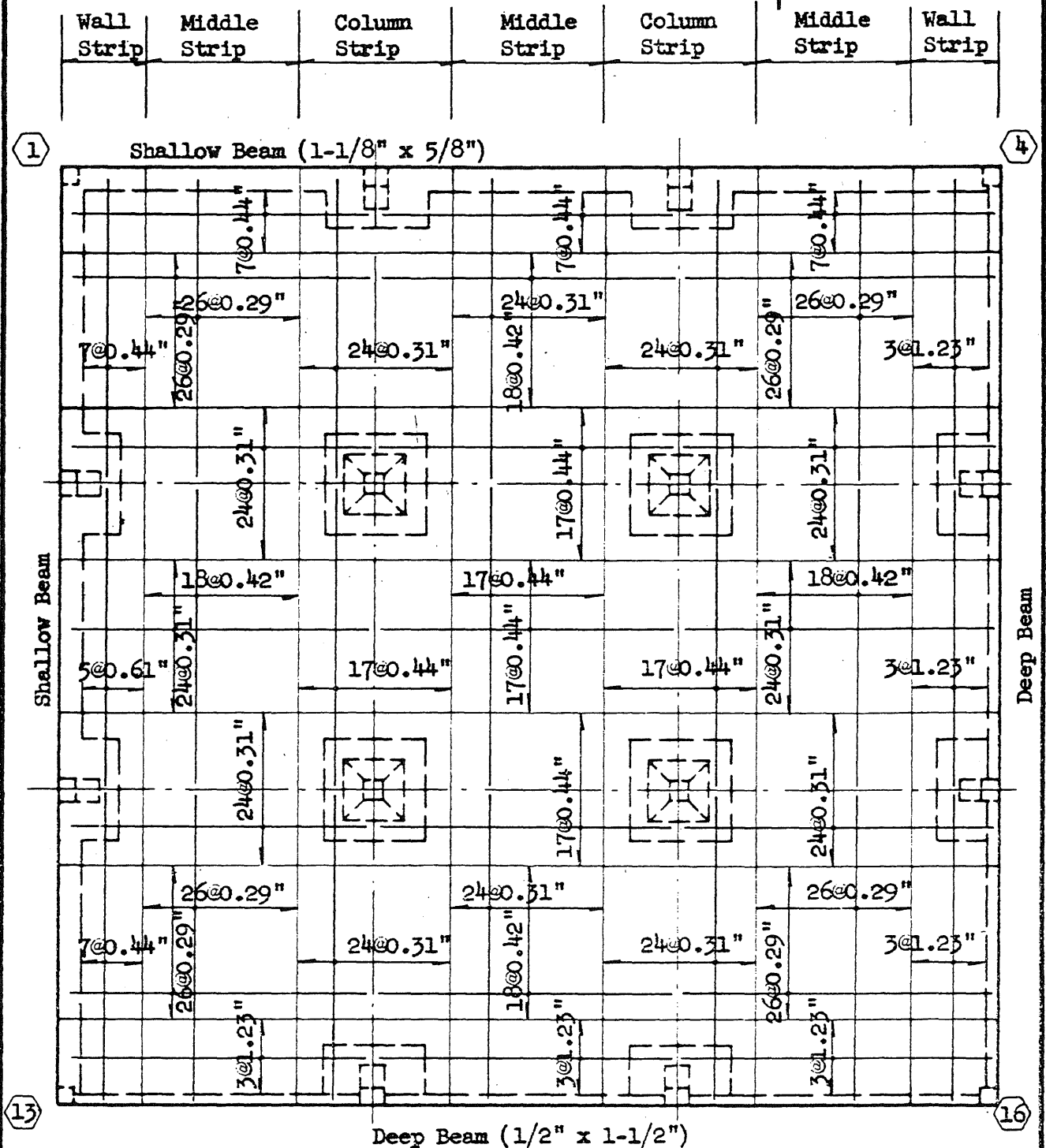
All stirrups 1/8-in. sq. bars. First stirrup 1/2" from face of column, first 6 stirrups closed.

FIG. 5.22 ARRANGEMENT OF REINFORCEMENT IN BEAMS OF TWO-WAY SLAB WITH SHALLOW BEAMS (T2)



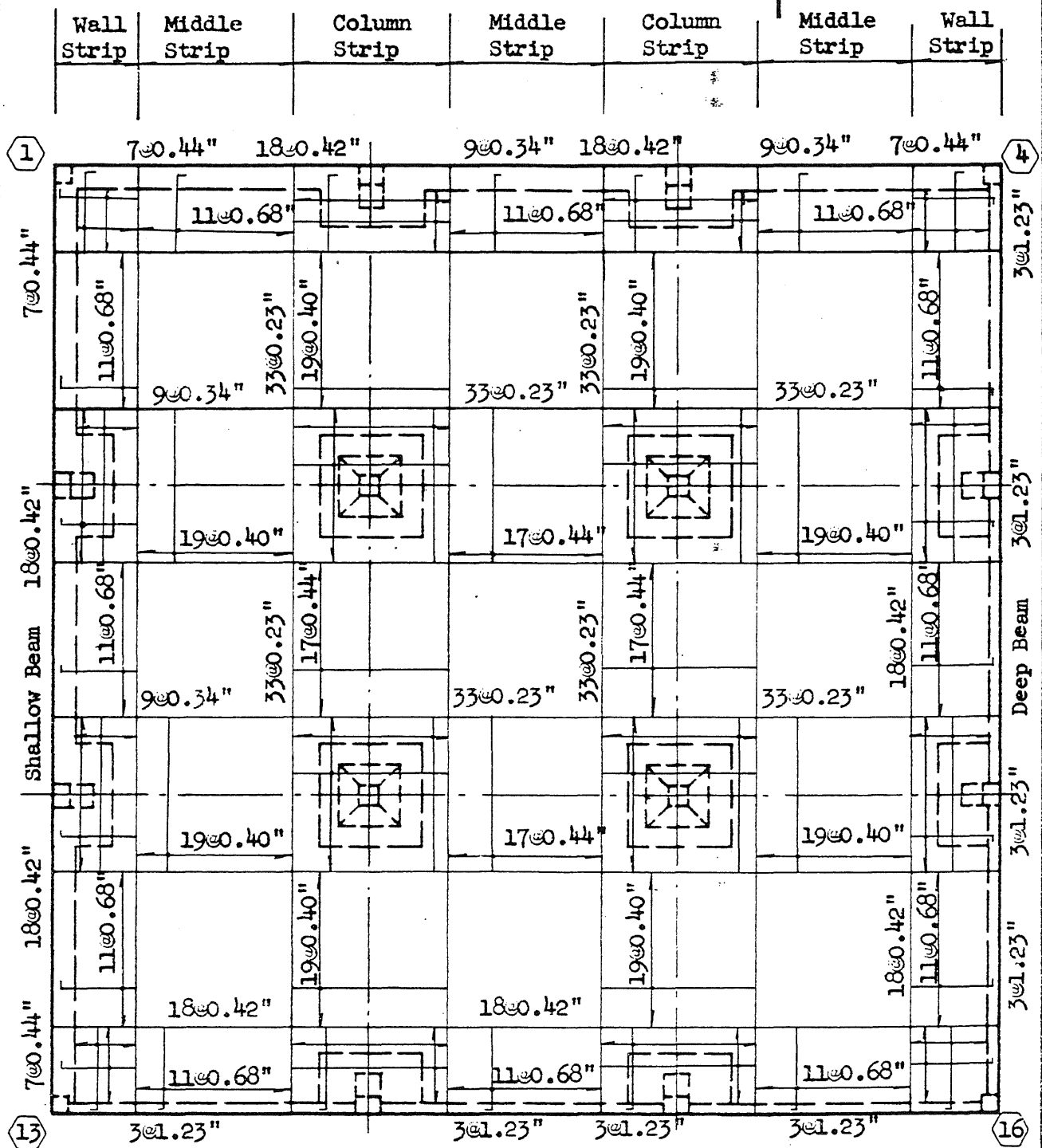
Note: Cover of 3/8 in. provided for vertical steel

FIG. 5.23 ARRANGEMENT OF COLUMN REINFORCEMENT IN TWO-WAY SLABS (T1, T2)



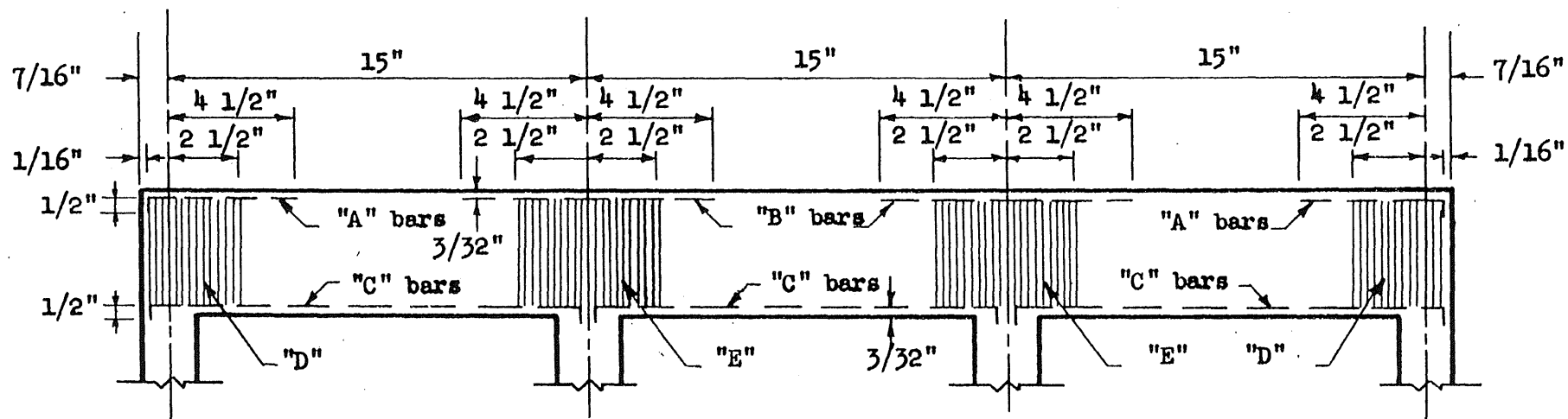
Note: All bars in middle and column strips were 15.0 in. or 7.5 in. in length and were placed alternately. All bars in the wall strips were 15.0 in. in length. All bar diameters were 0.0355 in.

FIG. 5.24 ARRANGEMENT OF BOTTOM REINFORCEMENT IN THE FLAT SLAB (F5)



Note: All bars in middle and column strips were 7.50 in. in length.
 All bars in wall strips were 4.10 in. in length with an
 additional 0.5 in. long hook. All bar diameters were 0.0355 in.

FIG. 5.25 ARRANGEMENT OF TOP REINFORCEMENT IN THE FLAT SLAB (F5)



Shallow Beam ($d = 1/2$ "

"A" bars - 16 Gauge Wire - 4 @ 5 1/2"

"B" bars - 16 Gauge Wire - 6 @ 9"

"C" bars - 16 Gauge Wire - 3 @ 16"

Deep Beam ($d = 1-3/8$ "

"A" bars - 16 Gauge Wire - 2 @ 5 1/2"

"B" bars - 16 Gauge Wire - 3 @ 9"

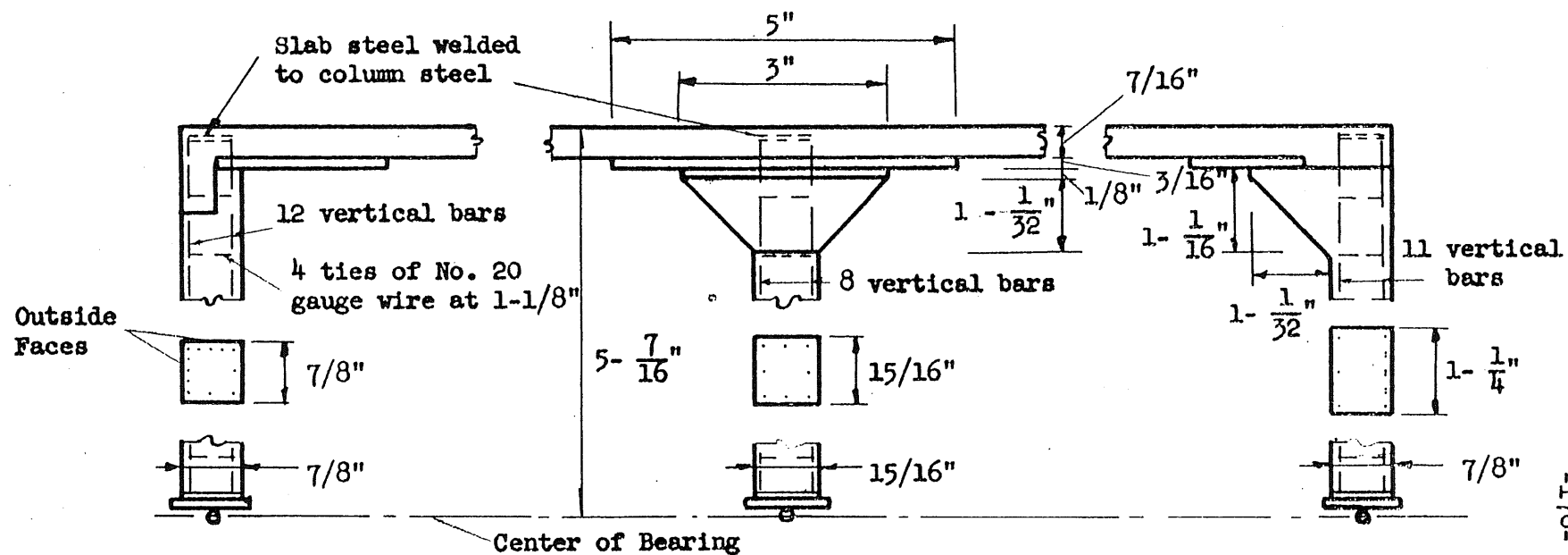
"C" bars - 16 Gauge Wire - 2 @ 16"

Shear - Torsion Reinforcement

"D" spiral - 20 Gauge Wire - 3" @ 1/4" intervals

"E" spiral - 20 Gauge Wire - 5" @ 1/4" intervals

FIG. 5.26 ARRANGEMENT OF BEAM REINFORCEMENT IN FLAT SLAB TEST STRUCTURE (F5)



Note: All vertical column reinforcement consisted of No. 16 gauge wire having a diameter of 0.063 in. and a cross-sectional area of 0.00312 square in. A cover of 1/16 in. was provided.

FIG. 5.27 ARRANGEMENT OF COLUMN REINFORCEMENT IN THE FLAT SLAB (F5)

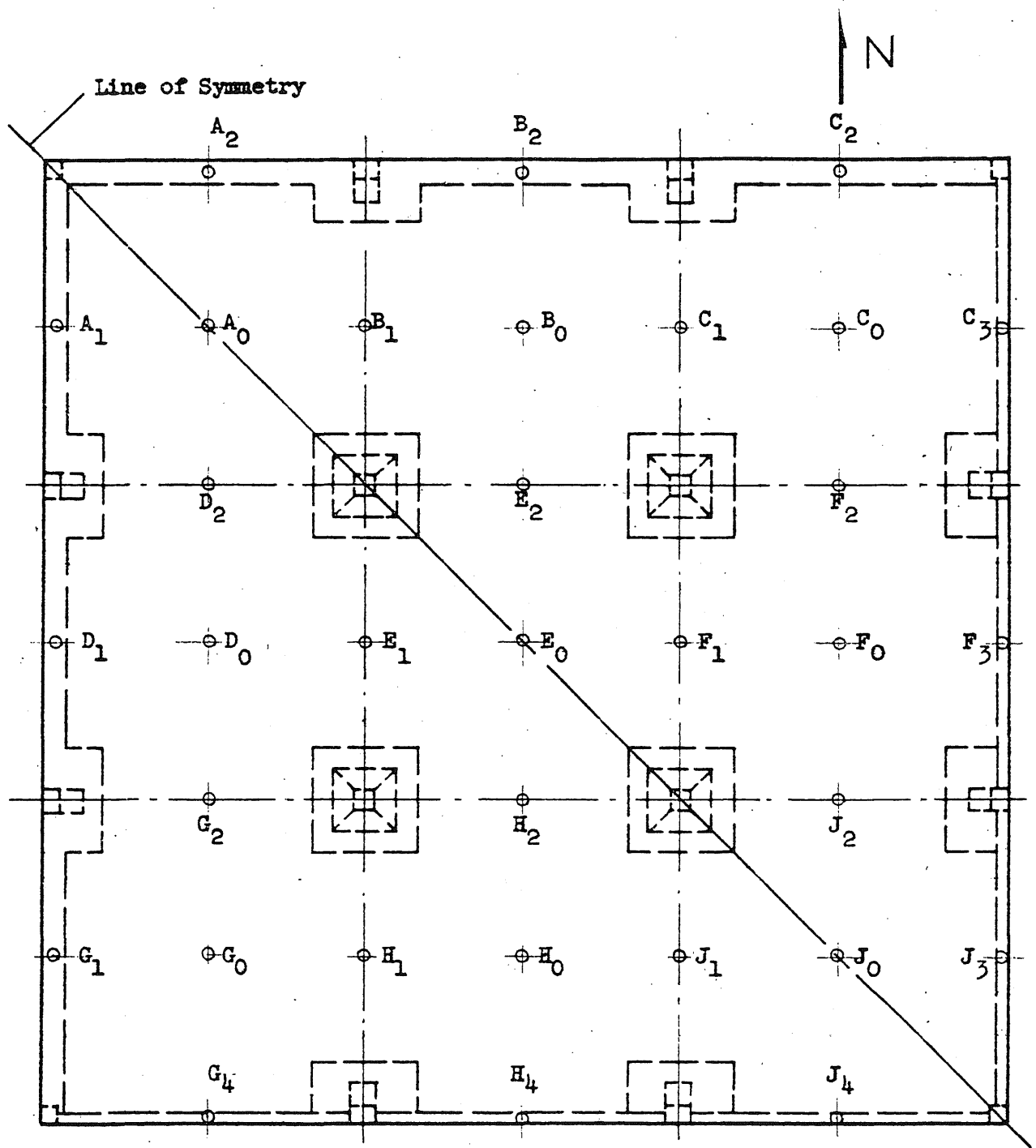


FIG. 5.28 LOCATION AND DESIGNATION OF DEFLECTION
DIAL GAGES FOR ALL TEST STRUCTURES

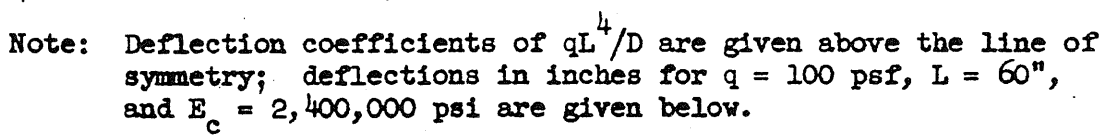
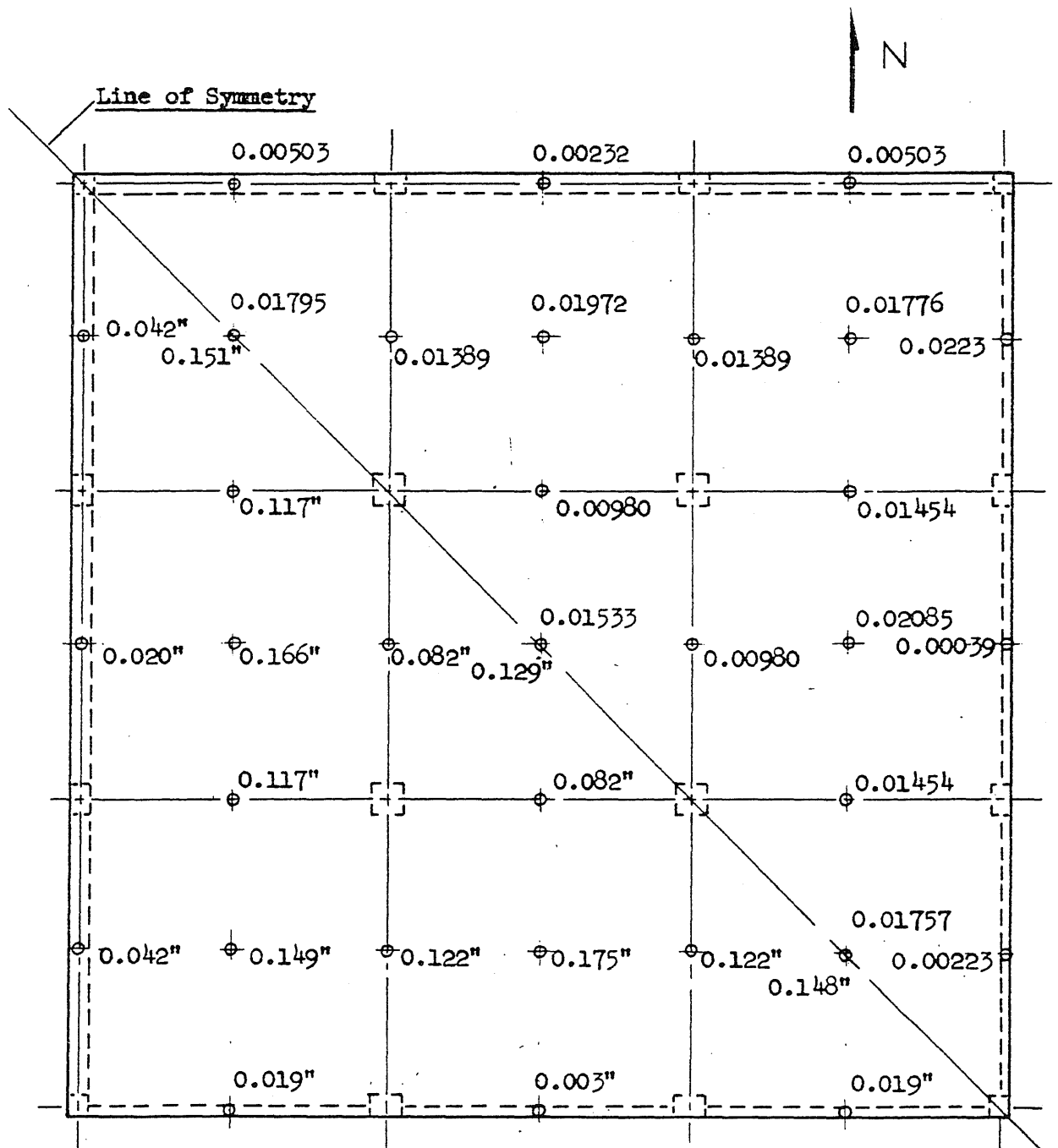


FIG. 5.29 DEFLECTIONS AND DEFLECTION COEFFICIENTS FOR THE FLAT PLATE (F1) BASED ON UNCRACKED SECTIONS



Note: Deflection coefficients of qL^4/D are given above the line of symmetry; deflections in inches for $q = 100$ psf, $L = 60"$, and $E_c = 2,400,000$ psi are given below.

FIG. 5.30 DEFLECTIONS AND DEFLECTION COEFFICIENTS FOR THE FLAT PLATE (F1) BASED ON FULLY CRACKED SECTIONS

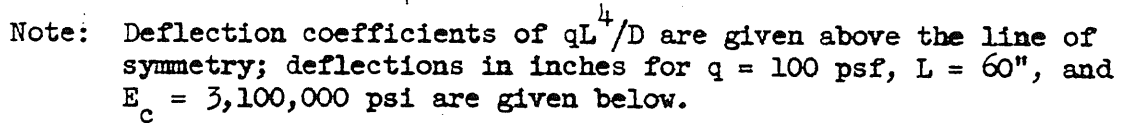
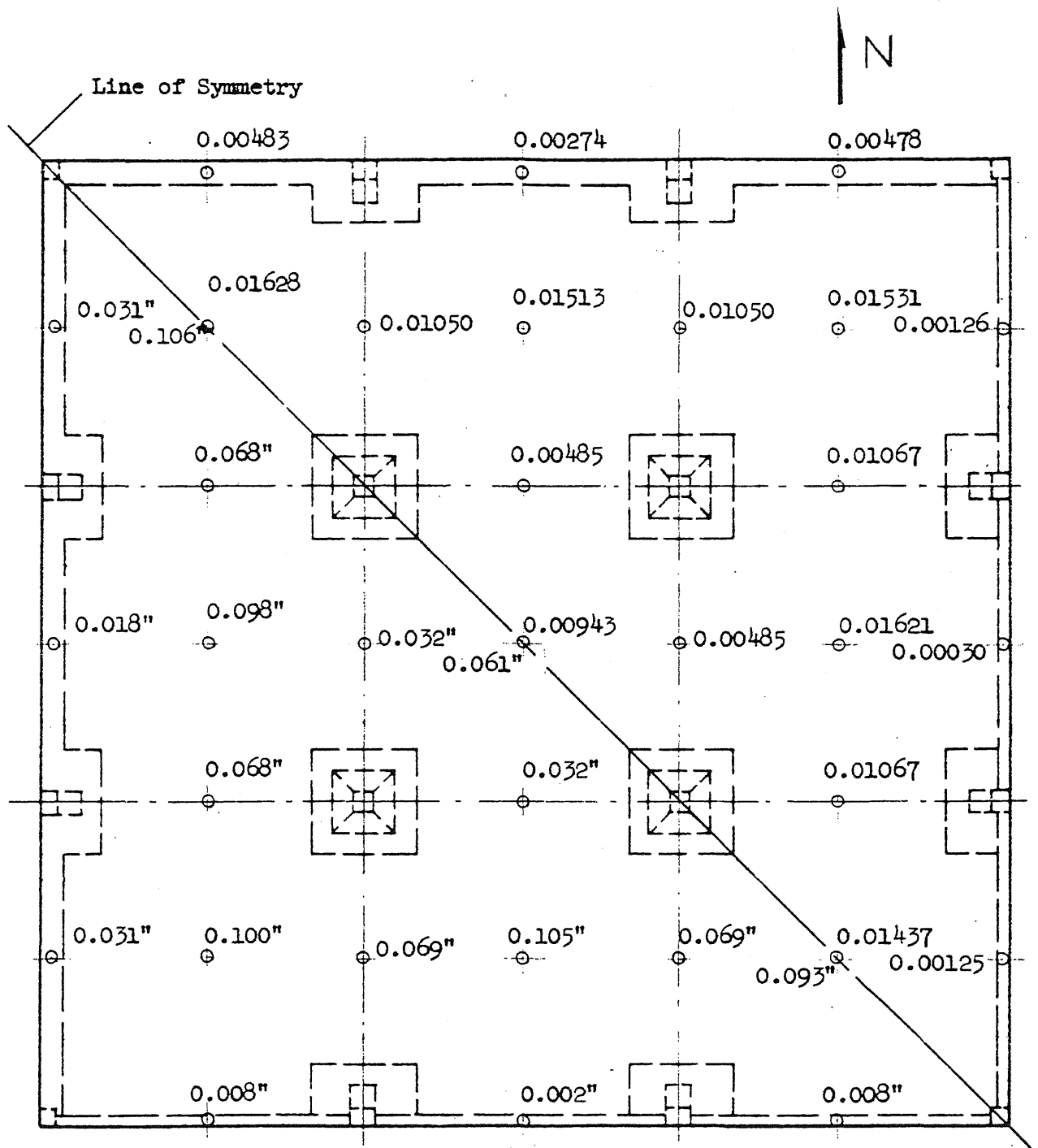
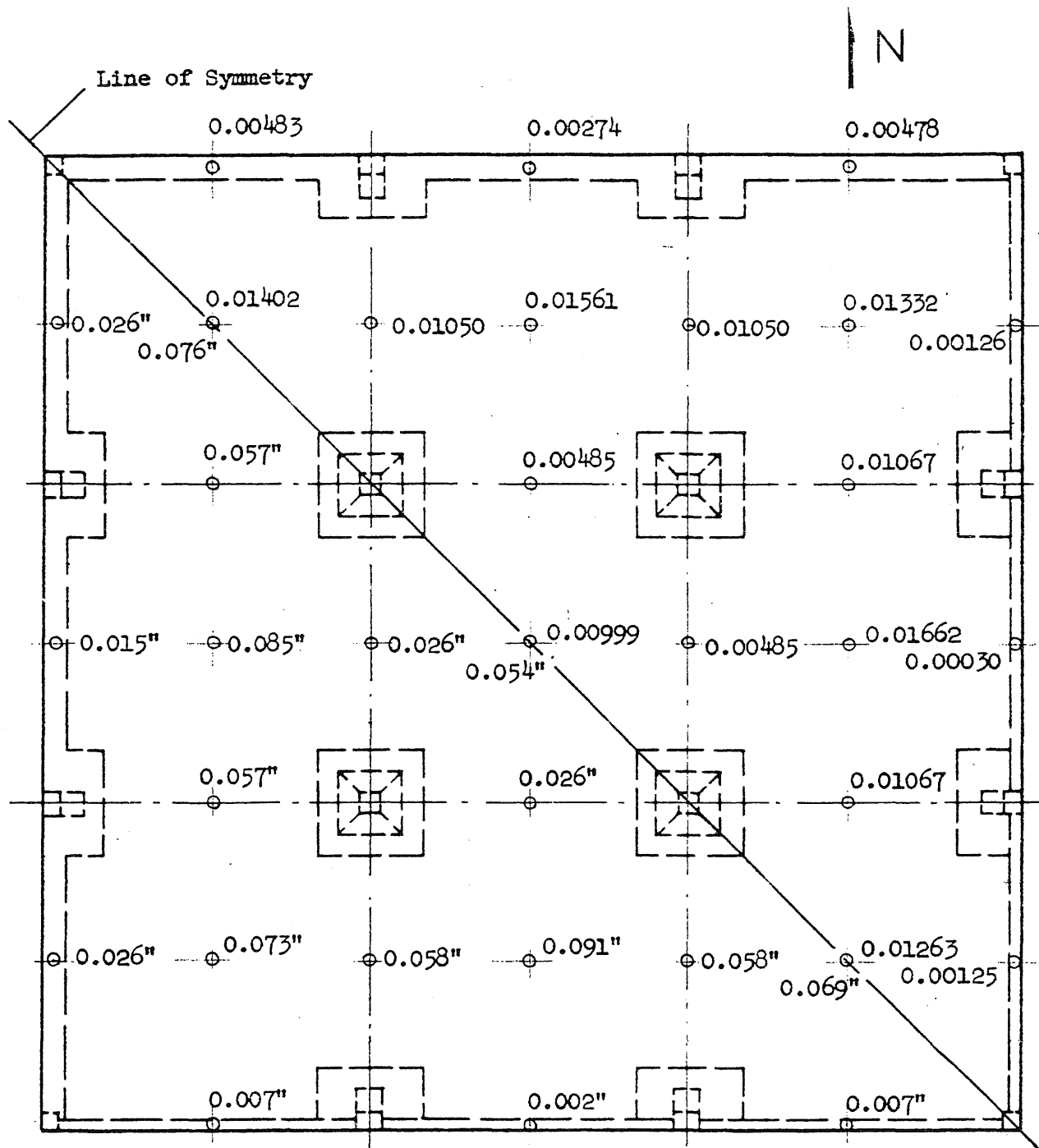


FIG. 5.31 DEFLECTIONS AND DEFLECTION COEFFICIENTS FOR THE FLAT SLAB (F2) BASED ON UNCRACKED SECTIONS.



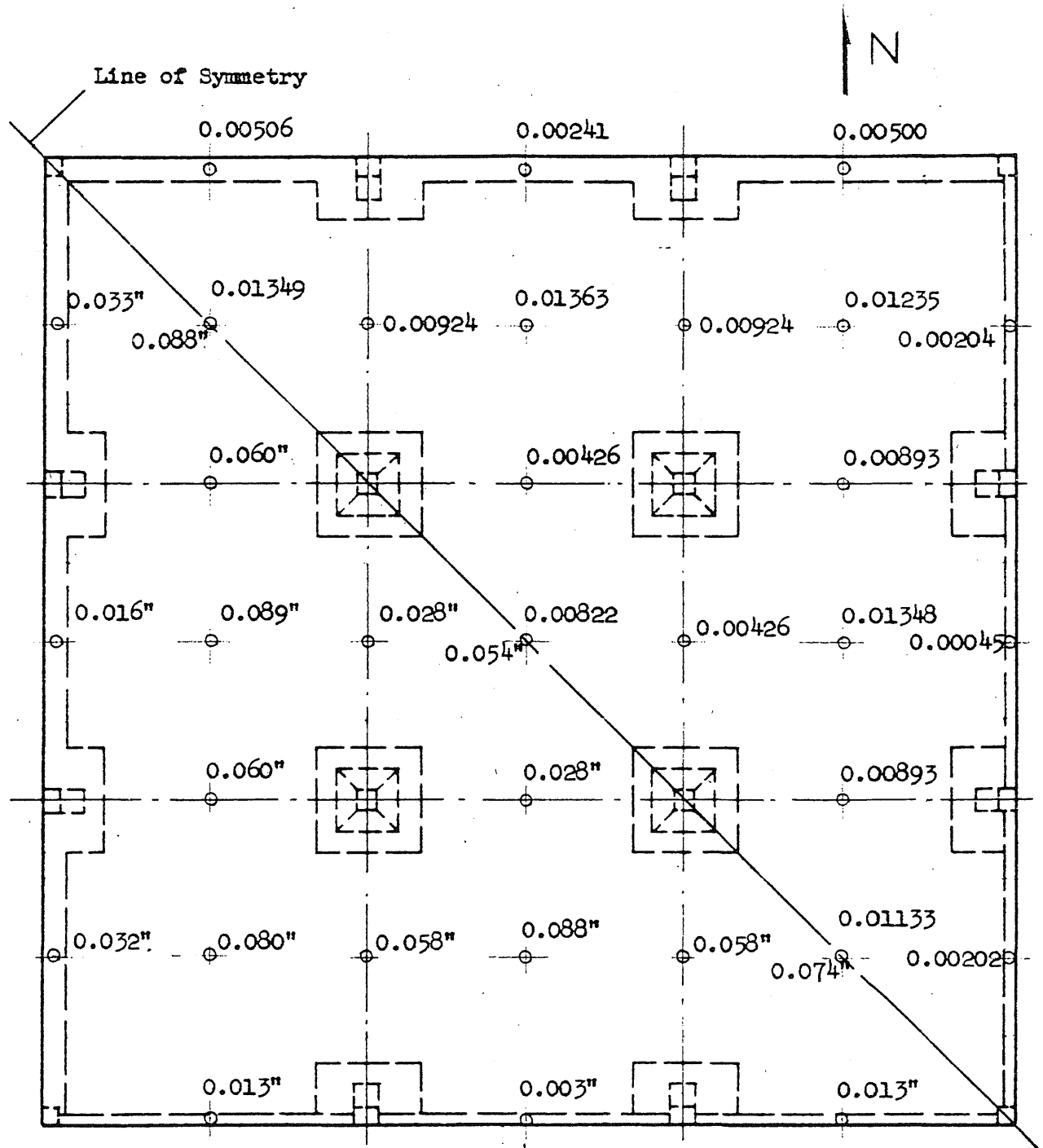
Note: Deflection coefficients of qL^4/D are given above the line of symmetry; deflections in inches for $q = 100$ psf, $L = 60"$ and $E_c = 3,100,000$ psi are given below.

FIG. 5.32 DEFLECTIONS AND DEFLECTION COEFFICIENTS FOR THE FLAT SLAB (F2) BASED ON FULLY CRACKED SECTIONS



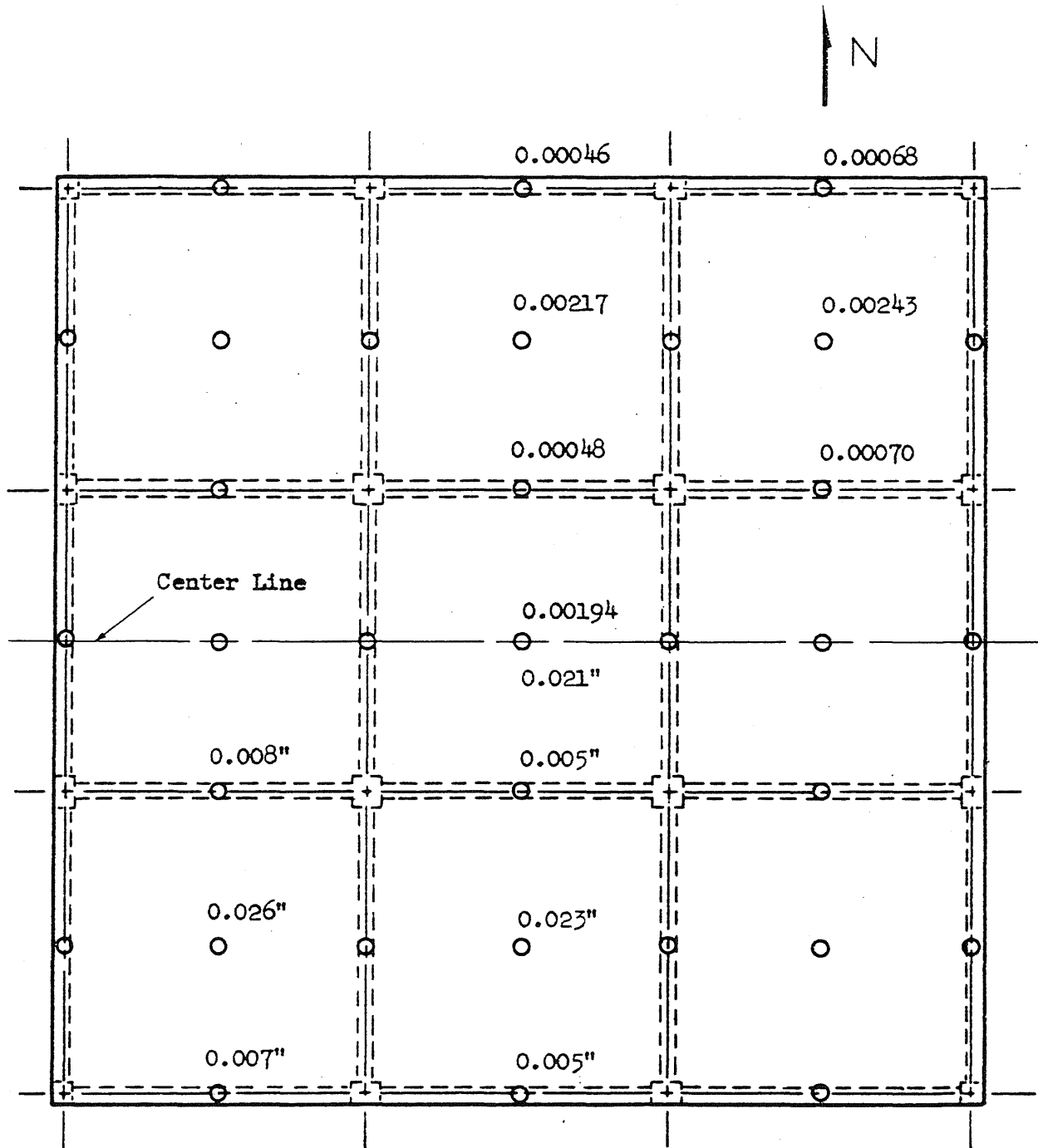
Note: Deflection coefficients of qL^4/D are given above the line of symmetry; deflections in inches for $q = 100$ psf, $L = 60"$, and $E_c = 3,700,000$ psi are given below.

FIG. 5.33 DEFLECTIONS AND DEFLECTION COEFFICIENTS FOR THE FLAT SLAB (F3) BASED ON FULLY CRACKED SECTIONS



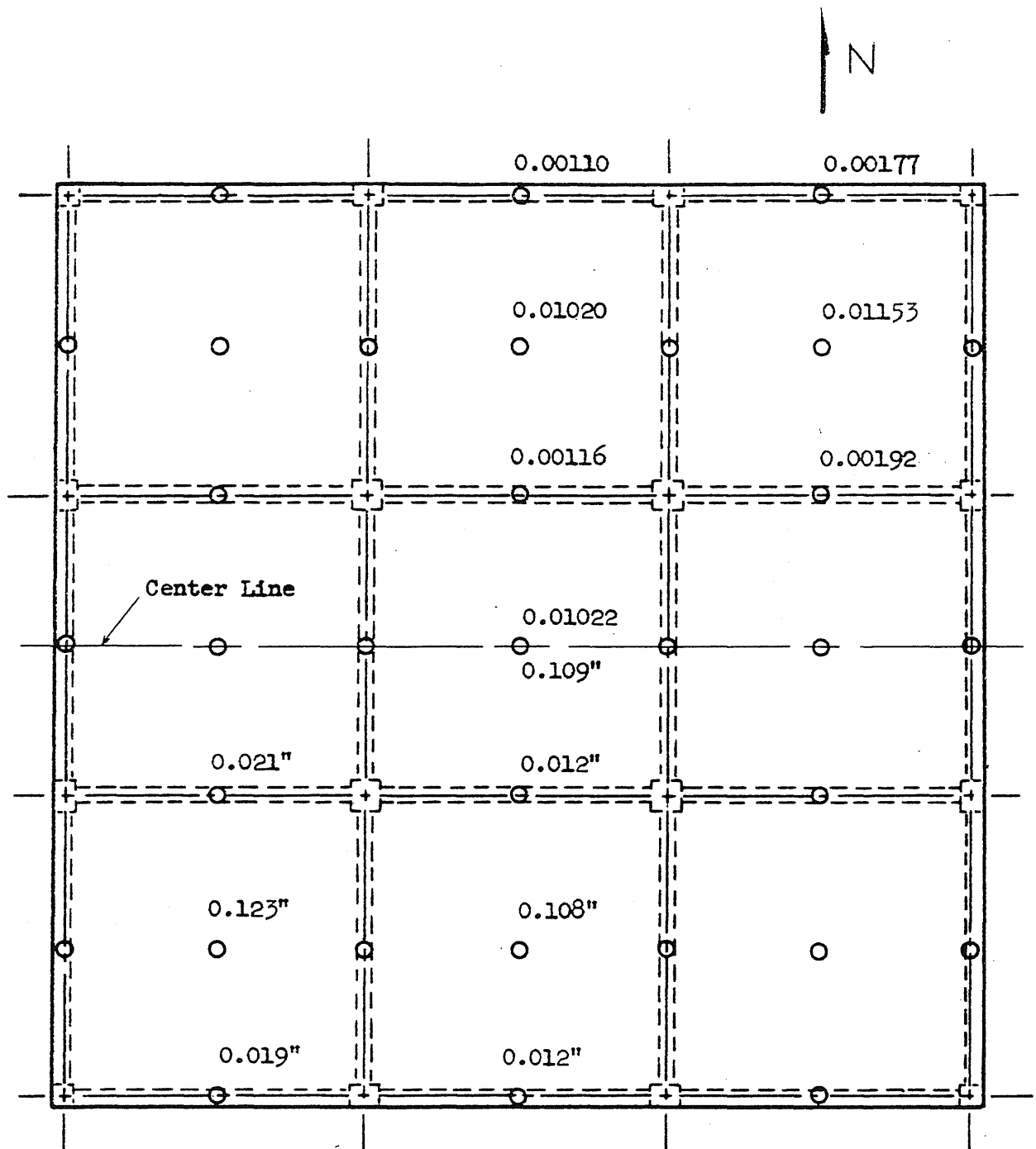
Note: Deflection coefficients of qL^4/D are given above the line of symmetry: deflections in inches for $q = 100$ psf, $L = 60''$, and $E_c = 3,100,000$ psi are given below.

FIG. 5.34 DEFLECTIONS AND DEFLECTION COEFFICIENTS FOR THE FLAT SLAB (F5) BASED ON FULLY CRACKED SECTIONS



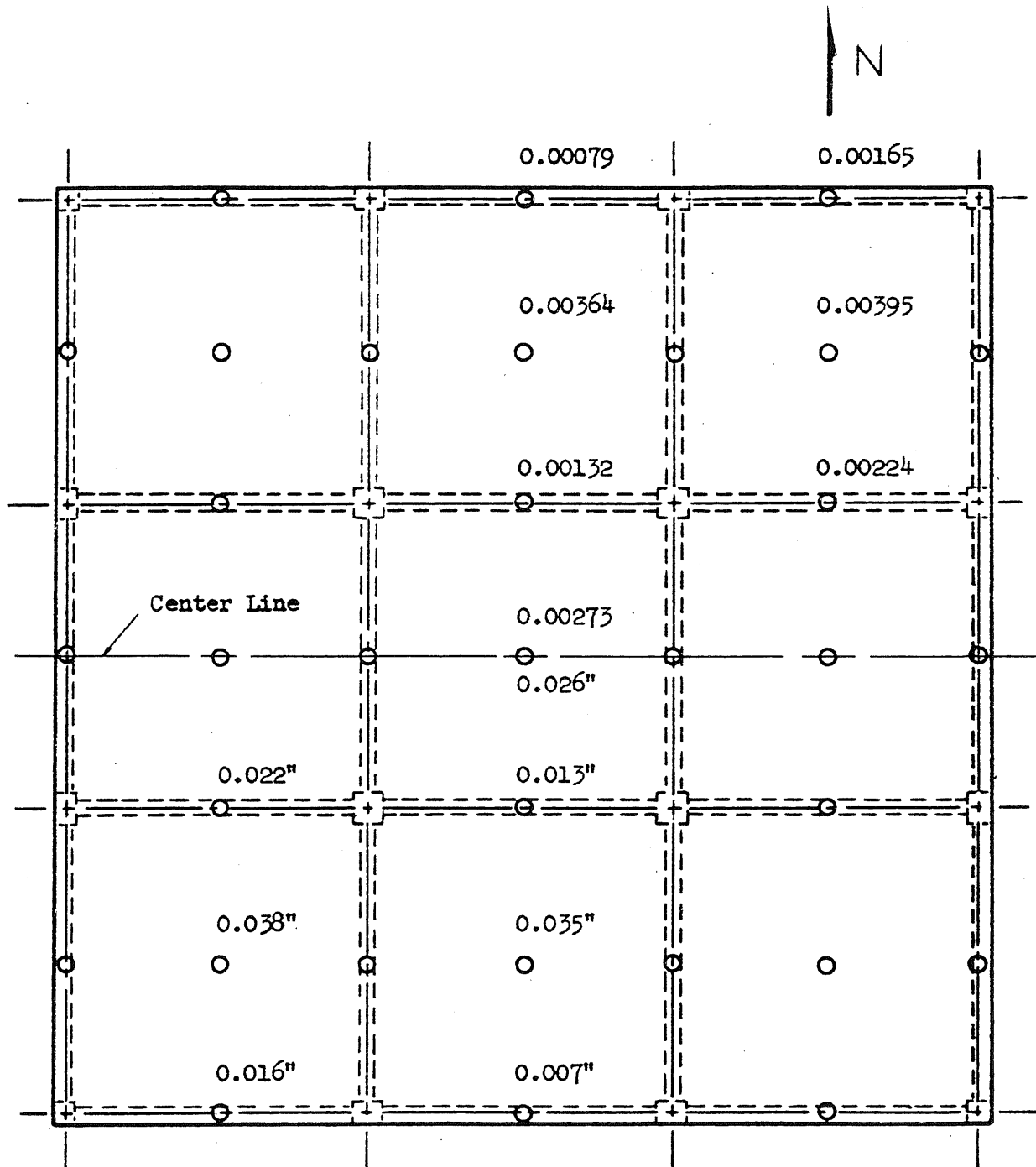
Note: Deflection coefficients of qL^4/D are given above the center line; deflections in inches for $q = 100$ psf, $L = 60"$, and $E_c = 3,000,000$ psi are given below.

FIG. 5.35 DEFLECTIONS AND DEFLECTION COEFFICIENTS FOR THE TWO-WAY SLAB WITH DEEP BEAMS (T1) BASED ON UNCRACKED SECTIONS



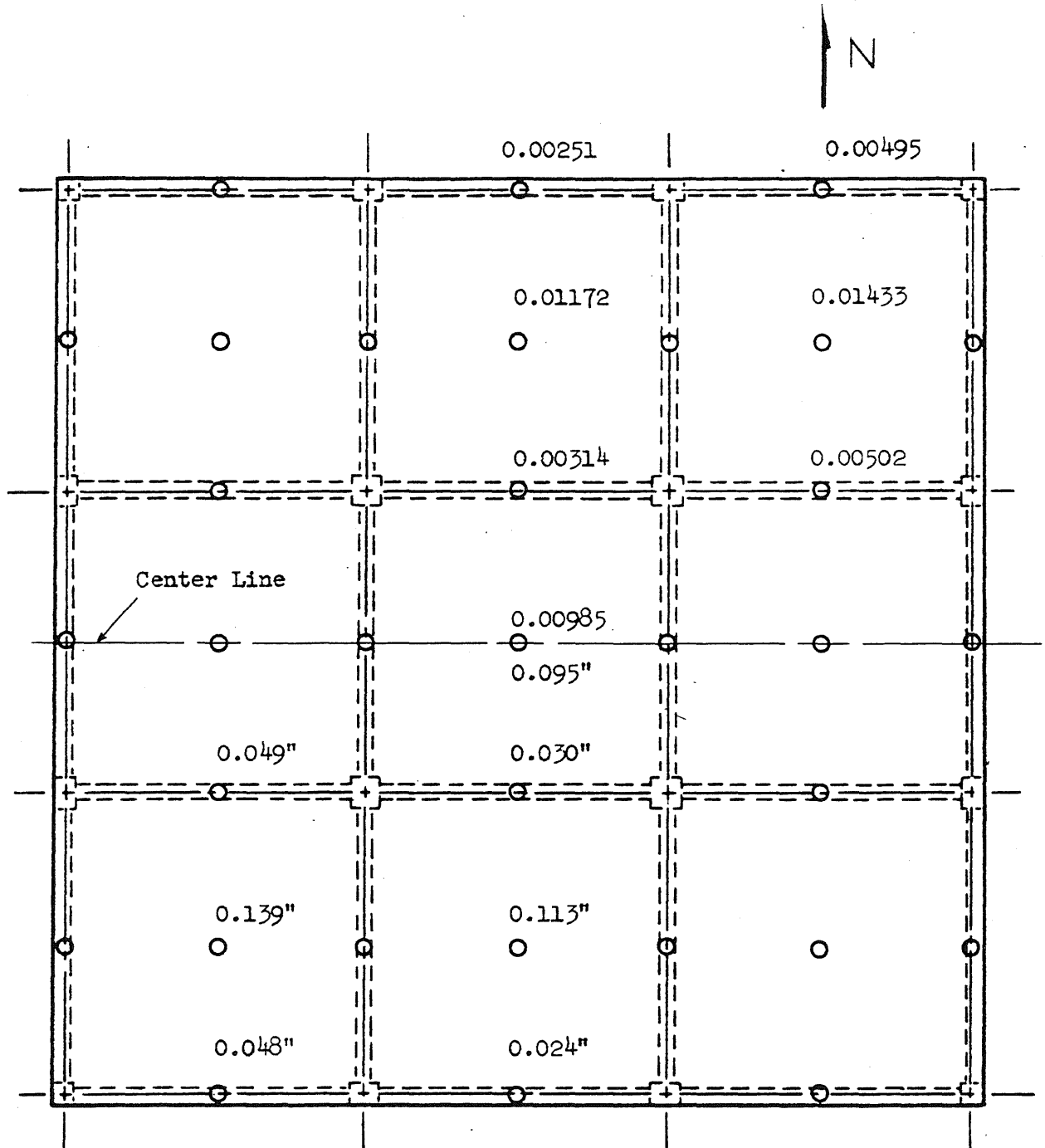
Note: Deflection coefficients of qL^4/D are given above the center line; deflections in inches for $q = 100$ psf, $L = 60$ ", and $E_c = 3,000,000$ psi are given below

FIG. 5.36 DEFLECTIONS AND DEFLECTION COEFFICIENTS FOR THE TWO-WAY SLAB WITH DEEP BEAMS (T1) BASED ON FULLY CRACKED SECTIONS



Note: Deflection coefficients of qL^4/D are given above the center line; deflections in inches for $q = 100$ psf, $L = 60$ ", and $E_c = 3,300,000$ psi are given below.

FIG. 5.37 DEFLECTIONS AND DEFLECTION COEFFICIENTS FOR THE TWO-WAY SLAB WITH SHALLOW BEAMS (T2) BASED ON UNCRACKED SECTIONS



Note: Deflection coefficients of qL^4/D are given above the center line; deflections in inches for $q = 100$ psf, $L = 60$ ", and $E_c = 3,300,000$ psi are given below.

FIG. 5.38 DEFLECTIONS AND DEFLECTION COEFFICIENTS FOR THE TWO-WAY SLAB WITH SHALLOW BEAMS (T2) BASED ON FULLY CRACKED SECTIONS.

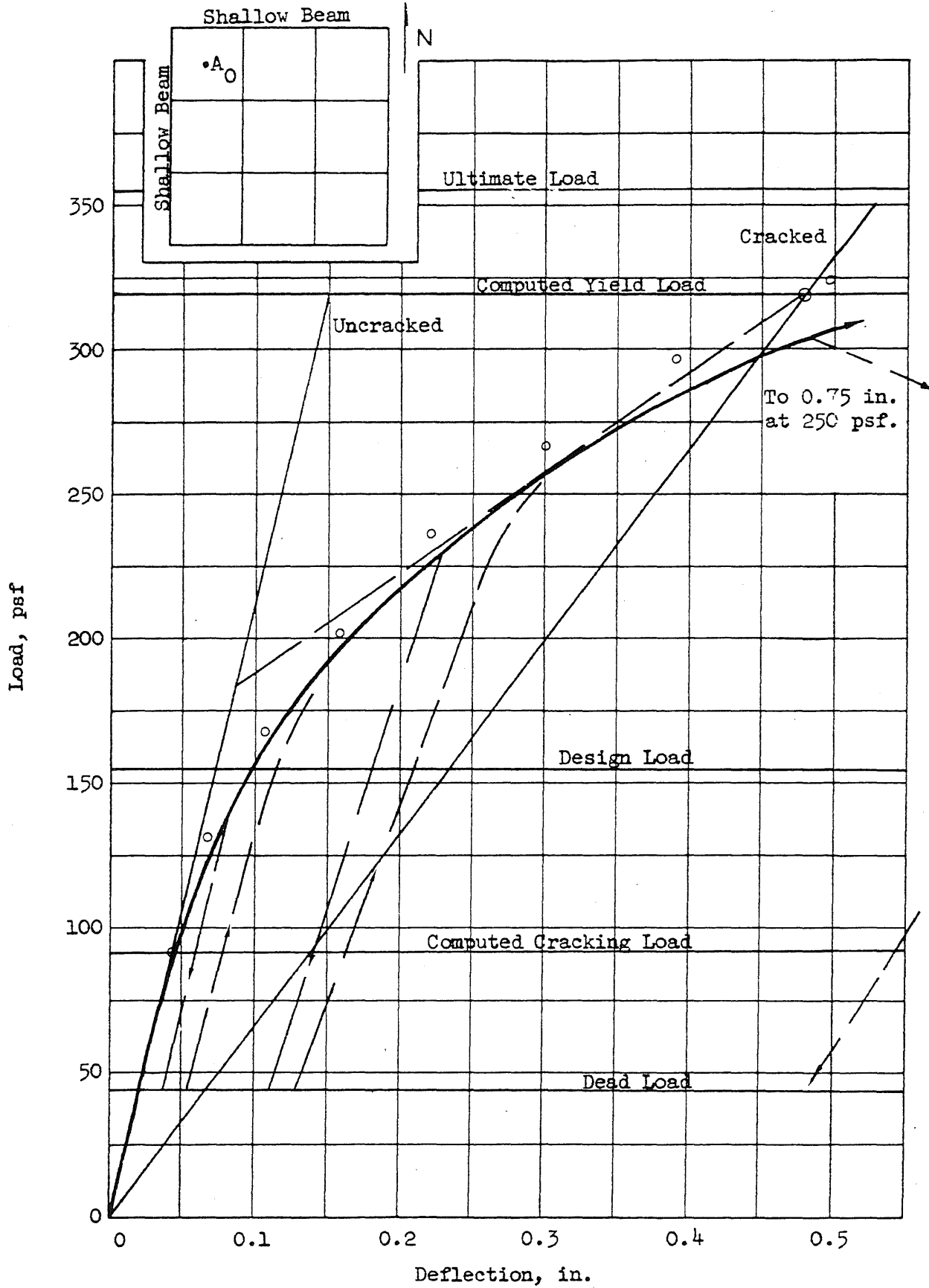


FIG. 5.39 LOAD-DEFLECTION CURVE, FLAT PLATE (F1), POINT A₀

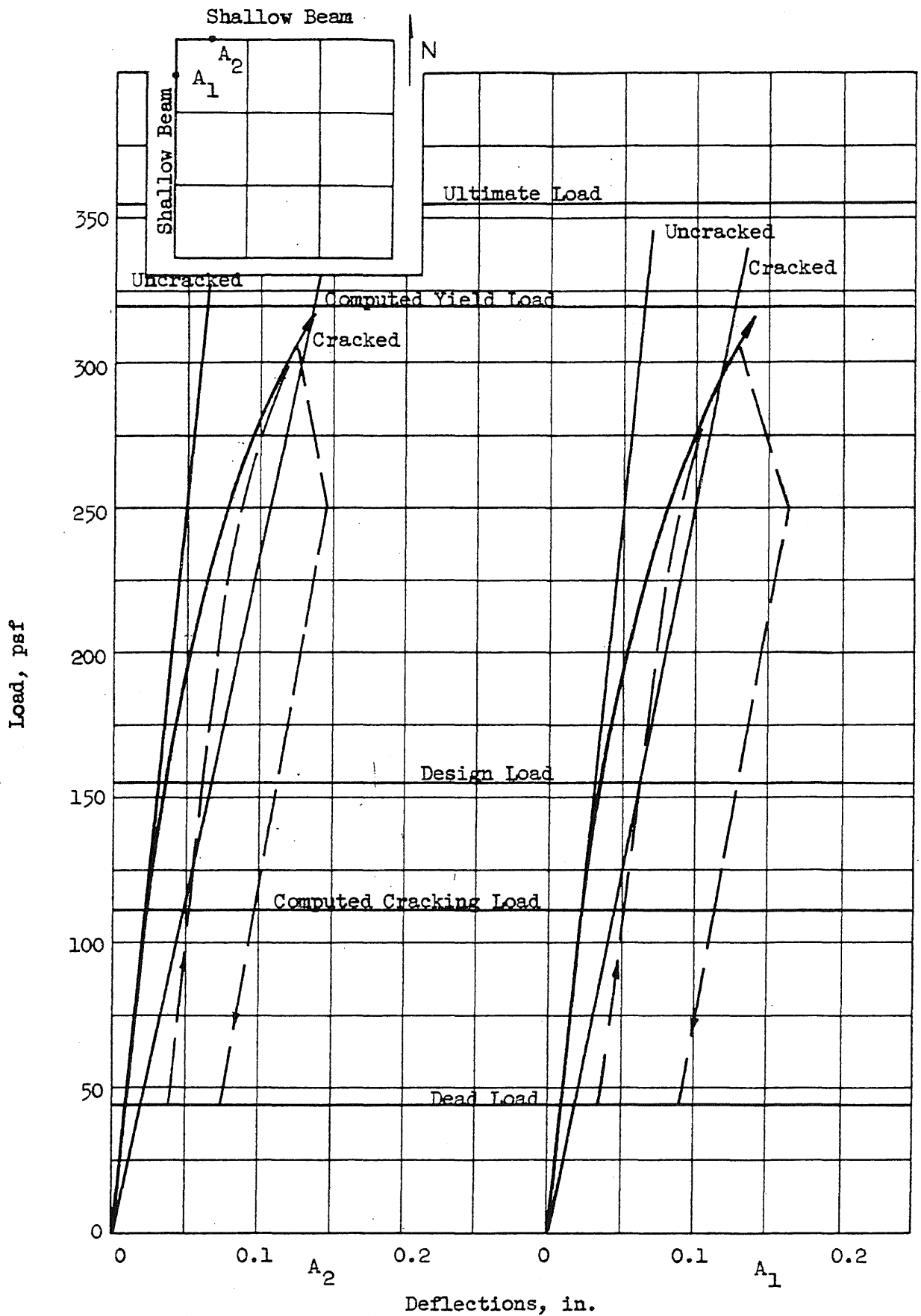


FIG. 5.40 LOAD-DEFLECTION CURVES, FLAT PLATE (F1), POINTS A_1 AND A_2

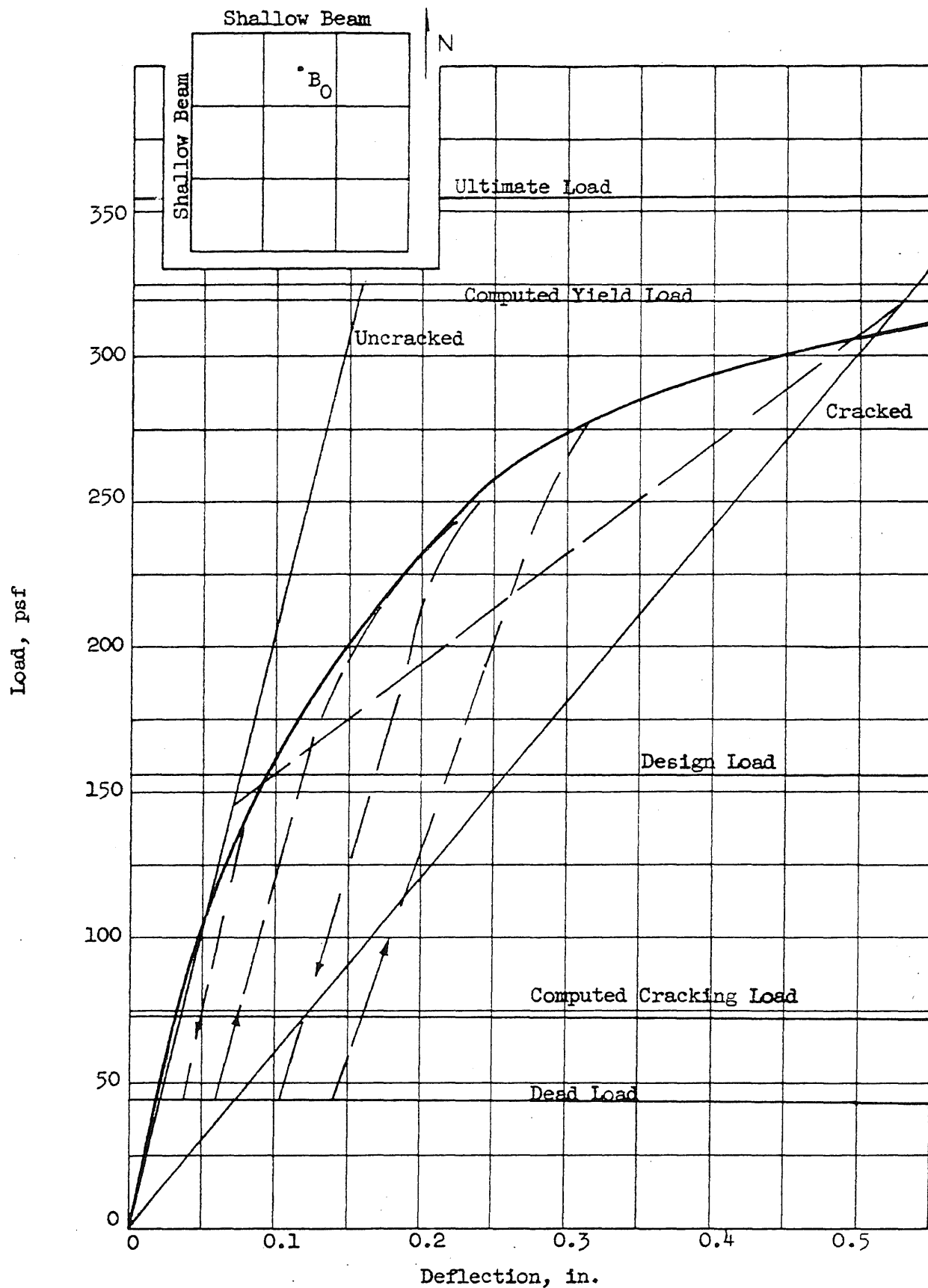


FIG. 5.41 LOAD-DEFLECTION CURVE, FLAT PLATE (F1), POINT B₀

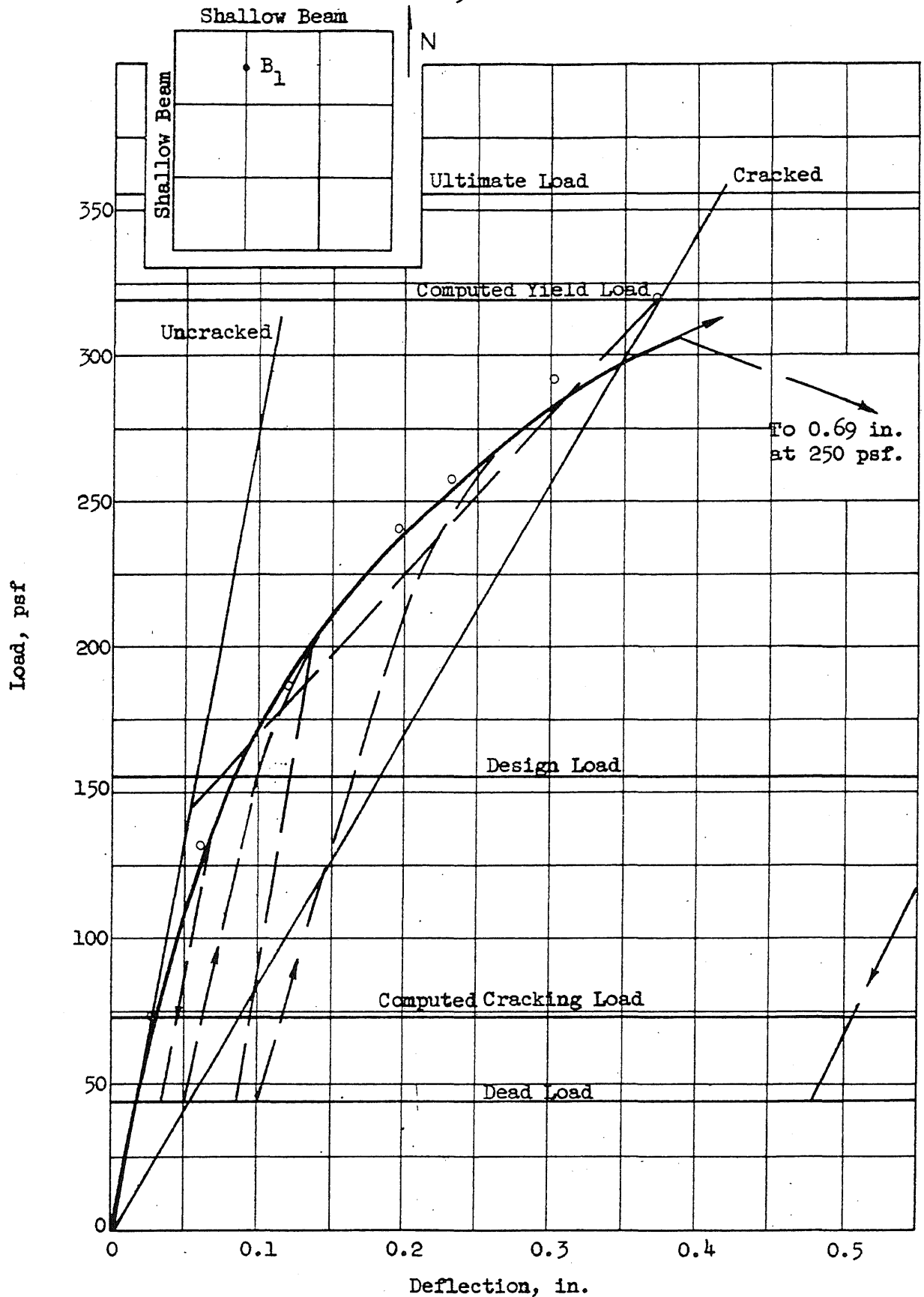


FIG. 5.42 LOAD-DEFLECTION CURVE, FLAT PLATE (F1), POINT B₁

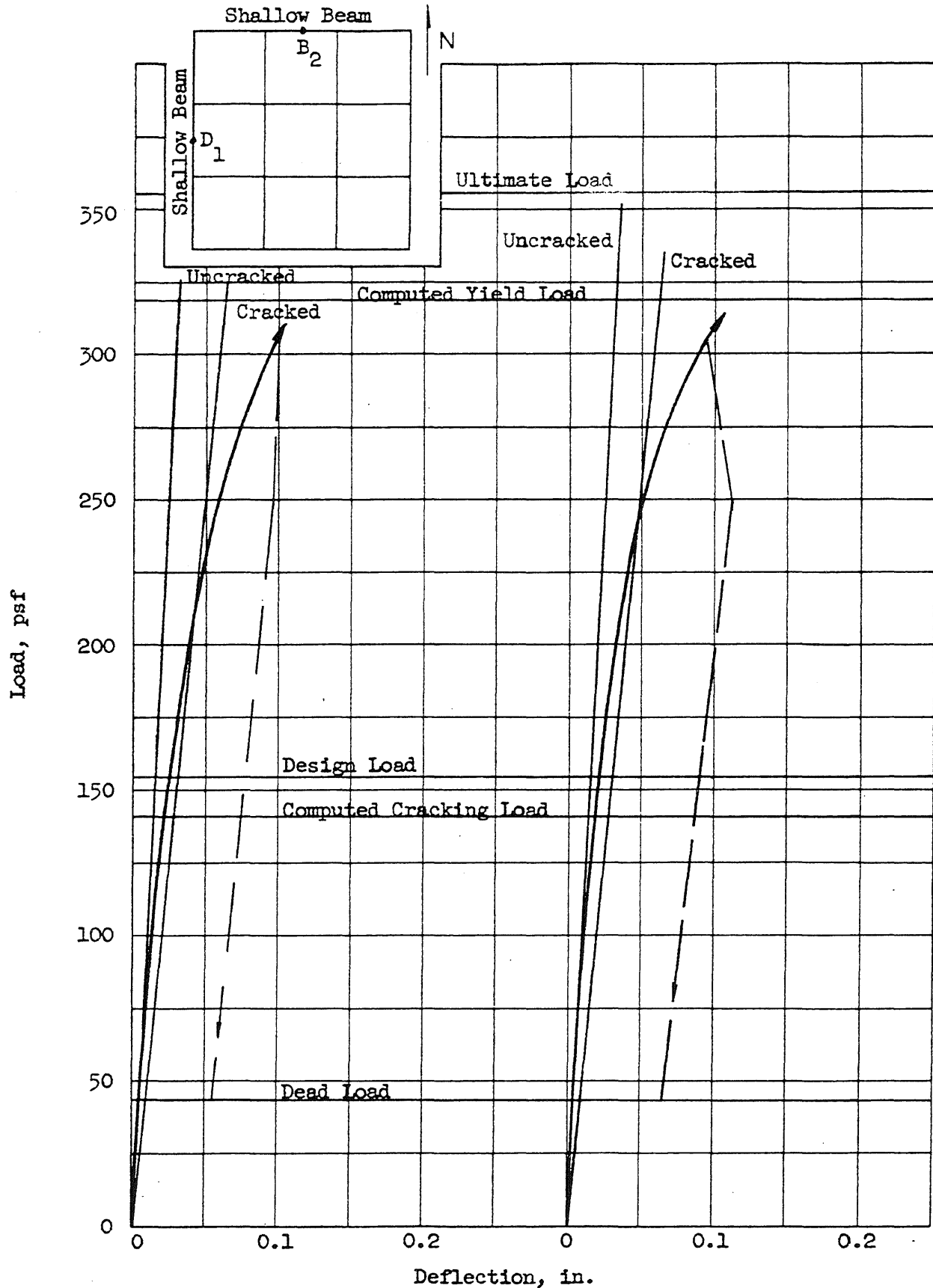


FIG. 5.43 LOAD-DEFLECTION CURVES, FLAT PLATE (F1), POINTS B₂ AND D₁

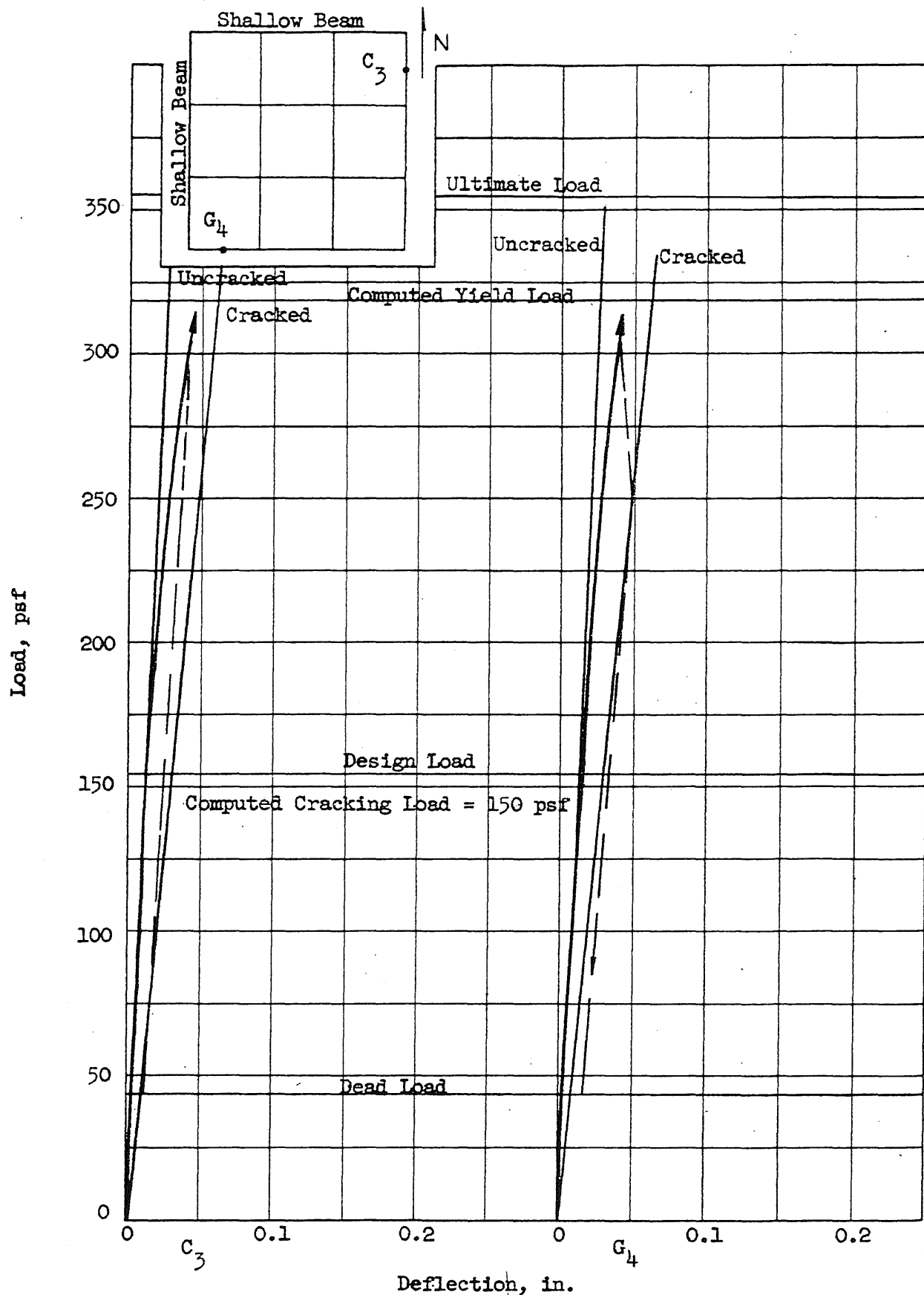


FIG. 5.44 LOAD-DEFLECTION CURVES, FLAT PLATE (F1), POINTS C_3 AND G_4

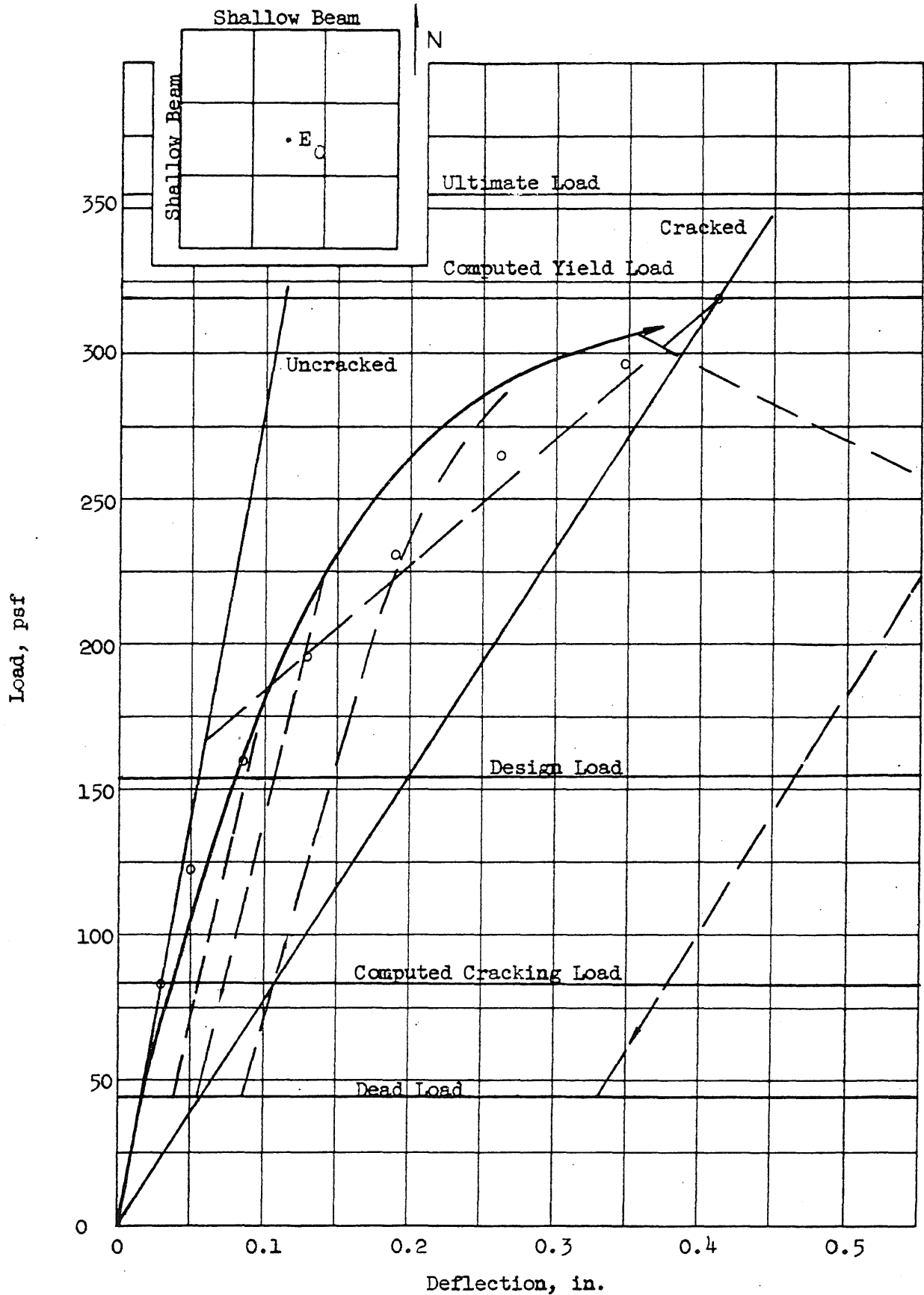


FIG. 5.45 LOAD-DEFLECTION CURVE, FLAT PLATE (F1), POINT E_0

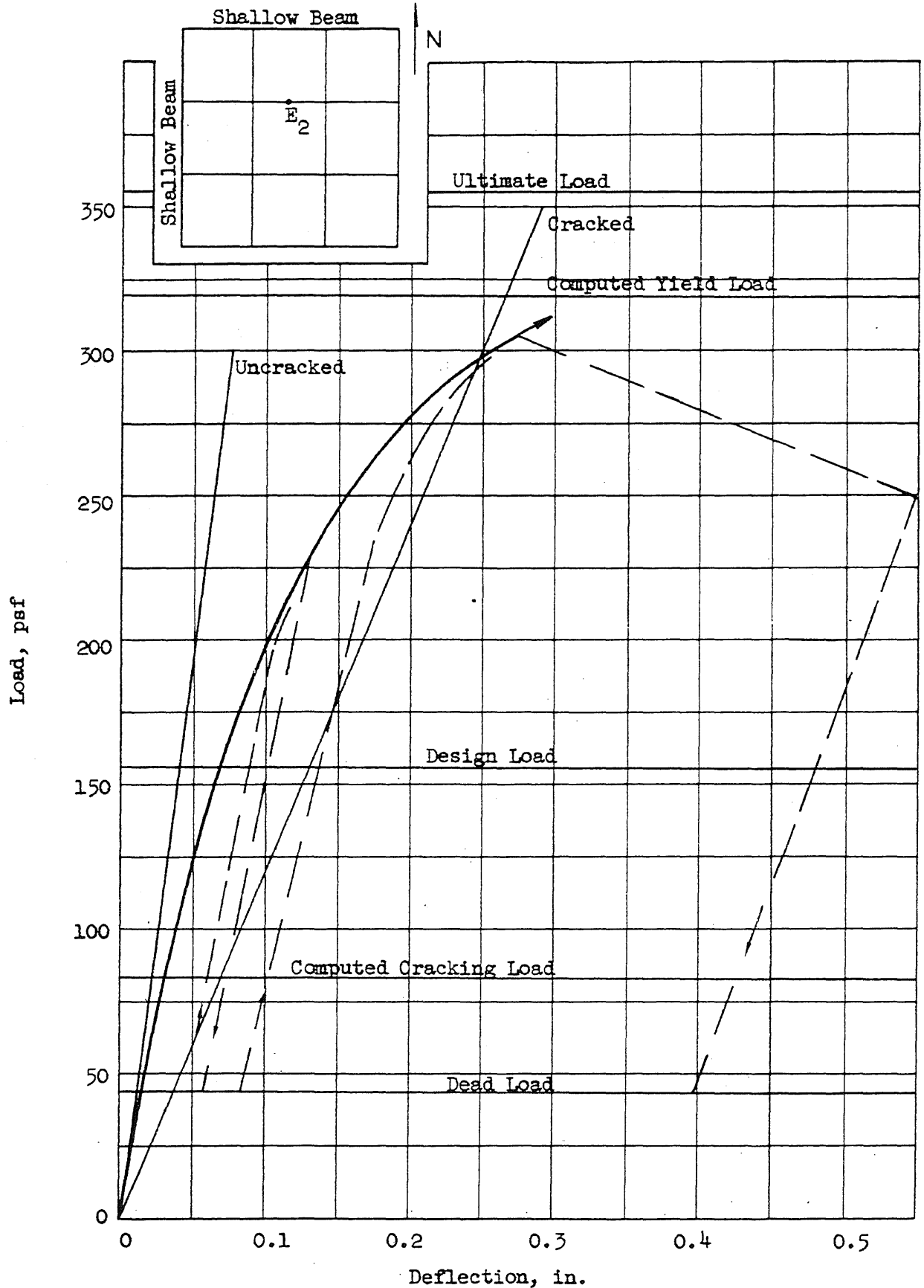


FIG. 5.46 LOAD-DEFLECTION CURVE, FLAT PLATE (F1), POINT E₂

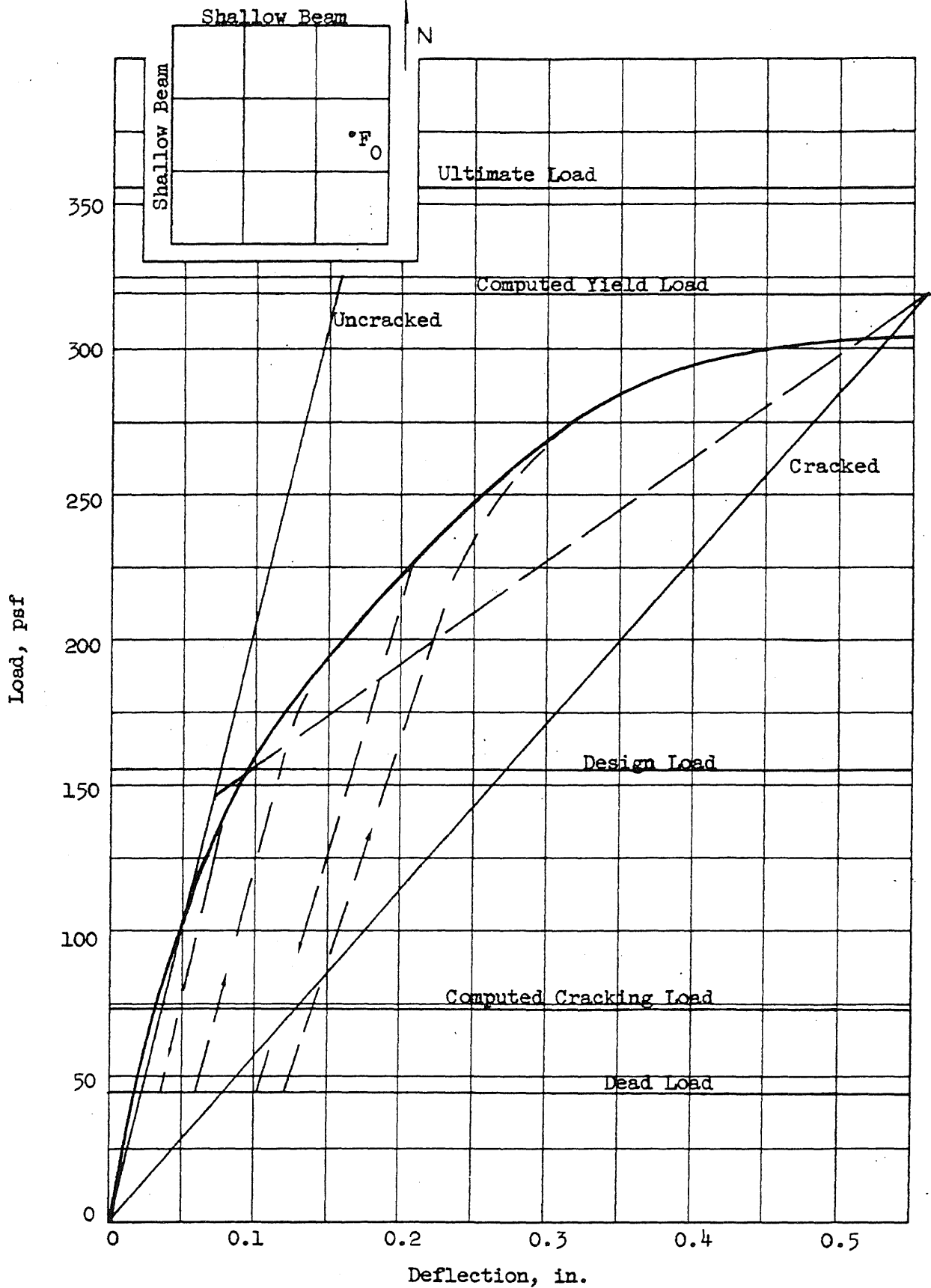


FIG. 5.47 LOAD-DEFLECTION CURVE, FLAT PLATE (F1), POINT F_0

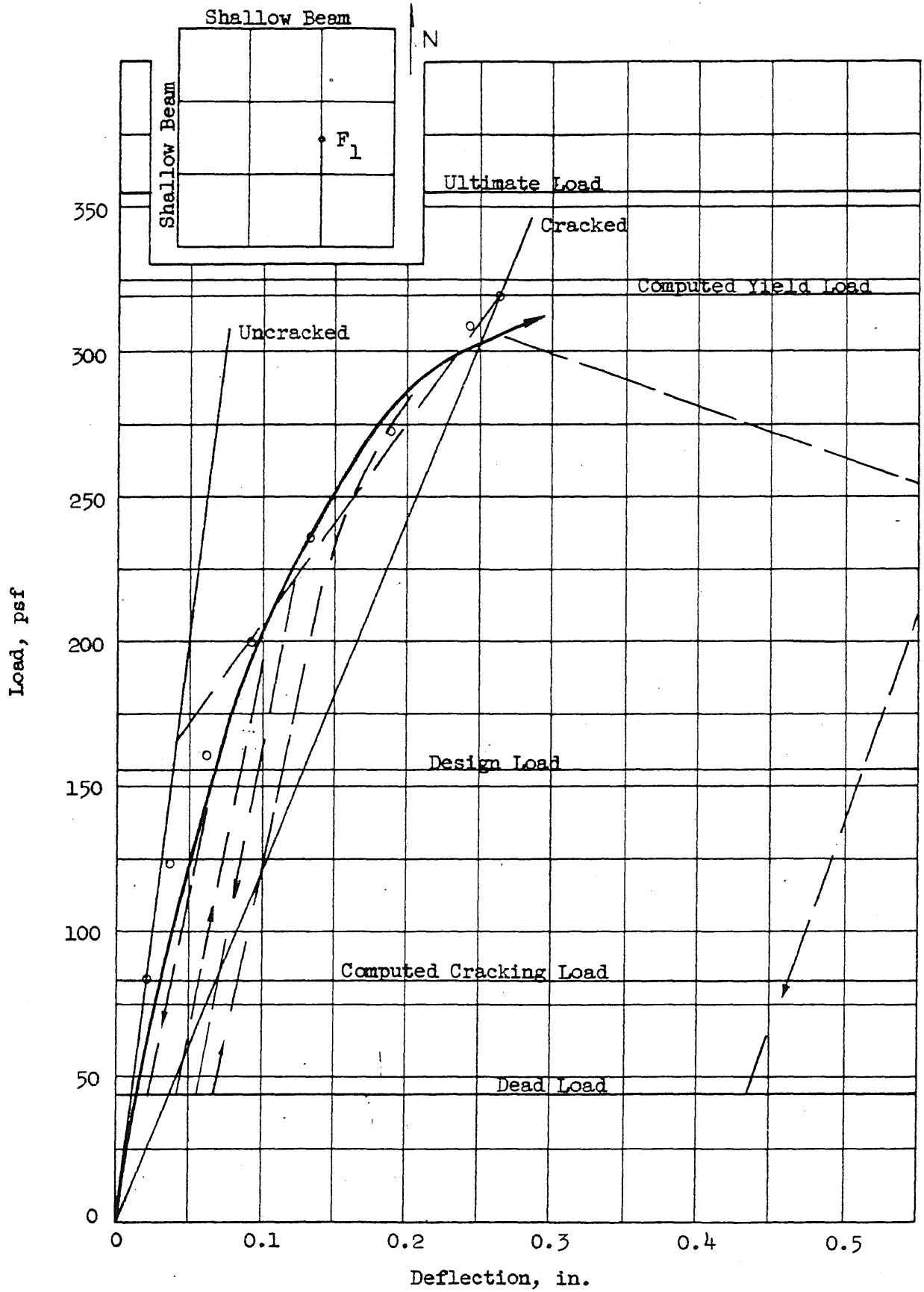


FIG. 5.48 LOAD-DEFLECTION CURVE, FLAT PLATE (F1), POINT F₁

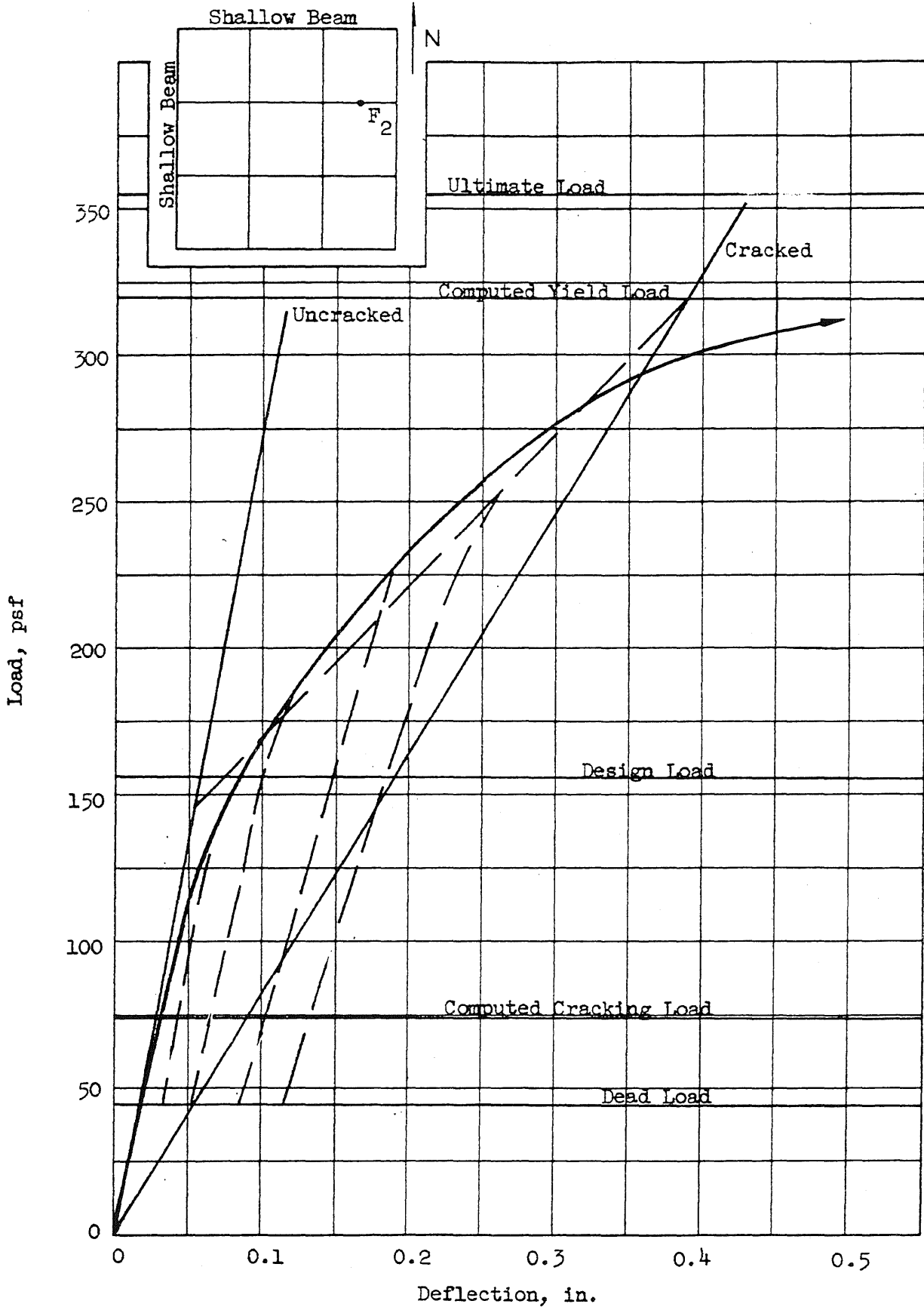


FIG. 5.49 LOAD-DEFLECTION CURVE, FLAT PLATE (F₁), POINT F₂

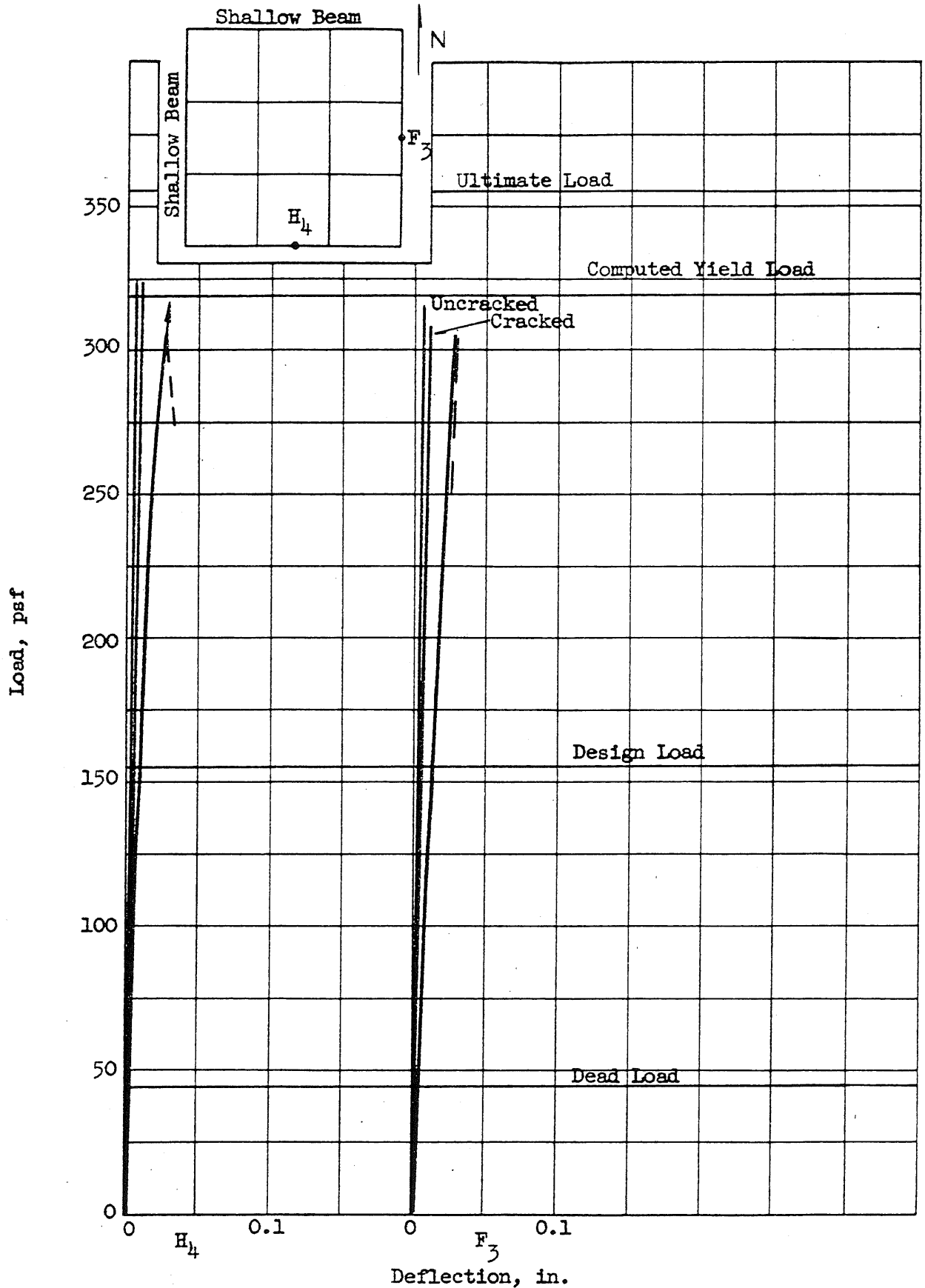


FIG. 5.50 LOAD-DEFLECTION CURVES, FLAT PLATE (F1) POINTS F_3 AND H_4

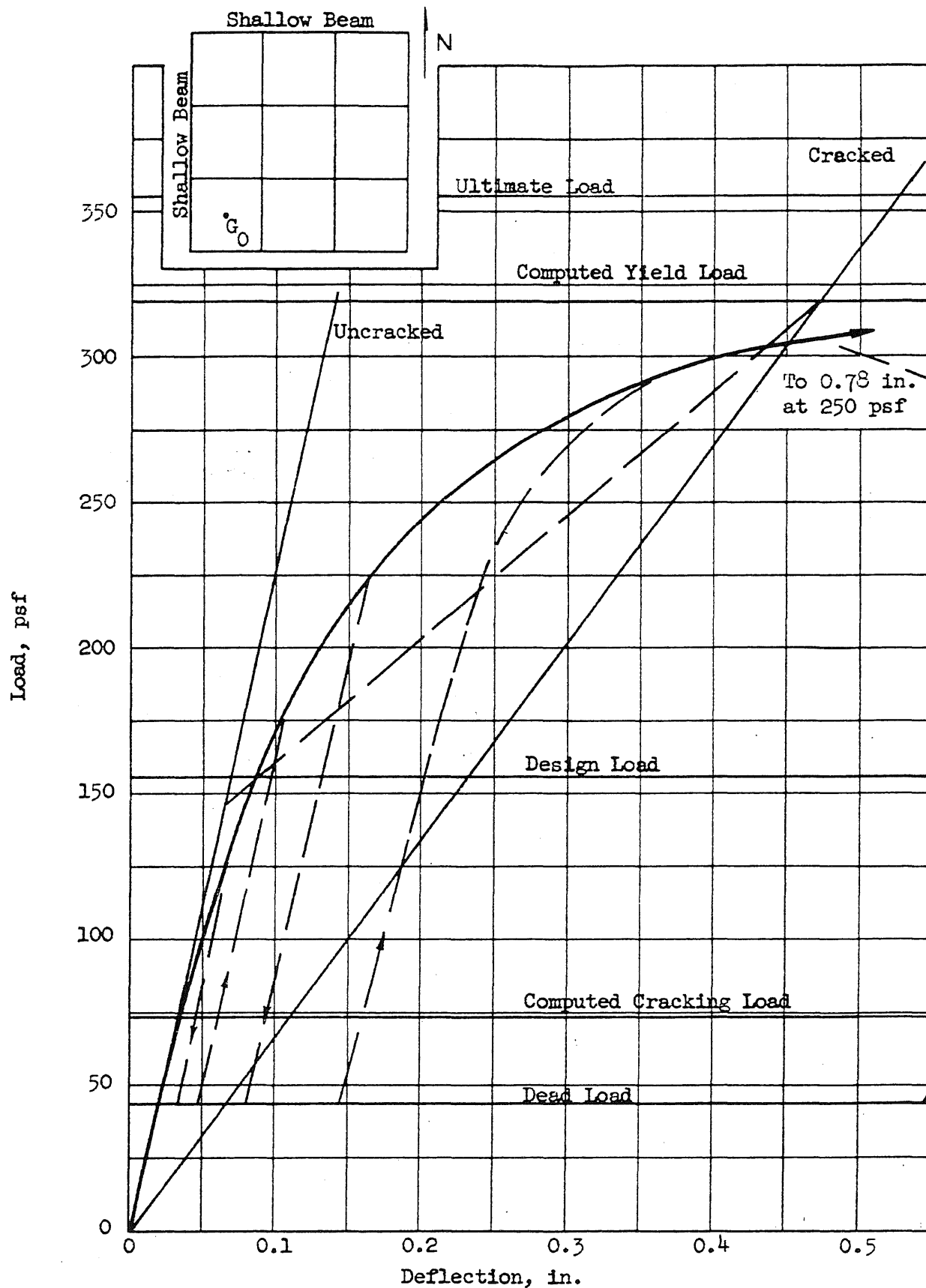


FIG. 5.51 LOAD-DEFLECTION CURVE, FLAT PLATE (F1), POINT G_0

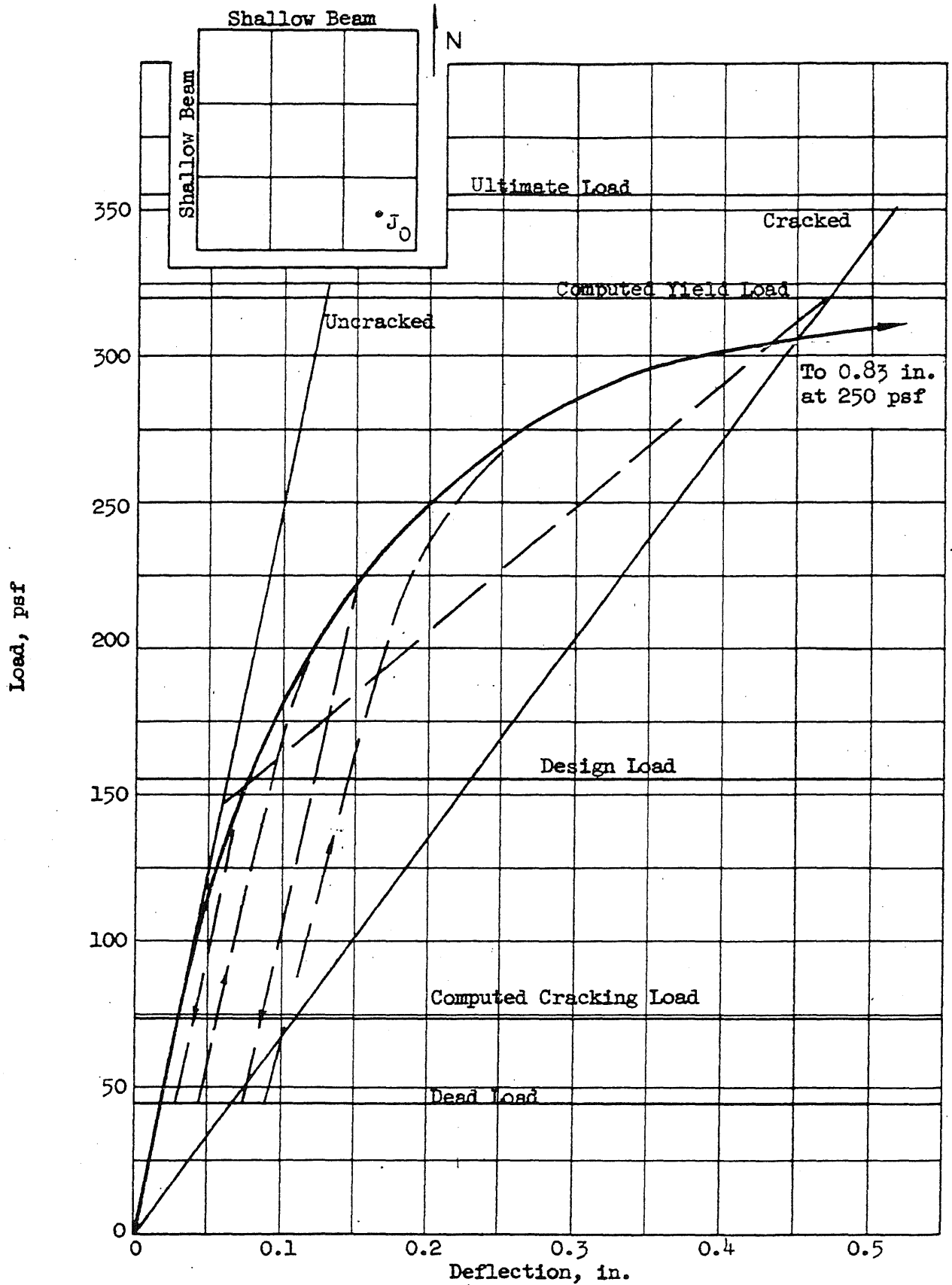


FIG. 5.52 LOAD-DEFLECTION CURVE, FLAT PLATE (F1), POINT J₀

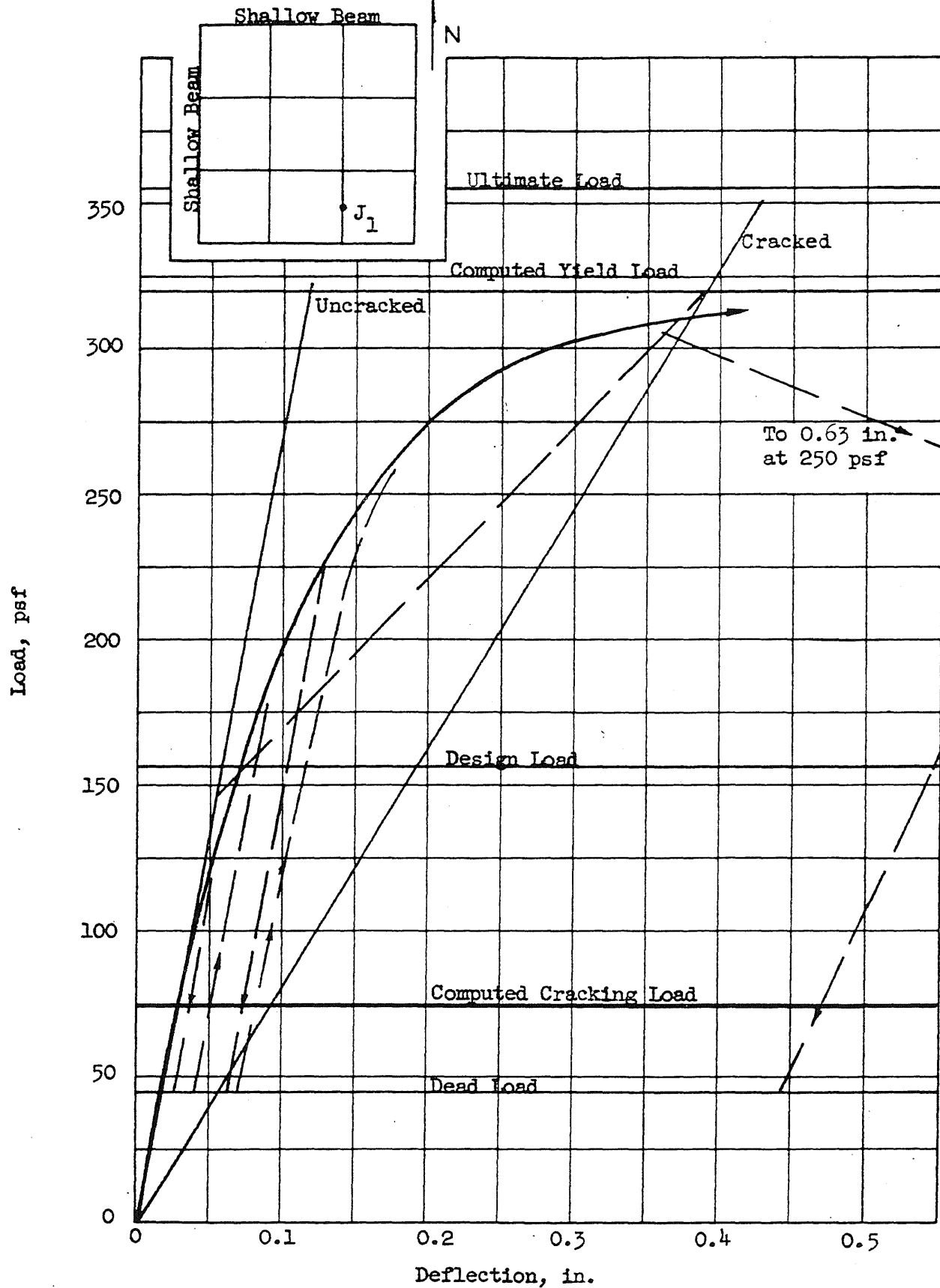


FIG. 5.53 LOAD-DEFLECTION CURVE, FLAT PLATE (F1), POINT J₁

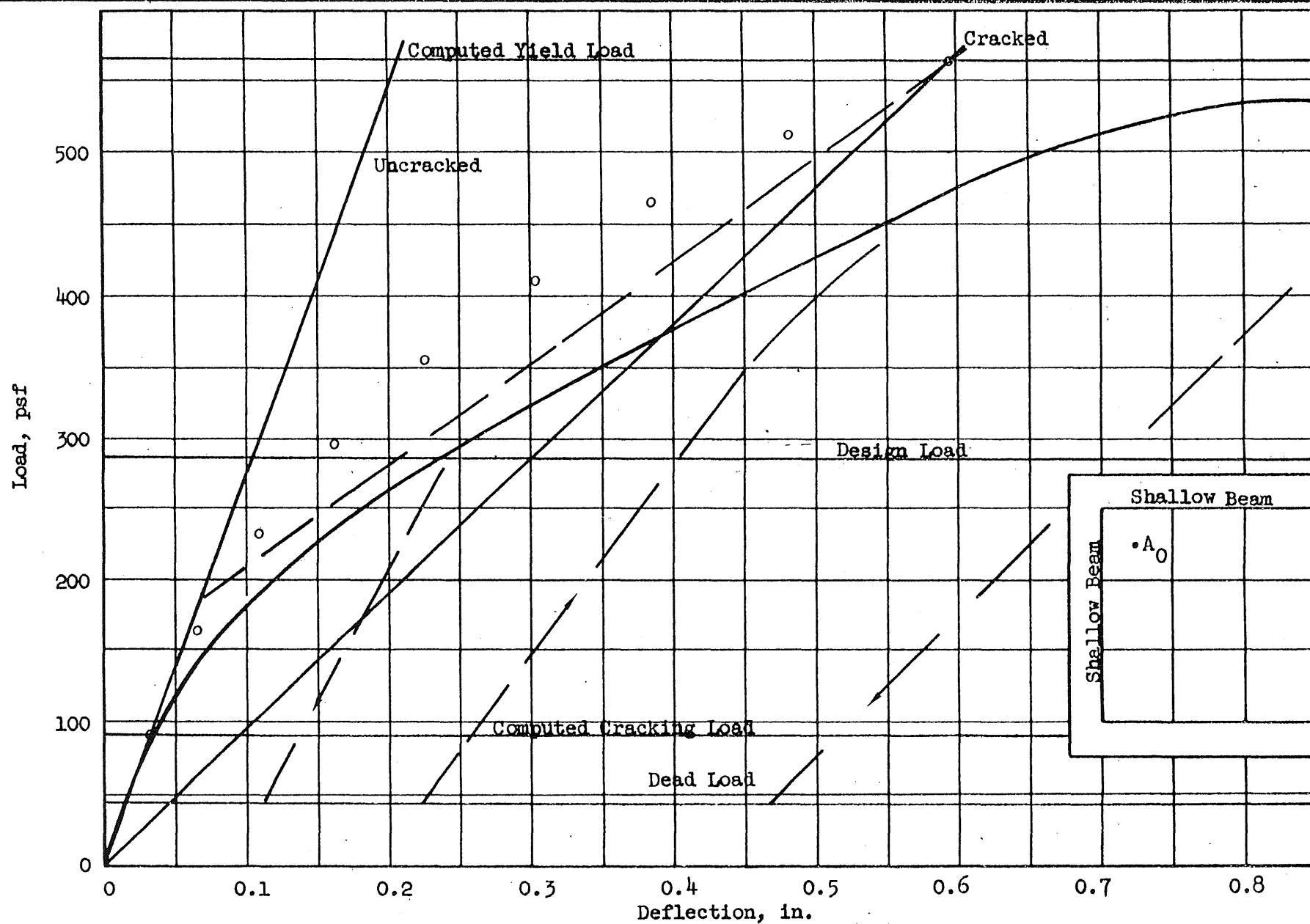


FIG. 5.54 LOAD-DEFLECTION CURVE, FLAT SLAB (F2), POINT A₀

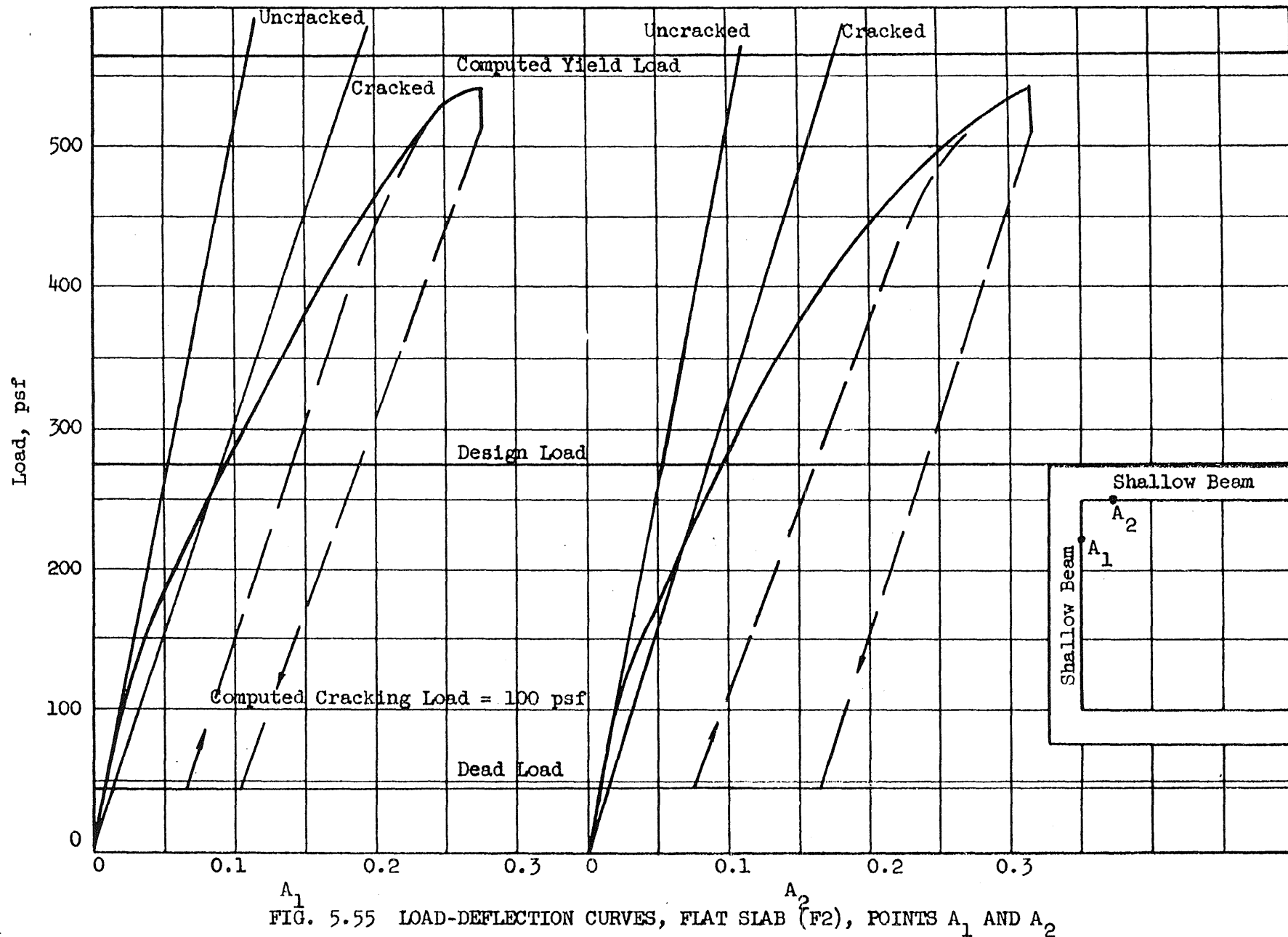


FIG. 5.55 LOAD-DEFLECTION CURVES, FLAT SLAB (F2), POINTS A₁ AND A₂

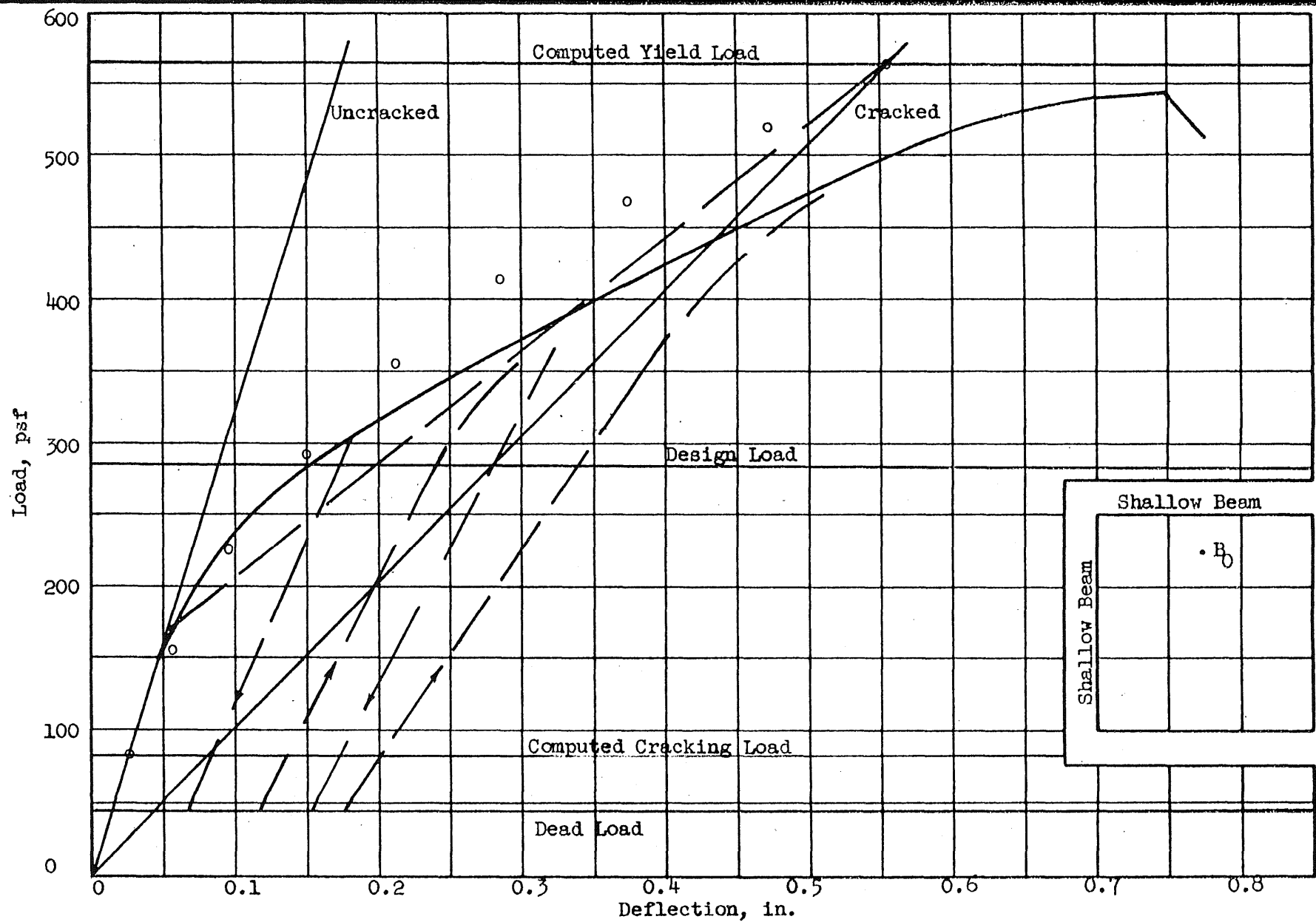


FIG. 5.56 LOAD-DEFLECTION CURVE, FLAT SLAB (F2), POINT B₀

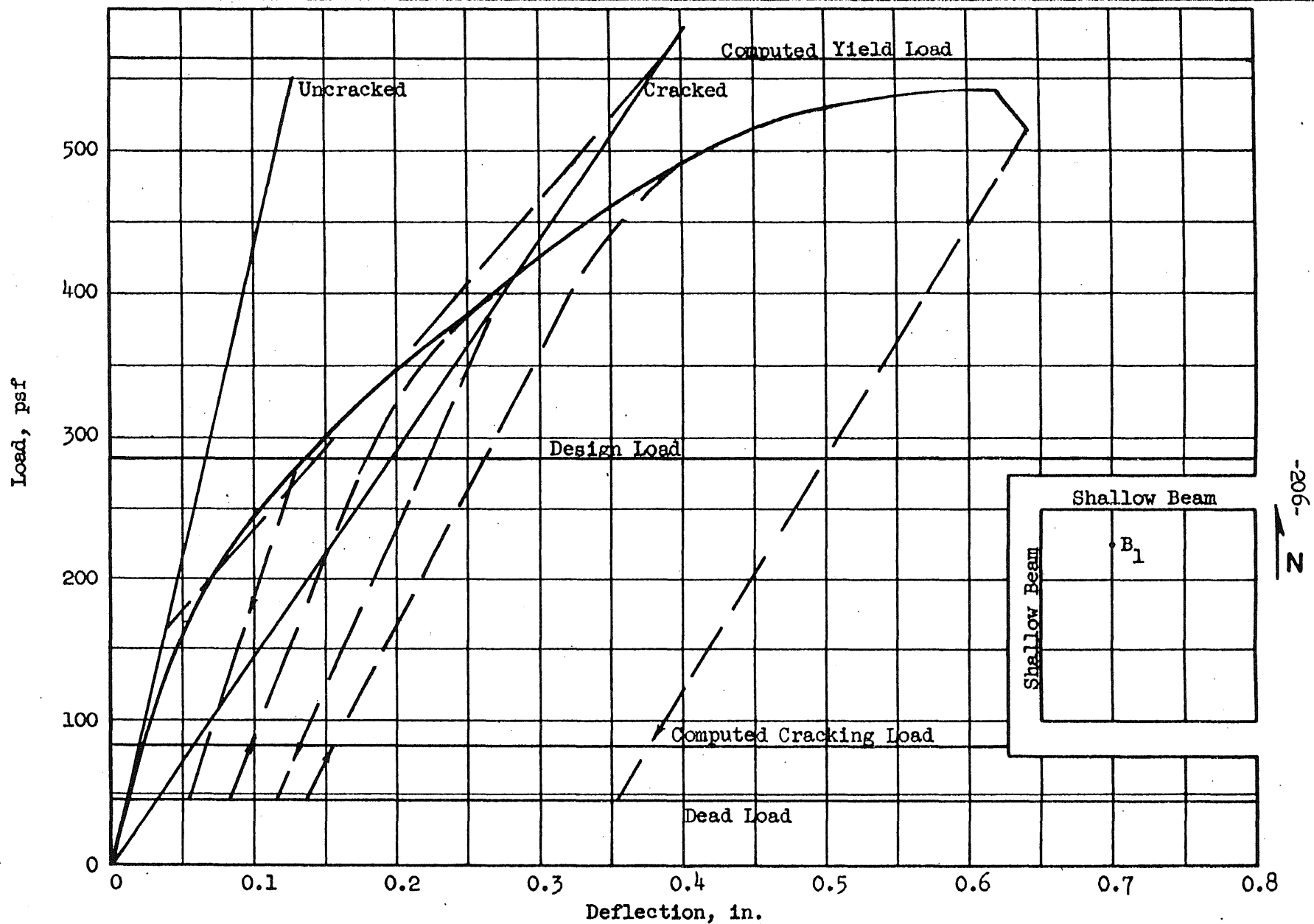


FIG. 5.57 LOAD-DEFLECTION CURVE, FLAT SLAB (F2), POINT B₁

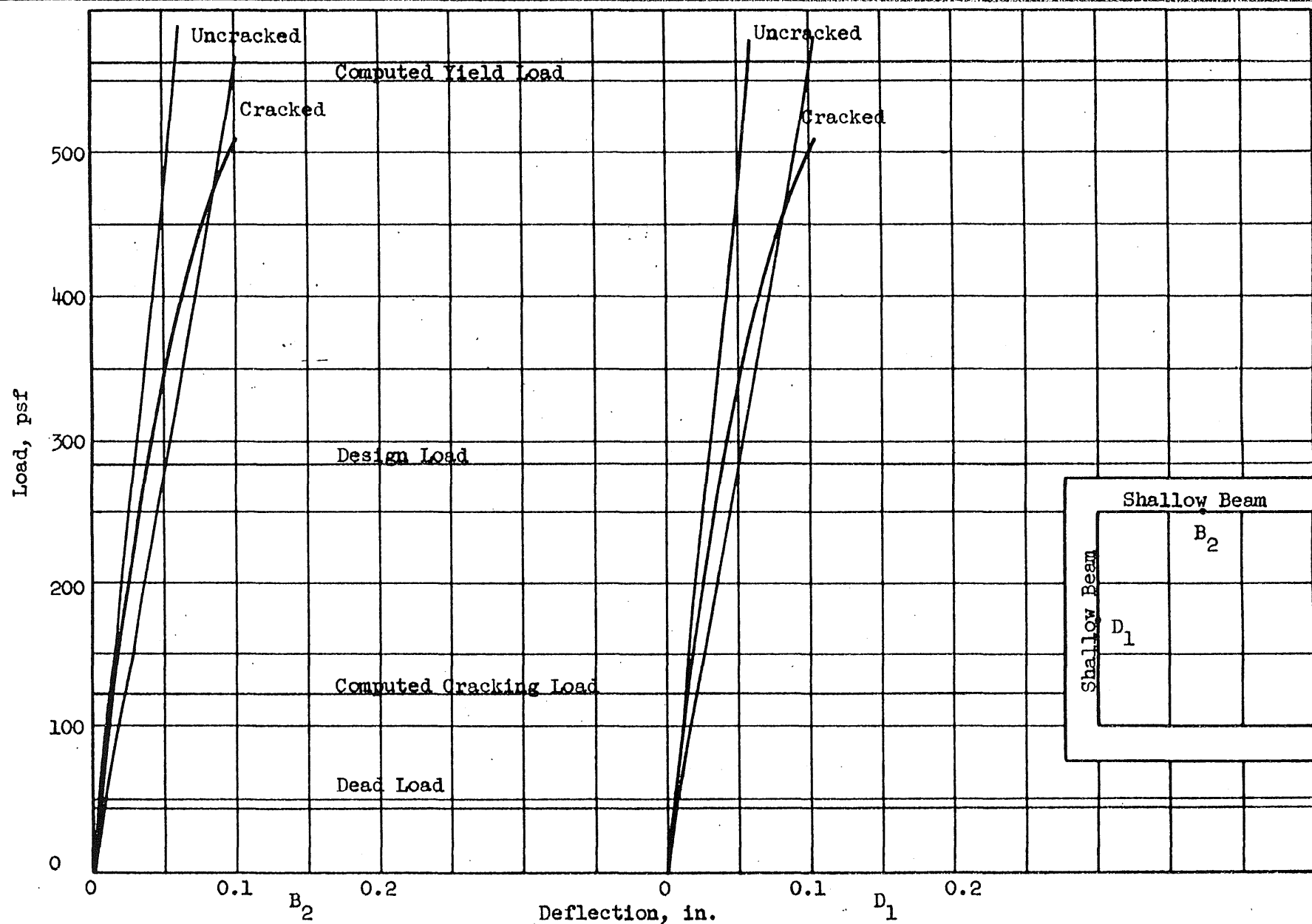


FIG. 5.58 LOAD-DEFLECTION CURVES, FLAT SLAB (F2), POINTS B_2 AND D_1

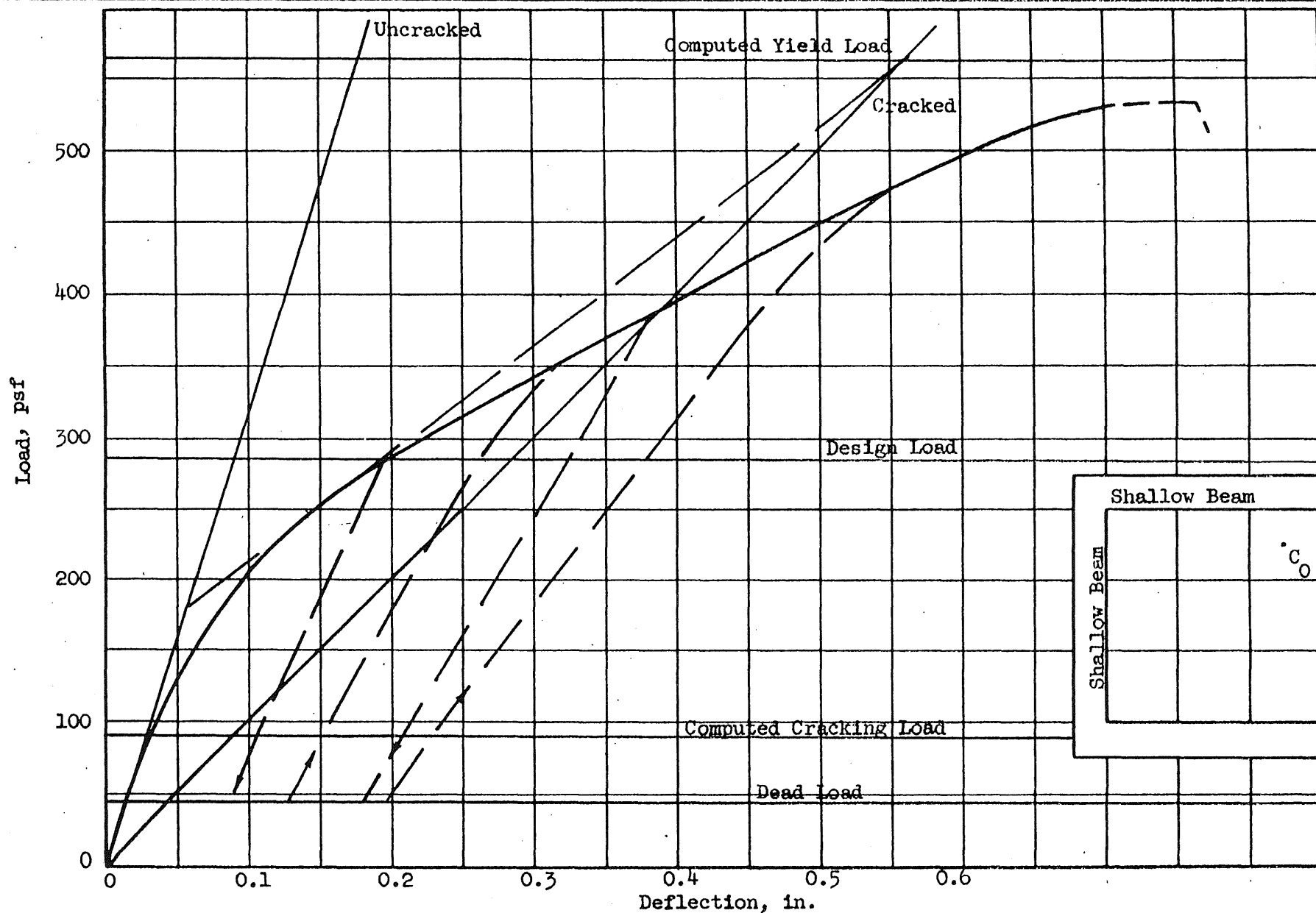


FIG. 5.59 LOAD-DEFLECTION CURVE, FLAT SLAB (F2), POINT C₀

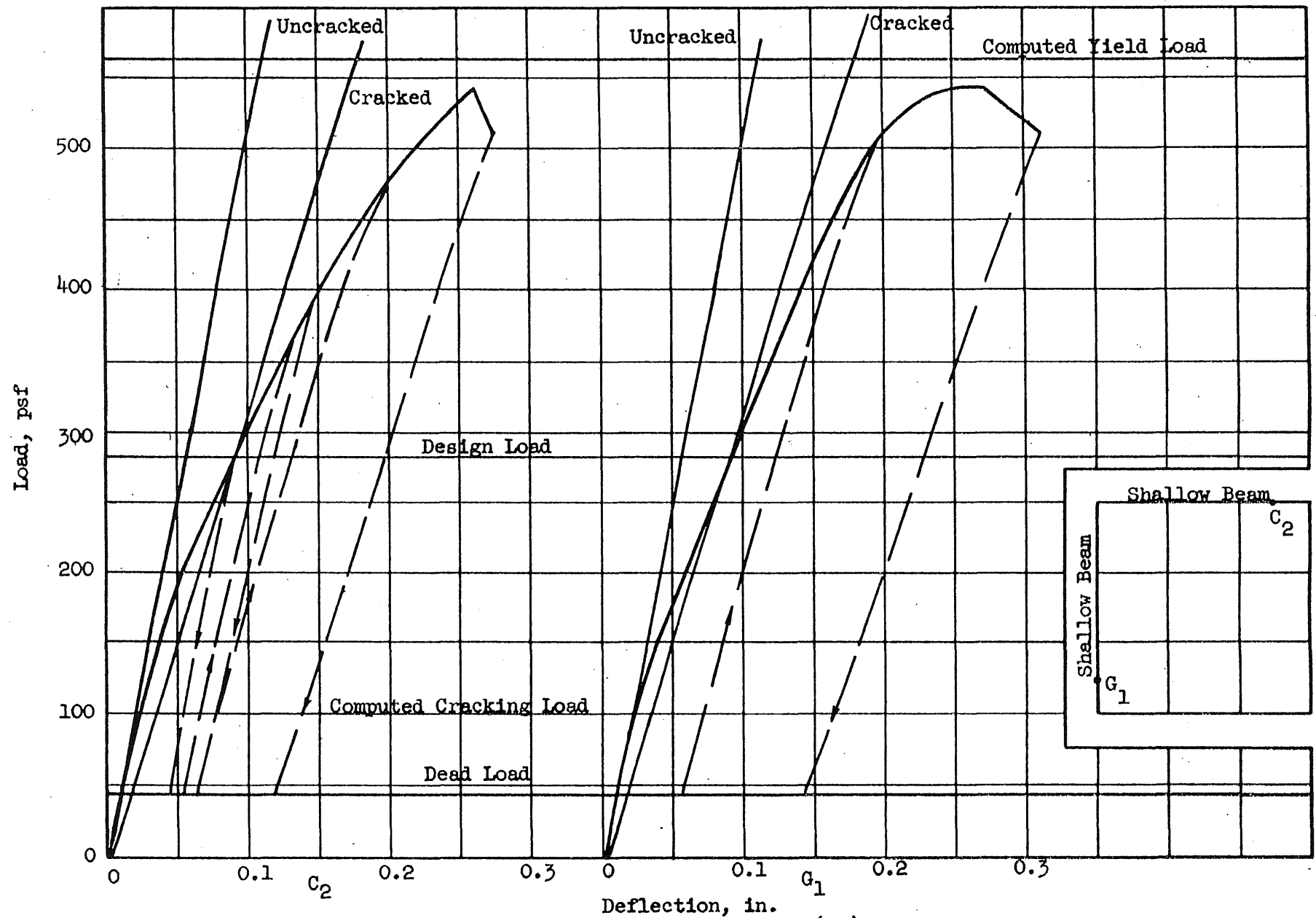


FIG. 5.60 LOAD-DEFLECTION CURVES, FLAT SLAB (F2), POINTS C_2 and G_1

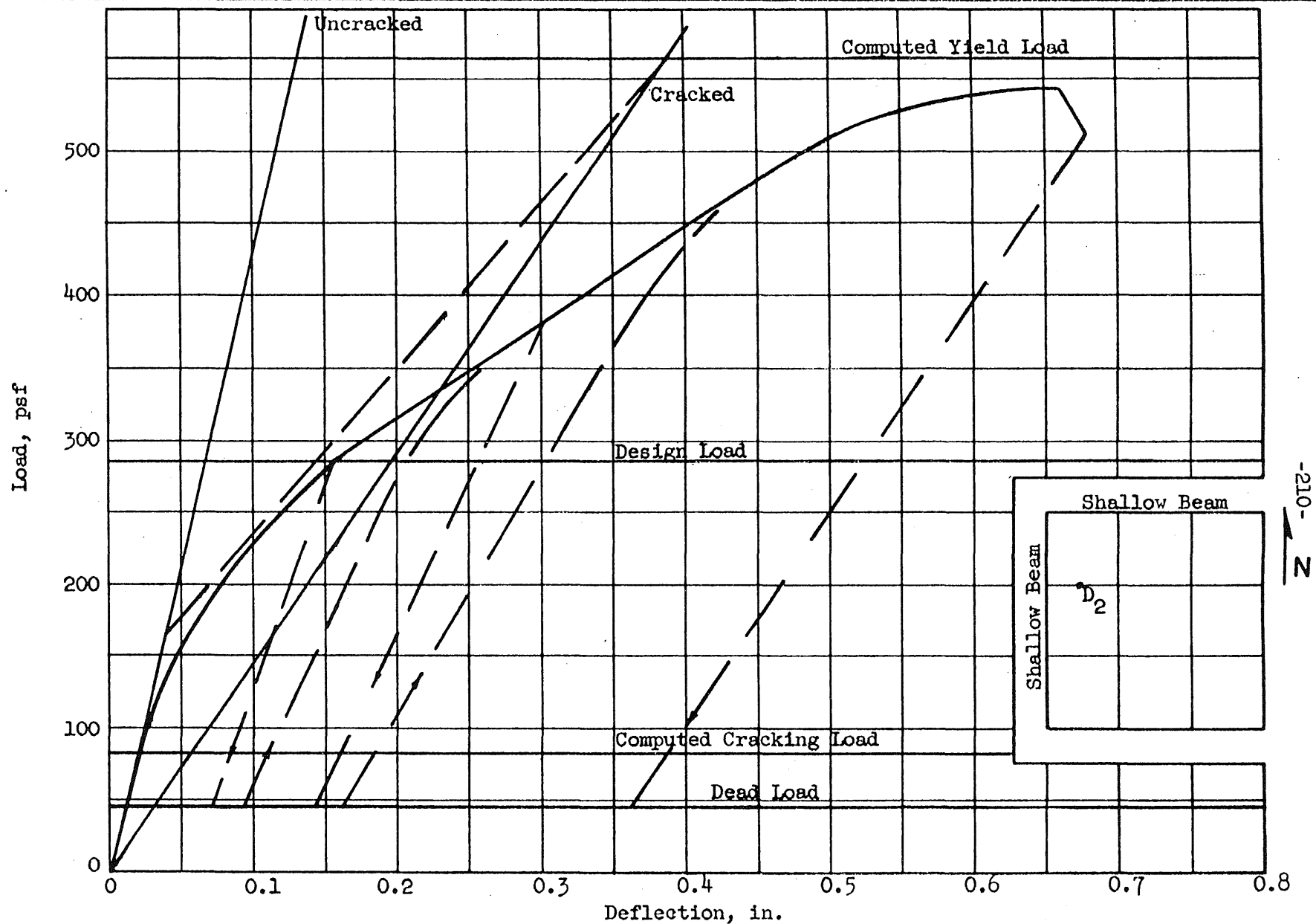


FIG. 5.61 LOAD-DEFLECTION CURVE, FLAT SLAB (F2), POINT D₂

-210-
N

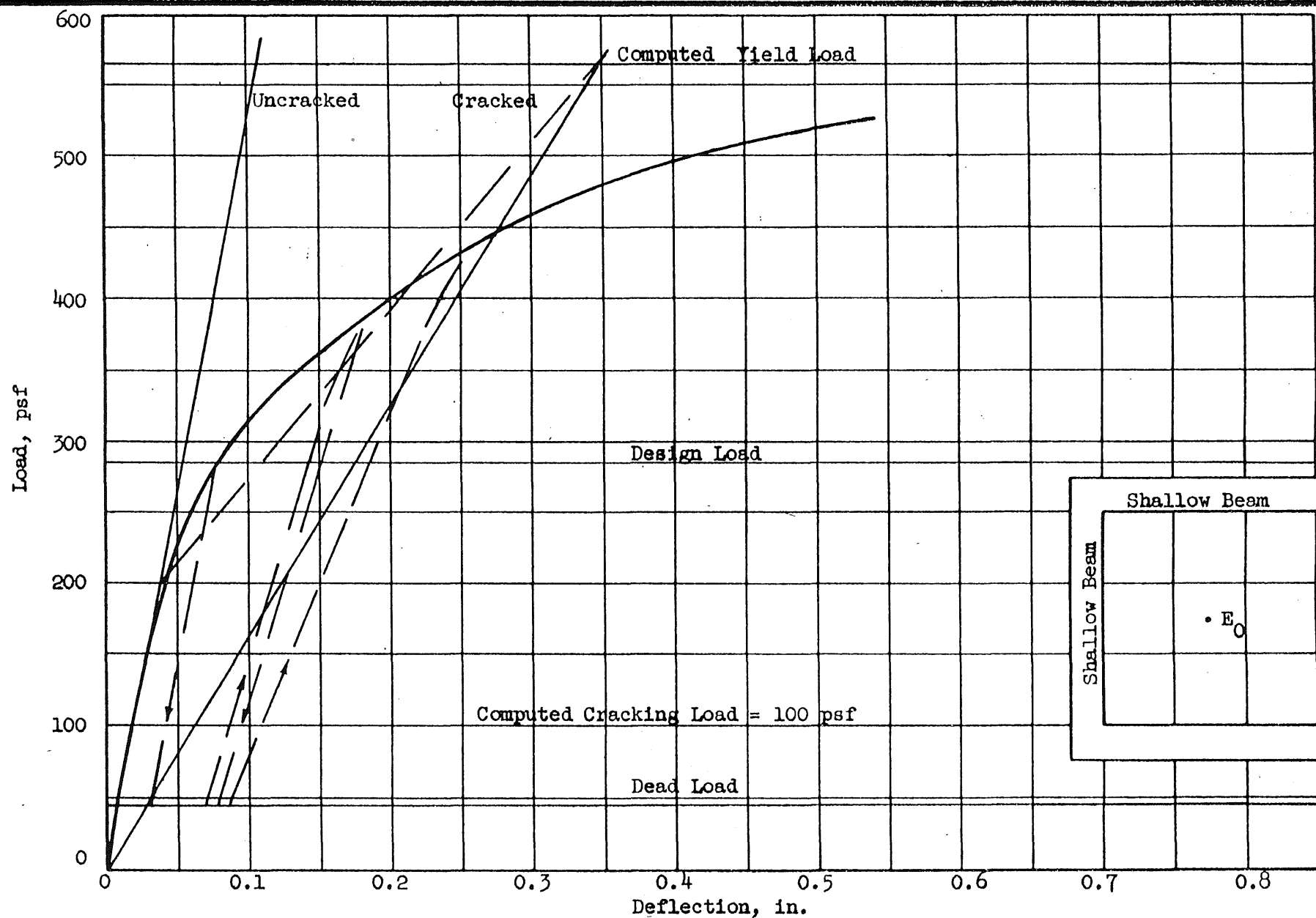


FIG. 5.62 LOAD-DEFLECTION CURVE, FLAT SLAB (F2), POINT E_0

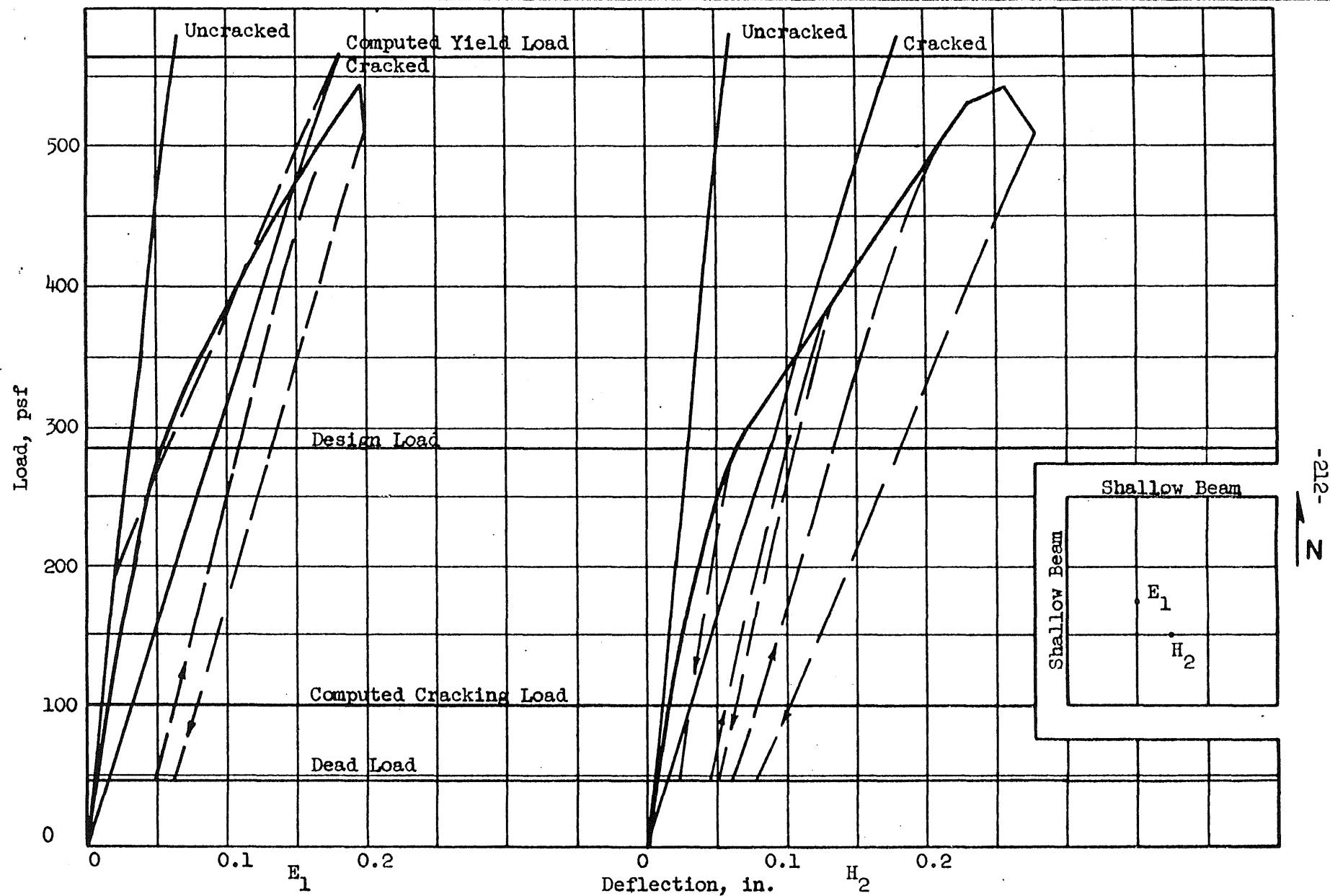


FIG. 5.63 LOAD-DEFLECTION CURVES, FLAT SLAB (F2), POINTS E_1 AND H_2

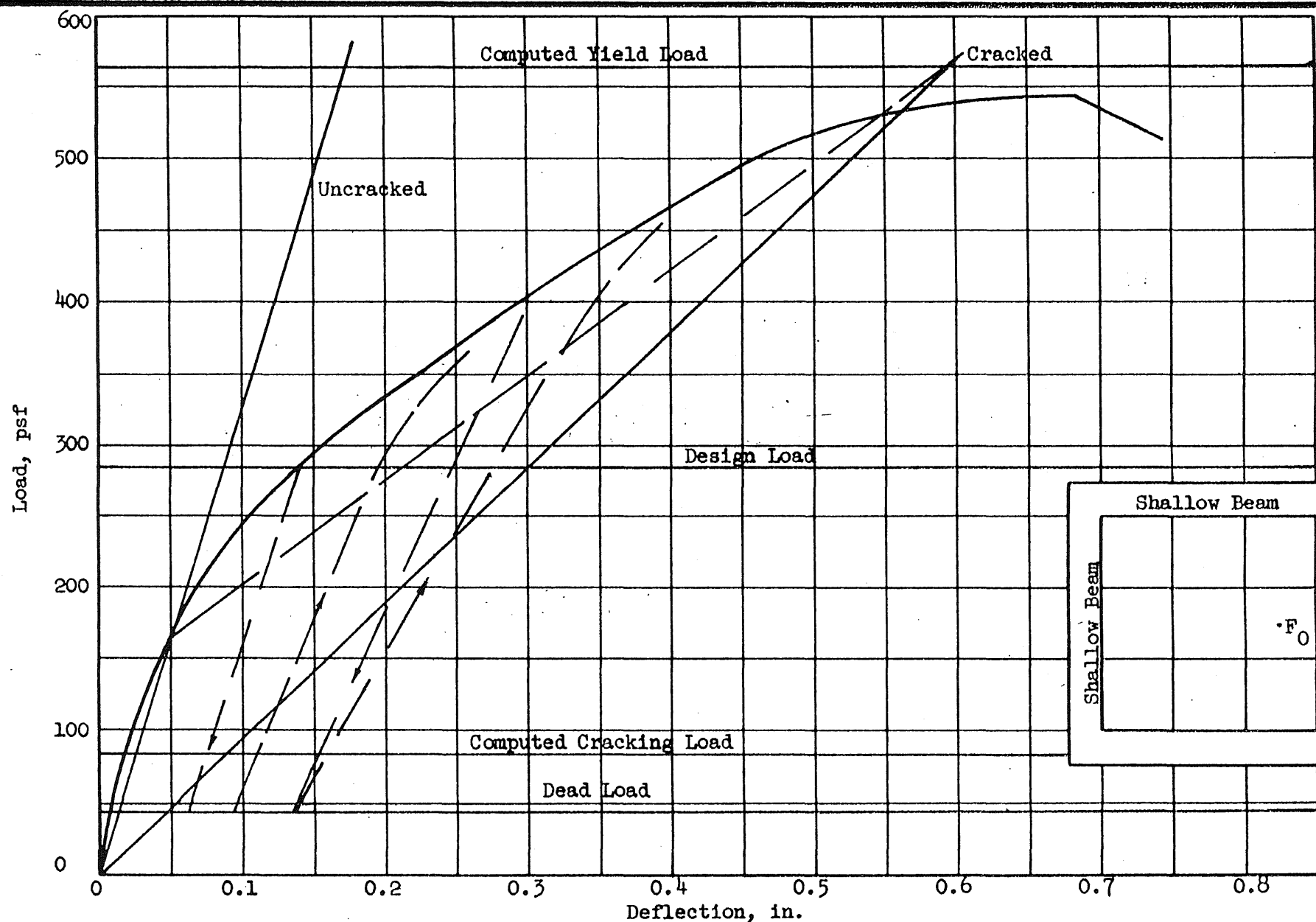


FIG. 5.64 LOAD-DEFLECTION CURVE, FLAT SLAB (F2), POINT F_0

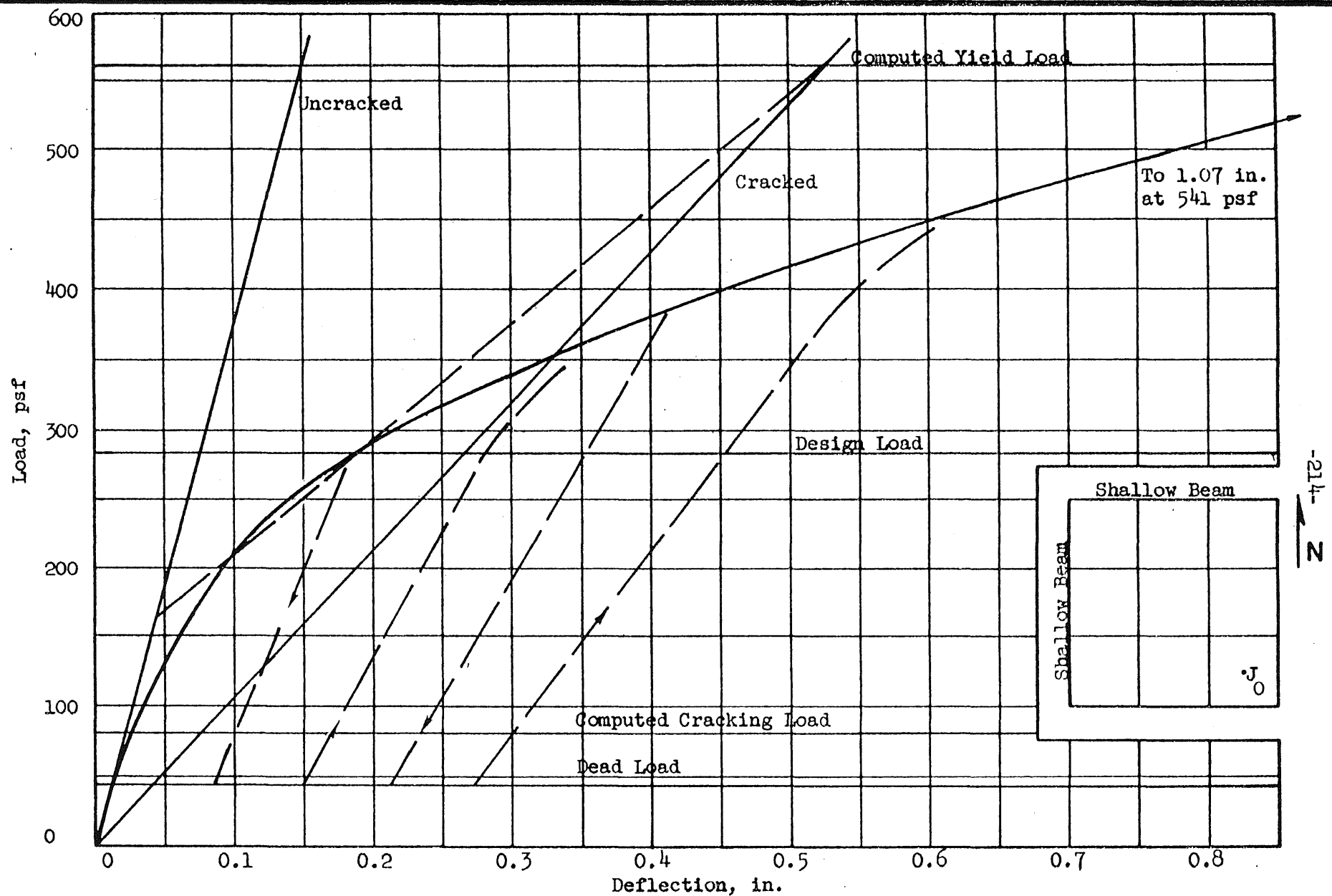


FIG. 5.65 LOAD-DEFLECTION CURVE, FLAT SLAB (F2), POINT J₀

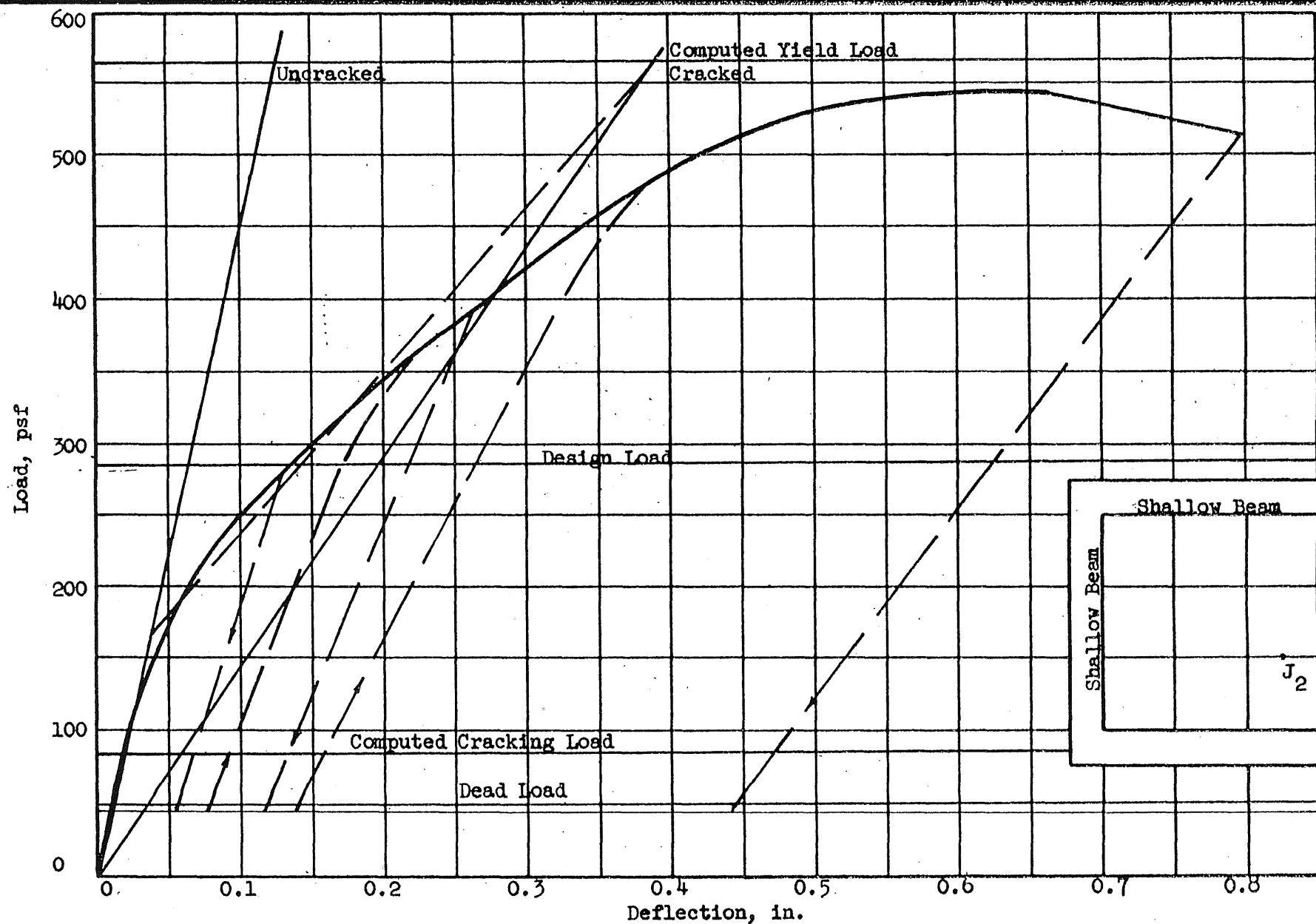


FIG. 5.66 LOAD-DEFLECTION CURVE, FLAT SLAB (F2), POINT J₂

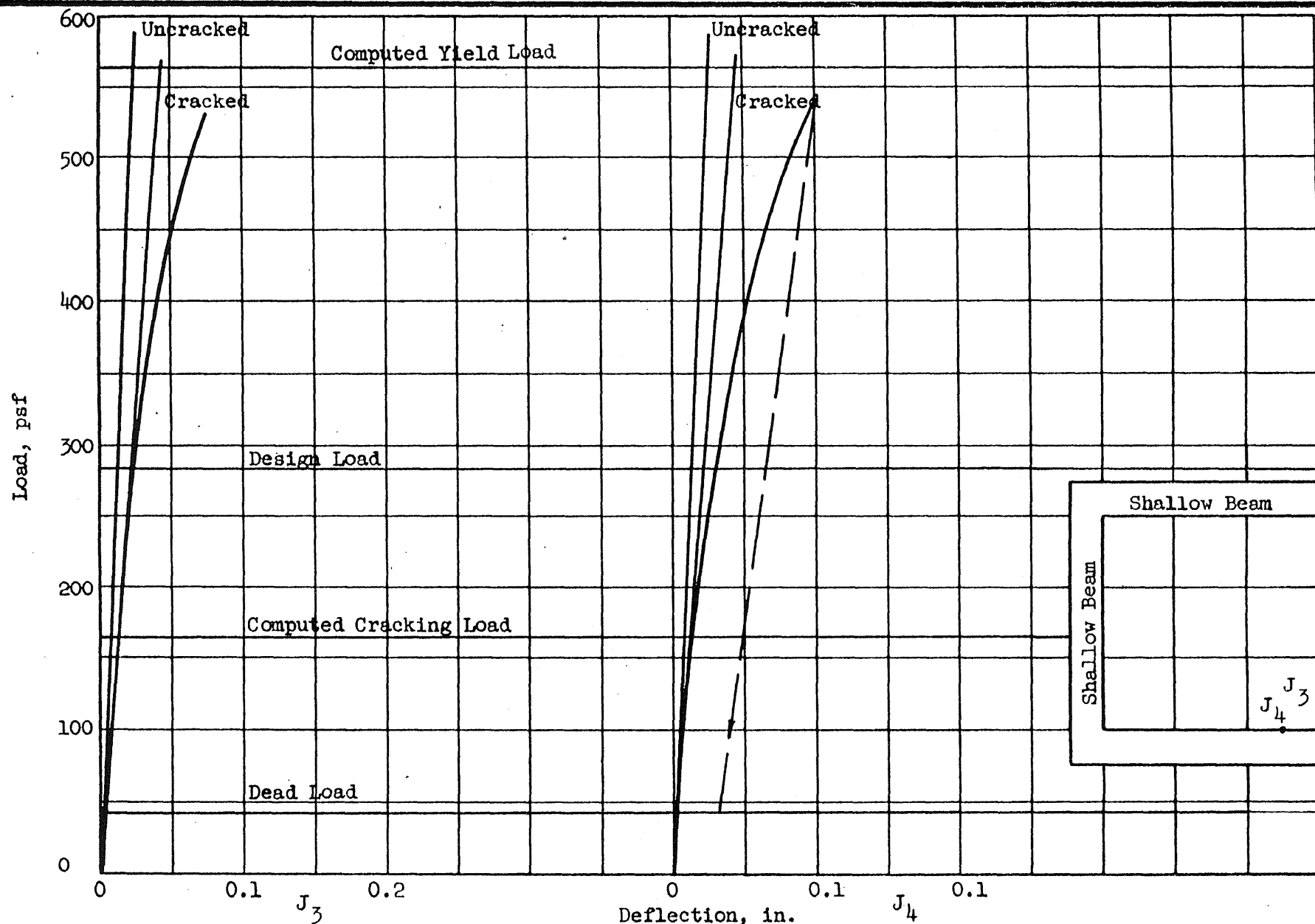


FIG. 5.67 LOAD-DEFLECTION CURVES, FLAT SLAB (F2), POINTS J_3 AND J_4

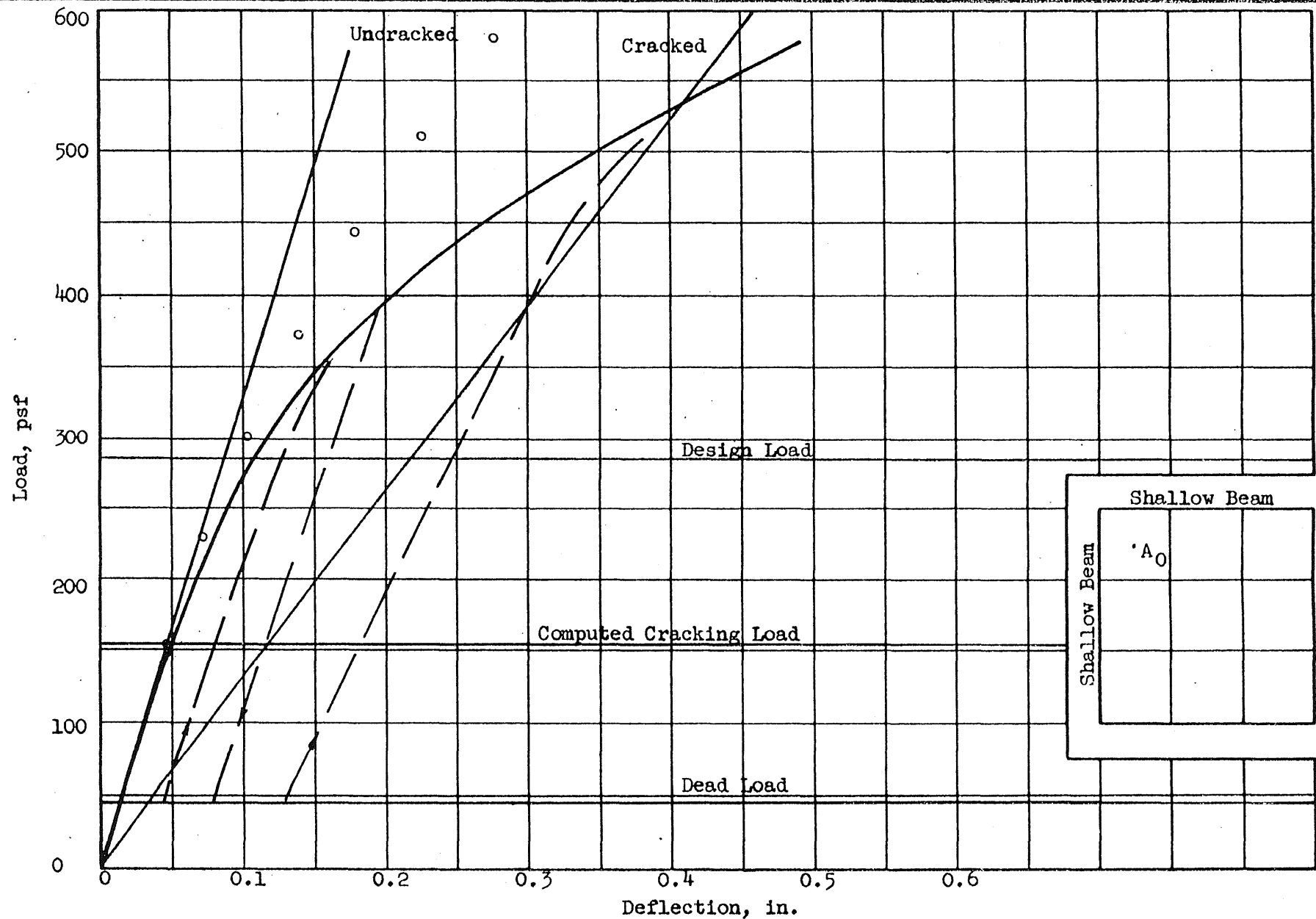


FIG. 5.68 LOAD-DEFLECTION CURVE, FLAT SLAB (F3), POINT A₀

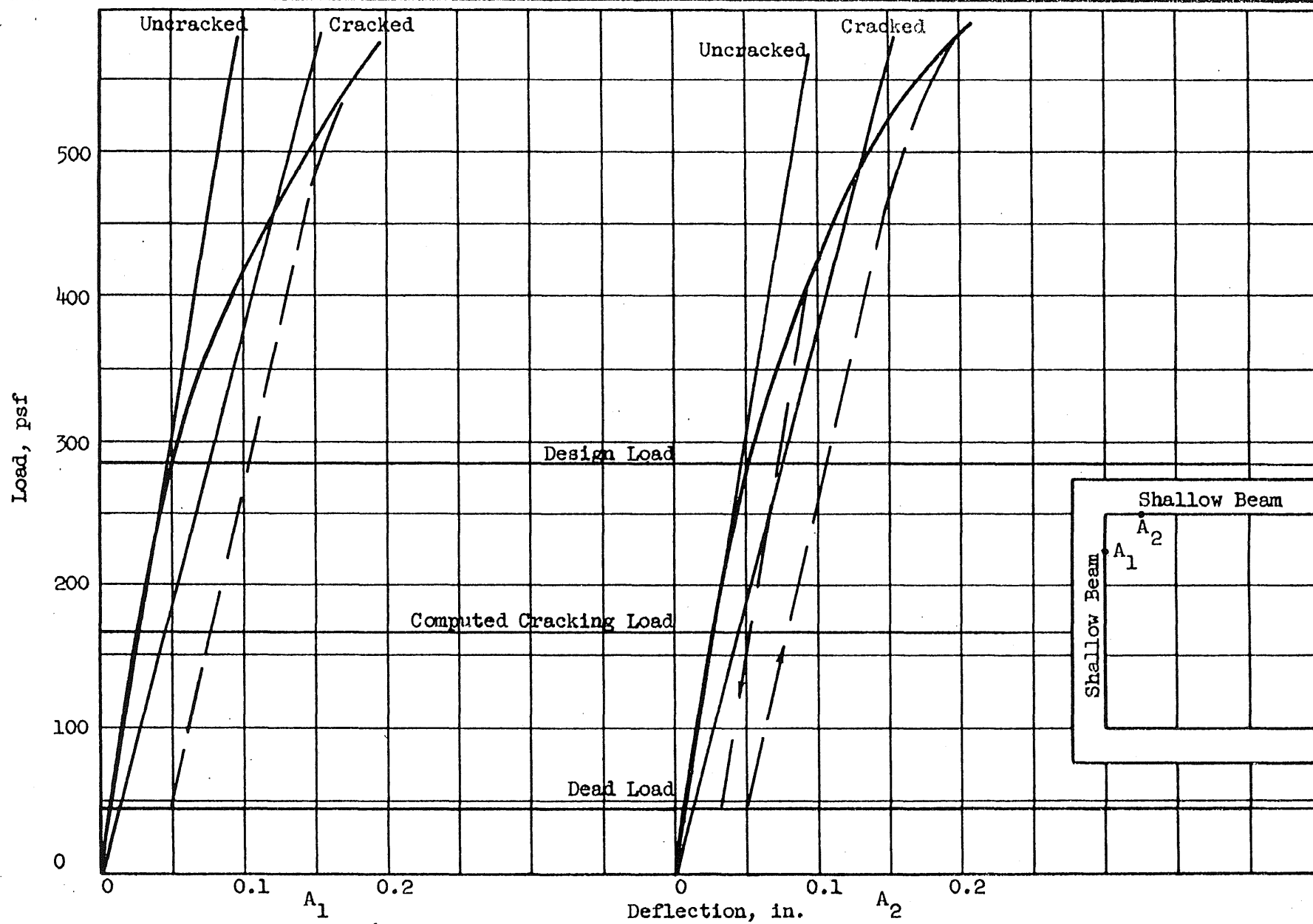


FIG. 5.69 LOAD-DEFLECTION CURVES, FLAT SLAB (F3), POINTS A₁ AND A₂

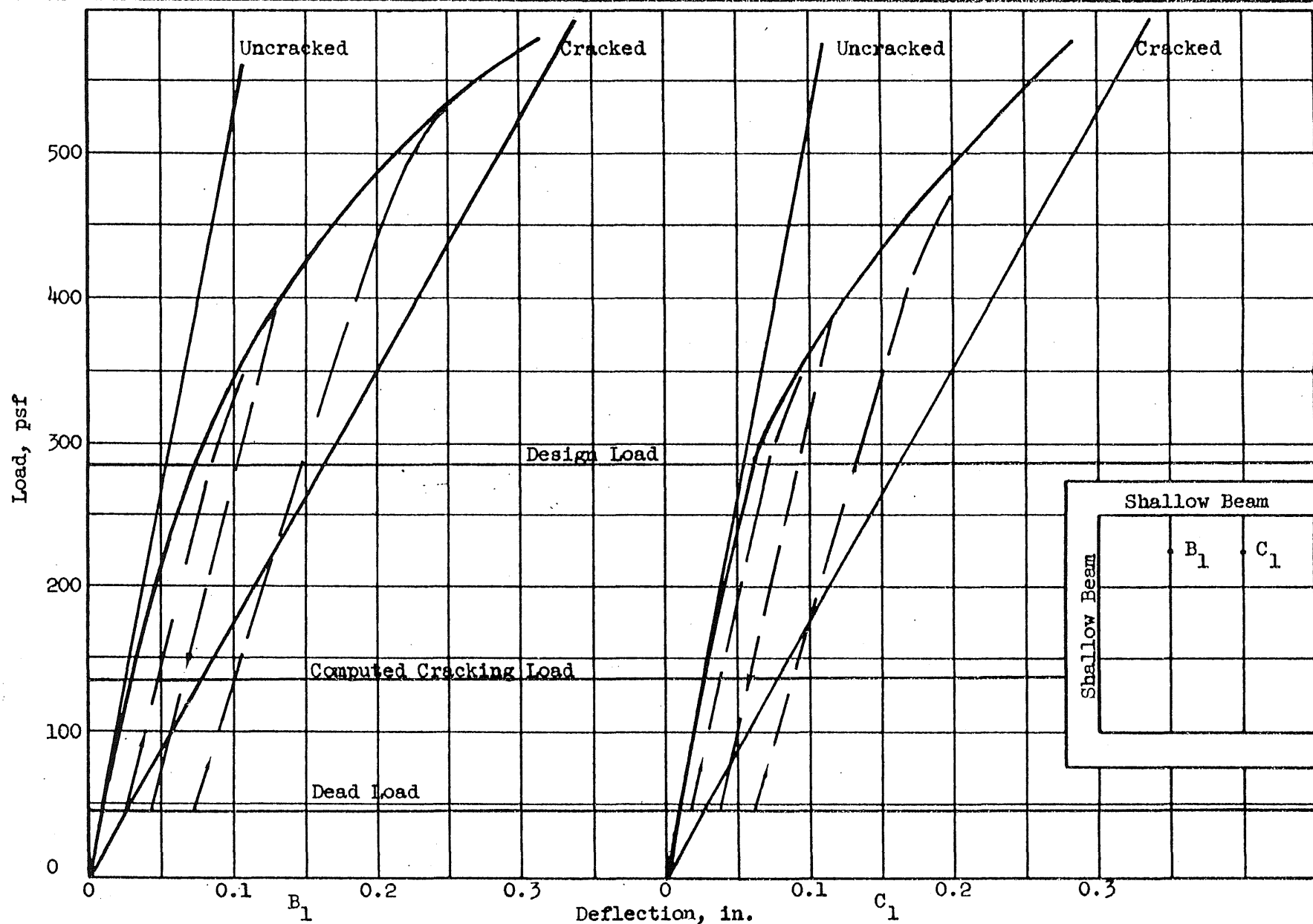


FIG. 5.70 LOAD-DEFLECTION CURVES, FLAT SLAB (F3), POINTS B_1 AND C_1

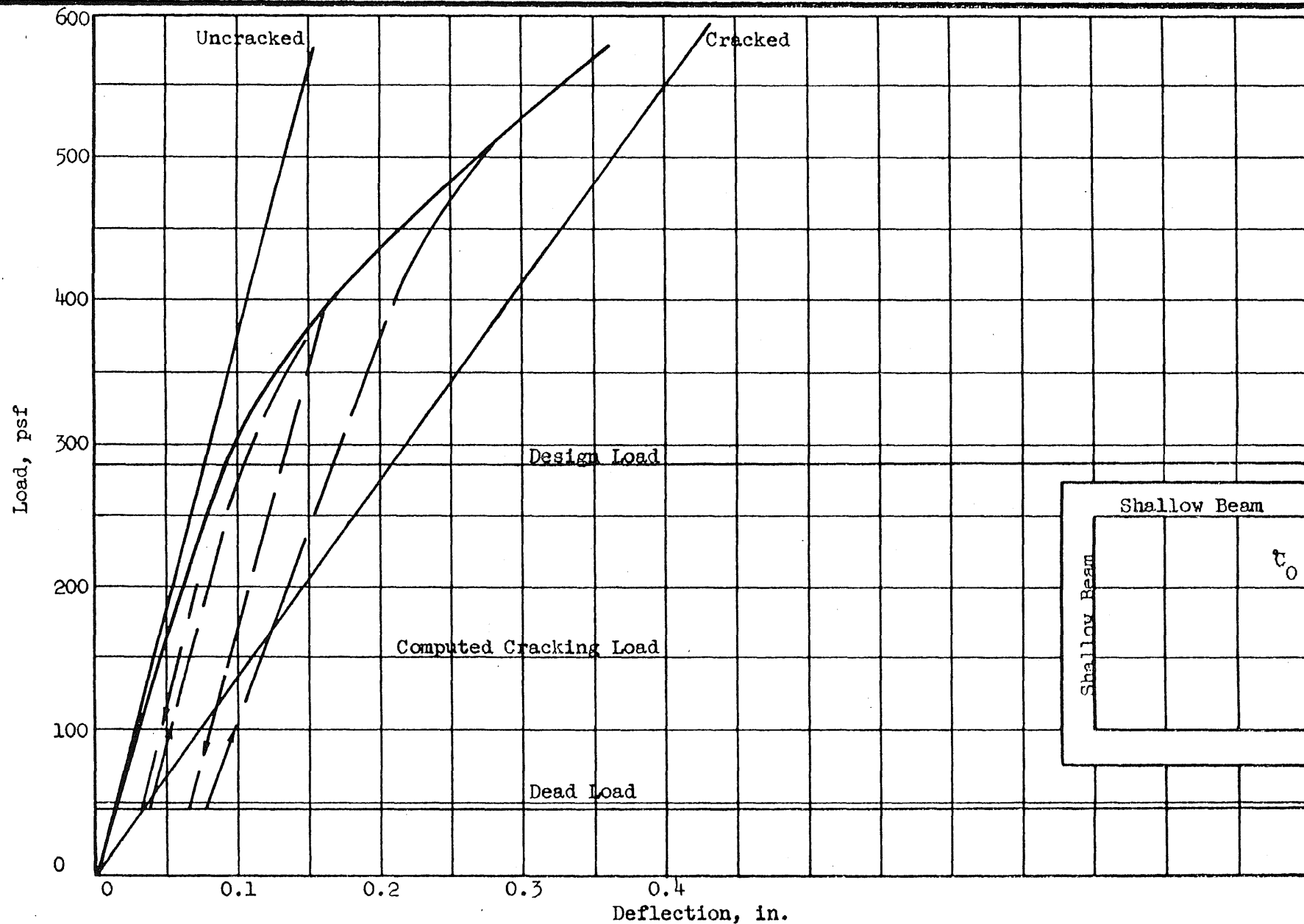


FIG. 5.71 LOAD-DEFLECTION CURVE, FLAT SLAB (F3), POINT C_0

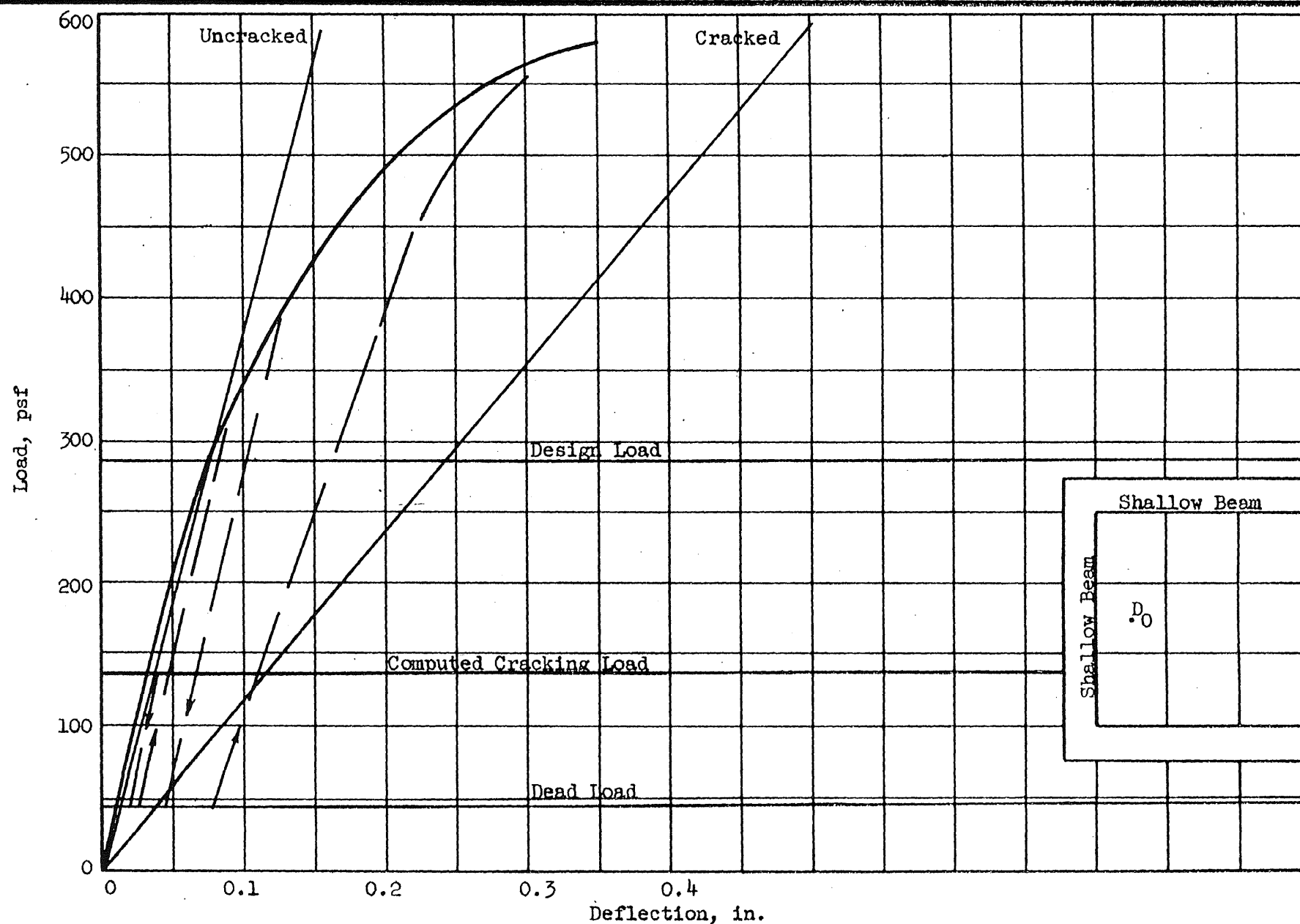


FIG. 5.72 LOAD-DEFLECTION CURVE, FLAT SLAB (F3), POINT D₀

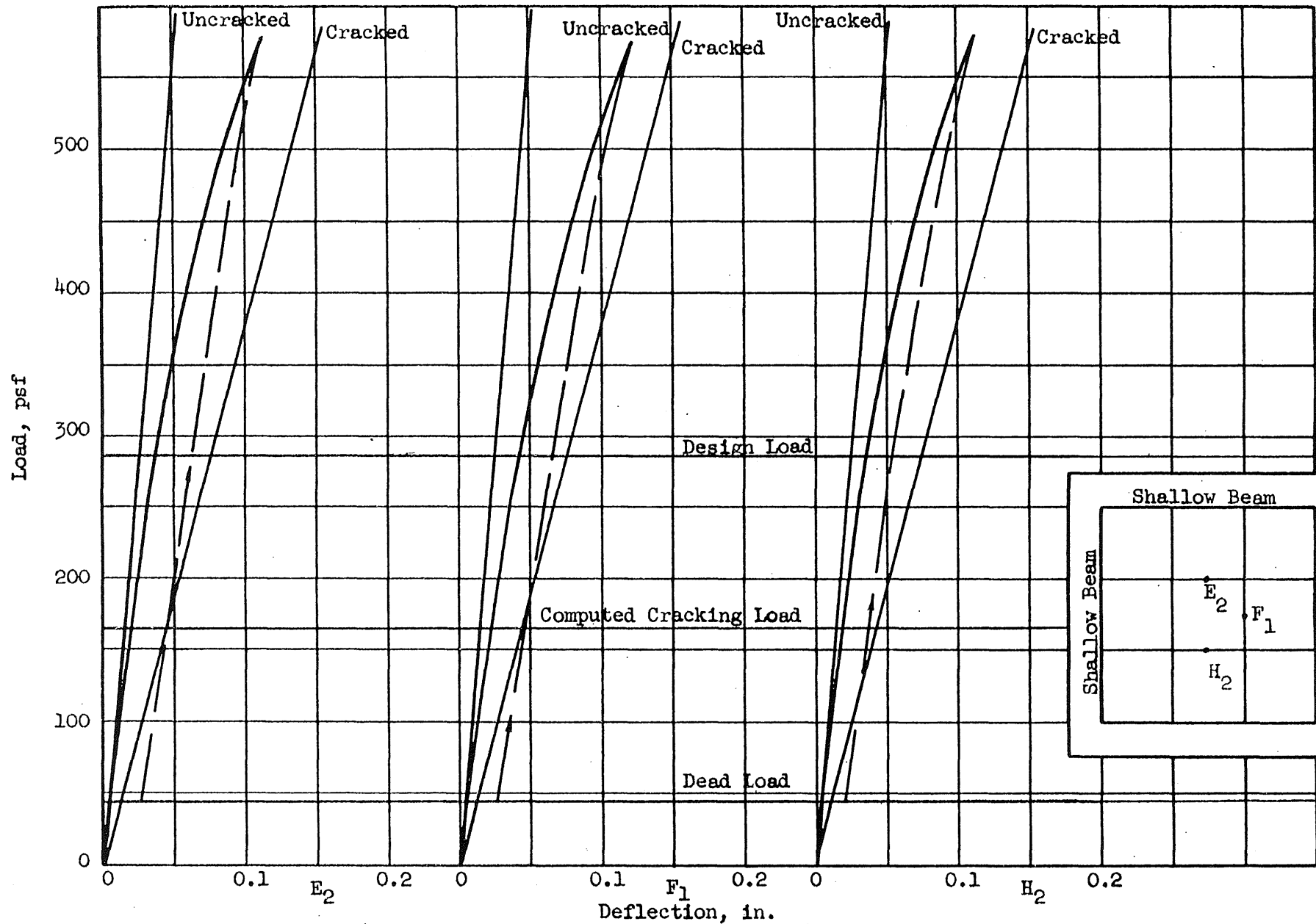


FIG. 5.74 LOAD-DEFLECTION CURVES, FLAT SLAB (F3), POINTS E_2 , F_1 , AND H_2

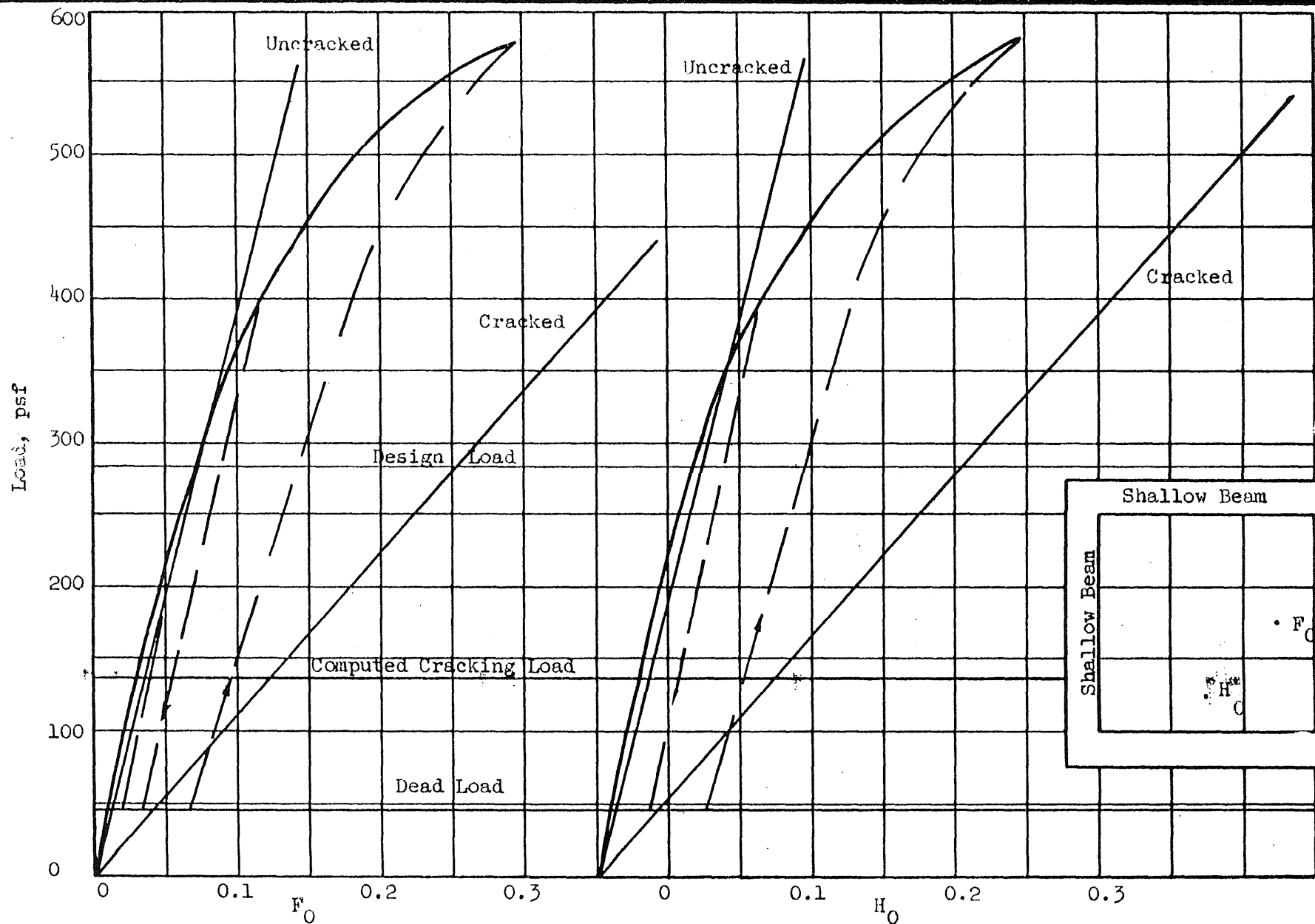


FIG. 5.75 LOAD-DEFLECTION CURVES, FLAT SLAB (F3), POINTS F_0 AND H_0

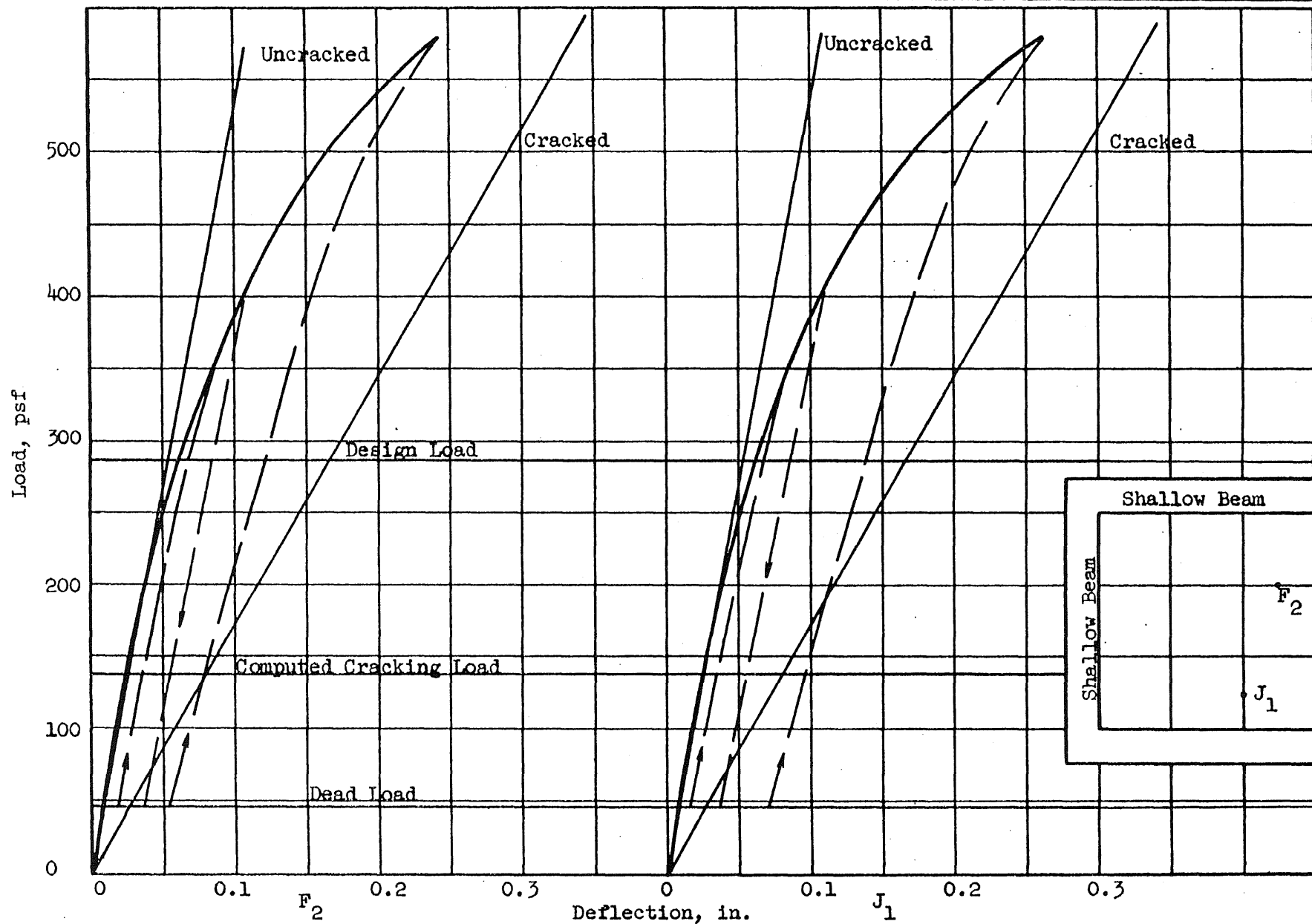


FIG. 5.76 LOAD-DEFLECTION CURVES, FLAT SLAB (F3), POINTS F_2 AND J_1

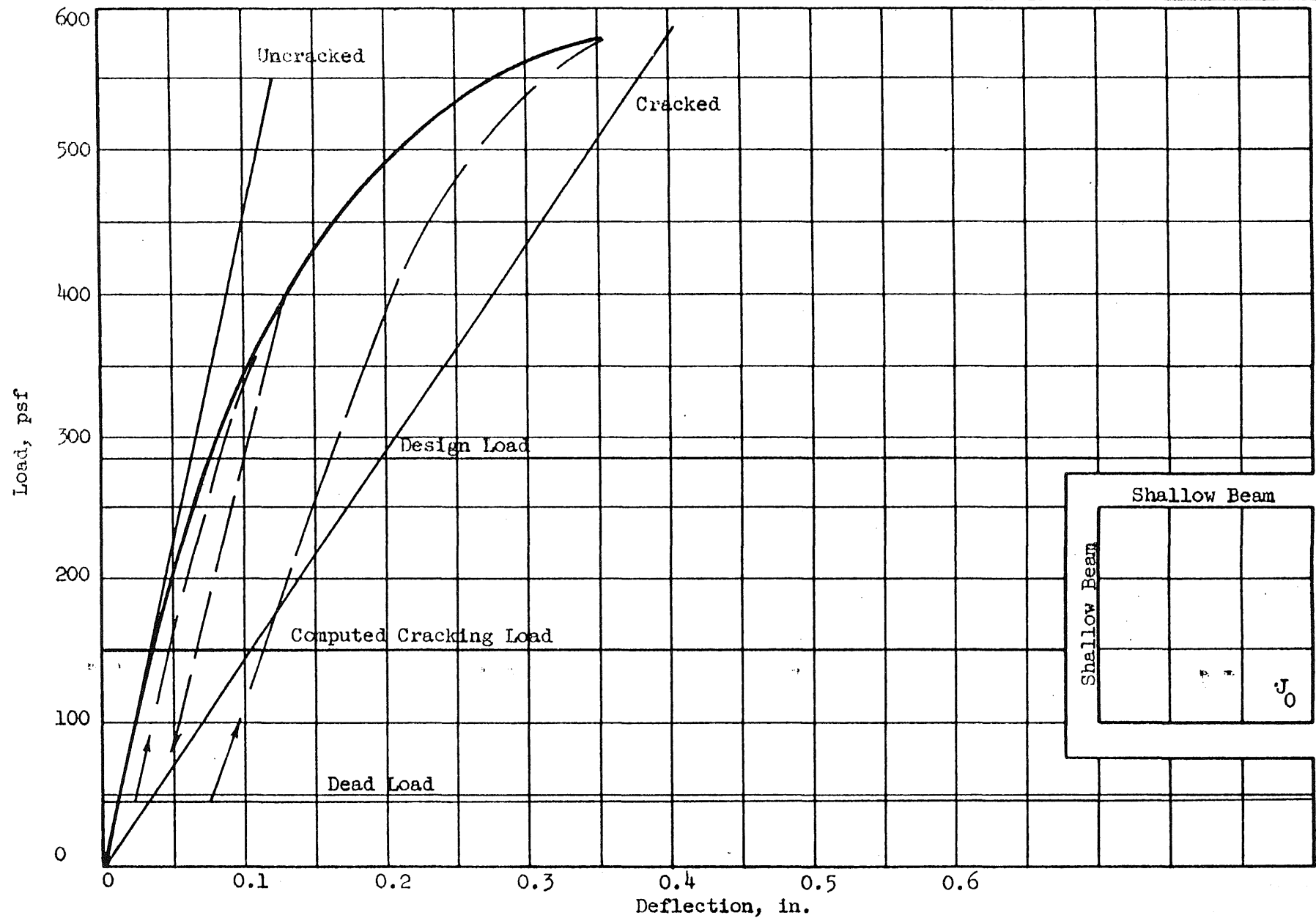


FIG. 5.77 LOAD-DEFLECTION CURVE, FLAT SLAB (F3), POINT J₀

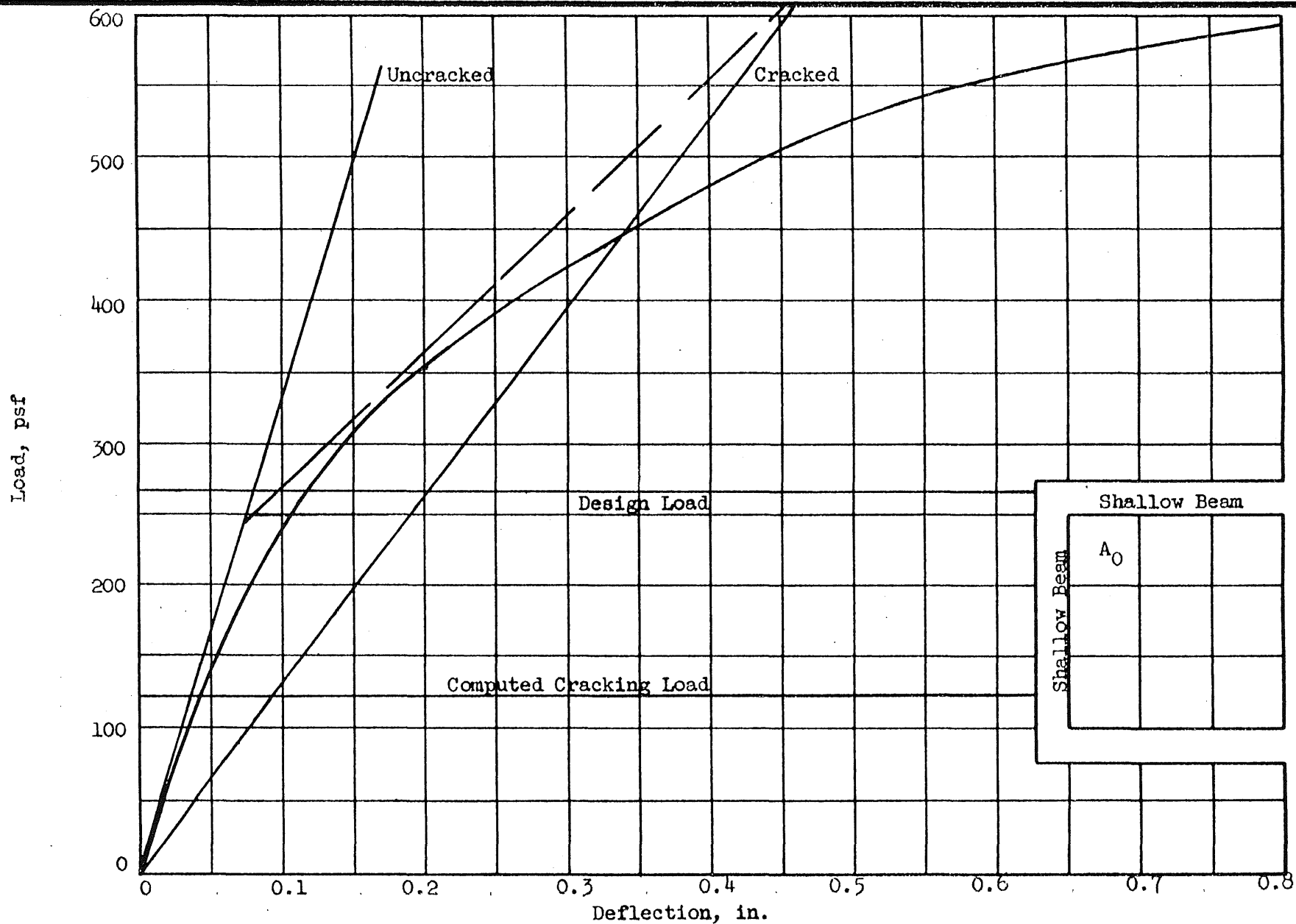


FIG. 5.78 LOAD-DEFLECTION CURVE, FLAT SLAB (F4), POINT A₀

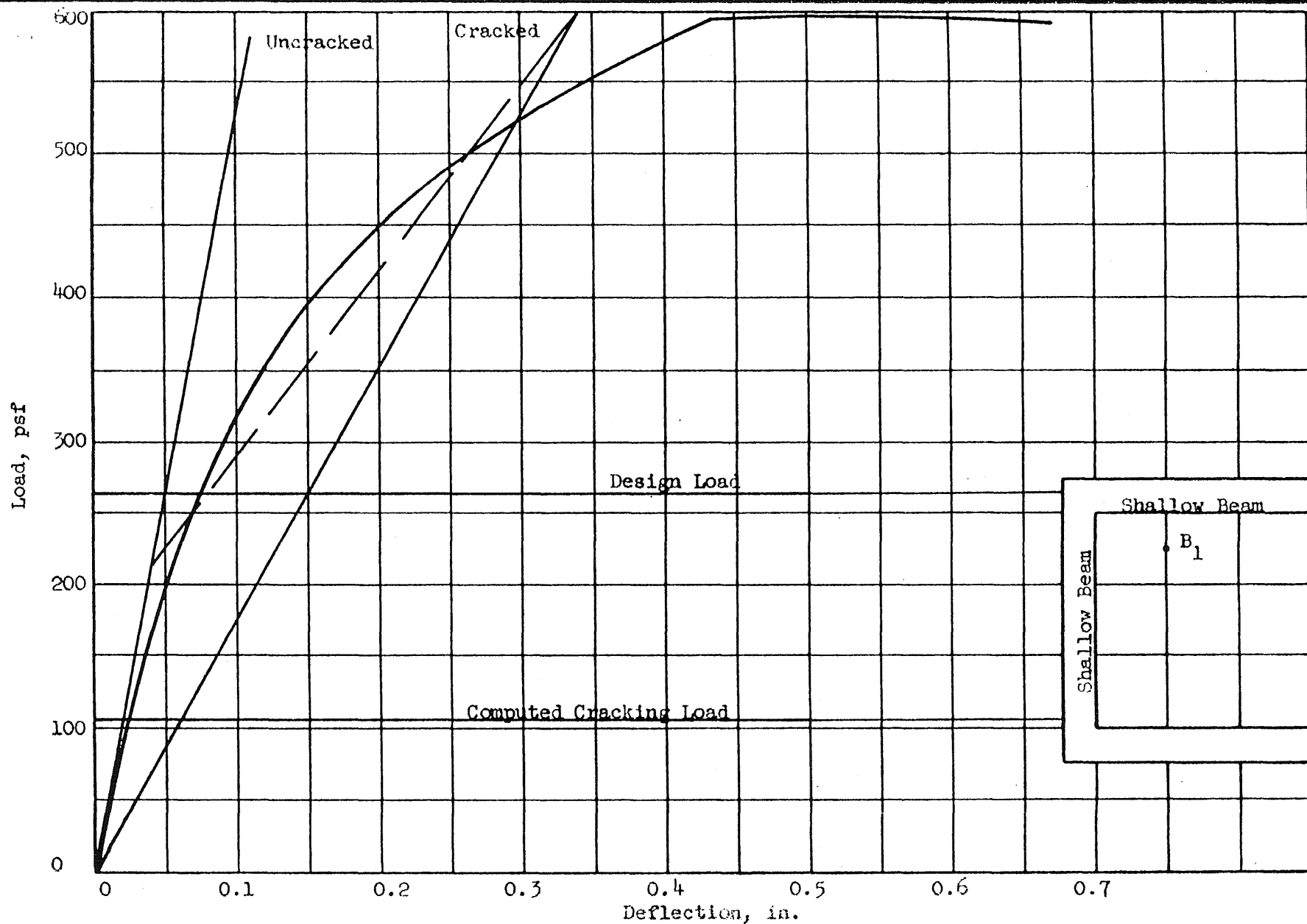
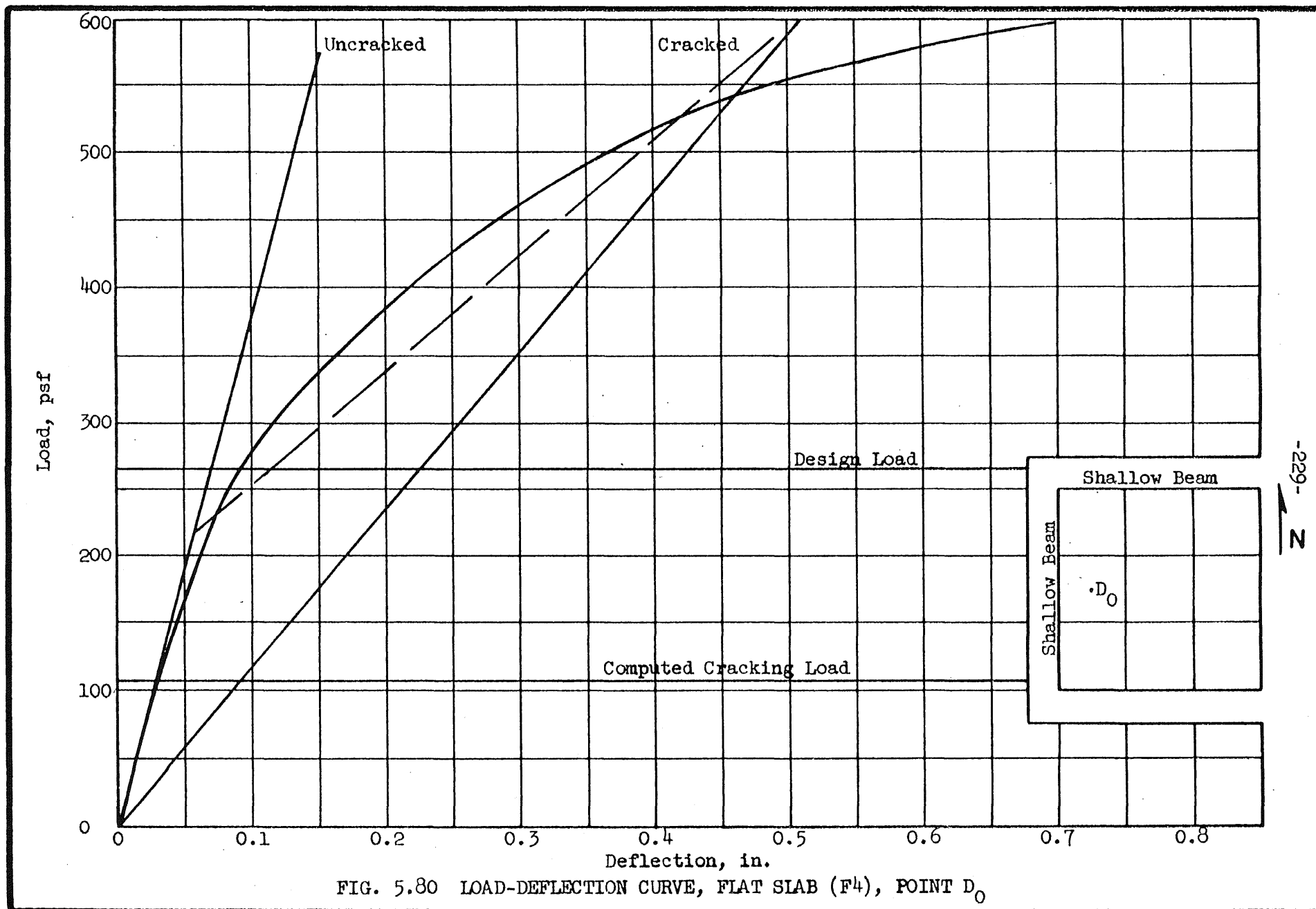


FIG. 5.79 LOAD-DEFLECTION CURVE, FLAT SLAB (F4), POINT B₁



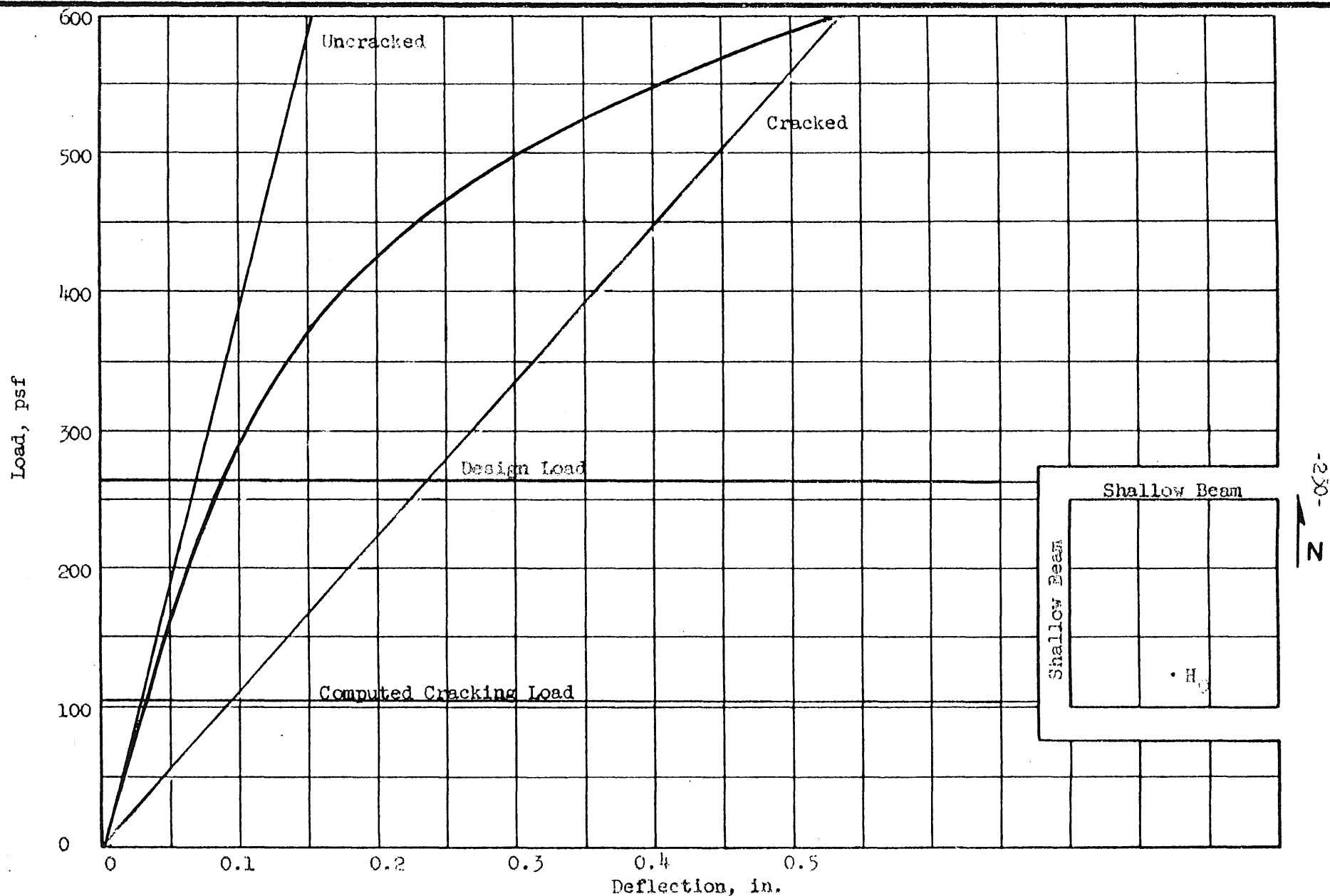


FIG. 5.81 LOAD-DEFLECTION CURVE, FLAT SLAB (F4), POINT H₀

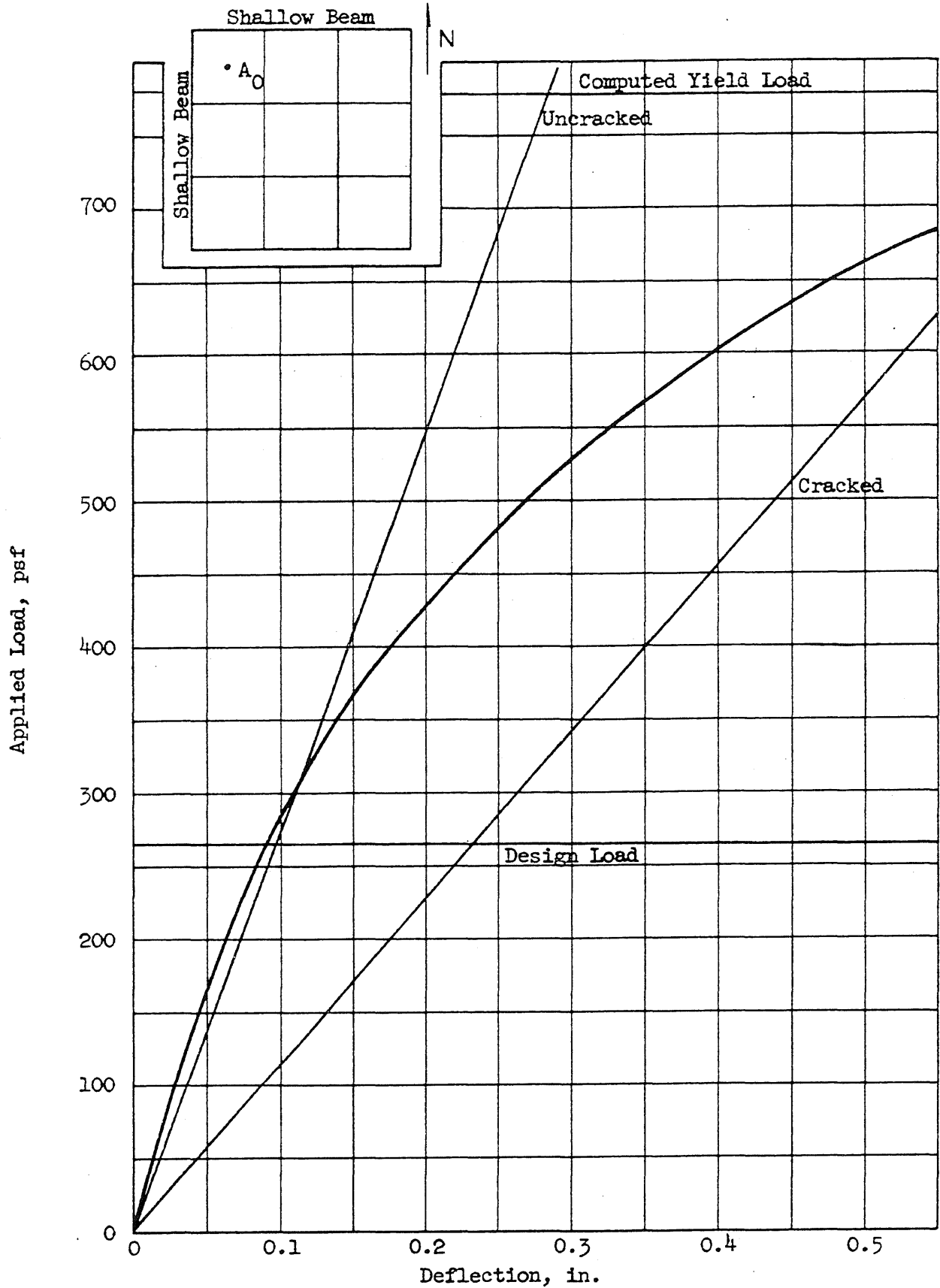


FIG. 5.82 LOAD-DEFLECTION CURVE, FLAT SLAB (F5), POINT A₀

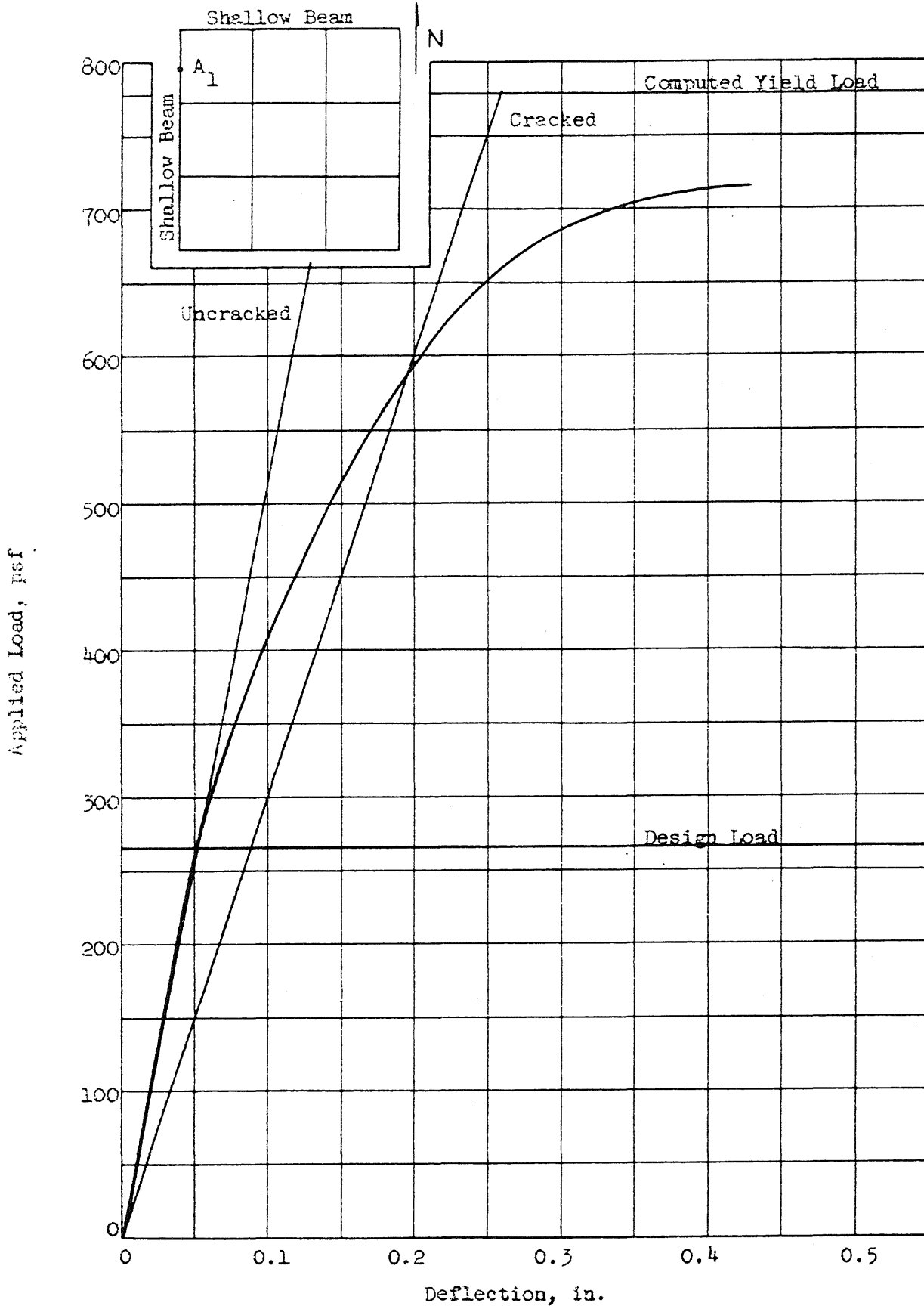


FIG. 5.33 LOAD-DEFLECTION CURVE, FLAT SLAB (F5), POINT A₁

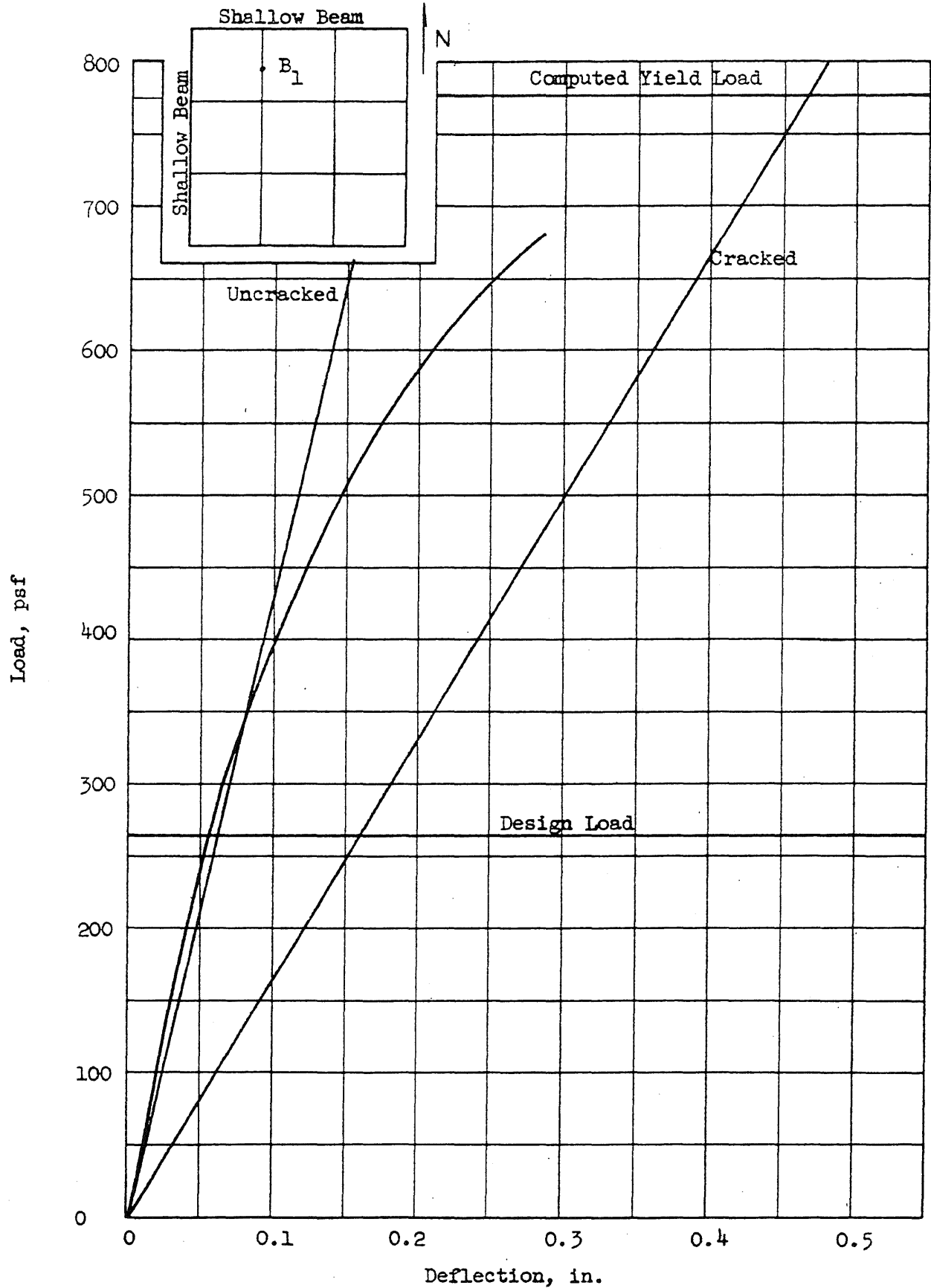


FIG. 5.84 LOAD-DEFLECTION CURVE, FLAT SLAB (F5), POINT B₁

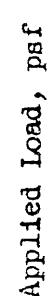


FIG. 5.85 LOAD-DEFLECTION CURVE, FLAT SLAB (F5), POINT D₀

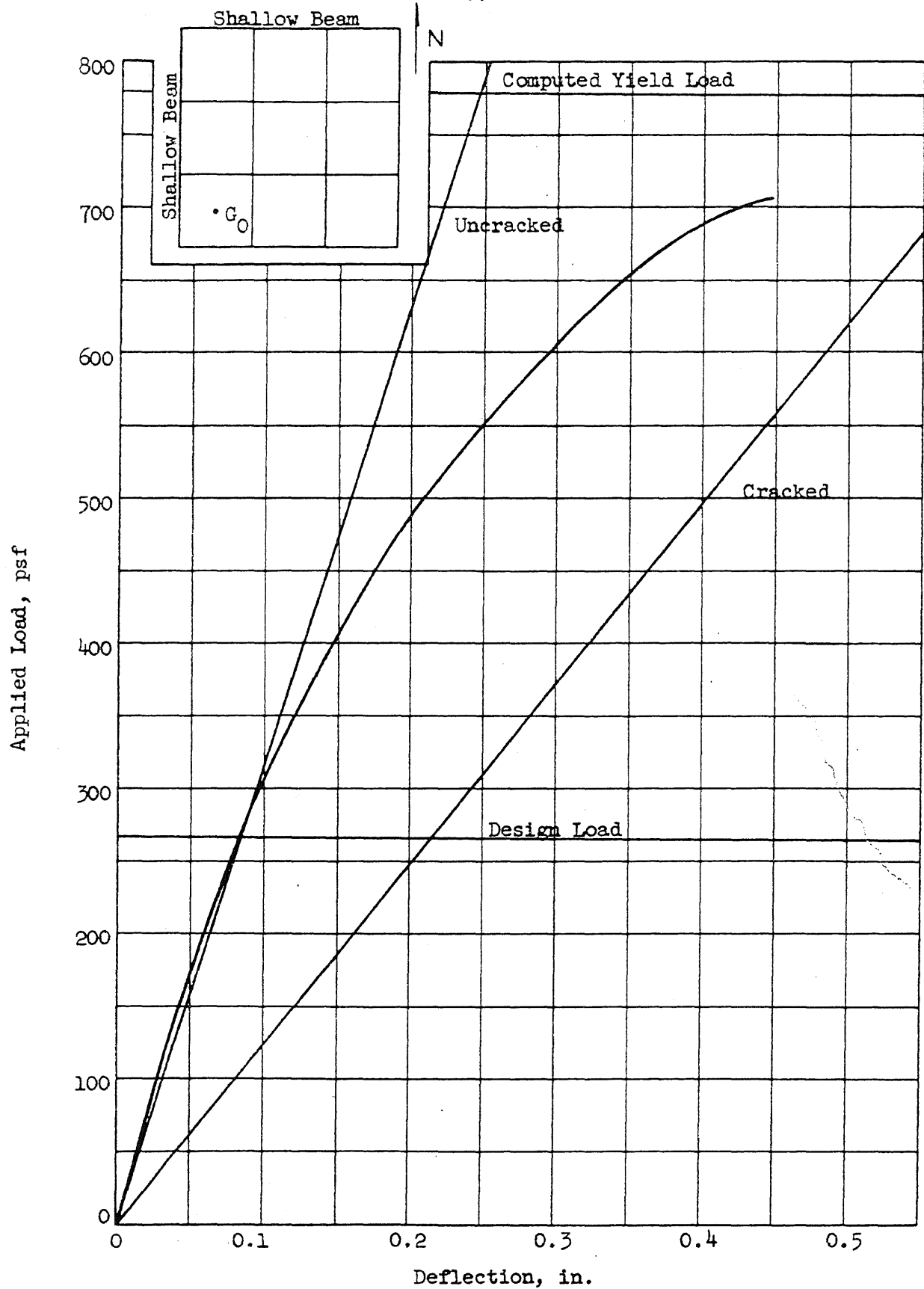


FIG. 5.36 LOAD-DEFLECTION CURVE, FLAT SLAB (F5), POINT G_0

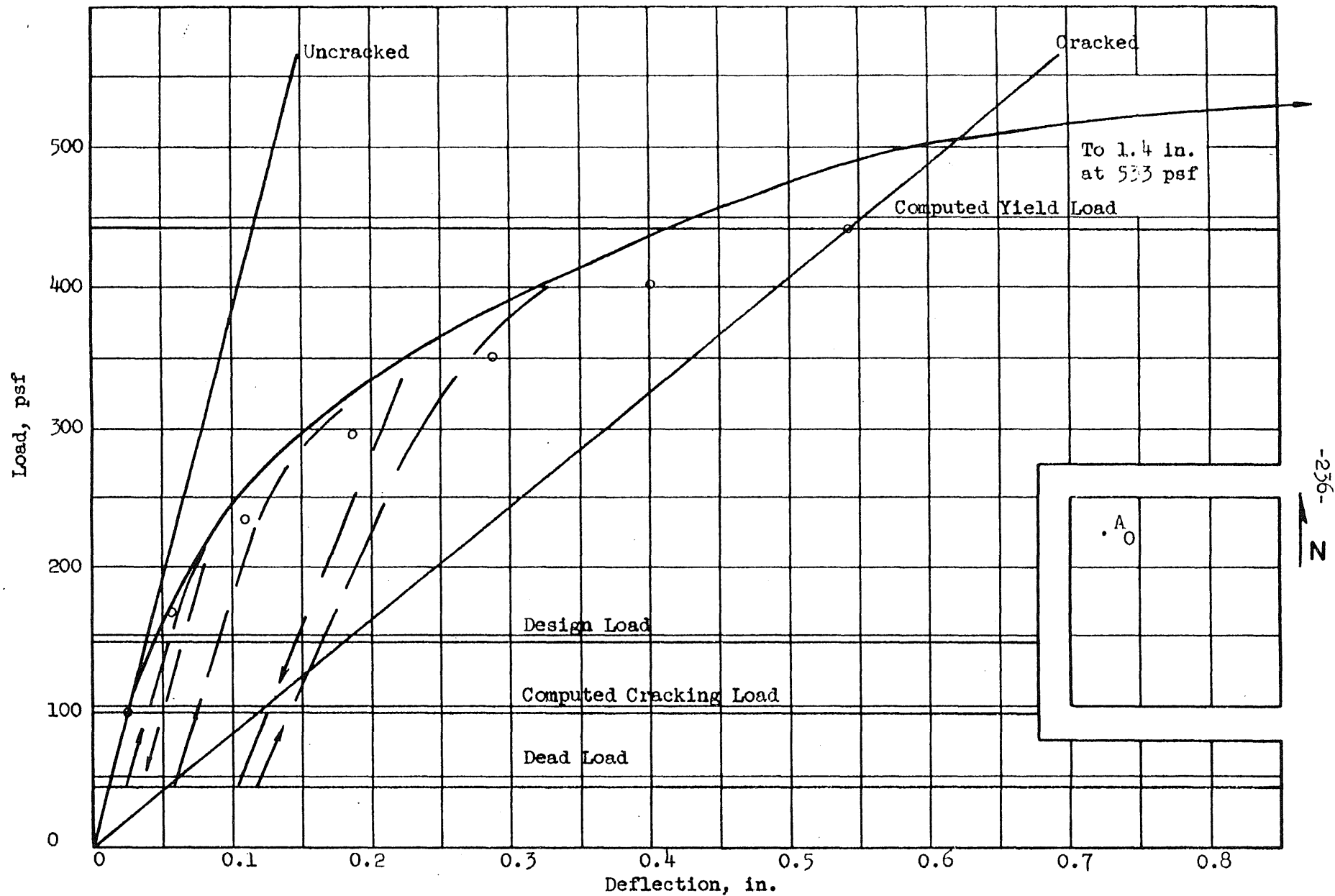


FIG. 5.87 LOAD-DEFLECTION CURVE, TWO-WAY SLAB (T1), POINT A₀

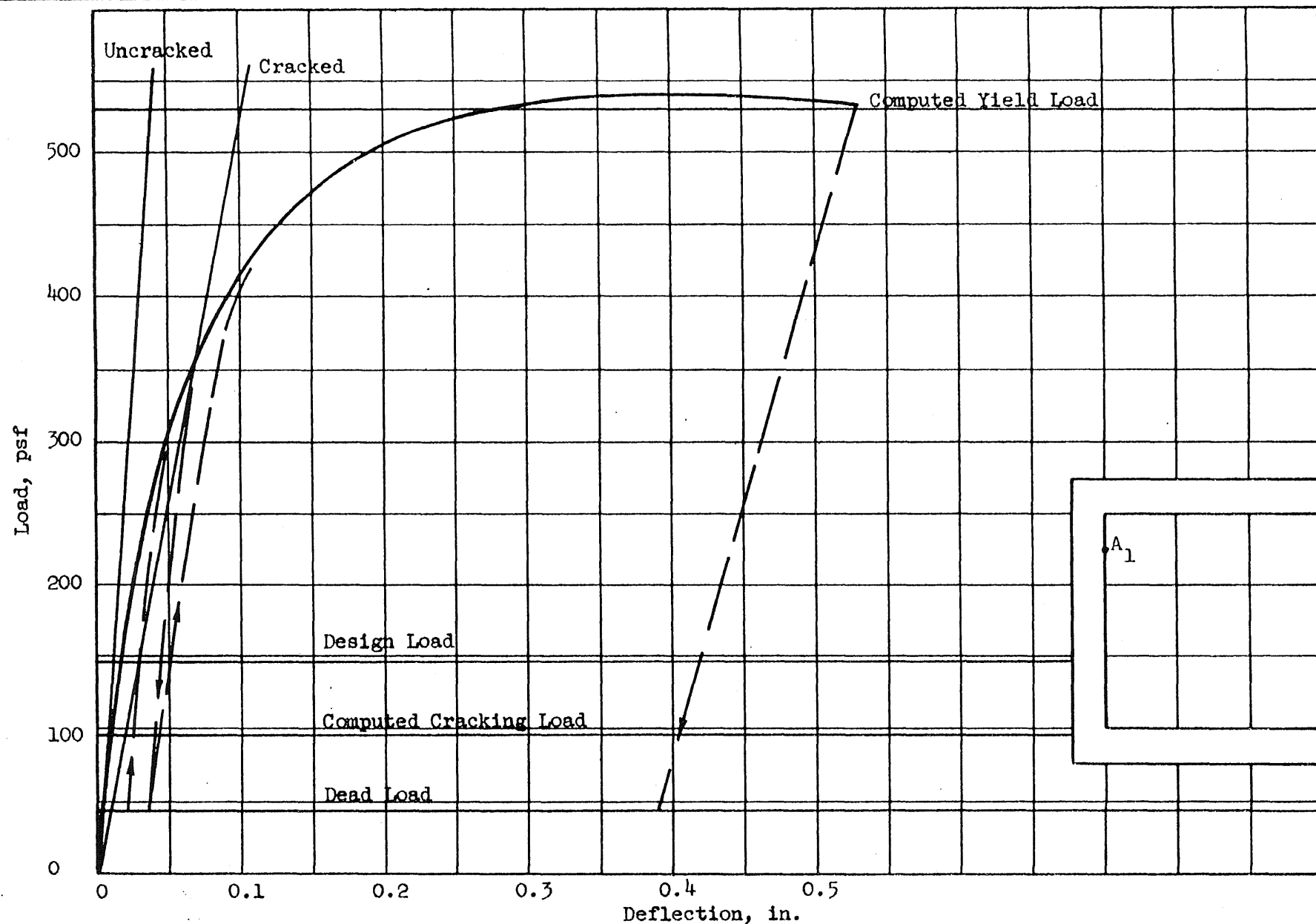


FIG. 5.88 LOAD-DEFLECTION CURVE, TWO-WAY SLAB (T1), POINT A₁

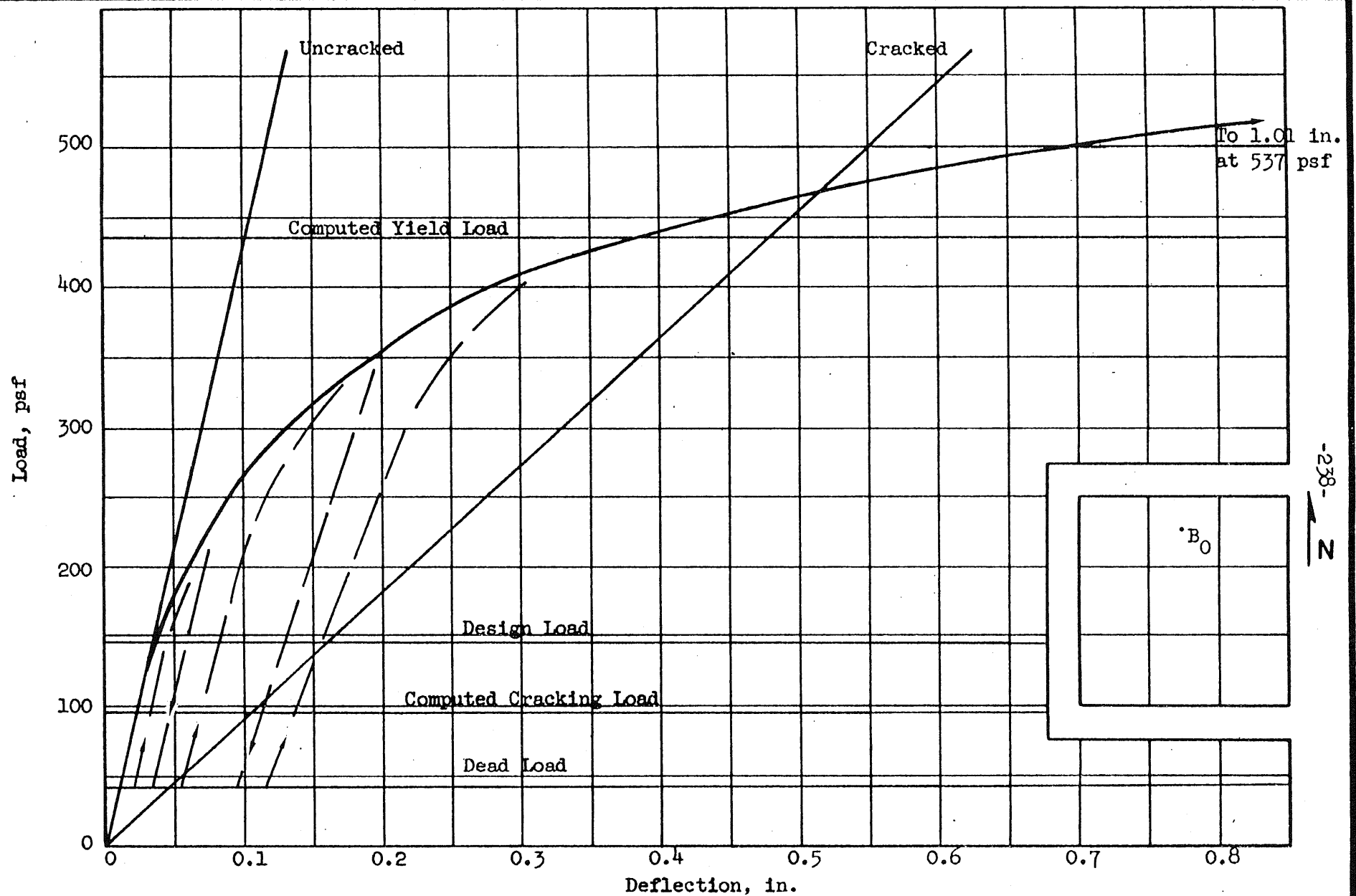


FIG. 5.89 LOAD-DEFLECTION CURVE, TWO-WAY SLAB (T1), POINT B₀

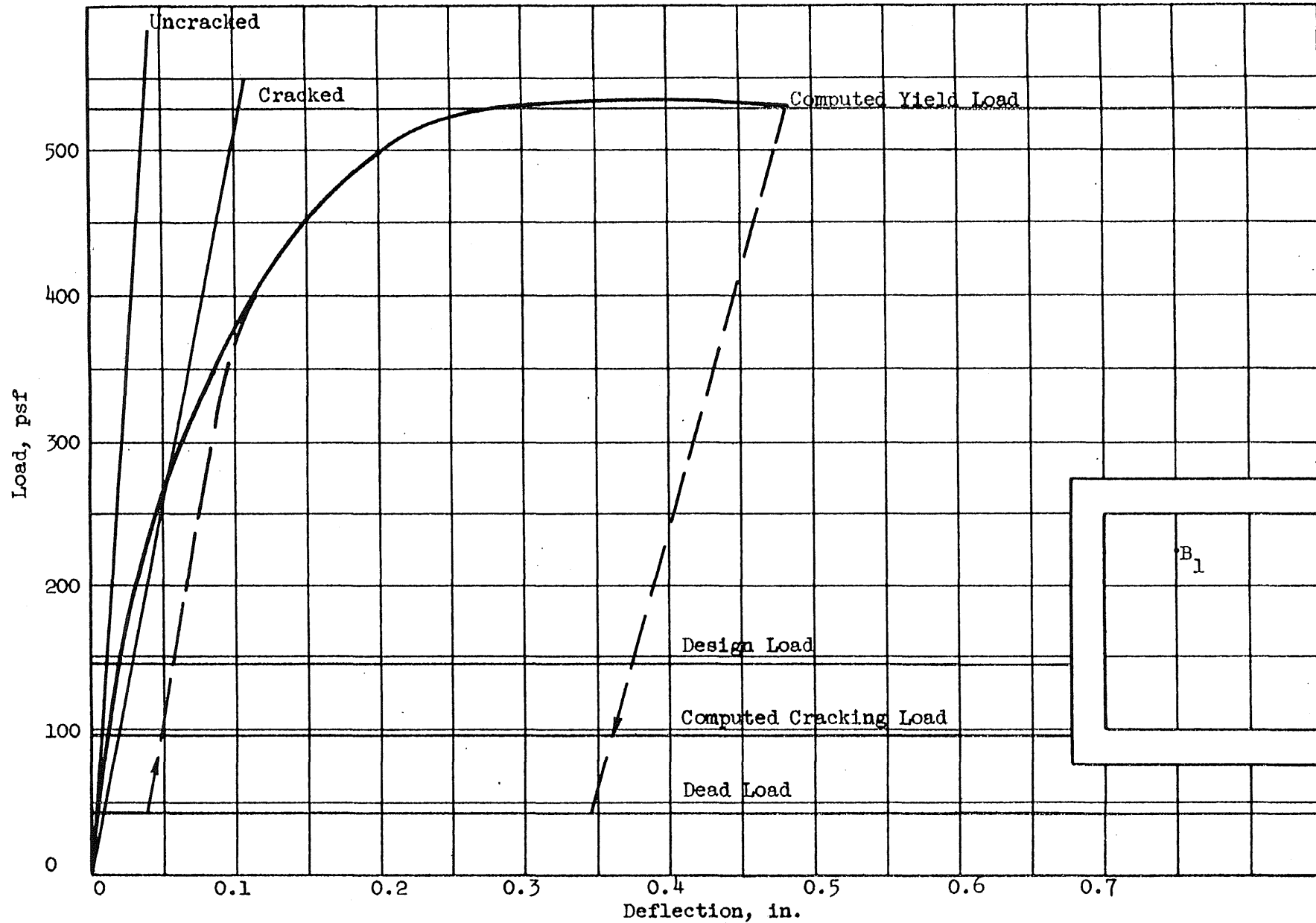


FIG. 5.90 LOAD-DEFLECTION CURVE, TWO-WAY SLAB (T1), POINT B₁

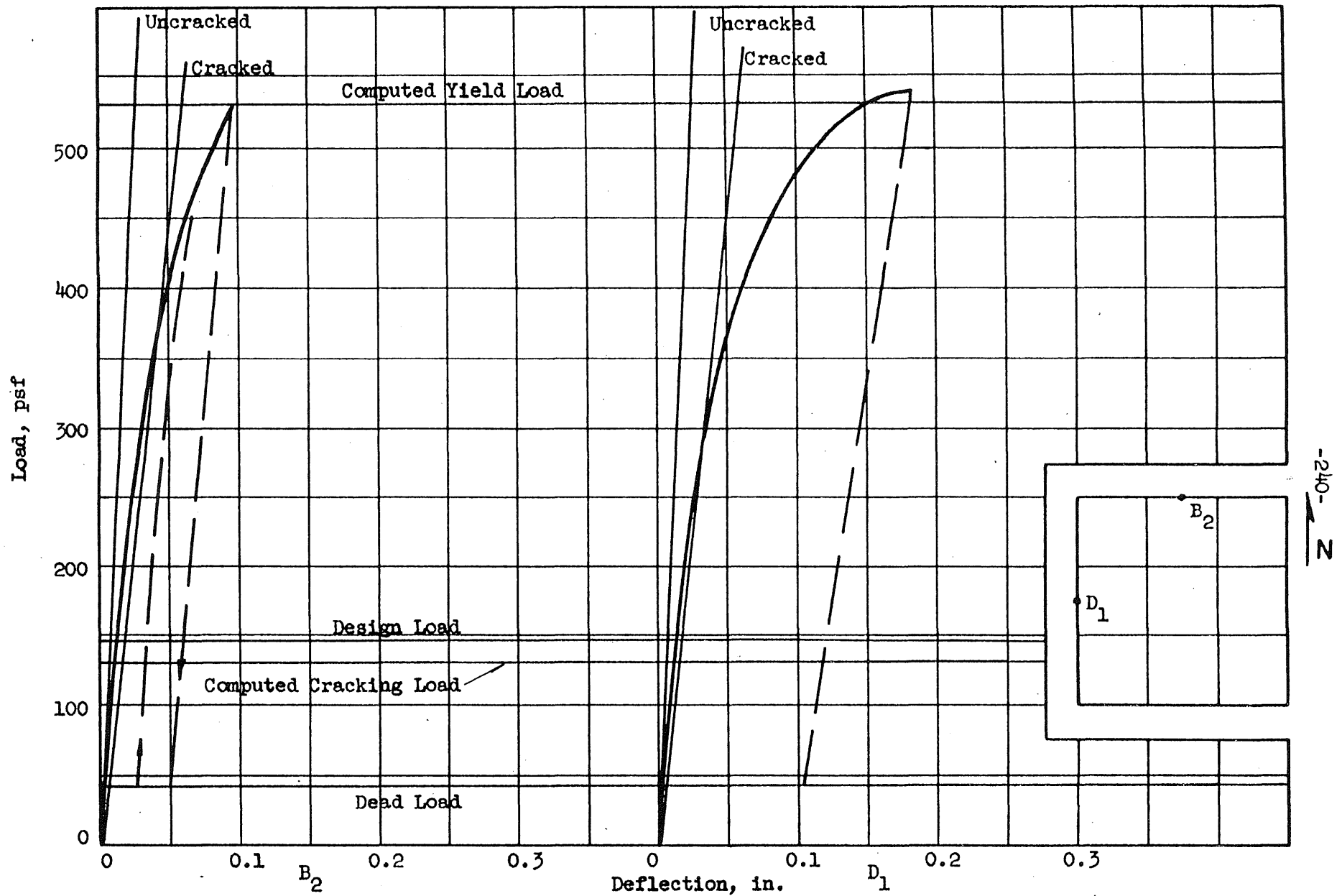


FIG. 5.91 LOAD-DEFLECTION CURVES, TWO-WAY SLAB (T1), POINTS B₂ AND D₁

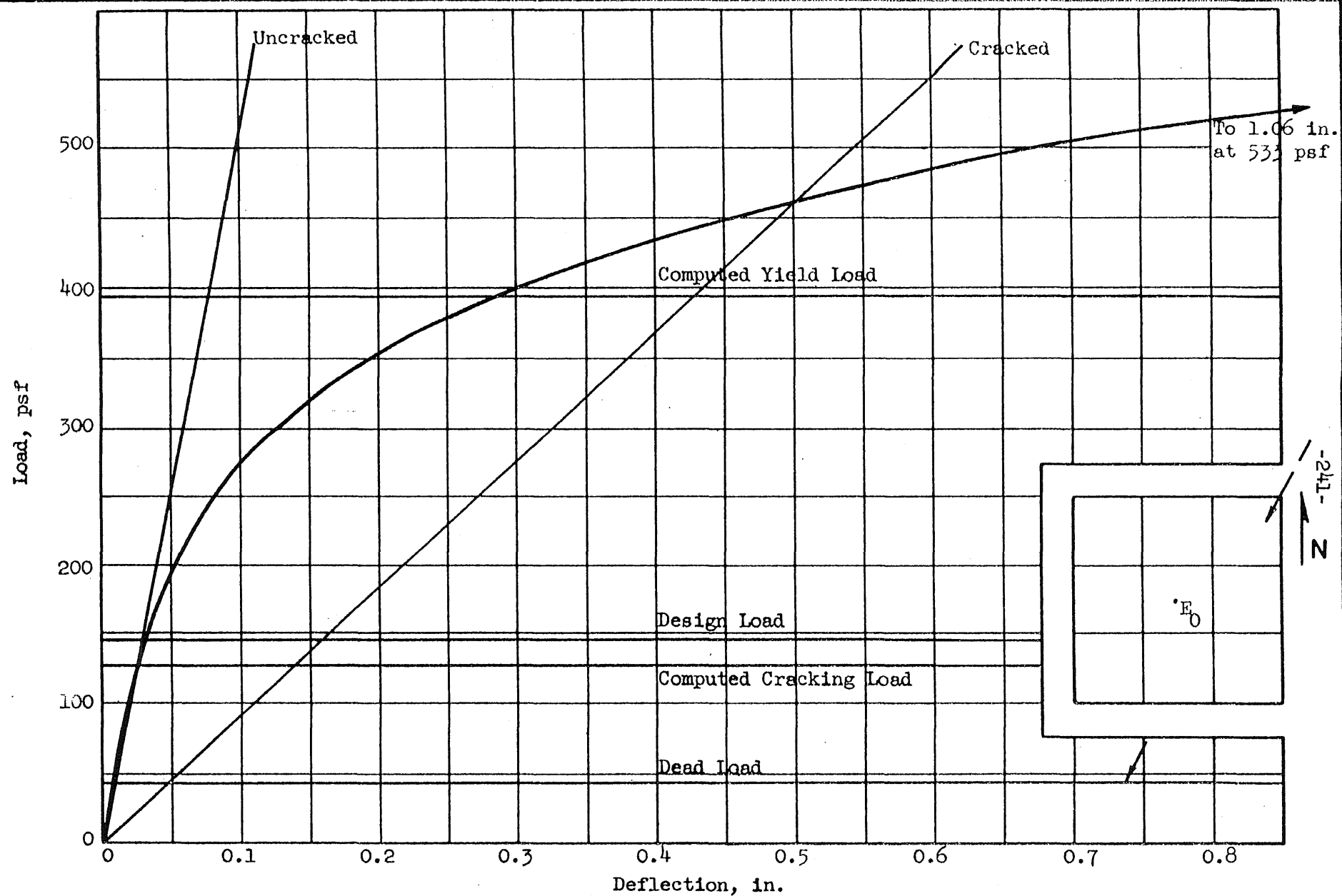


FIG. 5.92 LOAD-DEFLECTION CURVE, TWO-WAY SLAB (T1), POINT E₀

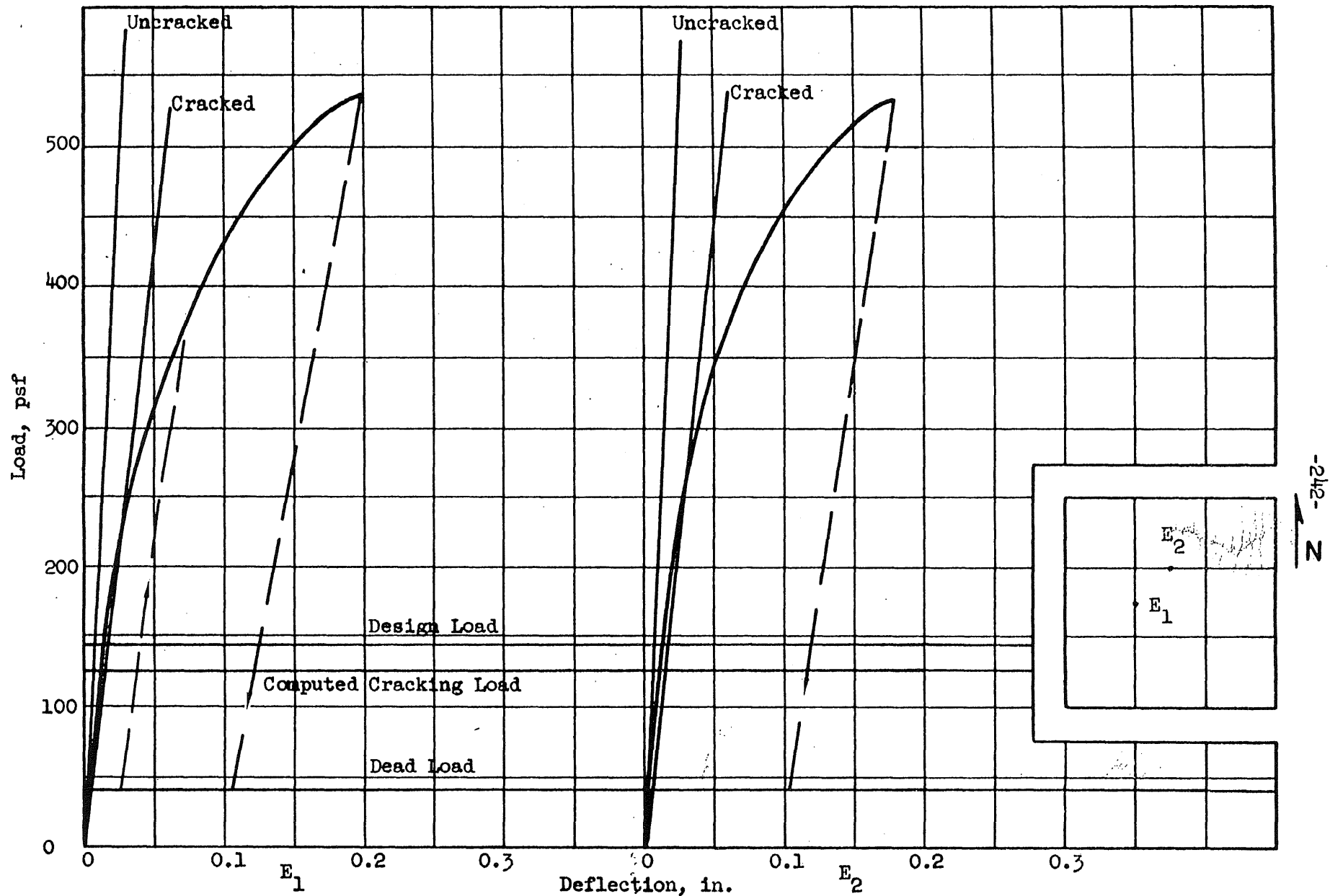


FIG. 5.93 LOAD-DEFLECTION CURVES, TWO-WAY SLAB (T1), POINTS E₁ AND E₂

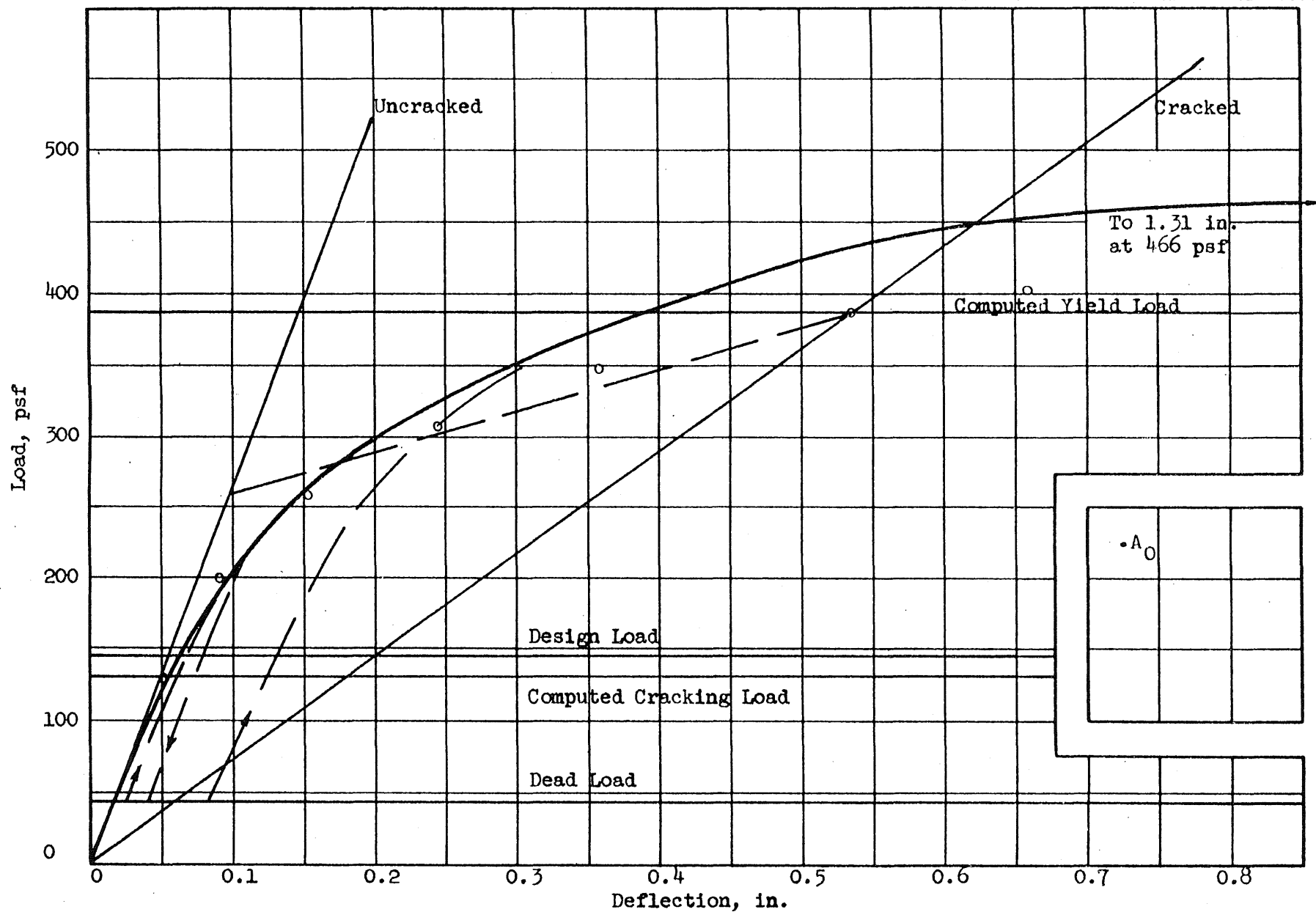


FIG. 5.94 LOAD-DEFLECTION CURVE, TWO-WAY SLAB (T2), POINT A₀

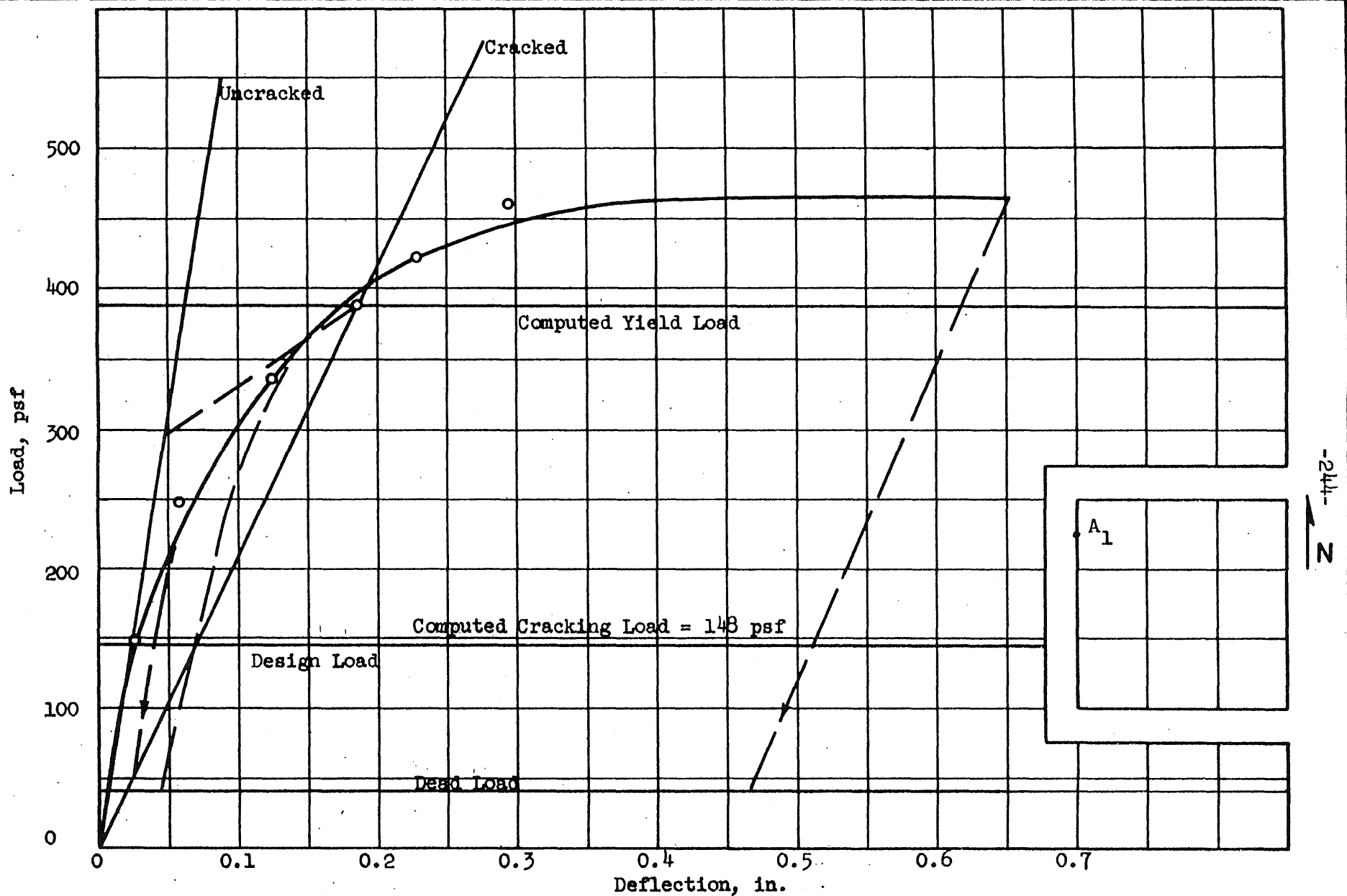


FIG. 5.95 LOAD-DEFLECTION CURVE, TWO-WAY SLAB (T2), POINT A₁

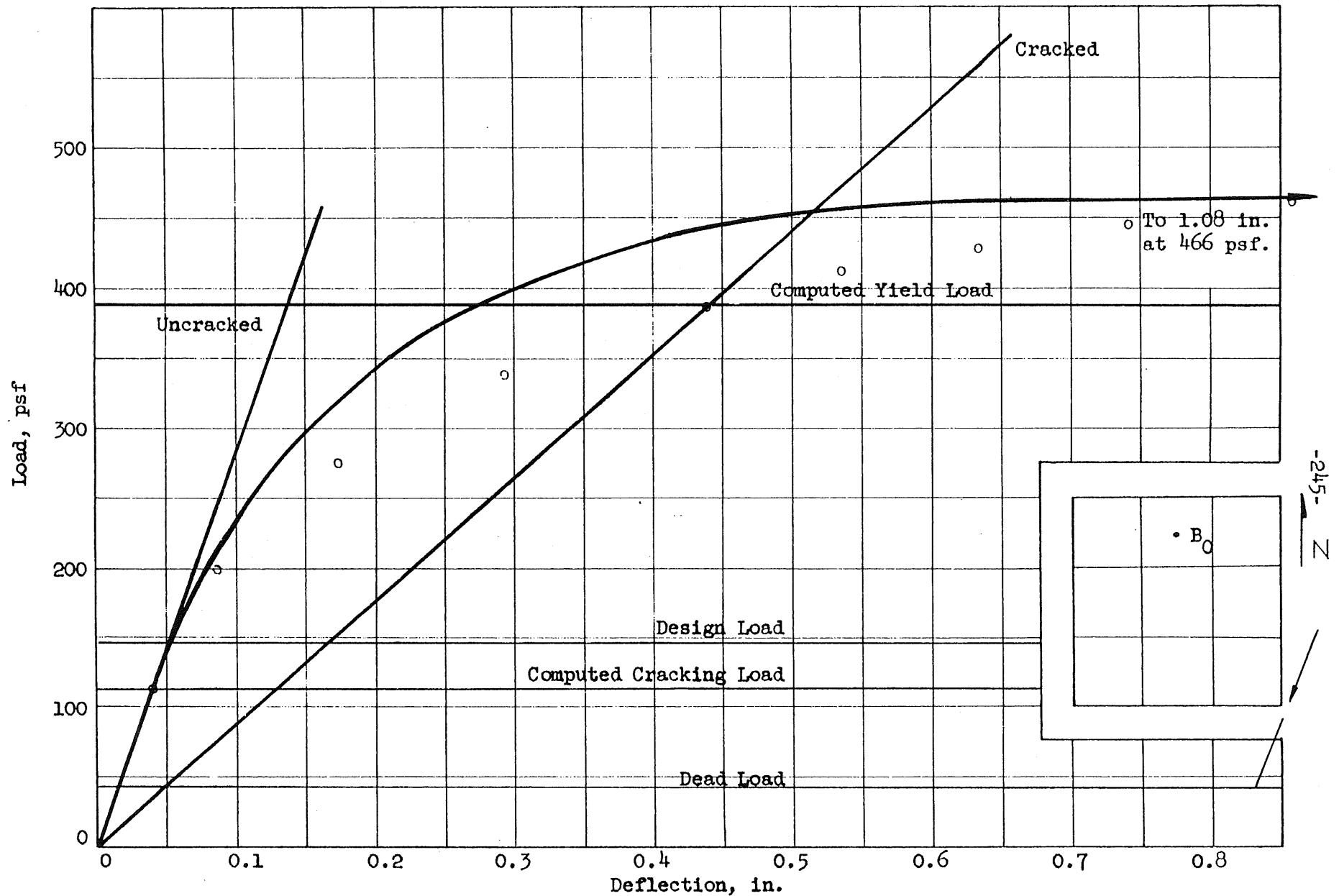


FIG. 5.96 LOAD-DEFLECTION CURVE, TWO-WAY SLAB (T2), POINT B_0

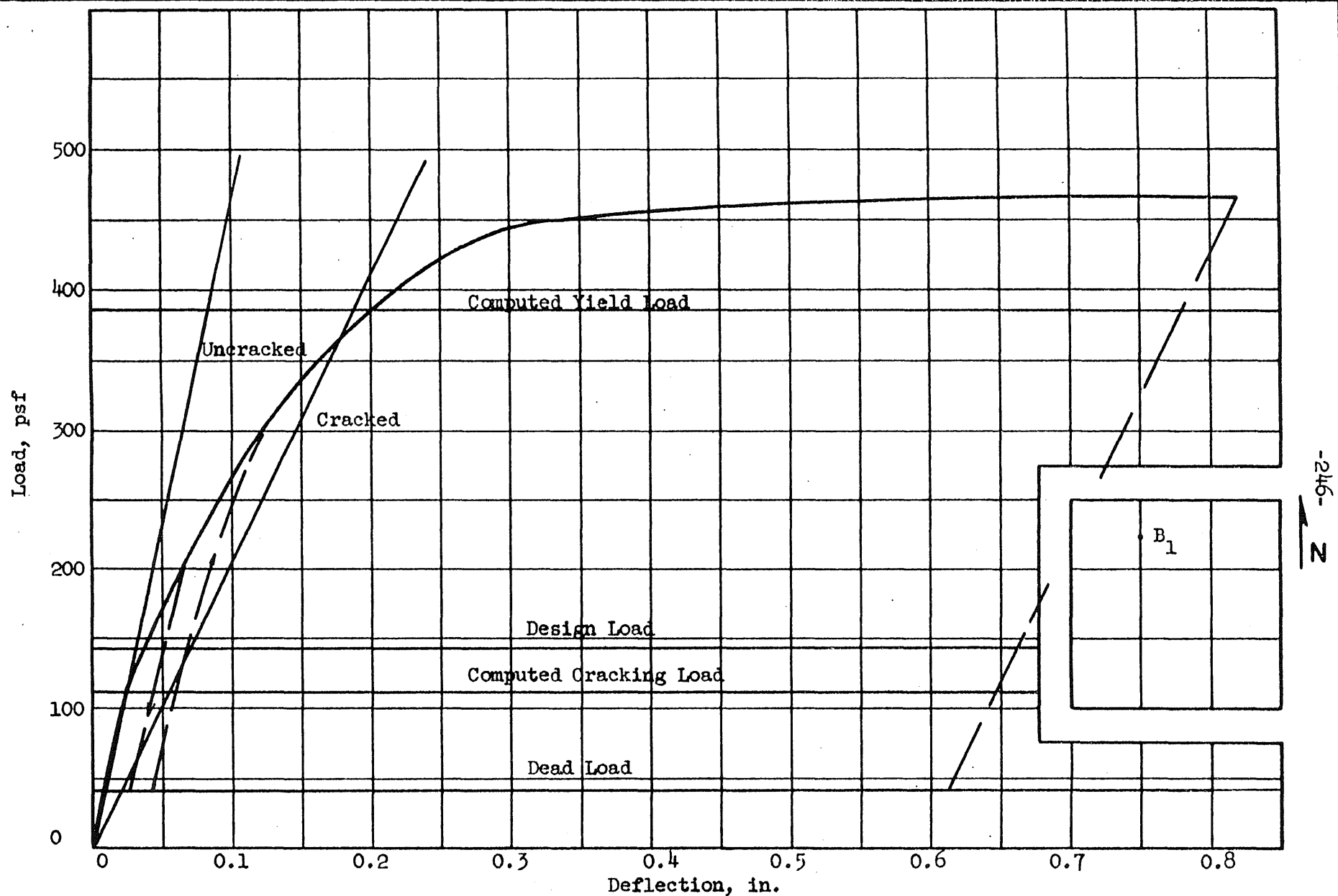


FIG. 5.97 LOAD-DEFLECTION CURVE, TWO-WAY SLAB (T2), POINT B₁

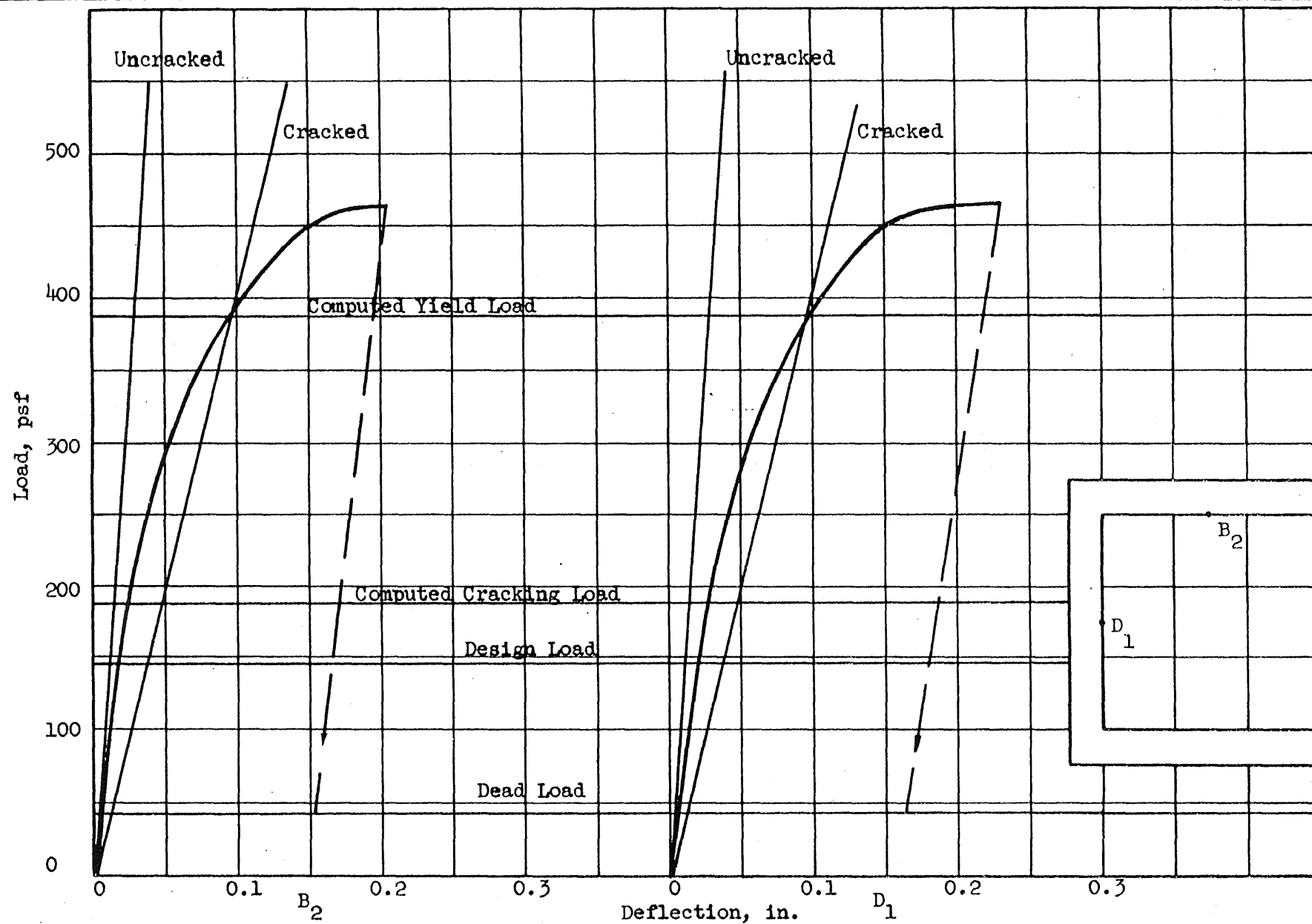


FIG. 5.98 LOAD-DEFLECTION CURVES, TWO-WAY SLAB (T2), POINTS B_2 AND D_1

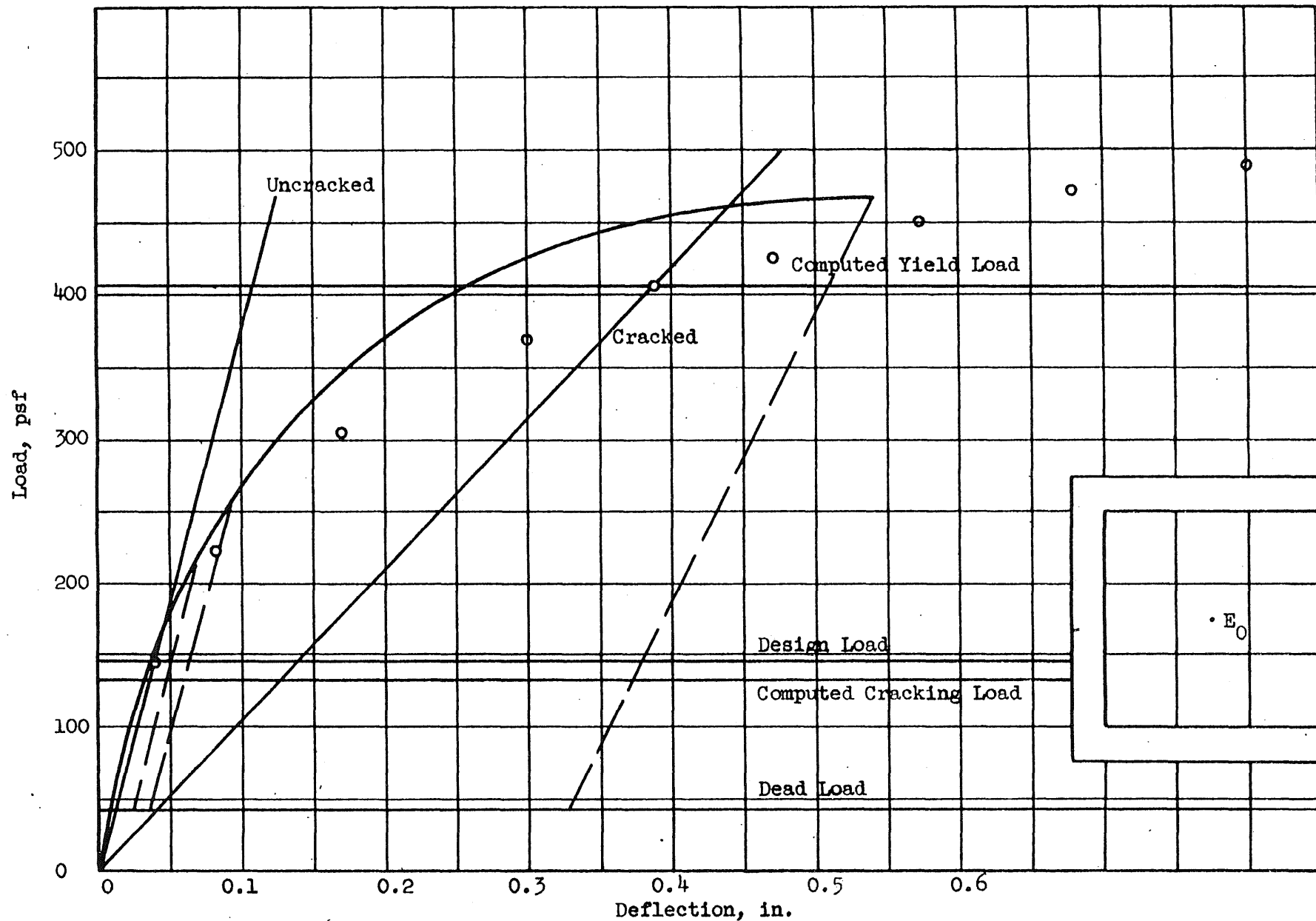


FIG. 5.99 LOAD-DEFLECTION CURVE, TWO-WAY SLAB (T2), POINT E_0

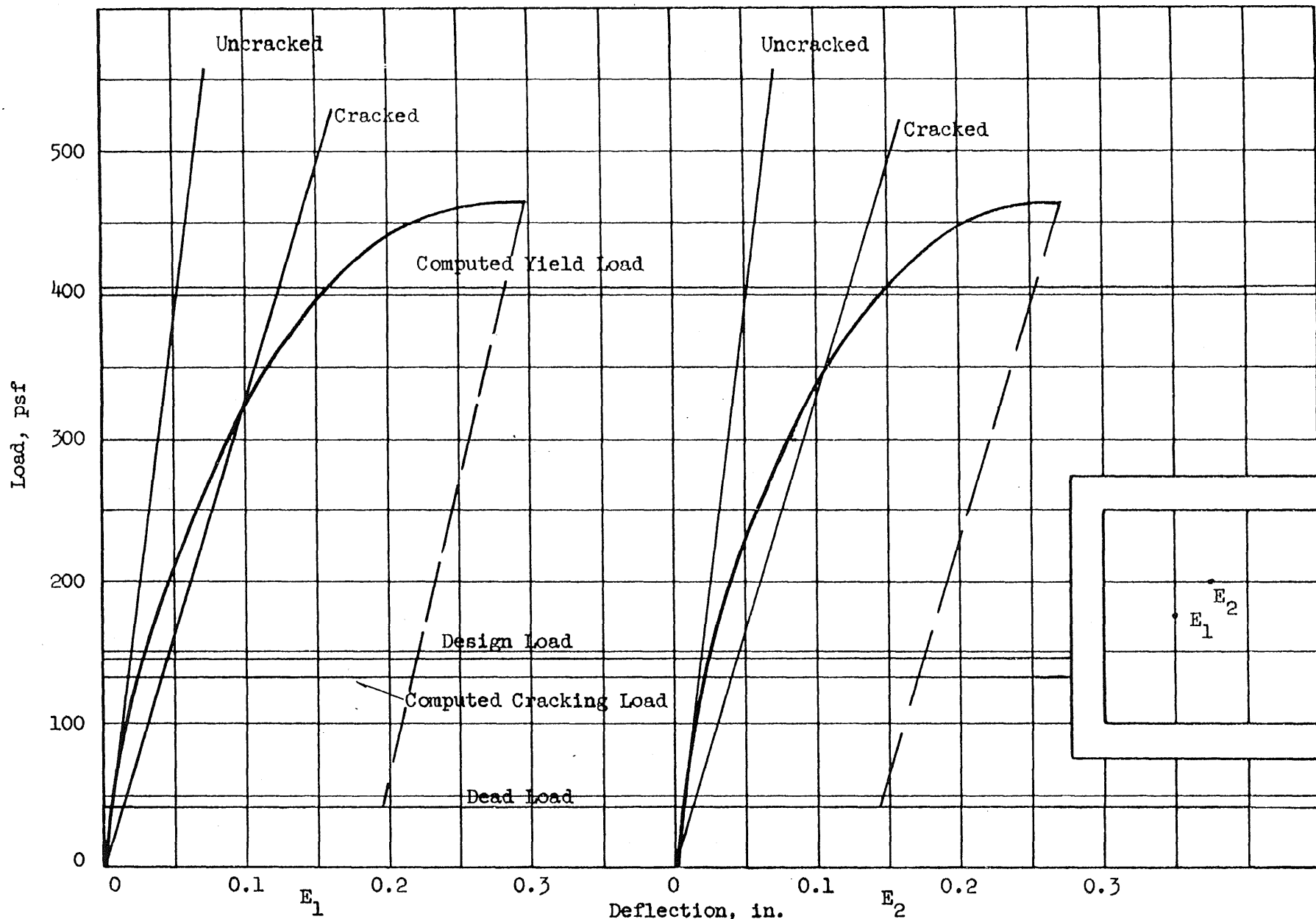


FIG. 5.100 LOAD-DEFLECTION CURVES, TWO-WAY SLAB (T2), POINTS E_1 AND E_2

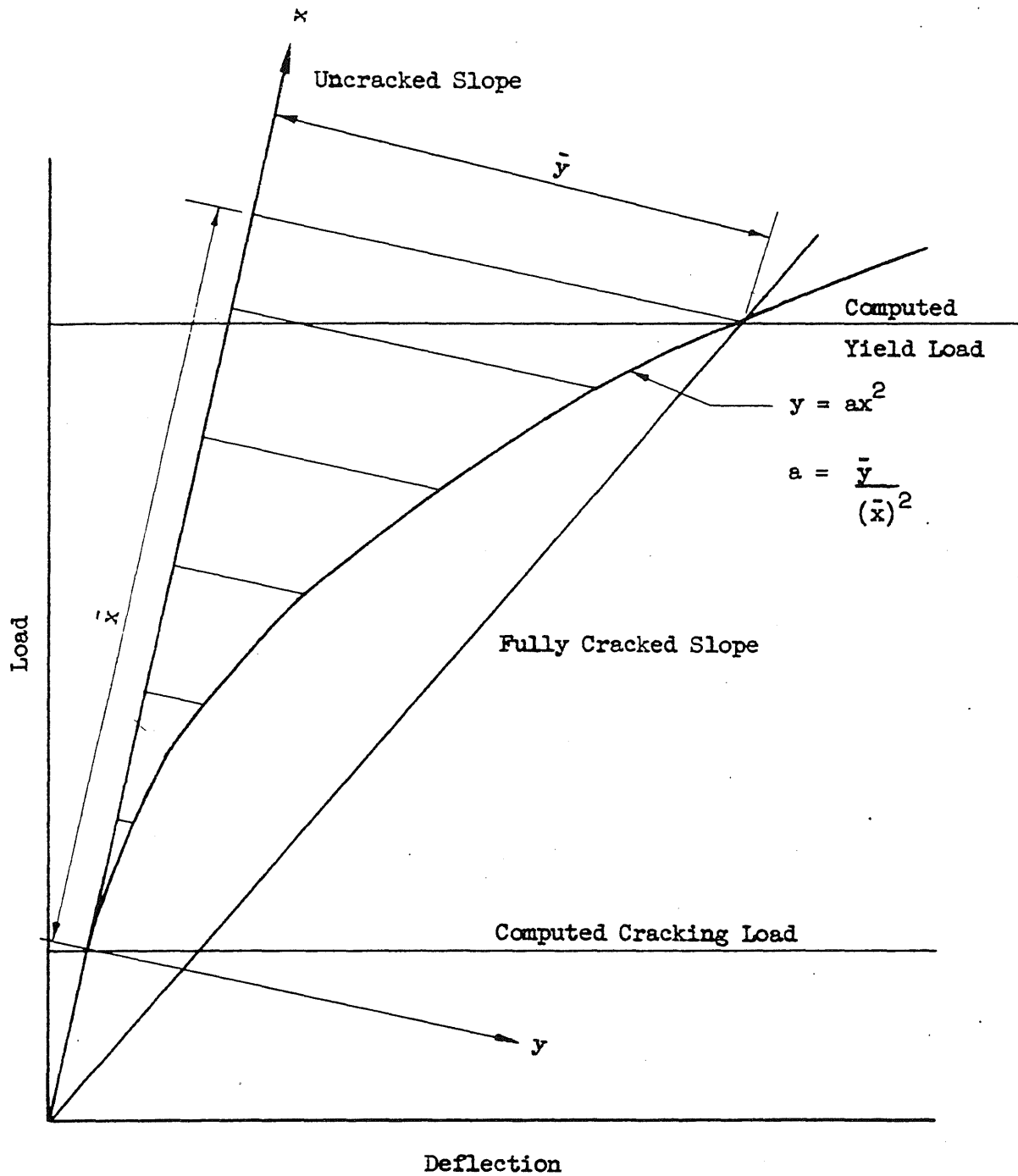
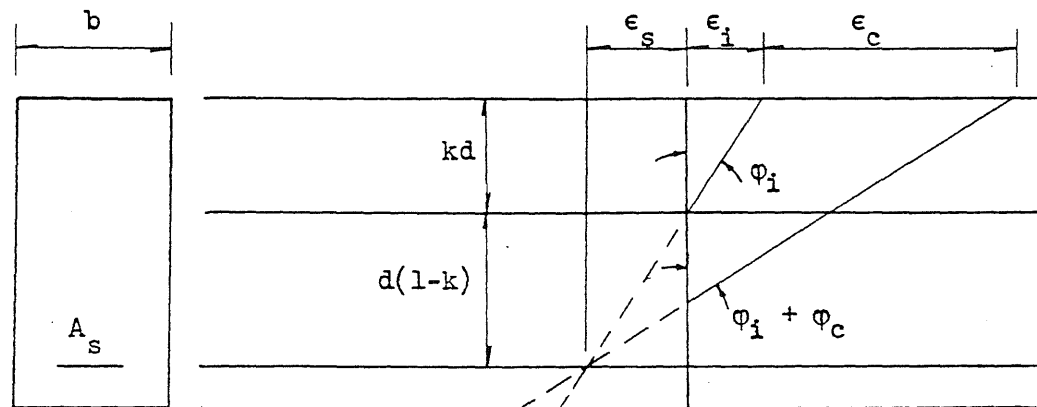
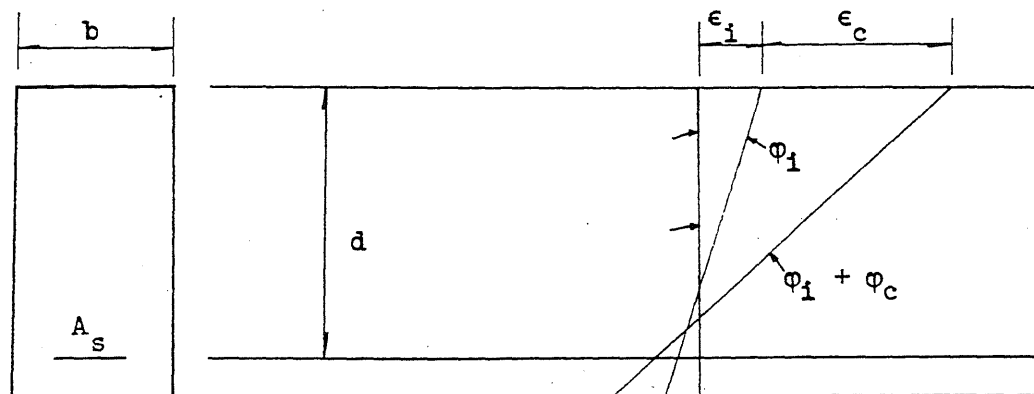


FIG. 5.101 METHOD OF CONSTRUCTION OF PARABOLIC TRANSITION CURVE

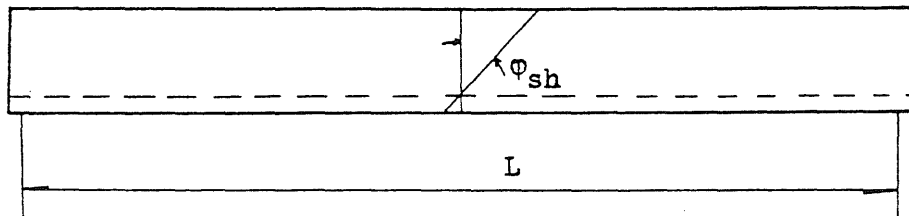


(a) Fully Cracked Section

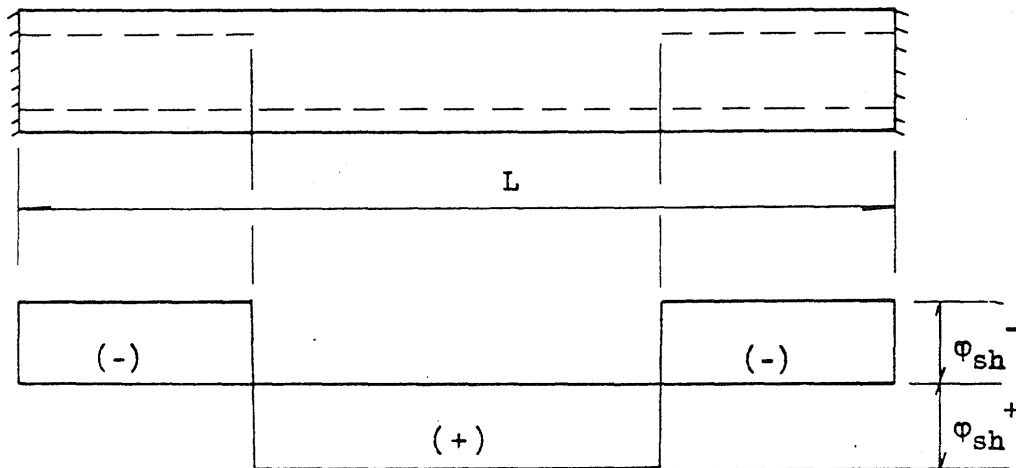


(b) Uncracked Section

FIG. 5.102 STRAIN DISTRIBUTION IN A REINFORCED CONCRETE BEAM

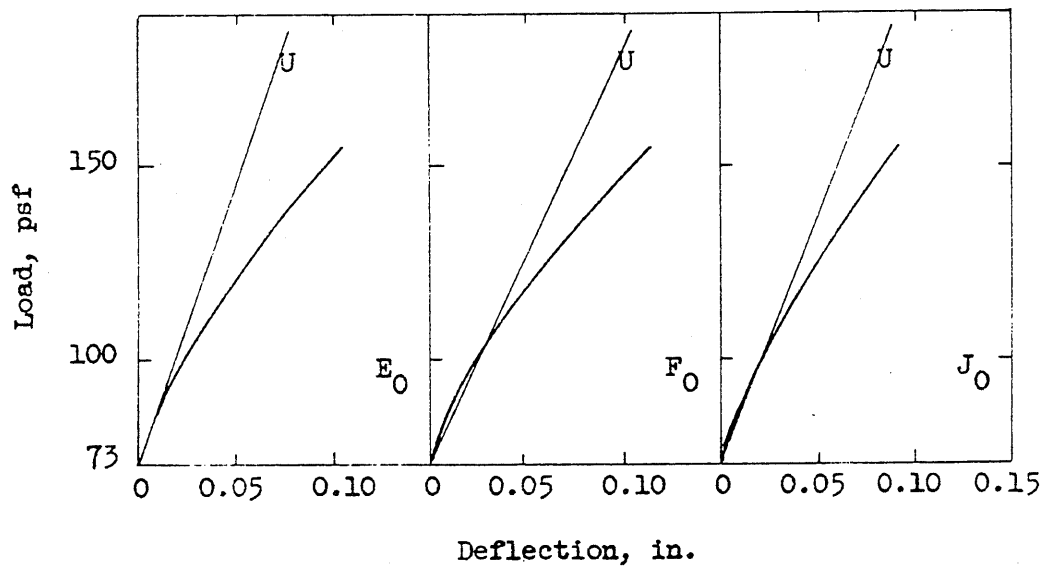
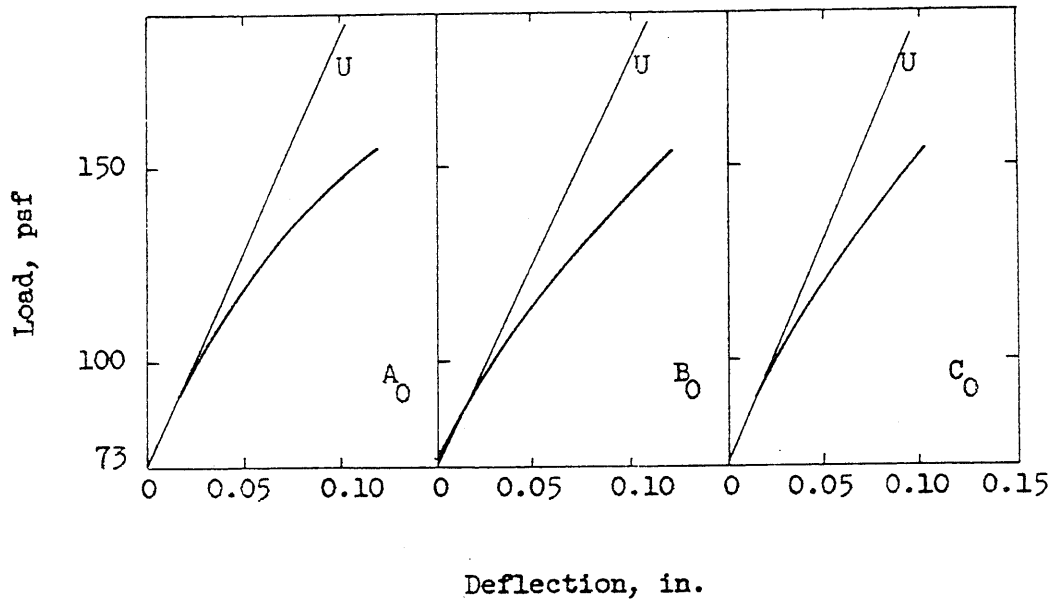


(a) Simply Supported Beam



(b) Fixed-Ended Beam

FIG. 5.103 SHRINKAGE CURVATURE IN REINFORCED CONCRETE BEAMS



Note: Straight lines marked U are slopes predicted on the basis of uncracked sections.

FIG. 5.104 LOAD-DEFLECTION CURVES FOR PCA TEST SLAB

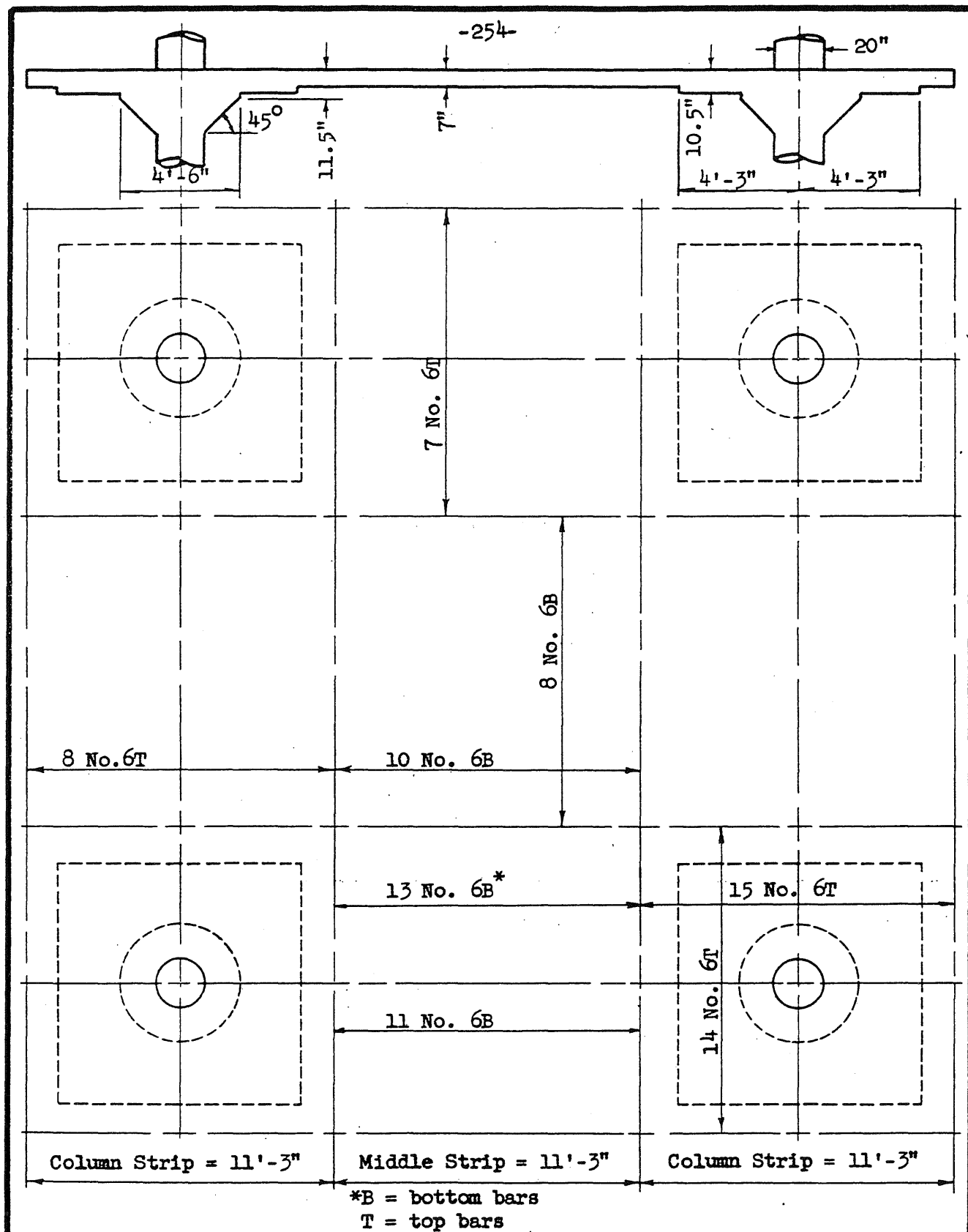


FIG. 5.105 TYPICAL INTERIOR PANEL, STRUCTURE C

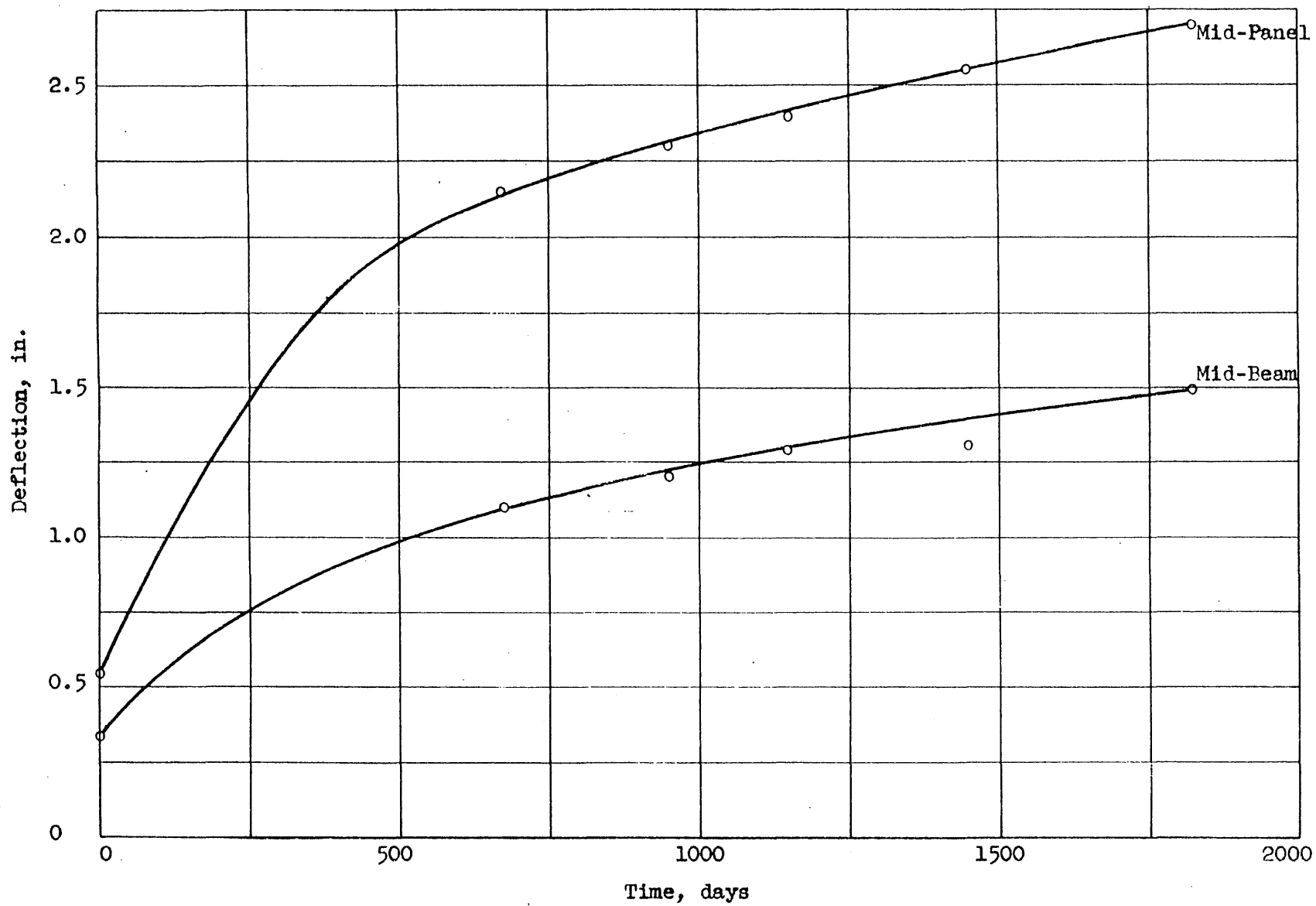


FIG. 5.106 DEFLECTION-TIME CURVES, INTERIOR PANEL, STRUCTURE C

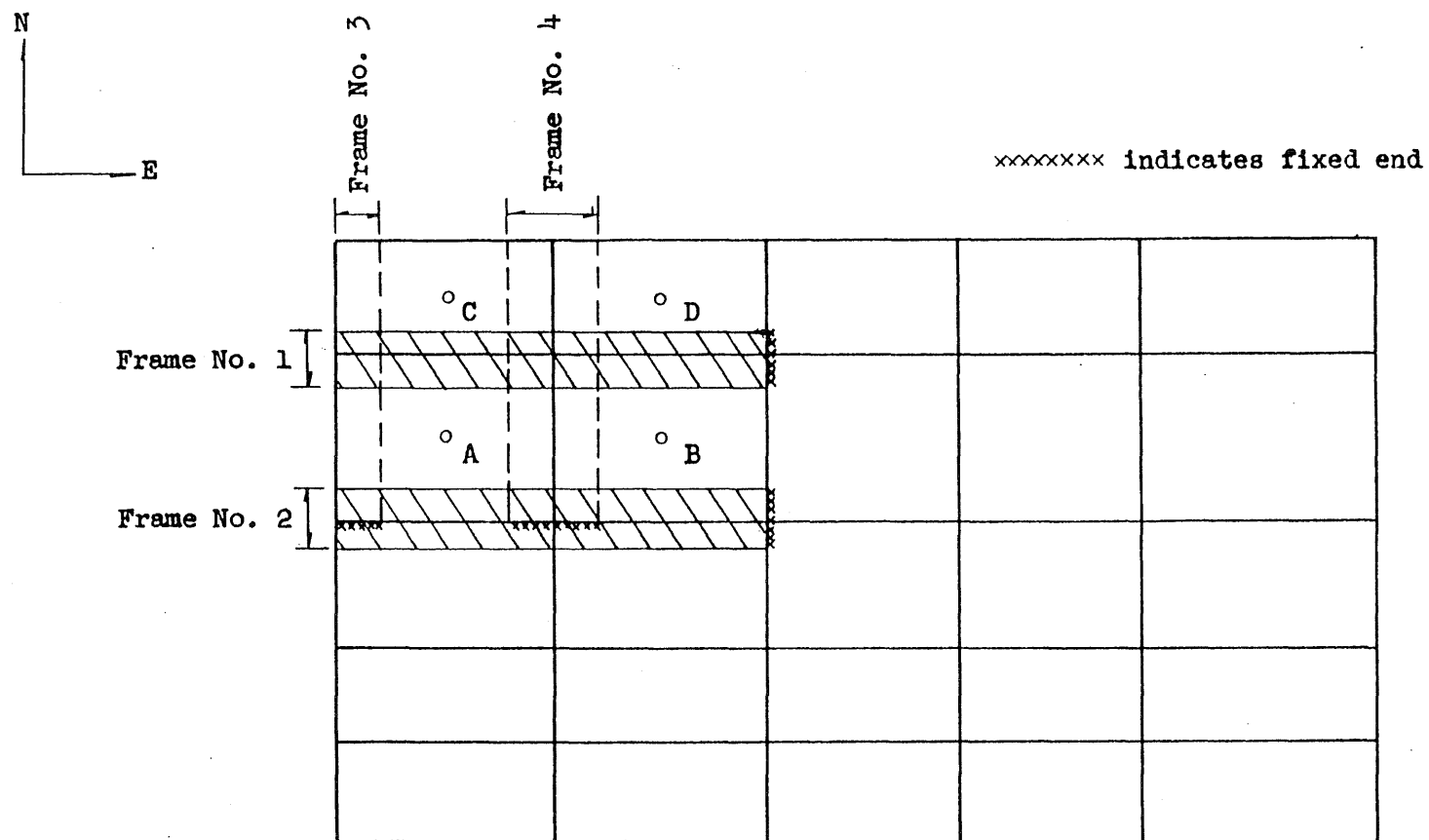


FIG. 6.1 SCHEMATIC LAYOUT OF A TYPICAL NONSYMMETRICAL STRUCTURE

APPENDIX A

EXTRACT FROM FRENCH BUILDING CODE ON DEFLECTIONS

A.1 Introductory Remarks

Material contained in the 1960 French Building Code (22) which pertains to deflections is given below. The French Code is a combined building code and commentary. Article 4.26 and the accompanying commentary discuss the minimum depth of beams. Article 4.36 incorporates Art. 4.26 in a discussion of the minimum allowable thickness of slabs. Portions of Articles 1.22-1.23 and 3.31 are included to clarify points listed in Arts. 4.26 and 4.36.

A.2 Extract on Deflections

Art. 4.26 Minimum Depth of Section

Rule

The deformations of joists and beams must be small enough so that surface coatings, partitions or other construction supported by the concrete members will not be damaged.

Commentary

Of the cases reported in the past few years of concrete structures becoming unserviceable, a large number were attributed to excessive deformations of flexural members.

Two types of difficulties are encountered in attempting to define the required rigidity of flexural members.

a) Uncertainties exist as to what modulus of elasticity and what moment of inertia should be used as well as to the effects of bond and shrinkage.

b) Statistics obtained from the study of failures do not at the present time permit the definition of the ratio of deflection to span, Δ/L ,

or of the absolute value of deflection that should be specified generally. Nor is it possible to define limits which indicate damage to parts of the structure.

The following areas must be considered:

a) Formulas defining minimum depth of slabs and beams for important works are needed.

b) The effects of the continual increases in allowable stresses on serviceability must be considered. These increases are permissible from a standpoint of strength but may result in excessive deformations.

c) Advances in construction procedures which lead to earlier decentering and earlier loading must be considered since these may have the effect of increasing creep.

Generally it may be assumed that for structures to be used as dwellings, schools, or offices it will not be necessary to define the required rigidity for members whose ratio d/L of depth of section to clear span is at least equal to $0.10 (M_t/M_o)$ where M_t is the maximum bending moment in the span, and M_o is the static moment or the maximum bending moment that would exist in the span under consideration, if it were simply supported. The additional stipulation is made that the area A_s of the tensile steel must be such that

$$\frac{100A_s}{bd} \leq \frac{4800}{f_y} \quad (A.1)$$

where b is the width of the flange, d the effective depth of the beam and f_y is the yield point of the reinforcement in kg/cm^2 .

For beams supporting slabs the ratio d/L must be at least $1/16$ regardless of the relative value of M_t .

If these conditions are not fulfilled then the following procedure may be used. Assume that for a simply supported beam of span L having a

constant cross section the mid-span deflection Δ_{t1} caused by instantaneous loads is equal to the sum of the deflection Δ_i caused by the instantaneous loads and the deflection Δ_1 caused by the long time loads. Thus

$$\Delta_{t1} = \Delta_i + \Delta_1 \quad (A.2)$$

The deflections are computed from the following relationships:

$$\Delta_i = \frac{L^2}{10dE_s\theta} \left[f_{si} + 15f_{ci} \right] \quad (A.3)$$

$$\Delta_1 = \frac{L^2}{10d} \left[0.000125 + \frac{1}{\theta} \left(\frac{f_{s1}}{E_s} + \frac{2.5f_{c1}}{E_{c1}} \right) \right] \quad (A.4)$$

where d = effective depth at the point of maximum moment,

E_s = modulus of elasticity for steel = 2,100,000 kg/cm²,

E_{c1} = modulus of elasticity for concrete (see Section 3.312),

f_{si} , f_{ci} = steel and concrete stresses under short time loading,

f_{s1} , f_{c1} = steel and concrete stresses under long time loading.

The term θ is taken as 1.00 when the percentage of steel $p = 100A_s/bd$ is greater than $0.25[5-f_y/2400]$. Otherwise

$$\theta = 2 - \left[\frac{4p}{5-f_y/2400} \right] \quad (A.5)$$

where p is the percent of reinforcement and f_y is the yield point of the reinforcement in kg/cm². For calculating Δ_1 the ratio f_{c1}/E_c shall not be taken as less than 0.00012θ .

For continuous or for fixed elements the deflection Δ at the center of the span considered shall be taken as

$$\Delta = \Delta_t + 0.5(\Delta_w + \Delta_e) \quad (A.6)$$

The terms Δ_t , Δ_w , and Δ_e are obtained by using Eqs. A.3 and A.4. The

deflection Δ_t is computed by replacing L by the distance L' between the points of inflection. In order to compute the deflection Δ_w (or Δ_e) replace L by $2a_w$ (or $2a_e$), where a_w (or a_e) designates the distance from the left (or right) support to the adjacent point of inflection.

The stresses f_{si} , f_{sl} , f_{ci} , f_{cl} are in each case the maximum stress in the steel and concrete under the action of the instantaneous loads or of the long-time loads in the fictitious span of length L' for Δ_t , in the left support for Δ_w and at the right support for Δ_e , and d is the effective depth in the span or at the supports according to the case considered.

For a cantilevered span of length L , the deflection at the free end is:

$$\Delta = \frac{L^2}{5d} \left[\frac{f_{si} + 15f_{ci}}{\theta E_s} + 0.000125 + \frac{1}{\theta} \left(\frac{f_{sl}}{E_s} + \frac{2.5f_{cl}}{E_{cl}} \right) \right] \quad (A.7)$$

The stresses are those in the steel and concrete at the section of effective depth d at the support and the length L is taken as the clear span.

The major difficulty lies in fixing the value of the allowable deflection-to-span ratio. This should be mainly a function of the type and use of the members. An approximate guide for admissible deflection-to-span ratio for elements supporting walls, partitions and fragile fixtures is $1/500$.

For large spans $1/500$ may not be a sufficient restriction and an absolute value of deflection may have to be specified, in order to reduce the risk of cracking of partitions.

Art. 4.36 Minimum Thickness of Slabs

4.360

Rule Deflections must be small enough that partitions etc., are not damaged.

Commentary

The methods of Art. 4.26 may be used for slabs.

If the following two conditions are met then deflections need not be considered.

a) Let M_x and M_y be the maximum unit bending moments in a simply supported slab of spans L_x and L_y . (M_x is assumed larger than M_y .) Let M_t be the unit moment in the x direction taking into account the effects of fixity and/or continuity. ($M_t \geq 0.75 M_x$). Then if the ratio d/L_x is equal to or greater than $\frac{1}{20} \frac{M_t}{M_x}$ the deflection is not considered objectionable.

b) Let A_s be the cross-sectional area of the tensile reinforcement for a width b , d the effective depth, and f_y the elastic limit of the reinforcement. Then the maximum percentage of steel $p = 100A_s/bd$ must be less than $.8 \times 2400/f_y = 1920/f_y$ where f_y has units of kilograms per square centimeter.

4.361

Rule Slabs cast in place should have a minimum thickness of 4 cm when they are constructed monolithically with beams or have an equivalent support. Otherwise, their minimum thickness should be 5 cm.

4.362

Rule Slabs prefabricated in shops must have a thickness at least 75 per cent of the above.

Note: The above regulations may be governed by rule 3.03 governing the testing of prefabricated members.

Art. 3.31 Modulus of Longitudinal Deformation

3.311 $E_s = 2,100,000 \text{ kg/cm}^2 [= 29,840,000 \text{ psi}]$

3.312

Unless special measures are taken, the longitudinal modulus of deformation of concrete, expressed in kg/cm^2 shall be taken as

$$E_{cl} = 7,000 \sqrt{f_j}$$

for permanent loads and as

$$E_{ci} = 21,000 \sqrt{f_j}$$

for loads remaining on the structure for 24 hours or less. The term f_j is the concrete strength at an age of j days (kg/cm^2).

These values can be used when the stresses do not exceed the limits fixed in Section 2.

If only the 28-day strength is available, one may assume that the values of E_1 and E_1 are those determined from f_{28} , increased by 20% for class 250/315 concretes and by 10% for class 315/400 and 355/550 concretes.

Art. 1.22 Class of Cement

The present code and commentary assumes the use of concretes containing cements of class 250/315*.

Other classes may be used if they present the characteristics requisite for the construction for which they are employed.

Art. 1.23 Proportion of Cement

The minimum amount of cement is used, in kg/m^3 , should not be less than $550 \sqrt[5]{c_g}$ where c_g is the minimum dimension of the aggregate.

* Note: The two numbers used in referring to a particular class of cement represent the cube compressive strengths in kg/cm^2 , at 7 and 28 days of age respectively, for a standard mortar mixture. The standard mortar mixture is prepared using the cement under consideration and sands of specified sizes.

APPENDIX B
DESCRIPTION OF COMPUTER PROGRAM

B.1 Introductory Remarks

This appendix contains a description of the computer program used in the investigation of the effects of finite column sizes upon deflections and bending moments for typical interior panels.

The program contained a main program and two sub-programs. The main program generated N simultaneous equations by applying a finite difference operator to N points on the plate. The first sub-program solved for the N unknowns, in this case the deflections at the N points, by triangulation of the matrix. The second sub-program used the N deflections in computing bending moments at each point in the orthogonal directions defined by the two centerlines of the plate. As a typical interior plate, which is one of an array of similar uniformly loaded plates, is symmetrical about both centerlines it was necessary to consider only one-fourth of a plate for purposes of analysis.

The program was coded in FORTRAN. Tables 10 - 12 were prepared using the Control Data Corporation No. 1604 electronic digital computer to execute the program. The remainder of Tables 7 - 15 were prepared using the IBM 7090. An off-line IBM 1401 was used to transfer the program and input data from cards to magnetic tape for input and for printing the output.

A description of the input data is given in Section B.2. The finite difference operator that was used is discussed in Section B.3. The flow diagrams are described in B.4. Output data and estimated running time are discussed in B.5. The validity of the program is shown in B.6 and the availability of the program is given in B.7.

B.2 Input Data

The three variables considered were the aspect ratio, the ratio of column size to panel size, and the ratio of beam to plate rigidity. The program was coded so that the length of the long side of a panel remained constant and only the length of the short side varied. The columns were taken as being square in cross section. Thus only the ratio of column width to the length of the long side of the panel or c/L ratio was required in the input data to define the column size. Parallel beams were assumed to have equal moments of inertia. The ratio of beam rigidity in the short direction to that in the long direction was taken as constant. Thus only one input parameter defining rigidity was required.

One input data card was prepared for each case considered. The first word contained the length of one-half of the short side, the second contained the c/L ratio and the third contained the H_L ratio.

B.3 Finite Difference Operator

For an interior panel, which is one of an array of similar uniformly loaded panels, there is no rotation of the edges of the panel. Thus the flexural stiffnesses of the columns and torsional stiffnesses of the beams have no effect and only the plate and beam rigidities need be considered in making an analysis.

The general pattern of the finite difference operator for a point on a beam is shown in "molecule notation" in Fig. B.1. This pattern is symmetrical about the point of application. The term H' is defined as

$$H' = \frac{EI}{Dh} \quad (B.1)$$

where $h = L/n$ = the spacing between grid lines or node points. A value of

$n = 20$ was used in coding the program. For a point not falling on a beam the H' terms in Fig. B.1 would be eliminated.

The ratio between the moment of inertia of a beam in the short direction to that in the long direction was taken as one of three constant values. These constant relationships were

$$I_S = I_L \quad (B.2a)$$

$$I_S = \left[\frac{S}{L} \right] I_L \quad (B.2b)$$

$$I_S = \left[\frac{S}{L} \right]^2 I_L \quad (B.2c)$$

From the definitions of H_S and H_L and equations B.1 and B.2 the following relationships are found:

$$H'_S = \frac{EI_S}{Dh} = \frac{EI_S n}{DL} = nH_S \quad (B.3)$$

$$H'_L = \frac{EI_L}{DL} = \frac{EI_L}{DSR} = \left[\frac{n}{R} \right] H_L \quad (B.4)$$

$$\frac{H'_S}{H'_L} = \left[\frac{I_S}{I_L} \right] \left[R \right] \quad (B.5)$$

where $R = S/L$.

The portion of the operator falling on a beam is given in Fig. B.1 as

$$\boxed{1+H'} \text{ --- } \boxed{-8-4H'} \text{ --- } \boxed{20+6H'} \text{ --- etc.} \quad (B.6)$$

This may be rewritten as

$$\boxed{1+nH} \text{ --- } \boxed{-8-4nH} \text{ --- } \boxed{20+6nH} \text{ --- etc.} \quad (B.7)$$

It was desired to use only values of H in the input data which would represent H_L . This necessitated the modification of Equation B.7 to read

$$\boxed{1+RnH} \text{ --- } \boxed{-8-4RnH} \text{ --- } \boxed{20+6RnH} \text{ --- etc.} \quad (B.8)$$

for use with a point lying on a long beam. For a point lying on a short beam equation B.7 would read

$$1+R'nH \quad -8-4R'nH \quad 20+6R'nH \quad \text{etc.} \quad (B.9)$$

where R' had the following values

$\frac{H_S}{H_L}$ Ratio	$\frac{I_S}{I_L}$ Ratio	R'
R	1	R
R^2	R	R^2
R^3	R^2	R^3

B.4 Flow Diagrams

A general flow diagram for the program is shown in Fig. B.2 and a detailed flow diagram corresponding to the FORTRAN coding is given in Fig. B.3. The numbers on Fig. B.2 refer to the notes given below.

Note 1: The program generated a matrix A (I,J) containing I rows and J columns with the maximum value of I being equal to N, the number of points on the quarter-plate, and the maximum value of J being equal to N+1. Column number N+1 was for the load term qh^4/D appearing on the right hand side of the equation given in Fig. B.1. This term was transposed to the left side of the equals sign for entry into the matrix. For the value of $h = L/20$ used in coding this term became -0.00000625. The array reserved for the matrix contained (N)(N+1) words.

Note 2: The operator was applied at a series of points I on the plate with I taking successive values from 1 to N. The thirteen elements of the operator could then be defined in reference to the point I by using the thirteen J

subscripts shown in Fig. B.1. Thus J7 would equal I, J2 would equal I+10, etc.

Note 3: After the J addresses were computed entries were made in the matrix by setting the proper $A(I,J)$ terms equal to their corresponding elements in Fig. B.1. Thus for $I = 17$, J2 would be 27, and the entry $A(17,27) = 2.0$ would be made into the 17th row and the 27th column of the matrix.

Note 4: For certain locations on the plate portions of the operator would fall on the column or outside of the lines of symmetry defining the quarter-plate. For these locations it was necessary to modify the general pattern of Fig. B.1. In order to determine the location of a given point on the plate it was necessary to establish a row and a column counter on the plate as shown in Fig. B.4. The IA counter established the number of rows and the JA counter established the number of columns of node points measured from the center of the plate. Note that there is no correspondence between the rows and columns of node points on the plate and the rows and columns of terms in the matrix. The testing to determine if modifications were necessary and the ensuing modifications of the basic pattern entailed the bulk of the coding effort.

Note 5: In order to check the program a number of test problems were run with the entire matrix of $(N)(N+1)$ terms being printed for each problem. These printed matrices were then checked by hand. After code checking showed that the program was performing satisfactorily this portion of the program was deleted.

Note 6: After the matrix was generated the N unknowns were solved using a standard subroutine ..

Note 7: Plate bending moments were computed using the relationship

$$m_p = -\frac{1}{h^2} \left[\begin{array}{c} \textcircled{1} \text{---} \textcircled{-2} \text{---} \textcircled{1} \end{array} \right] \quad (\text{B.10})$$

where m_p represents the unit plate bending moment. Moments were computed in the two orthogonal directions defined by the two centerlines of the plate. Moments were computed for a value of Poisson's ratio equal to zero. Beam bending moments in the long direction were computed using the relationship

$$M_b = \frac{-HR}{h^2} \left[\begin{array}{c} \textcircled{1} \text{---} \textcircled{-2} \text{---} \textcircled{1} \end{array} \right] \quad (\text{B.11})$$

For beams in the short direction the term R appearing in equation B.11 was replaced by R' .

Figure B.3 is a detailed flow diagram for the main program. The subprogram for computing moments used a similar detection scheme and is not shown. Two detection symbols are used in the flow diagram, one corresponding to a two-way branch, and the other corresponding to a three-way branch. This was done to simplify the flow diagram. The numbers on Fig. B.3 refer to the explanatory notes given below. The program was coded only for the range of the c/L and S/L ratios given in Tables 7 - 15.

Note 1: The addresses of the terms making up the operator shown in Fig. B.2 were computed.

Note 2: The IA and JA counters were computed. For example, for points lying north of the column $IA = 1 + (I-1)/M2$ and $JA = I - (IA-1)(M2)$.

Note 3: The operator was applied to the point in question and the proper entries made into the matrix.

Note 4: The operator was modified for effects of symmetry and/or portions of the operator falling on the column.

Note 5: The c/L ratio was referred to as LC in coding. Thus for $c/L = 0$, LC was 0, for $c/L = 0.1$, LC was 1, etc.

B.5 Output Data and Estimation of Running Time

Output Data: Output data consisted of the deflections and moments at the N points of the quarter-plate considered. Deflections were given as coefficients of qL^4/D and moments were given as coefficients of qL^2 for plate moments and as coefficients of qL^3 for beam moments. Appropriate page headings listing the input parameters and other pertinent information were printed on each page of output data.

Estimation of Running Time: Machine time required for processing of the FORTRAN program into a machine language program was about two minutes. The maximum number of equations was obtained for the case of a square plate having a c/L ratio of zero. For this case N was 120. The total time required for generating the matrix, solution of the matrix, computation of moments, and storage of all output data on the magnetic tape for eventual printing was about three minutes for this case. For other values of N the time required for solution of the matrix would vary nearly as the third power of the ratios of N and the time required for the other portions of the program would vary about linearly. The total machine time required for the solutions summarized in Tables 7 through 15 was about one hour.

B.6 Validity of Program

The program was used to solve a number of known cases in order to check the validity and accuracy of the program. In Fig. B.5 deflection coefficients obtained by Sutherland (26) and from the program are shown plotted versus H_L for an aspect ratio of 0.8 and a c/L ratio of zero. A smooth curve

can be drawn through all the points obtained by the two methods for a given location on the plate thus showing the validity of the program. In general, the deflection coefficients obtained using the program were up to four percent greater than those obtained by other methods. For example, for a square panel having no supporting beams and point columns Timoshenko (23) gives a mid-panel deflection coefficient of 0.00581 while the coefficient obtained using the program was 0.00599 which was 3.1 percent greater. Similar agreement was found for the bending moments.

B.7 Availability

A copy of the program including a listing of the input deck has been placed in the Computer Program Library of the Civil Engineering Department, University of Illinois

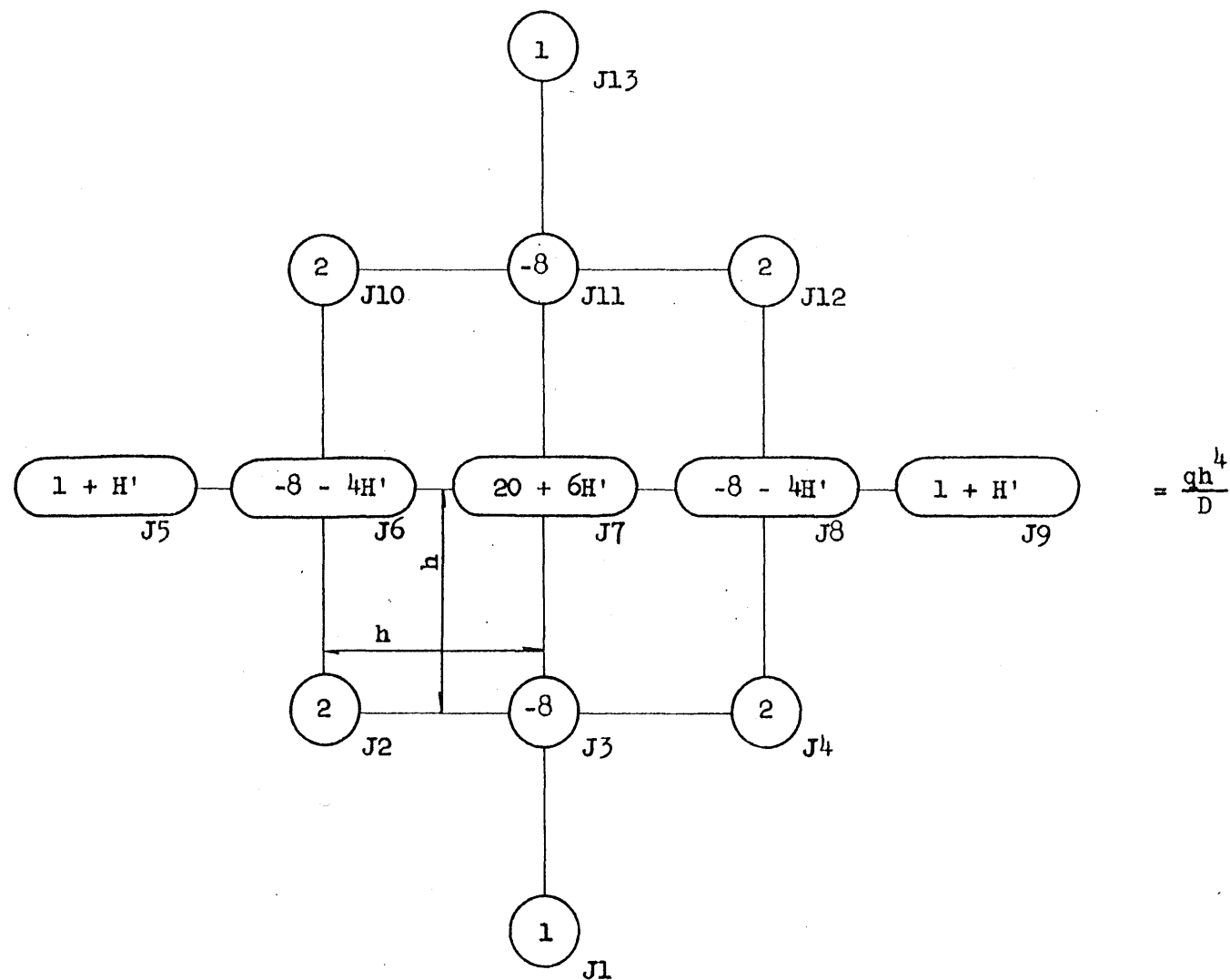


FIG. B.1 FINITE DIFFERENCE OPERATOR PATTERN AND ADDRESSES

-272-

Start

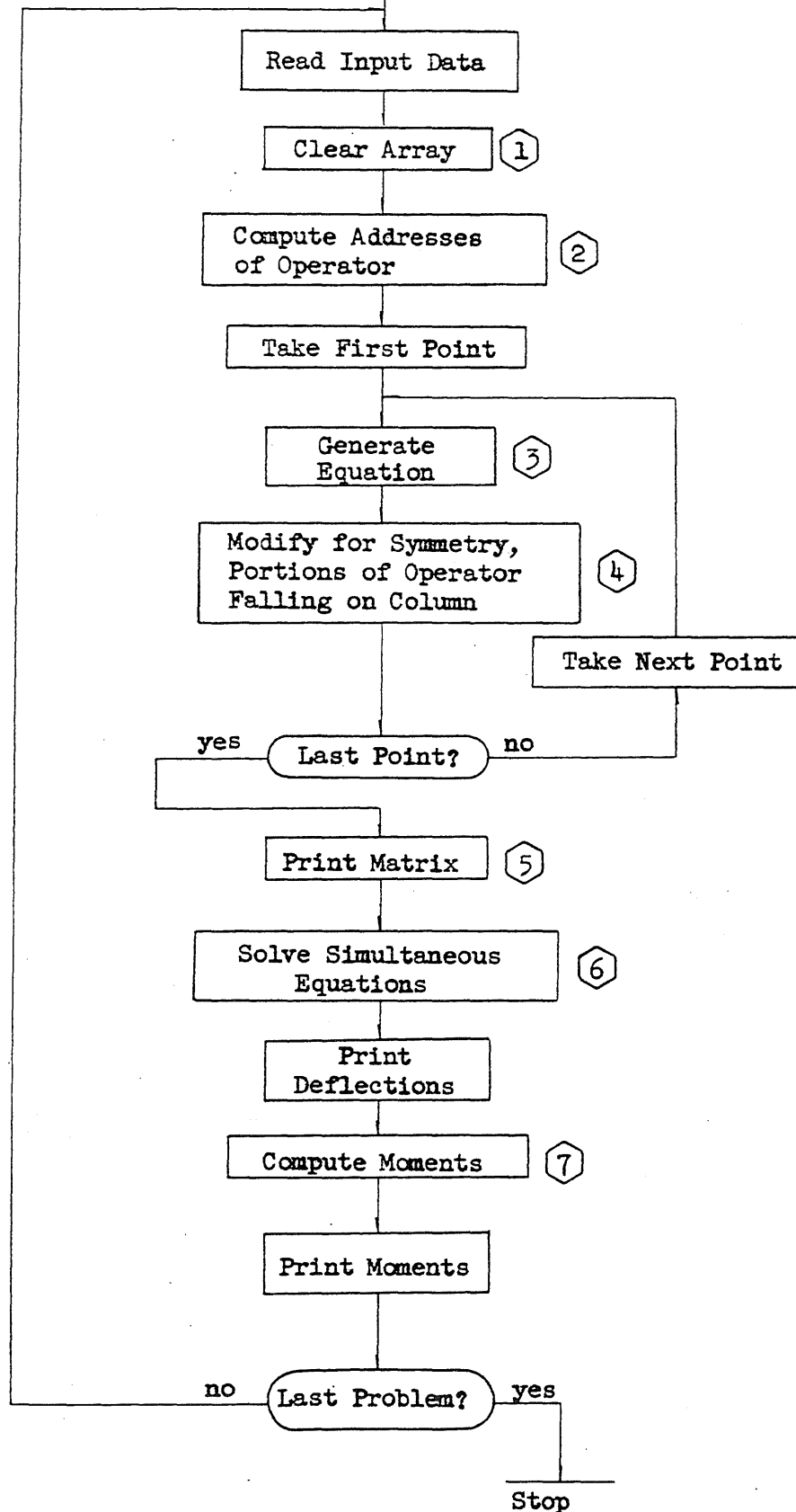


FIG. B.2 GENERAL FLOW DIAGRAM



FIG. B.3 DETAILED FLOW DIAGRAM

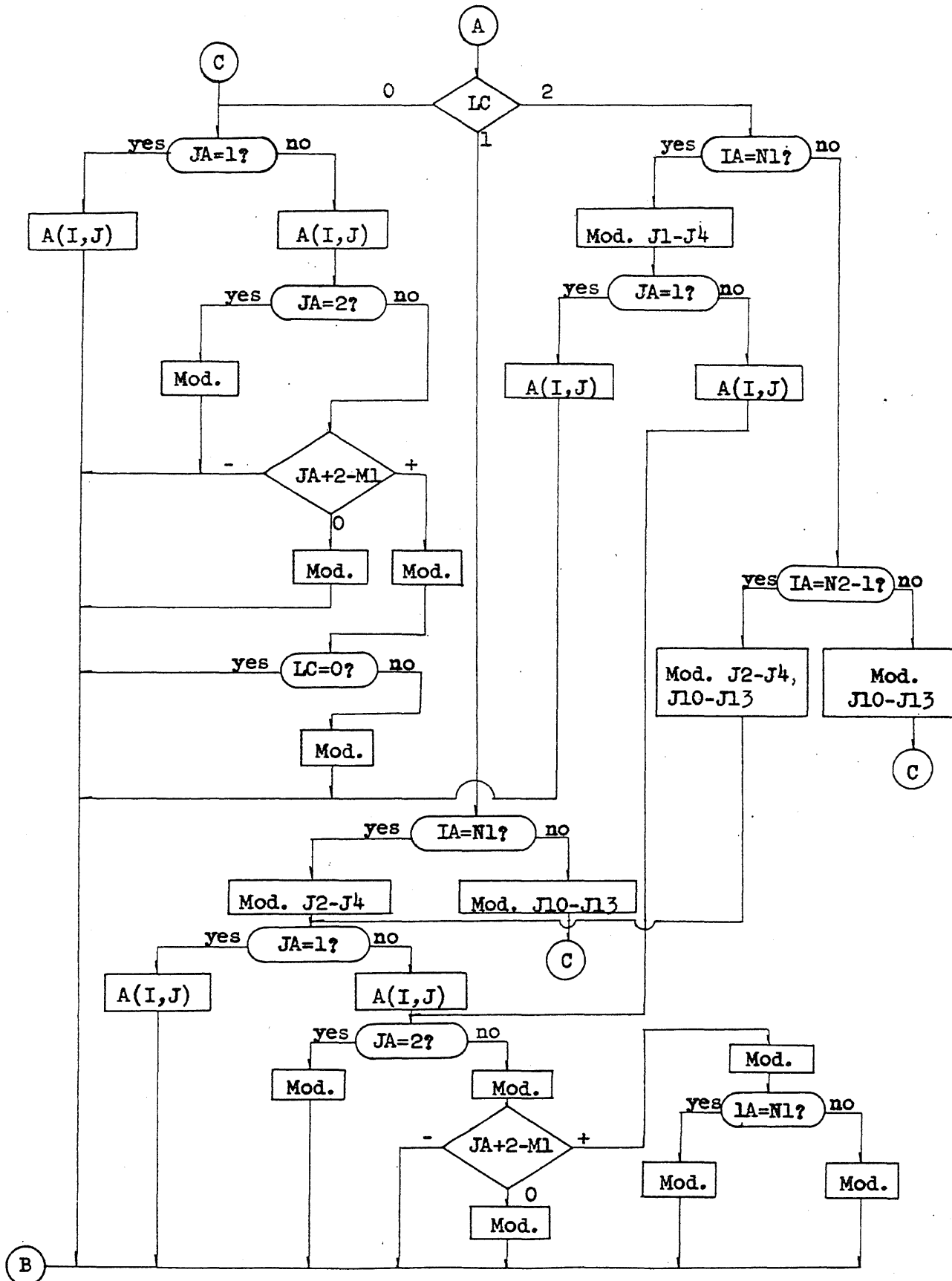


FIG. B.3 (Cont.) DETAILED FLOW DIAGRAM

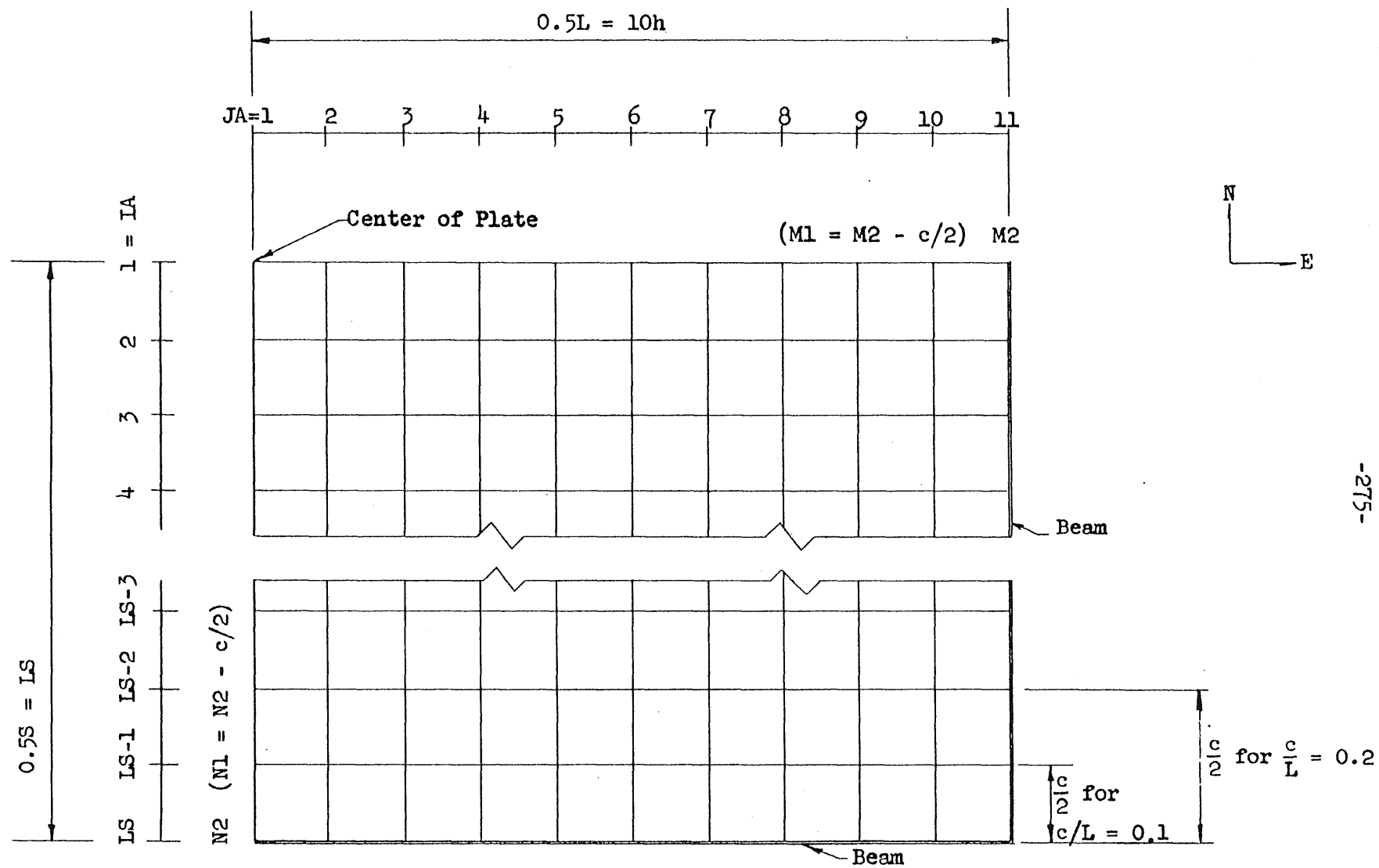


FIG. B.4 LAYOUT OF ONE-QUARTER OF INTERIOR PLATE

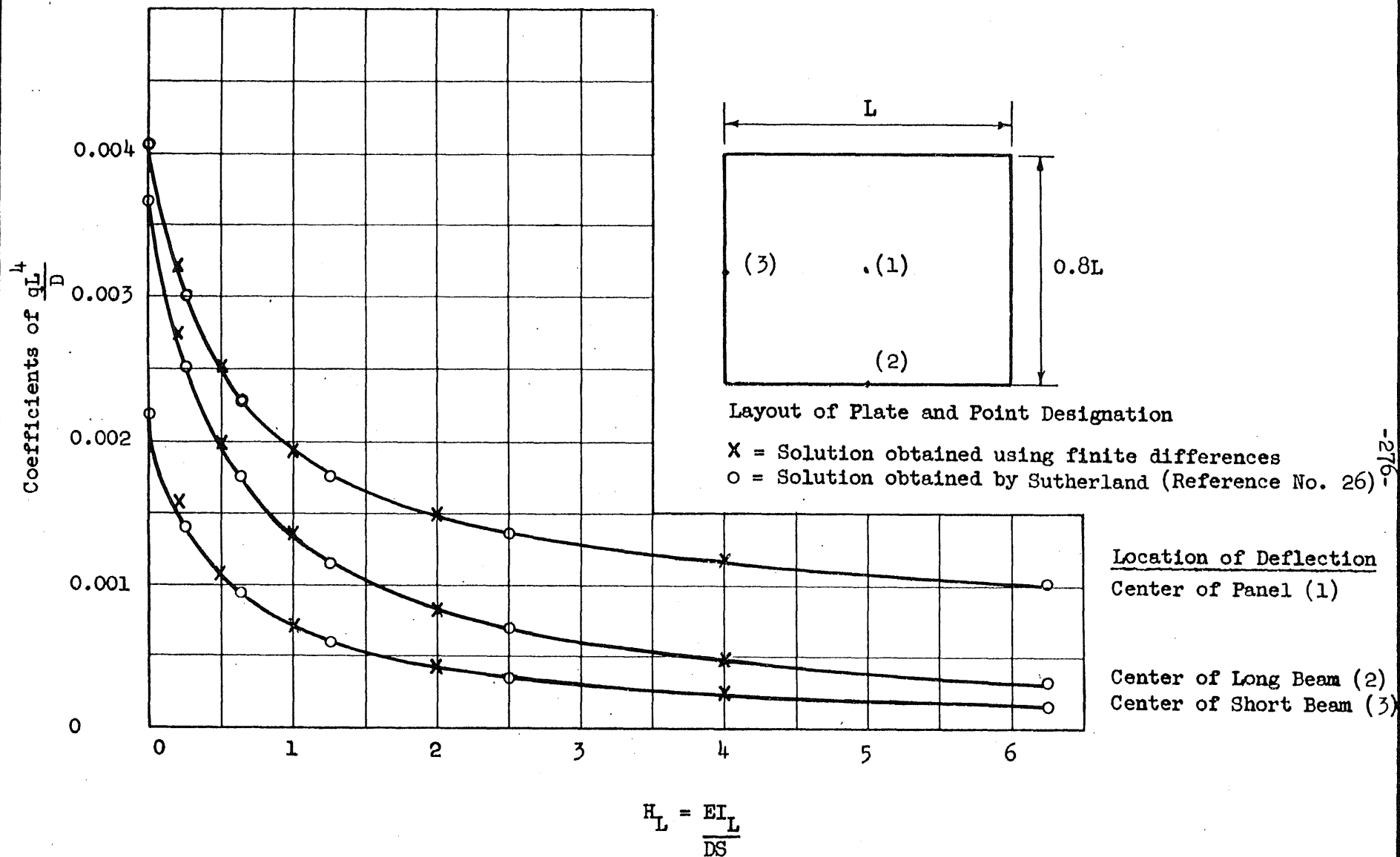


FIG. B.5 CHECK ON VALIDITY OF COMPUTER PROGRAM, $S/L = 0.8$, $c/L = 0$

APPENDIX C

ILLUSTRATIVE EXAMPLE

C.1 Introductory Remarks

This appendix contains a description of the procedure followed in using the frame analysis method to determine the deflections of the two-way slab with shallow beams (T2). Only the salient points of the computations are given; routine calculations are omitted. The layout and dimensions of the test structure are shown in Fig. 5.16. The arrangement of the reinforcement is shown in Figs. 5.21 - 5.23. The total design load, including 75 psf dead load, was 145 psf.

For purposes of discussion the computations involved in performing the frame analysis are divided into the following five areas:

- (1) Selection of frames,
- (2) Computations of stiffnesses and carry-over factors,
- (3) Determination of loading,
- (4) Computations of moments, slopes, and deflections based on uncracked sections, and
- (5) Computations of slopes and deflections based on fully cracked sections.

C.2 Selection of Frames

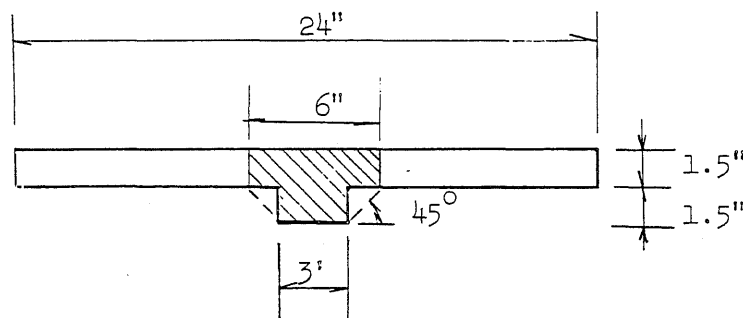
The two-way slab with shallow beams was symmetrical about both centerlines and about both diagonals. Hence it was necessary to analyze only two frames. One frame contained an interior row of columns and beams and is termed the interior frame. The other frame contained an edge row of columns and beams and is termed the edge frame. The dimensions of these two frames are shown in Fig. C.1.

C.3 Computations of Stiffness and Carry-Over Factors

The following computations are for the interior frame. Those for the edge frame are performed in a similar manner. There are two different types of flexural members in the interior frame, the interior and the end beams. There are two types of flexural-torsional members, the edge column-edge beam combination and the interior column-interior beam combination.

(a) Interior Beam

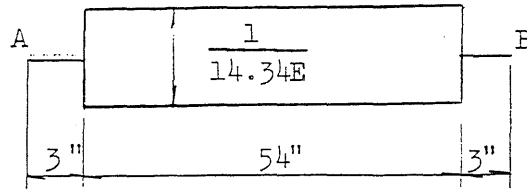
In cross section the interior beam has the shape shown in sketch A.



SKETCH A

The moment of inertia of this section is computed by considering it to be made up of two parts as described in Section 4.4. The distance to the centroid of the cross-hatched part, measured from the upper surface, is 1.25 in. The moment of inertia of this part is 9.28 in.^4 and that of the remainder of the section is 5.06 in.^4 . The beam rigidity EI may be expressed in terms of the total plate rigidity DL . The moment of inertia of a unit width of plate is 0.281 in.^3 . Taking L as 60 in. gives the relationship $EI = 0.850DL$. For the edge frame this relationship is $EI = 0.643DL$.

Based on the assumption that the beam may be considered as infinitely stiff from the face of a column to its center, the $1/EI$ diagram for the interior beam has the shape shown in sketch B. Using the column analogy, the stiffness at either end is computed to be $1.250E$. The choice of units is immaterial as

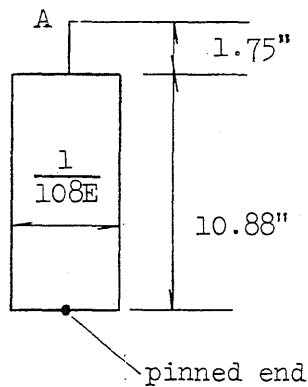


SKETCH B

long as all stiffness computations are made using the same units, in this case inches. The carry-over factor is 0.575.

(b) Interior Beam-Column

Assuming the interior column to be infinitely stiff from its intersection with the bottom of the interior beam to the centroid of the interior beam, the $1/EI$ diagram for this column has the shape given in sketch C.



SKETCH C

The dimension 1.75 in. is the distance from the bottom of the interior beam to the centroid of the area shown cross-hatched in sketch A. A somewhat larger distance would be taken if the centroid of the entire cross section shown in sketch A were used. However, studies have shown that the stiffnesses computed are relatively insensitive to changes in this dimension. The flexural stiffness at A in sketch C is $40.2E$.

The stiffness of the combined flexural-torsional element may be computed from the relationship

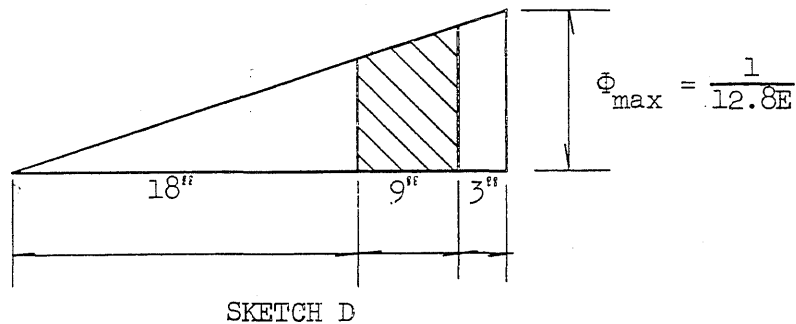
$$K_{bc} = \frac{m_c}{\theta_t + \theta_f} \quad (C.1)$$

where the notation is described in Section 4.4. The value of θ_f may be computed from the flexural stiffness of the interior column as

$$\theta_f = \frac{0.9}{40.2E} = \frac{0.0224}{E} \quad (C.2)$$

The torsional stiffness of the beam framing into the column from a direction perpendicular to the longitudinal axis of the frame may readily be determined once the value of C has been computed. Using Fig. 4.4 the value of C for the section shown cross-hatched in sketch A is found to be 12.8 in.⁴ for the edge beam the value of C is 12.0 in.⁴

The assumed unit rotation diagram for one-half of the interior beam, measured from center of beam to center of column, is shown in sketch D.

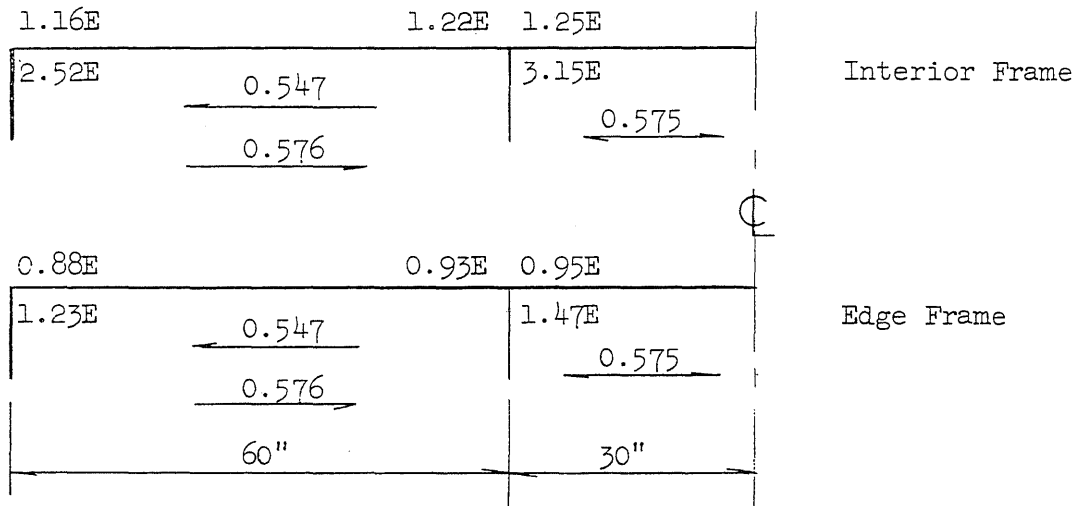


The value of θ_t , which is equal to one-half the area shown as cross hatched in sketch D, is computed to be 0.264/E.

The final stiffness of the combined torsional-flexural member is

$$K_{bc} = \frac{0.9}{0.264/E + 0.0224/E} = 3.15E \quad (C.3)$$

The stiffnesses and carry-over factors for both the interior and edge frames are shown in sketch E. The direction for which each carry-over factor is valid is indicated by an arrow.



SKETCH E

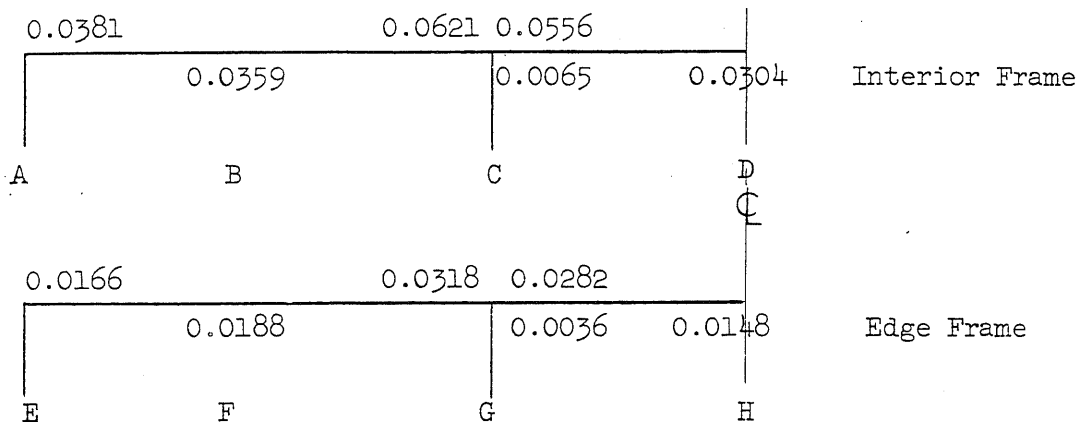
C.4. Determination of Loading

Since each panel of the structure was square the loading to be applied to each of the frames was the same as that shown in Fig. 4.2.

C.5. Computations of Moments, Slopes, and Deflections for Uncracked Sections

(a) Moments

The line representation of each of the frames is shown in sketch E above. The fixed-end moments for each of the spans of the interior frame, computed by taking "a" as 0.2, "b" as 0.0 and "q'" as $0.6qL$ in Table 18, are $0.05448qL^3$, and the static moment is $0.0860qL^3$. The fixed-end moments and static moments for the edge frame spans are one-half those for the interior frame. The final end moments and mid-span moments determined using the Cross moment-distribution procedure are shown in sketch F. The moments are given in terms of qL^3 .



SKETCH F

(b) Slopes

The slope at the end of a beam may be determined by dividing the moment acting on the column into which the beam frames by the stiffness of the column. The stiffness for the interior column is $3.15E$. Note that the "column" referred to here is the combined flexural-torsional element and not the purely flexural element shown in sketch C. The stiffness of the interior column may be expressed in terms of the unit plate rigidity D as follows:

$$\frac{(3.15E)(60)(\frac{I}{14.34})(0.850DL)}{EI} = 11.17D \quad (C.4)$$

Dividing the bending moment acting on column C in sketch F by this stiffness gives

$$\theta_C = \frac{0.0065qL^3}{11.17D} = 0.00058 \frac{qL^3}{D} \quad (C.5)$$

A summary of the slopes computed for the columns shown in sketch F is given below.

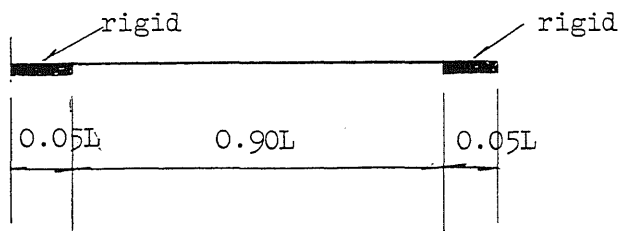
<u>Point</u>	<u>Slope</u>
A	0.00431
C	0.00058
E	0.00381
G	0.00069

The slopes are given in units of qL^3/D . The sense of the slopes may be determined from sketch F.

(c) Deflections

The total deflection at the center of a span of the ersatz frame is the sum of the deflections caused by the applied loads with the ends fixed and the deflections resulting from the end rotations. The deflection caused by the uniformly distributed portion of the load may be readily computed using known coefficients. The deflection caused by the "roof-top" portion of the load may be determined using Table 18. The deflection at mid-span of a beam of length L caused by an induced end rotation of magnitude θ is $\theta L/8$ assuming the end not rotated to be fixed. There is an additional deflection at the mid-span of the beam resulting from the deflection of the ends of the beam in respect to the columns into which it frames.

The computations for the deflection at point D in sketch F are given below. In making these computations it is necessary to deal with the clear span. The portions of the total span lying between column centers and column faces are assumed to be rigid as shown in sketch G.



SKETCH G

Effect of uniformly distributed load

$$\Delta = \frac{5}{384} \frac{0.4qL(0.9L)^4}{0.850DL} = 0.000804 \frac{L^4}{D} \quad (C.6)$$

Effect of "roof-top" loading

$$a = \frac{0.15}{0.90} = 0.167, \quad b = 0$$

$$\Delta = \frac{5.58}{3840} \frac{0.6qL(0.9L)^4}{0.850DL} = 0.000673 \frac{qL^4}{D} \quad (C.7)$$

Effect of θ_C (both ends)

$$\Delta = \frac{\theta_C L}{4} = \frac{-0.00058}{4} (0.9L) \frac{qL^3}{D} = -0.000131 \frac{qL^4}{D} \quad (C.8)$$

Effect of End Deflection (both ends)

$$\Delta = (\theta_C)(0.05L) = -0.00058 \frac{qL^3}{D} (0.05L) = -0.000029 \frac{qL^4}{D} \quad (C.9)$$

The final deflection is the sum of the four terms listed above and is

$$\Delta = 0.00132 \frac{qL^4}{D} \quad (C.10)$$

In like manner the deflections at the remaining mid-beam points may be determined. Once the mid-beam deflections and the column rotations are known, the mid-panel deflections are computed using Eqs. 4.8 - 4.10. Thus the deflection at the center of the interior panel is computed as

$$\Delta = 0.00132 \frac{qL^4}{D} + 0.00153 \frac{qL^4}{D} - 0.2L(0.00058 \frac{qL^3}{D}) = 0.00273 \frac{qL^4}{D} \quad (C.11)$$

C.6 Computations of Slopes and Deflections Based on Fully Cracked Sections

The rotation of a column, assuming it to be fully cracked, is computed by multiplying the rotation computed on the basis of the uncracked

section to that of the cracked section. The rotations computed in this manner are given below in terms of qL^3/D .

<u>Point</u>	<u>Slope</u>
A	0.0202
C	0.0016
E	0.0179
G	0.0019

The mid-beam "fully cracked deflection" is computed by multiplying the "uncracked deflection" by the ratio of the "uncracked moment of inertia" to the average "fully cracked moment of inertia." For the interior beam containing point D in sketch F the uncracked moment of inertia is 14.34 in.^4 and the average fully cracked moment of inertia is 6.04 in.^4 . Hence the mid-beam deflection is

$$\Delta = 0.00132 \frac{qL^4}{D} \frac{14.34}{6.04} = 0.00314 \frac{qL^4}{D} \quad (C12)$$

For a member which contains no compressive reinforcement the moment of inertia of the fully cracked section may be computed using the relationship

$$I_{cr} = nA_s d^2 (1-k)j \quad (C.13)$$

where I_{cr} is the cracked moment of inertia,

n is the modular ratio $= E_s/E_c$,

E_s, E_c = moduli of elasticity of steel and concrete, respectively,

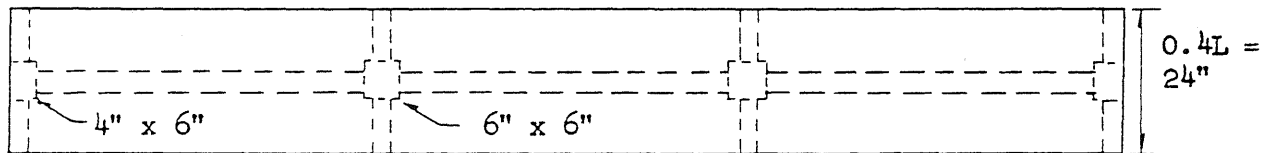
A_s = cross-sectional area of tensile reinforcement,

d = depth from compressive face of member to centroid of tensile reinforcement,

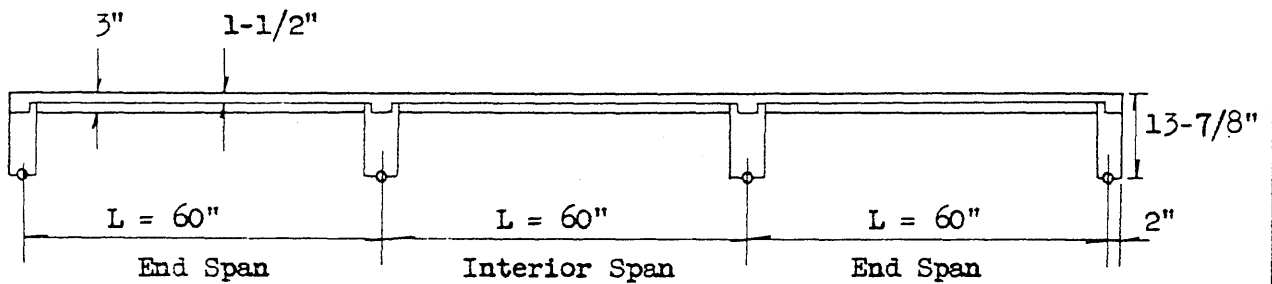
kd = depth from compressive face of member to point of application of resultant of compressive stresses, and

jd = distance between points of application of resultants of compressive and tensile forces.

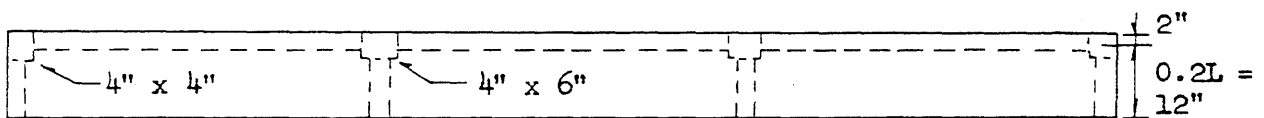
For a member containing compressive reinforcement the moment of inertia for the fully cracked section may be computed using Table 11 in the Reinforced Concrete Design Handbook, Second Edition, 1955.



Interior Frame



Section



Edge Frame

Note: All beams 3" x 3"

FIG. C.1 ERSATZ FRAMES FOR TWO-WAY SLAB WITH SHALLOW BEAMS (T2)

[illegible]